TESLA - COLLABORATION

Transparencies from the Workshop on

Thin Film Coating Methods for Superconducting Accelerating Cavities

Ed.: D. Proch

DESY

August 2000, TESLA 2000-15

Table of Contents, TESLA Report 2000-15

Thin Film Coating Methods for Superconducting Accelerating Cavities, DESY, July 10, 2000

D.Proch

DESY, 19.7.2000-07-19

Summary of the One day workshop on thin film coating methods for superconducting accelerating cavities 10.July 2000, DESY

This workshop was organised one day prior to the TTF meeting as a brainstorming about cavity coating methods. The scope of discussion was to:
- review of coating techniques
- reports of ongoing activities
- discuss about the evidence of Hc1 as the limiting field
- propose superconducting candidates for new cavity coating experiments
- find out, whether we should we try CVP, or wet coating of Nb, laser ablation,..
- discuss the question, whether Cu is the best substrate
-organize new collaborations.

In the meeting not all of these items could be covered intensively, but a lot of worthwhile information was exchanged. The following write-up presents a short (may be not complete) summary of the presentations and discussions. There was a general consensus, that such meetings should be continued in the near future.

Classification and Overview of Various Deposition Technologies - J. Langner/Soltan Institute

A nice review about coating methods was presented by Langner. The following remarks should be made:

• There is no experience in our community with chemical vapour deposition techniques. This might simply be due to lack of chemists in our working field. Effort should be launched to get in contact with expertise groups in the field of chemical vapour deposition methods.

• The exclusively used magnetron sputter method for producing Nb-Cu resonators seems to be a mature technology (see CERN report on this subject). An intrinsic drawback of this method is the relative low impact energy of the Nb ions (1-10 eV) and the need of a carrier gas.

• Vacuum arc deposition might be an interesting alternative to magnetron sputtering:
-the impact energy of metal ions is in the range of 10 to 100 eV. This results in a quasi in situ cleaning of the substrate to be coated and in a denser growing film. A problem might arise from the contamination of the film by large size droplets (around 1 um).
There is collaboration between the Soltan Institut (Langner) and INFN Roma (Tazzari) in preparing Nb film samples by this method. It was proposed by these partners to include DESY in this effort. Details of the joined programme will be discussed soon.

Exotic Superconducting Materials and Related Deposition Technologies for Coated Superconducting Cavities - E. Palmieri/INFN Legnaro

Palmieri discussed the superconducting properties in terms of three fundamental (and rather easy measurable) quantities: Tc, specific heat and normal state low temperature resistivity. Applying the selection criterion of low BCS resistance, promising candidates must experience high Tc and low resistivity. There are two large groups of superconductors, which on paper provide the required characteristics:
-B1 compounds. They are characterized by a NaCl type structure and are formed by a transition metal with Nitrogen and/or carbon (e.g. NbN)
-A15 compounds like Nb3Sn or V3Si.
For those materials which have been RF measured, increasing losses are observed when raising the stored cavity energy: Nb3Sn, NbN, (NbTi)N, V3Si, MoRe,... Very active work with dielectric resonators is carried out at INFN Neapel to optimize sputter/co-evaporation parameters for good film performance.
Other important characteristics in defining promising candidates for coating are:
-large area of stability in the phase diagram, especially when lowering the temperature
-stable superconducting properties for changes in stoichiometry.
Also in this respect Nb3Sn is an interesting material. So far Nb3Sn has been produced by Sn vapor on a solid Nb cavity body (see talk by G. Mueller). In order to avoid the high costs of the Nb material coating a Cu cavity by co-evaporation should be tried out. The high thermal conductivity of Cu as compared to Nb would be another advantage.

Nb Sputtered Films on Cu Cavity - S. Calatroni/CERN

Sputter parameters have been investigated and optimised in respect to high Q-values (up to gradients of the order of 10 MV/m):
-physical properties of the substrate (spinning, hydroforming, electro-polishing)
-variation of the sputter gas (Ar, Kr, ...)
High Q-values of 10^11 could be established. But there still exists the Q-drop when raising the accelerating gradient. Above 10 MV/m all measured curves merge to the same Q slope. The best high gradient cavity reached 28 MV/m at a Q-value of 0.5*10^9. A conclusive explanation for the Q-drop is still missing.
In situ pre cleaning of the Cu substrate by inserting a special cathode before the Nb sputtering has been used in the past, and will be tested again in view of producing films as similar to the bulk as possible.
Hc1 of thin sputtered Nb films was measured by the induction method: it is of the order of 50 mT. As compared to the maximum values reached so far, clearly Hc1 is surpassed in RF applications. It was argued, however, whether the low measured value for flux penetration in thin films can be interpreted as Hc1 (as defined for a bulk superconductor).

Nb Sputtered Cavities: Present Experience and Future Plans - P. Bosland/Saclay

At Saclay single cell Nb-Cu cavities have been coated by magnetron sputtering. Here the cavity can be heated up to 400°C during the coating process, and the Cu cavities are polished by a special mixture of sulphuric and nitric acid, but not by electro-polishing. The highest field reached was 25 MV/m at a Q-value of 1.2*10^9 limited by power.
The effect of substrate roughness was studied on samples using a thermometric method for surface resistance measurements. BCS surface resistance is not affected by roughness, but there is a clear correlation between the value of the residual resistance as well as the Q-slope

versus the growth defect density. These defects, typical of sputtering technique, are generated by small defects of the copper surface before deposition: substrate roughness defects, dust particles already on the surface or coming from the magnetron cathode during sputtering. However, the growth defect density is not the only origin of the reduced performance of sputtered Nb/Cu cavities. Sometimes the Q-slope is reduced after baking at 90°C for 20 hours. Several new Cu cavities were produced by hydro-forming. It was proposed to electro-plolish these resonators prior to coating.

Nb3Sn for RF Application - G. Mueller/Uni Wuppertal

There is a long lasting experience with vapour diffusion coating of Nb resonators with Nb3Sn at University of Wuppertal. The high quality factor of 10^10 at 4.2 K (1.5 GHz, CEBAF frequency) clearly demonstrated the promise of lower Rbcs for Nb3Sn as compared to pure Nb. At 5 MV/m the gradient was still above the specified value for CEBAF. This resonator was produced from high RRR 300 Nb, coated at Wuppertal and measured by P.Kneisel at Jlab. After Ti heat treatment high RRR Nb cavities show large grain size. This unfavourable situation for uniform growth of NB3Sn grains was overcome by Sn nucleation during SnCl2 treatment at 200°C.
Discussion started about a possible continuation of the work with Nb3Sn in collaboration with Wuppertal, Saclay and DESY. Unfortunately there was no report about the detailed plans at Saclay, but H.Safa expressed his interest in this work during private conversation at the last EPAC.

Example for Coating by Sublimation:TiN for RF Windows , J. Lorkiewicz/DESY

The coating of RF windows with Ti by sublimation was reported as example for this technology. The conversion to TiN is done by using NH3 during deposition at a pressure of 10^-3 mbar . The conversion is completed by a further Ammonia pressure of around 400 mbar for another 20 hour after Ti coating.

Report about Joint Coating Project between INFN Roma and Soltan Institute - R. Russo/INFN Roma2

There is a collaboration between Soltan institute and INFN, Roma about building and operating a planar arc source for sample coating. Main question is, whether microdroplets are a problem in this coating procedure. As pointed out in Langners talk, the vacuum arc method promises to produce a cleaner (no carrier gas) and more compact (higher impact energy of metal ions) Nb film. It is expected to get a conclusion in two years about the relevance of this method for cavity coating.

Report about Activities for Coating Cavities for the Muon Accelerator - Hasan Padamsee/Cornell University

A Fermilab neutron factory study calls for a 200 MHz SRF linac. Because of the large cavity size at this low frequency, bulk cavity production would be very expensive. Therefore an R&D program is started with the aim of demonstrating 15 MV/m gradient in three years with Nb coated Cu resonators. One challenging item is the high stored energy of about 1000 Joule per cavity. Also in this respect a Nb-Cu cavity has advantages because of stability against quenching.

List of attendees

Benvenuti, C., CERN, EST/SM,	cristoforo.benvenuti@cern.ch
Bloess, D.,	dietrich.bloess@cern.ch
Bosland, P., CEA-Saclay, DSM/DAPNIA/SEA,	pbosland@cea.fr
Brinkmann, Arne, DESY, MHF-SL,	arne.brinkmann@desy.de
Calatroni, Sergio, CERN,	sergio.calatroni@cern.ch
Dwersteg, B., DESY, MHF-SL,	bernhard.dwersteg@desy.de
Goessel, Andre, DESY, MHF-SL,	andre.goessel@desy.de
Haebel, E.,	ernst.haebel@cern.ch
Kouptsidis, Johannes, DESY, MVA,	johannes.kouptsidis@desy.de
Langner, J., SINS Warsaw,	langner@ipj.gov.pl
Lorkiewicz, J., DESY, MHF-SL,	jerzy.lorkiewicz@desy.de
Moeller, W.-D., DESY, MHF-SL,	wolf-dietrich.moeller@desy.de
Mueller, G., Uni Wuppertal,	mueller@wpos4.physik.uni-wuppertal.de
Padamsee, H., Cornell University,	hsp@cesr10.lns.cornell.edu
Palmieri, E., INFN Legnaro,	palmieri@lnl.infn.it
Proch, D., DESY, MHF-SL,	dieter.proch@desy.de
Reschke, D., DESY, MHF-SL,	detlef.reschke@desy.de
Russo, Roberto, Universita di Roma, Physics Dept.	roberto.russo@roma2.infn.it
Schulz, Eberhard, DESY, MVA,	eberhard.schulz@desy.de
Sekutowicz, Jacek, DESY, MHF-SL,	jacek.sekutowicz@desy.de
Singer, W., DESY, MPL,	waldemar.singer@desy.de
Singer. X., DESY, MPL,	xenia.singer@desy.de
Tiessen, J., DESY, MVA,	jens.tiessen@desy.de
Twarowski, K., DESY, MHF-SL,	krzysztof.twarowski@desy.de
Vogel, H.P., Accel,	vogel@accel.de

Agenda for the Meeting about Thin Film Cavity Coating

July 10, 2000, Seminarroom 1, Bldg. 1, Starting time: 11:00 h
(The TESLA Board Meeting is held in a different part of the same building (seminarroom 4, Bldg. 1b)

Sequence of talks and duration might be modified. The schedule is only a guideline.

11:00 Classification and Overview of Various Deposition Technologies - J. Langner/Soltan Institute (60 min)
- evaporative technologies
- sputtering
- arc
- IBAD
- lasers

Sputtering
- ion beam sputtering
- glow discharge DC sputtering
- DC magnetrons
- reactive sputtering

Vacuum Arc-Based Technologies
- categories of vacuum arcs
- coatings from arcs

12:00 Exotic Superconducting Materials and Related Deposition Technologies for Coated Superconducting Cavities - E. Palmieri/INFN Legnaro (40 min)

13:00 Lunch

14:00 Nb3Sn for RF Application - G. Mueller/Uni Wuppertal (40 min)

14:40 Nb Sputtered Films on Cu Cavity - S. Calatroni/CERN (40 min)

15:20 Nb Sputtered Cavities: Present Experience and Future Plans - P. Bosland/Saclay (40 min)

16:00 Report about Joint Coating Project between INFN Roma and Soltan Institute - R. Russo/INFN Roma2 (20 min)

16:30 Coffee

17:00 Report about Activities for Coating Cavities for the Muon Accelerator - H. Padamsee/Cornell University (10 min)

17:10 Example for Coating by Sublimation: TiN for RF Windows - J. Lorkiewicz, DESY (10 min)

CLASSIFICATION AND OVERVIEW OF VARIOUS DEPOSITION TECHNOLOGIES

Introduction

-CVD, PVD

Evaporative Methods

Sputtering

-DC magnetron
-reactive sputter deposition
-bias sputtering
-unbalanced magnetron
-sustained self-sputtering

Vacuum arc

Film Quality

Conclusions

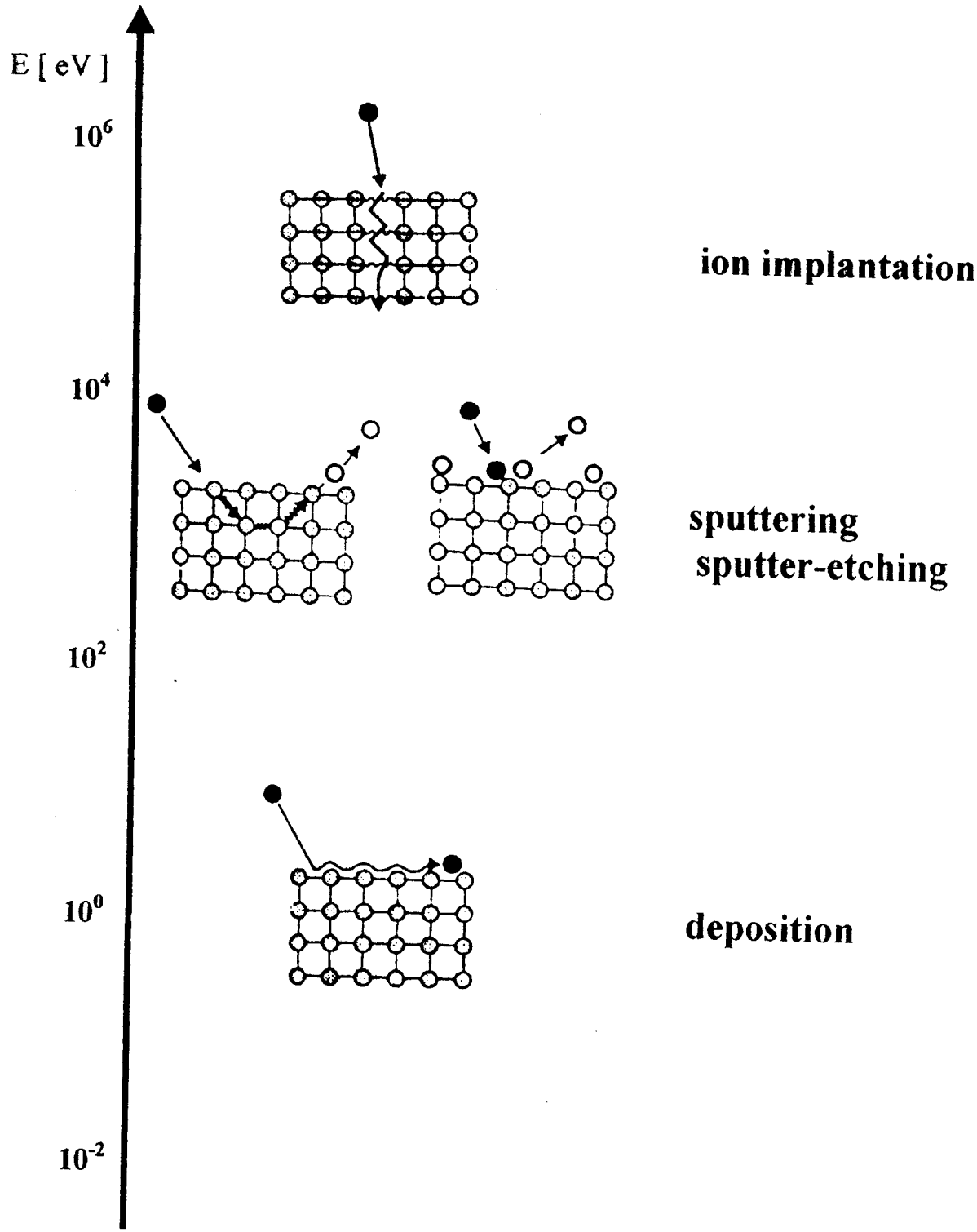
E [eV]
10^6
10^4
10^2
10^0
10^-2
ion implantation
sputtering
sputter-etching
deposition

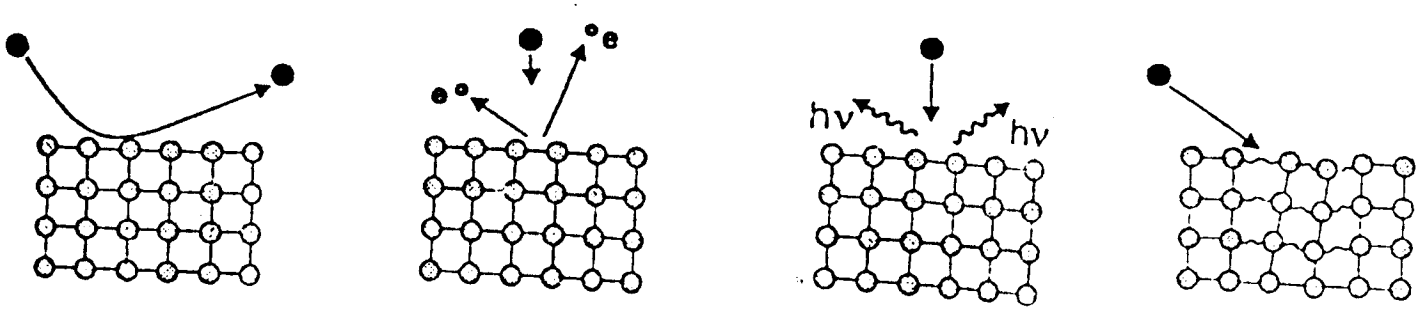
e
hν
hν

DEPOSITION

CVD

PVD

Chemical Vapour Deposition

Physical Vapour Deposition

Thin film crystallize due to chemical reaction of a gas or vapour introduced into reactor

Vapours (ofen ionized) of metal, alloy or compound are a source of films.

AP CVD

LP CVD

PA CVD

Evaporation

Sputtering

Arc

Laser

microelektronics

hard coatings

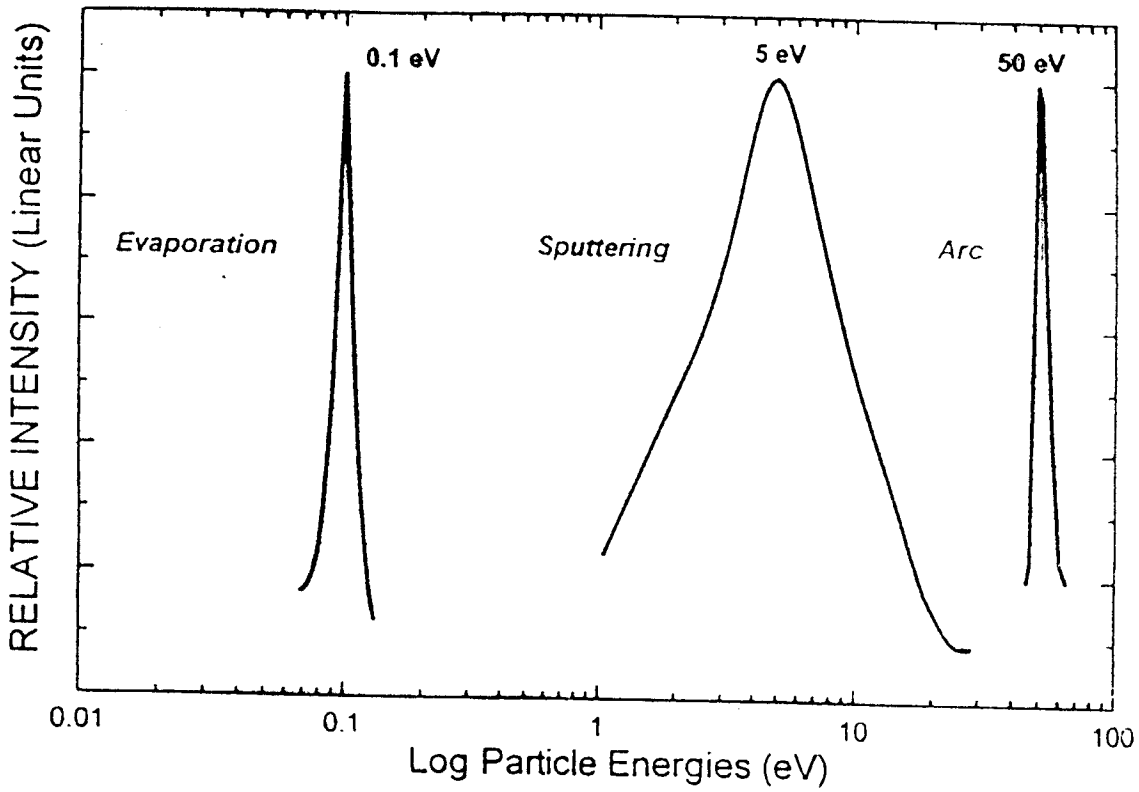

Fig. 1. Characteristic energies of metal species in PVD.

Evaporative Methods
ION PLATING

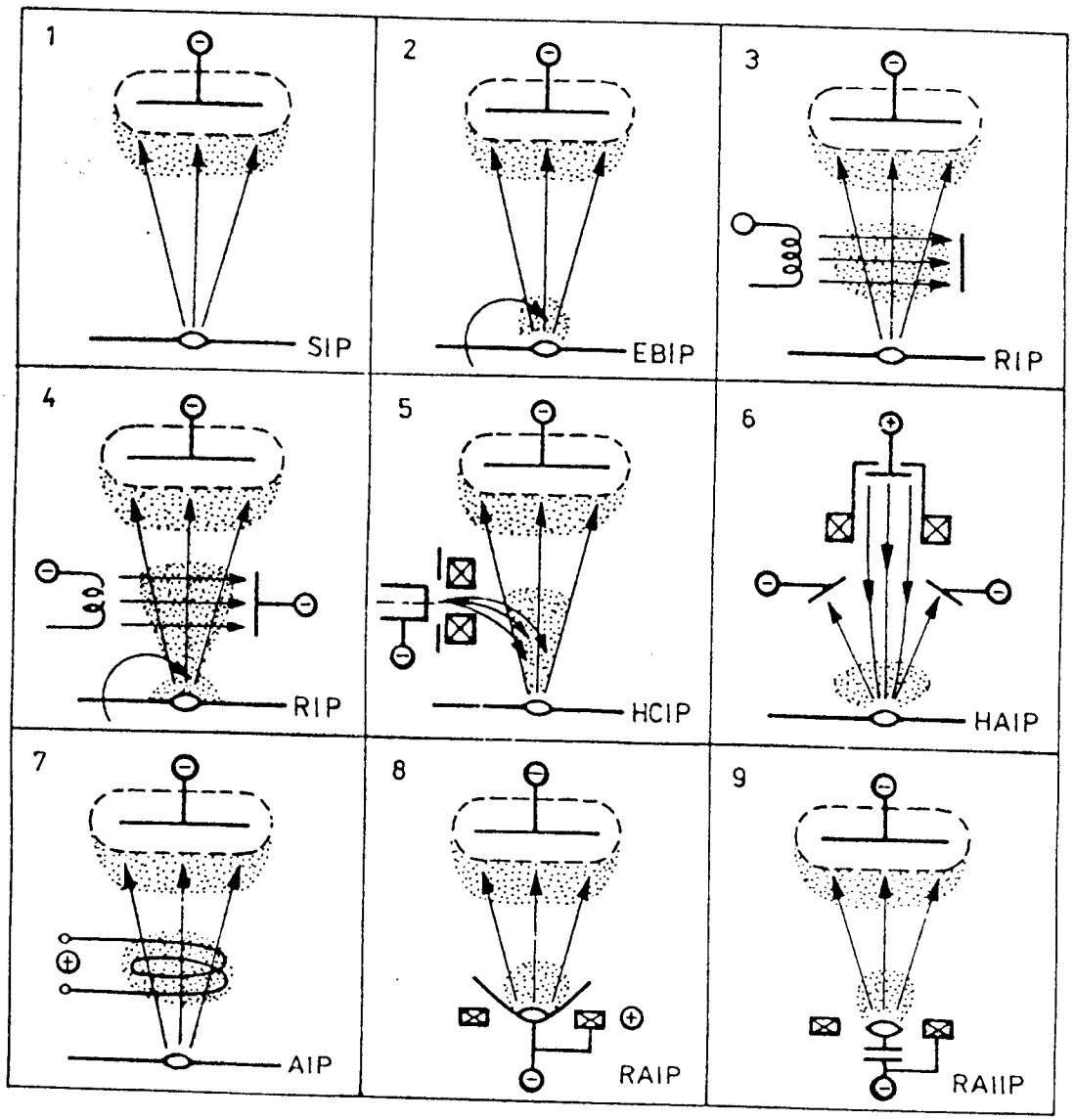

Sputtering

-ejection of atoms or molecules of a surface when the surface is struck by a fast incident particle.

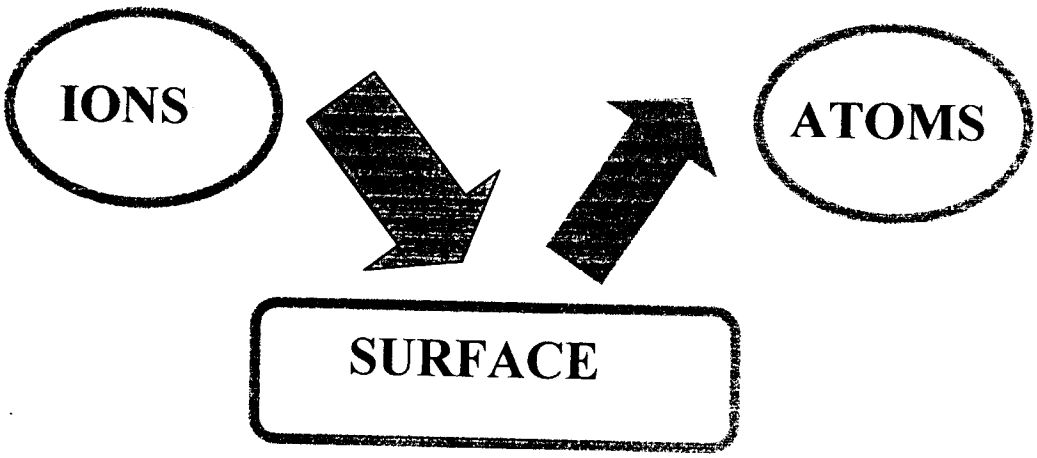

-energy of sputtered atoms – 5 – 10eV
-angular distribution- $E = F(\cos\Psi)$

-sp uttering yield – $Y = N_a/N_i$
$Y = Y(E_i, M_i, \alpha, \ldots)$
-threshold energy -20eV

Ion Beam Sputtering

Glow Discharge DC Sputtering

DC Magnetron

RF Sputtering

Diode Sputtering

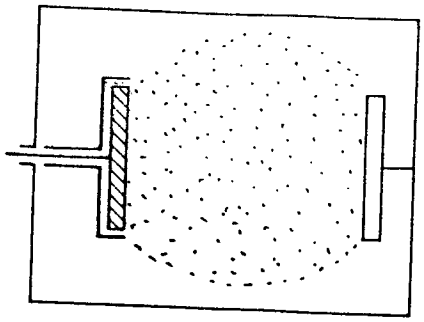

Triode Sputtering

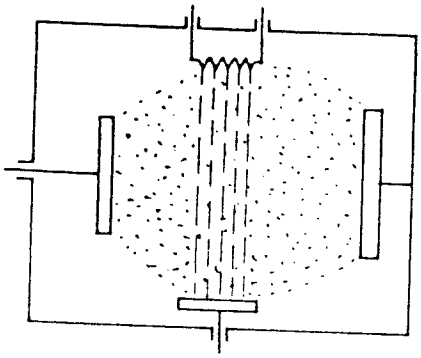

Hollow Cathode Sputtering

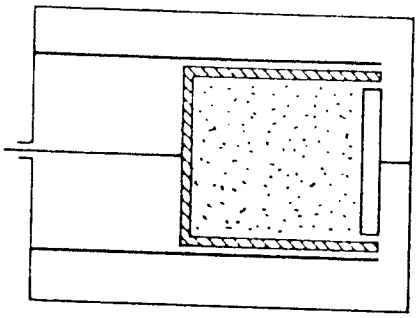

Electron Cyclotron Resonanse Sputtering

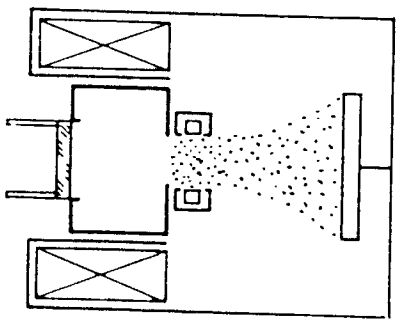

Ion Beam Sputtering

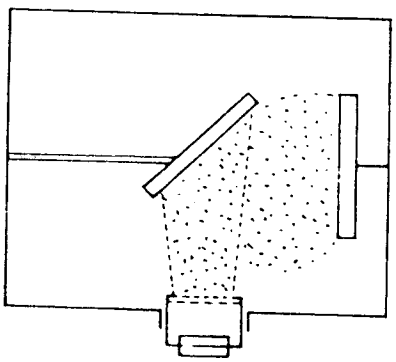

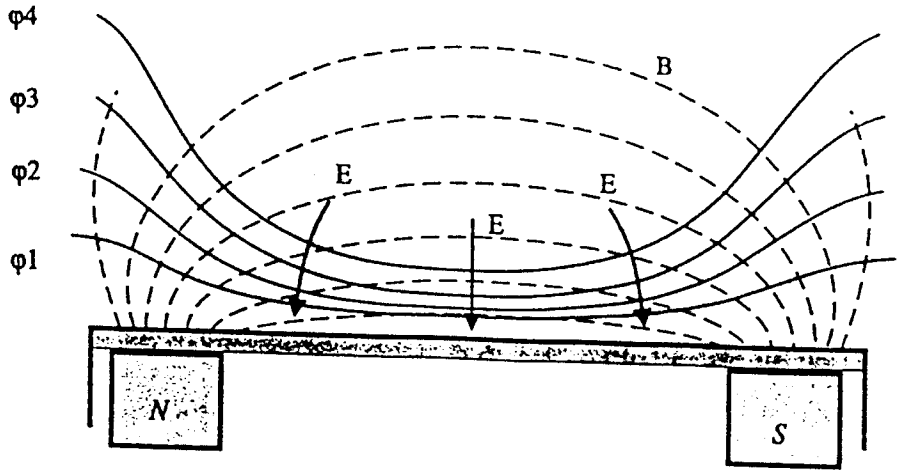

Rys. 9. Rozkład potencjału i trajektorie elektronów w obszarze pola elektrycznego nad katodą magnetronowego urządzenia rozpylającego

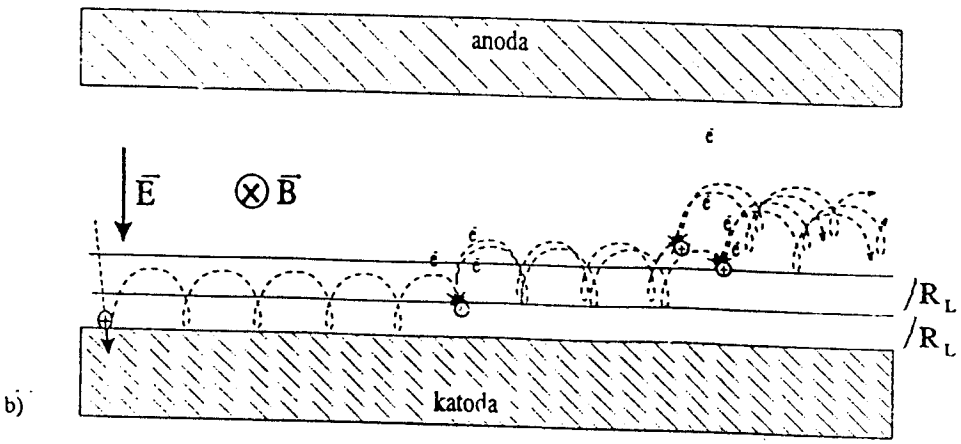

Rys. 18. Ruch elektronu w obszarze skrzyżowanych pól elektrycznego i magnetycznego (a) oraz trajektoria elektronów i powstawanie lawin elektronowych w obszarze katody urządzenia magnetronowego (b), [5]

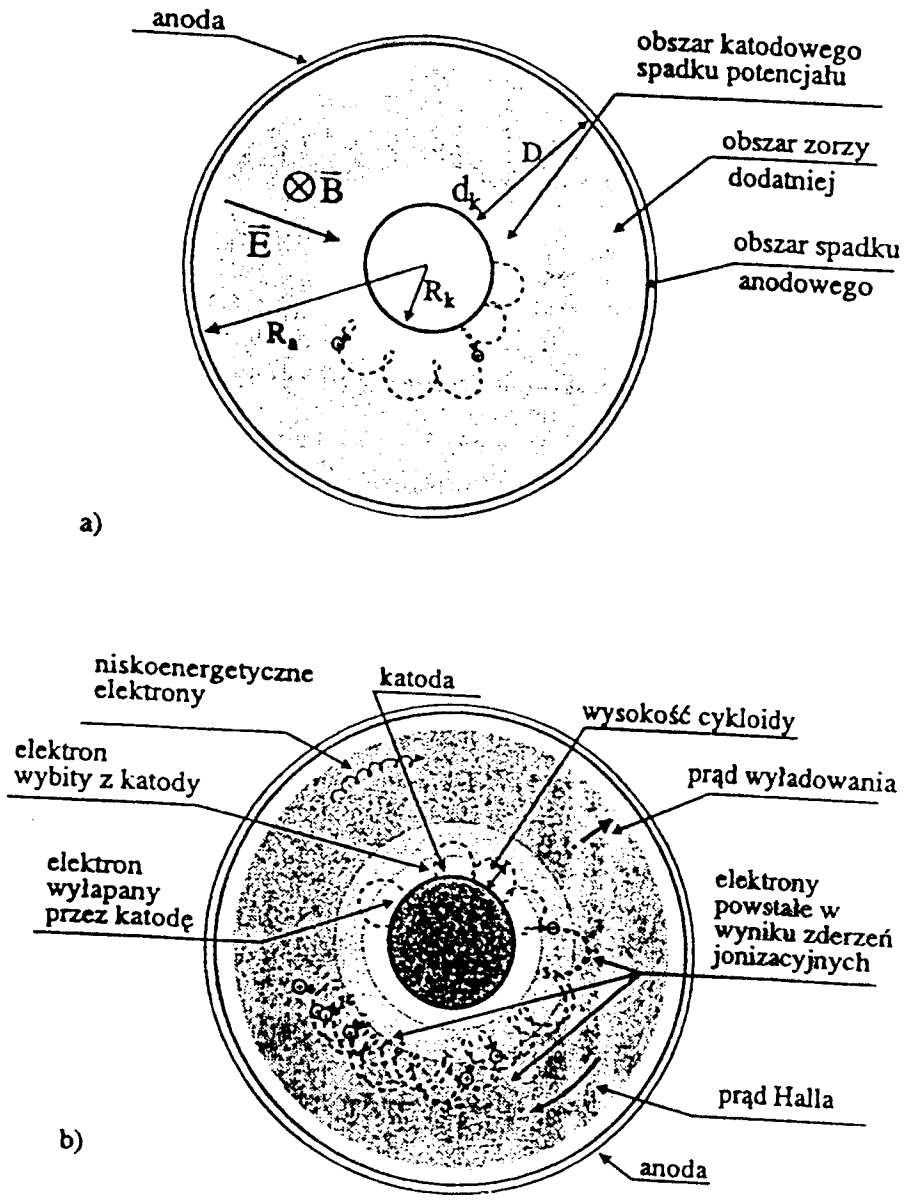

Rys. 26. Obszary wyładowania w układzie magnetronu cylindrycznego (a) oraz charakter ruchu elektronów w obszarze wyładowania wg Thorntona (b). [57]

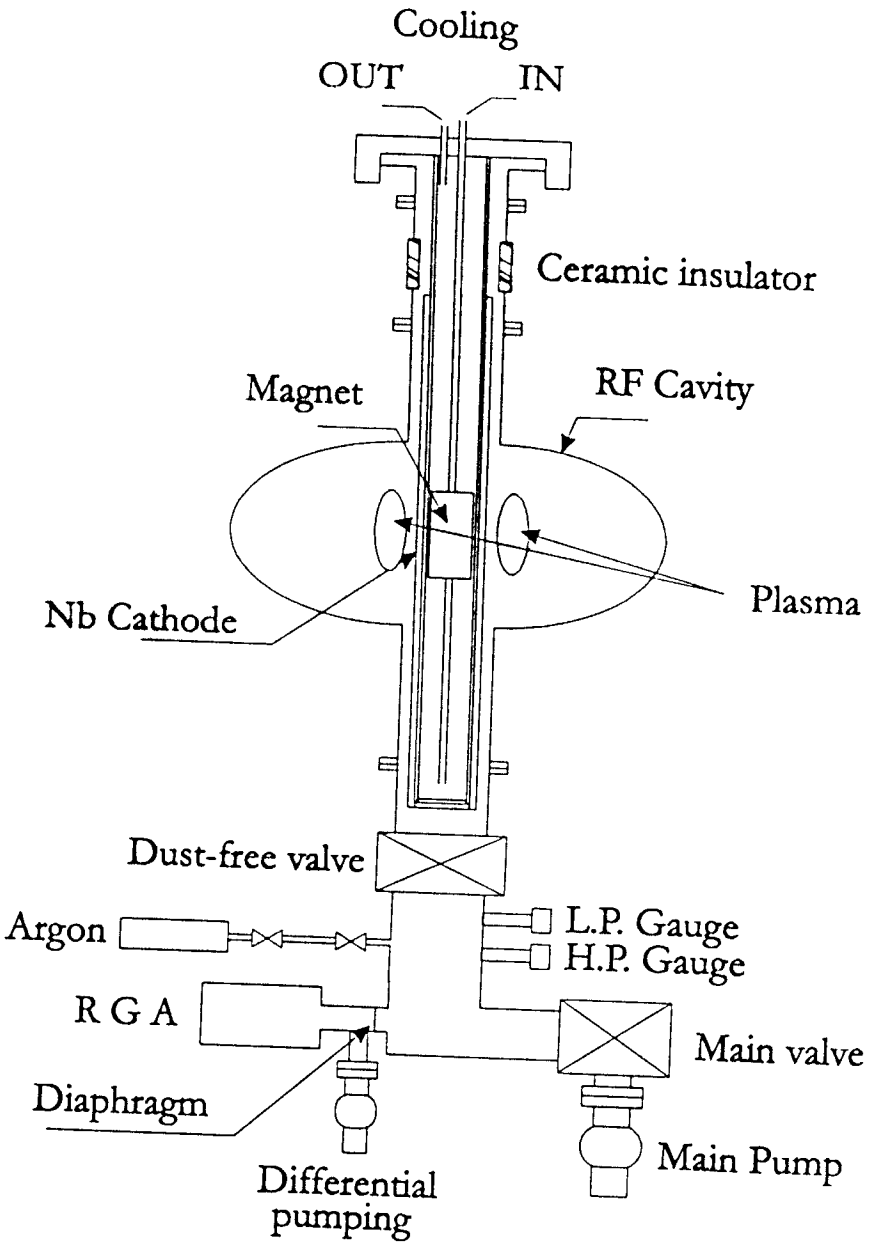
Cooling
OUT
IN
Ceramic insulator
Magnet
RF Cavity
Plasma
Nb Cathode
Dust-free valve
Argon
L.P. Gauge
H.P. Gauge
R G A
Main valve
Diaphragm
Main Pump
Differential
pumping

Fig. 2

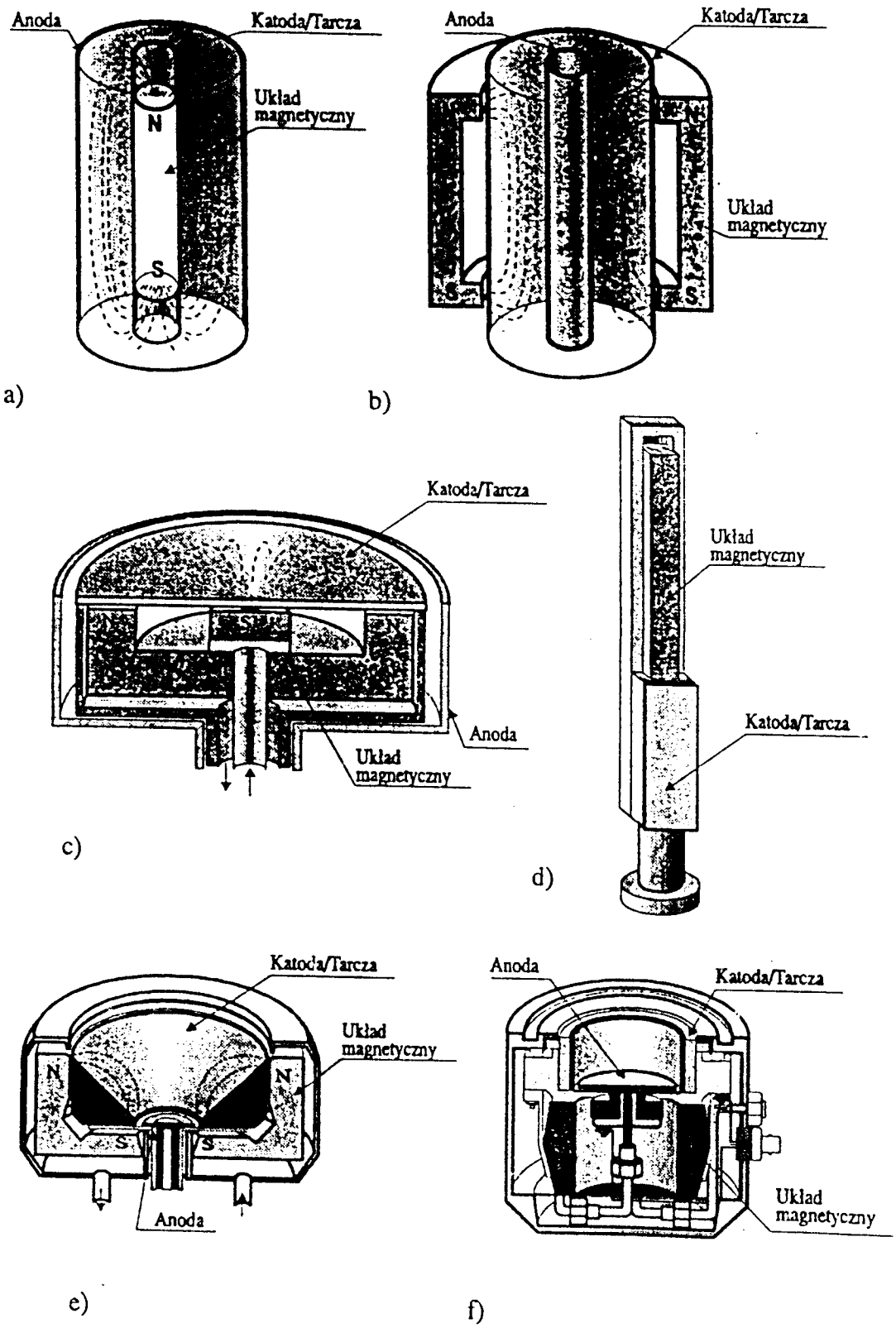

Rys. 3. Główne grupy magnetronowych urządzeń rozpylających: a) cylindryczne prętowe, b) cylindryczne wnękowe, c) płaskie, d) liniowe, e) kątowe, f) działa rozpylające

16

Reactive Sputter Deposition

-sputtering of a metal, alloy or compound in a reactive gas mixture (Ar/N_2, Ar/O_2, $Ar/C_2/H_2$...) in order to deposit a coumpound thin film (TiN, TiC, TiAlN, MoN, NbN,Al_2O_3...).

-chemical reactions;

on the substrate surface
in the gas phase
at the target

-problems with stechiometry (hysteresis effects)
control of plasma parameters (spectrometer, RGA)
-negative ion emision(respattering of substrate)
-arcing (for cylindrical magnetron)

Bias

Unbalanced magnetron

Bias Sputtering

-growing film is ion bombarded during deposition due to negatively biased substrate with respect to anode.

-useally--50V –150V (sputtering yield very low)

-desirable effects;

-re-sputtering of loosely bonded atoms

-increasing of a surface mobility incoming atoms

-desorption of gases (sputtering gas)

-low-energy ion implantation

-in result;

<u>improved film quality</u>

UNBALANSED MAGNETRON

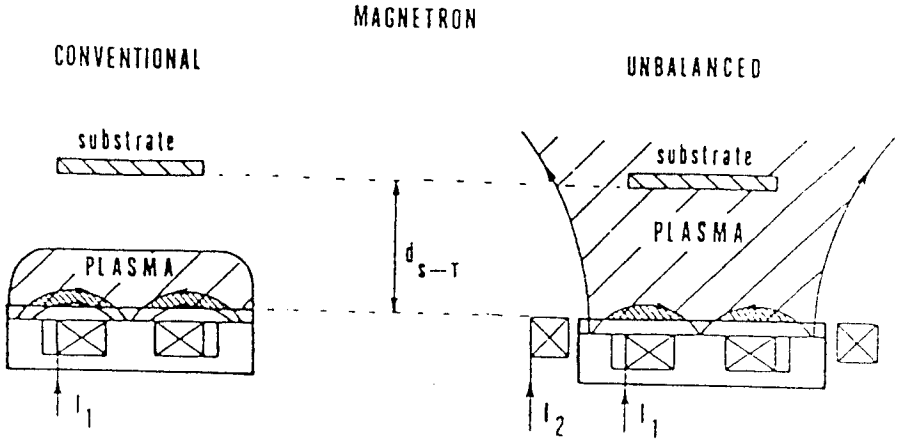

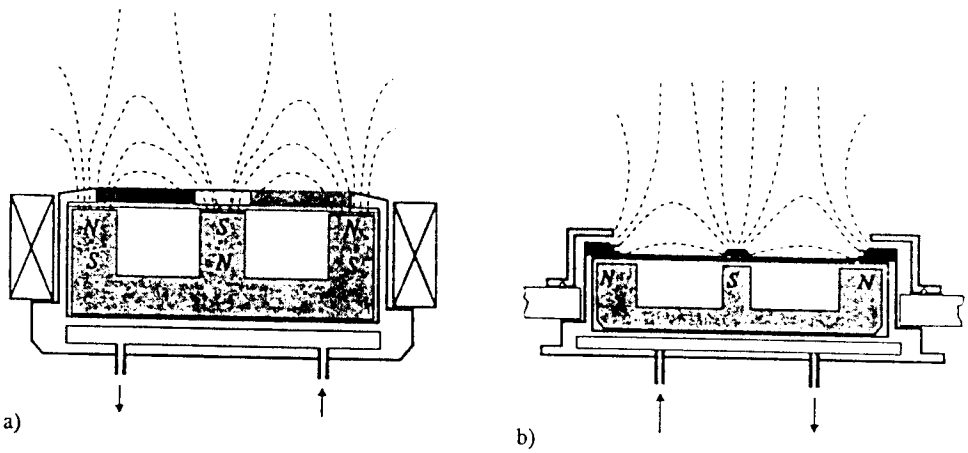

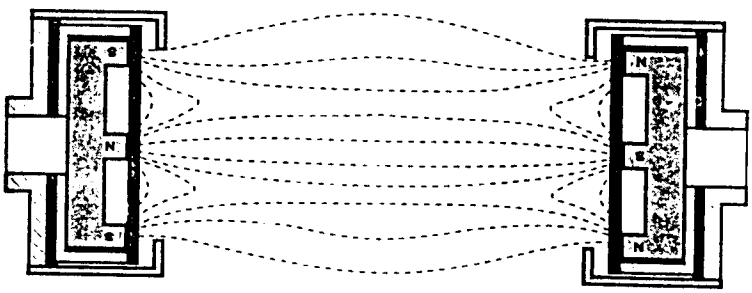

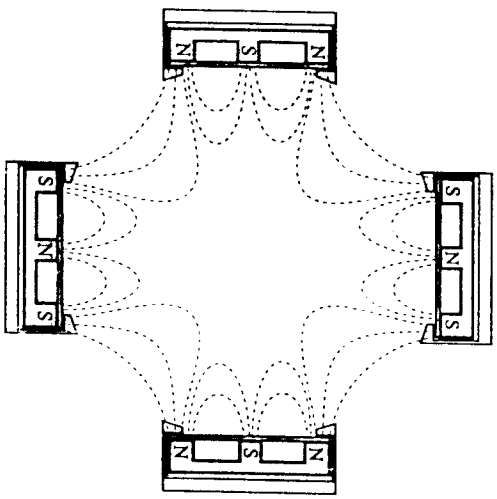

higher degree of ionisation → **improved film properties**

Sustained self-sputtering

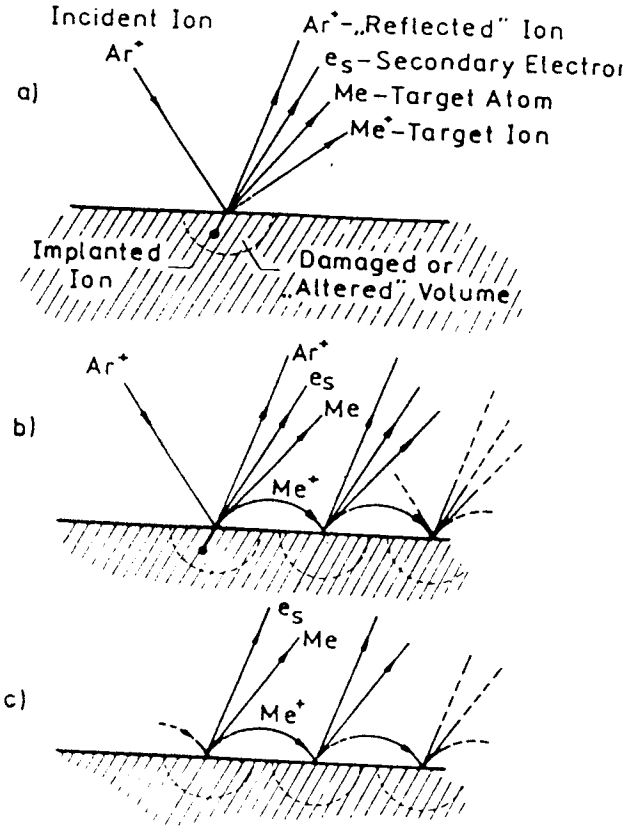

Mode	Ions effectively bombarding target	Gas pressure (argon) (mTorr)
1	Ar^+	≥ 0.5
2	Ar^+, Me^+	0–0.5
3	Me^+	0

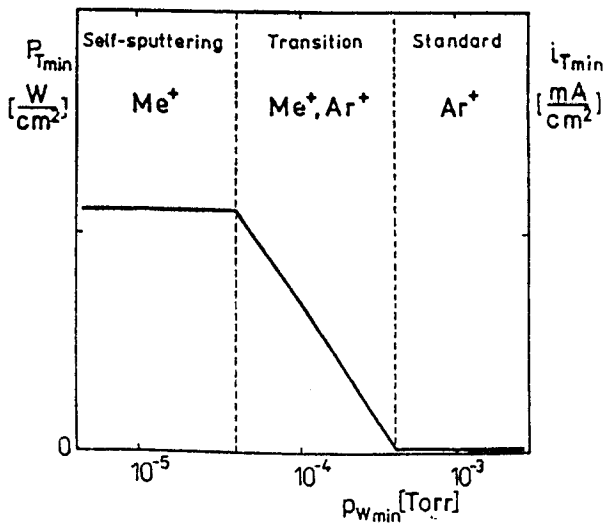

VACUUM ARC

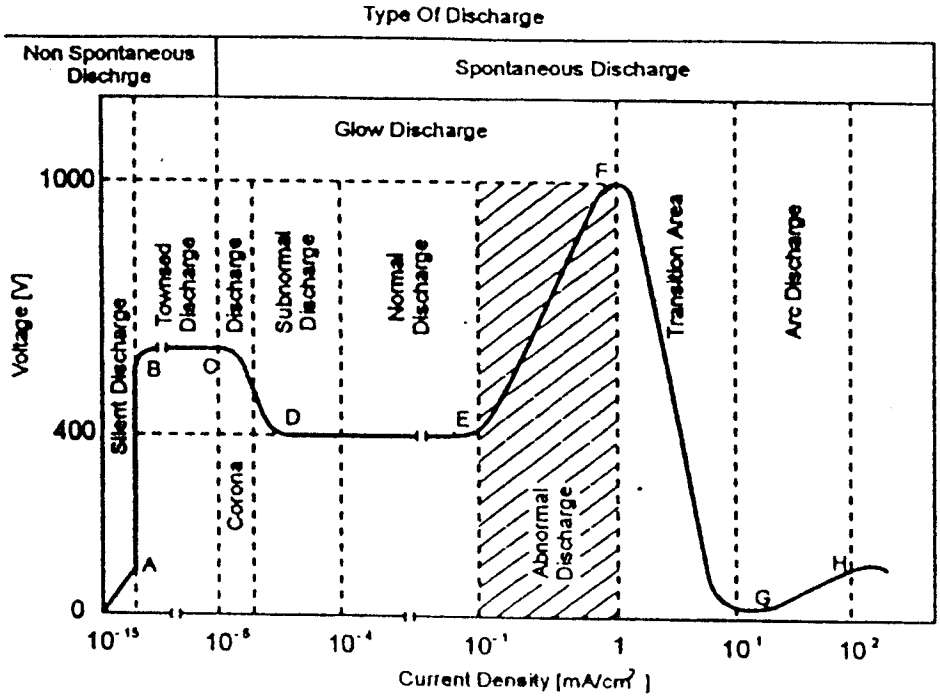
Type Of Discharge
Non Spontaneous Dischrge
Spontaneous Discharge
Glow Discharge
Voltage [V]
1000
400
0
Silent Discharge
Townsed Discharge
Corona
Discharge
Subnormal Discharge
Normal Discharge
Abnormal Discharge
Transition Area
Arc Discharge
A
B
C
D
E
F
G
H
10^{-15}
10^{-8}
10^{-4}
10^{-1}
1
10^{1}
10^{2}
Current Density [mA/cm^2]

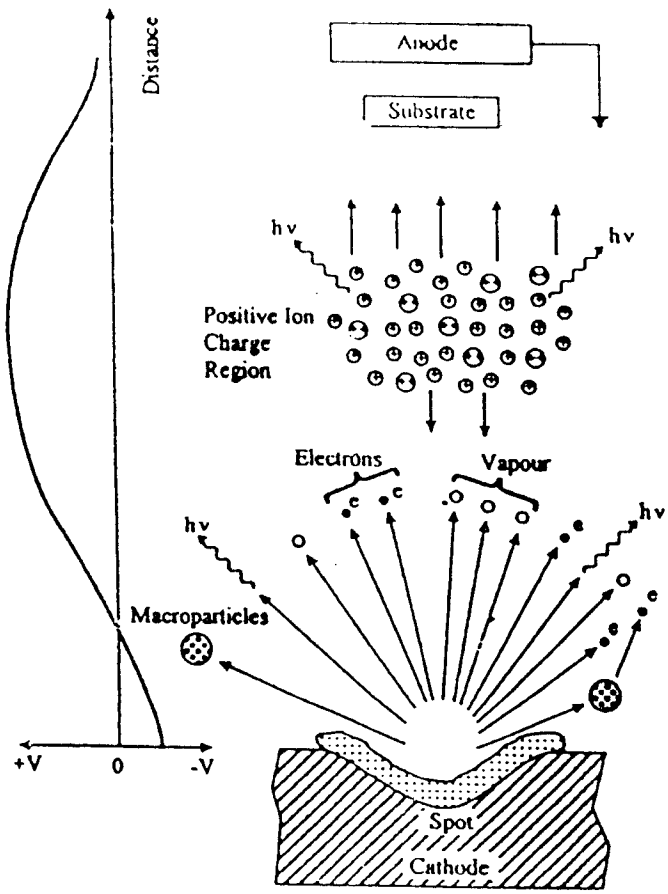
Distance
Anode
Substrate
hv
hv
Positive Ion Charge Region
Electrons
Vapour
hv
hv
Macroparticles
+V
0
-V
Spot
Cathode

VACUUM ARC

Vacuum arc – low-voltage (20-40V), high current discharge (50-200A) in vapour of the cathode material

Arc plasma – energy of ions– 10-100ev
degree of ionization up to 90%
multiply charged ions +2,+3
microdroplets order of μm

Categories of vacuum arcs

<u>discrete cathodic arc</u>
-random
-steared
distributed cathodic arc (hot cathode)
anodic arc (hot anode)

Types of arc devices

planar
<u>linear</u>
arc-ion-gun

Modes of operation

DC
AC (pulsed)

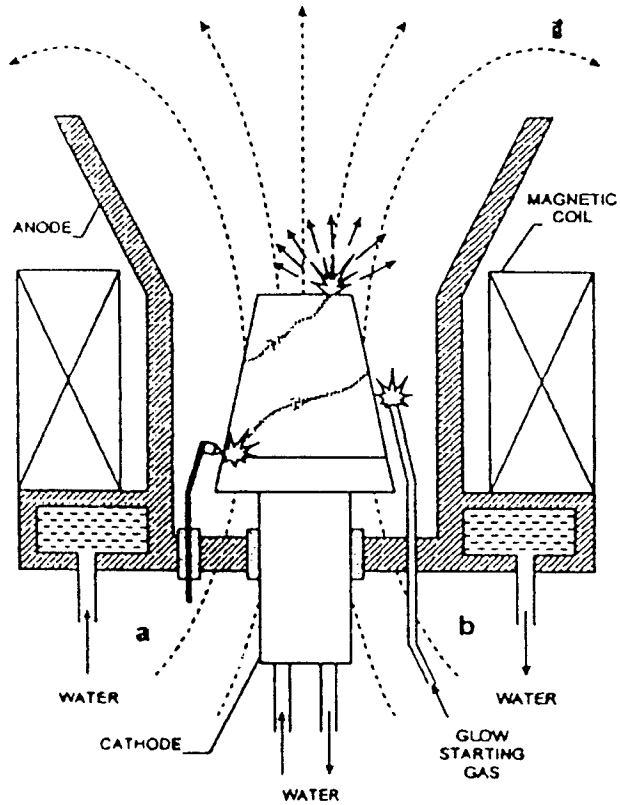
ANODE
MAGNETIC COIL
a
b
WATER
WATER
CATHODE
GLOW STARTING GAS
WATER

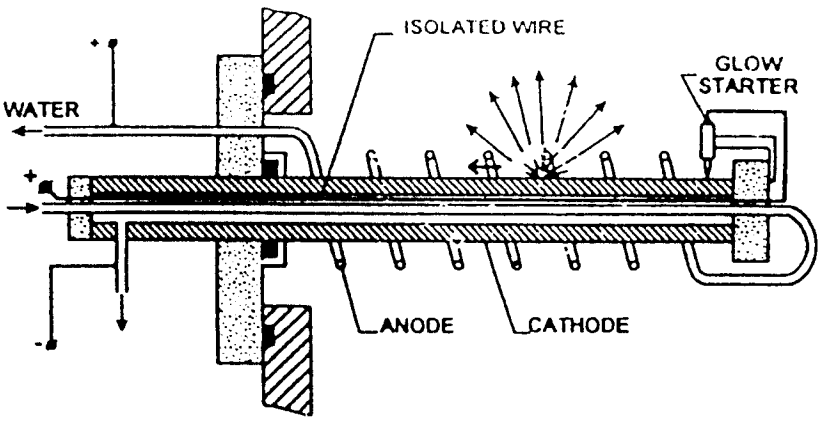
ISOLATED WIRE
GLOW STARTER
WATER
+
-
ANODE
CATHODE

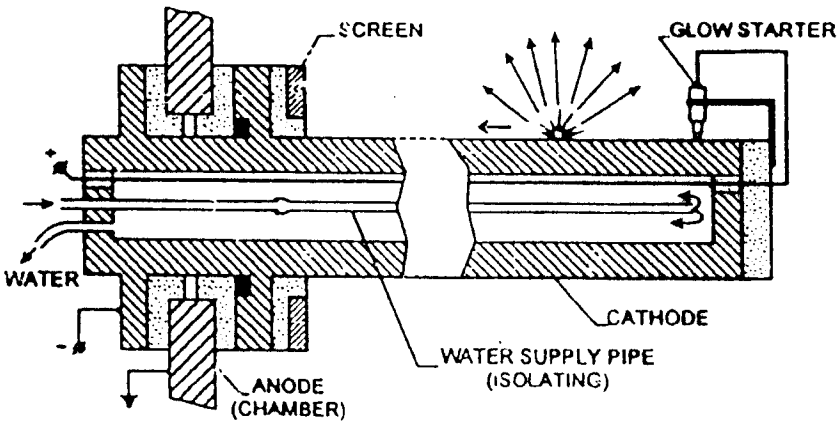
SCREEN
GLOW STARTER
+
WATER
-
CATHODE
WATER SUPPLY PIPE (ISOLATING)
ANODE (CHAMBER)

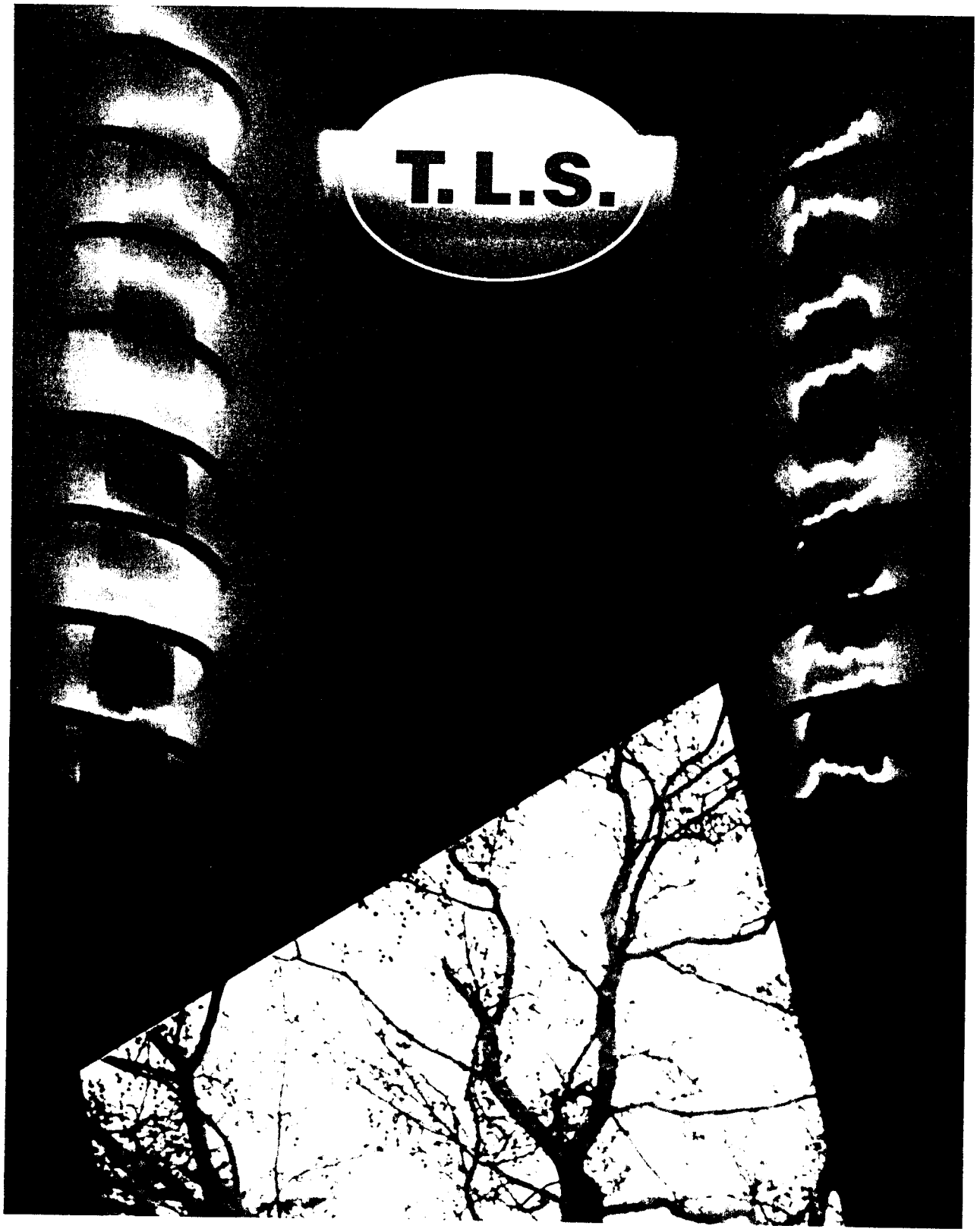
T.L.S.

Film Quality

-film purity
-film structure (microstructure)
    -density
    -grain size
    -porosity
-surface morfology (roughness.)
-adhesion
-stress

-can be modified by:

    -vacuum condition
    -deposition temperature
    -gas pressure
    -atom (ion) flux
    -ion energy
    -ion/atom arrival ratio
    -angle of incidence
    -surface preparation

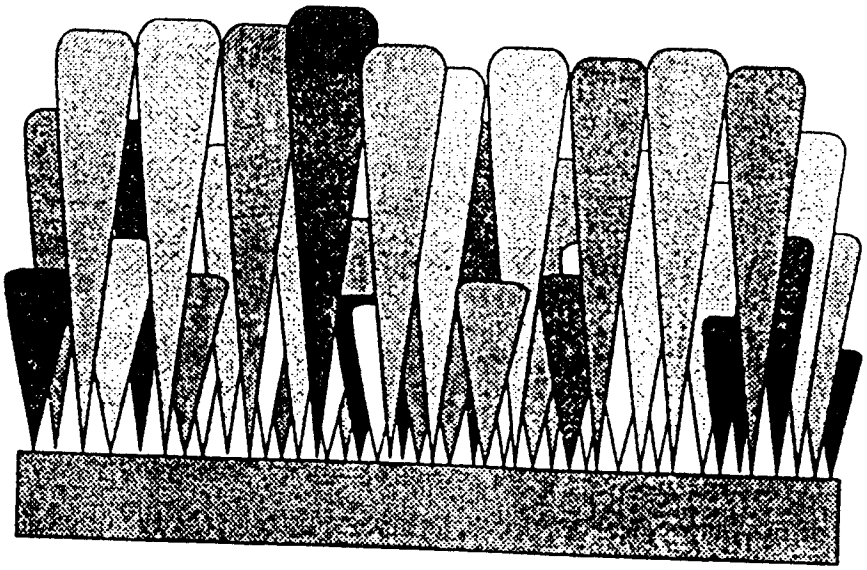

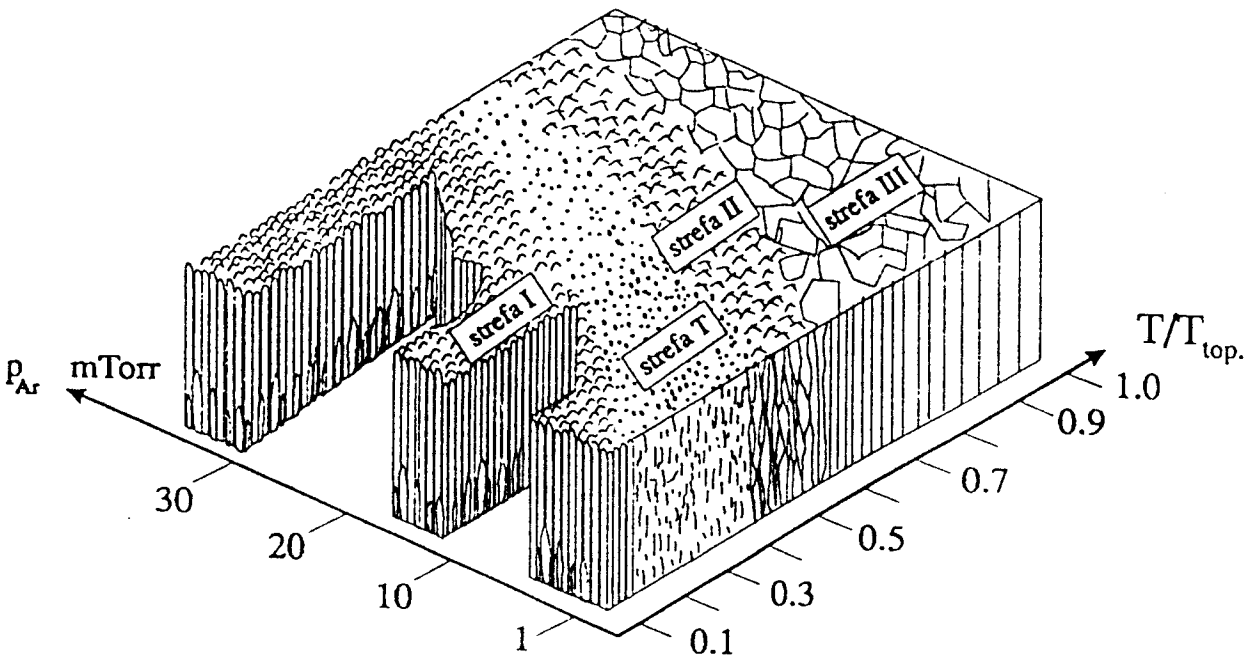
strefa I
strefa II
strefa III
strefa T
p_{Ar} mTorr
30
20
10
1
$T/T_{top.}$
1.0
0.9
0.7
0.5
0.3
0.1

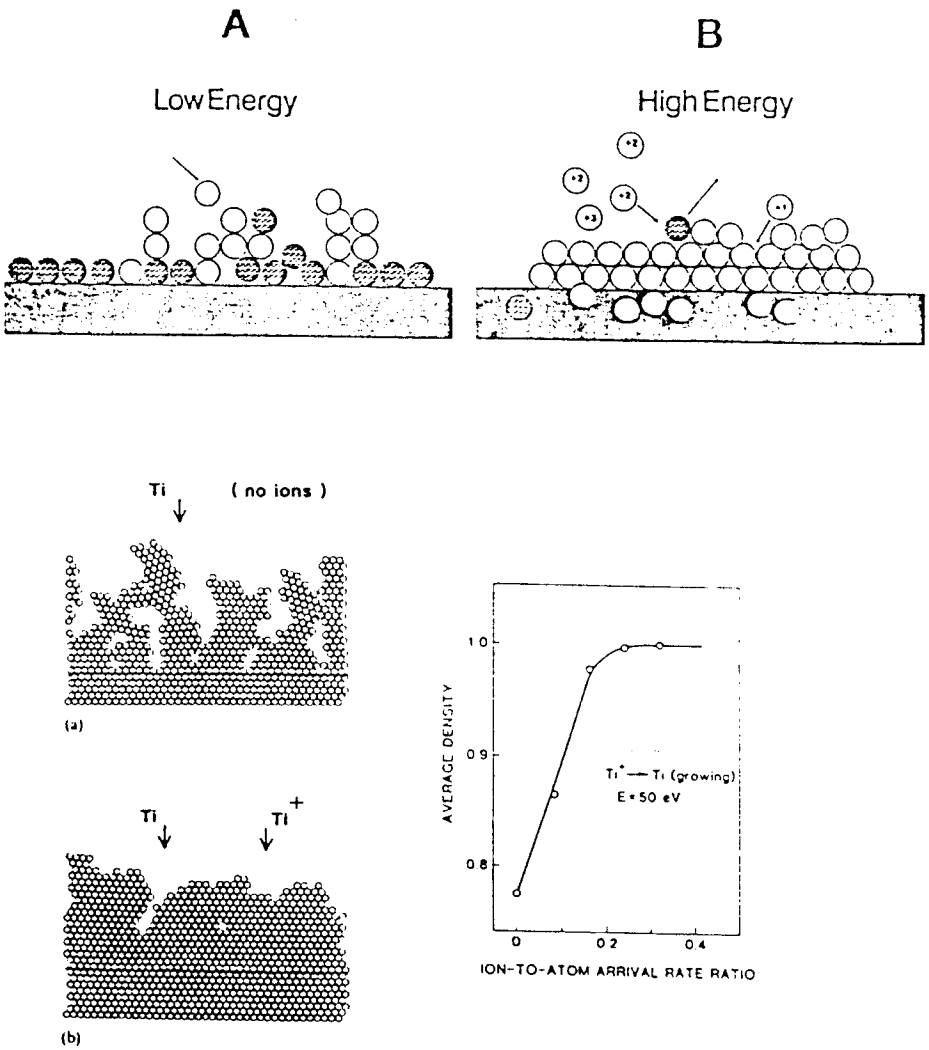

Figure 10: Results of a molecular dynamic modeling calculation carried out by P.J. Martin, et.al., in Ref. 10. Used with permission.

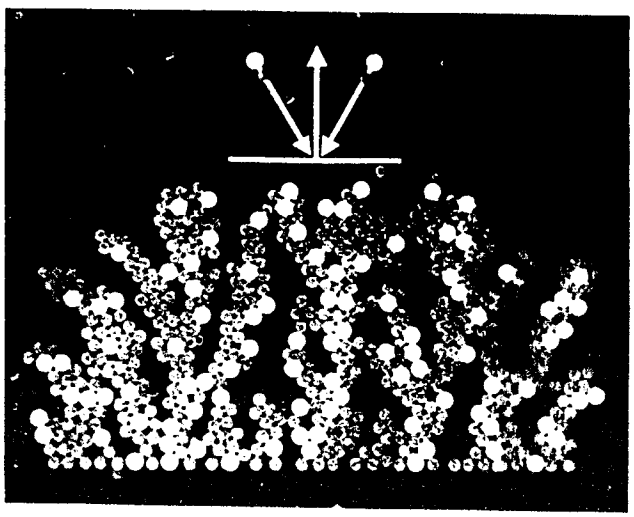

Sp

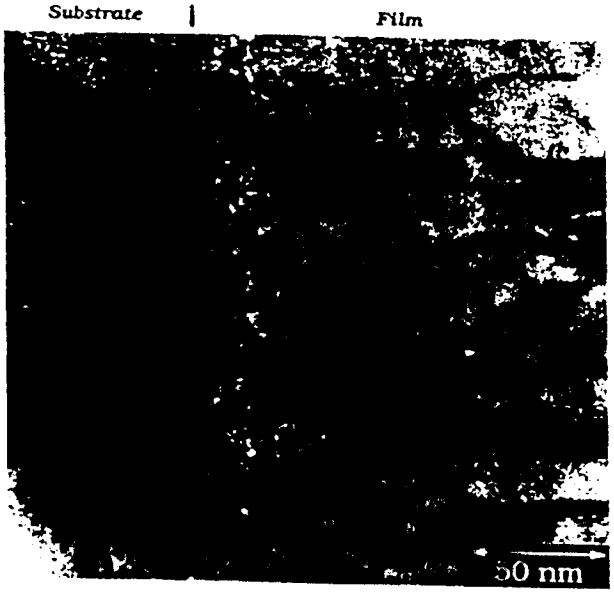
Substrate
Film
50 nm

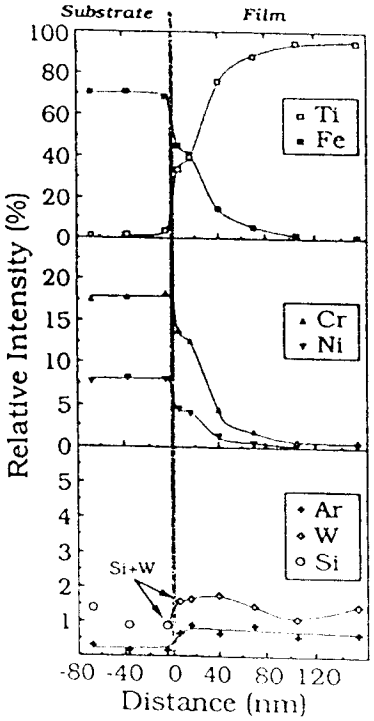
Substrate
Film
Ti
Fe
Cr
Ni
Ar
W
Si
Si+W
Relative Intensity (%)
Distance (nm)

St-Arc


Substrate
Recryst.
Film
50 nm

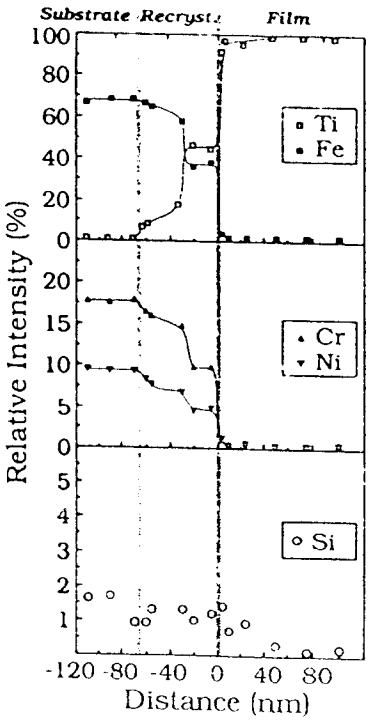
Substrate
Recryst.
Film
Ti
Fe
Cr
Ni
Si
Relative Intensity (%)
Distance (nm)

Fig. 5. Columnar growth of $Ti_{0.5}Al_{0.5}N$ coating with fissures and pores at $U_B = 0$ V (transmission electron micrograph, University of Linköping, Sweden).

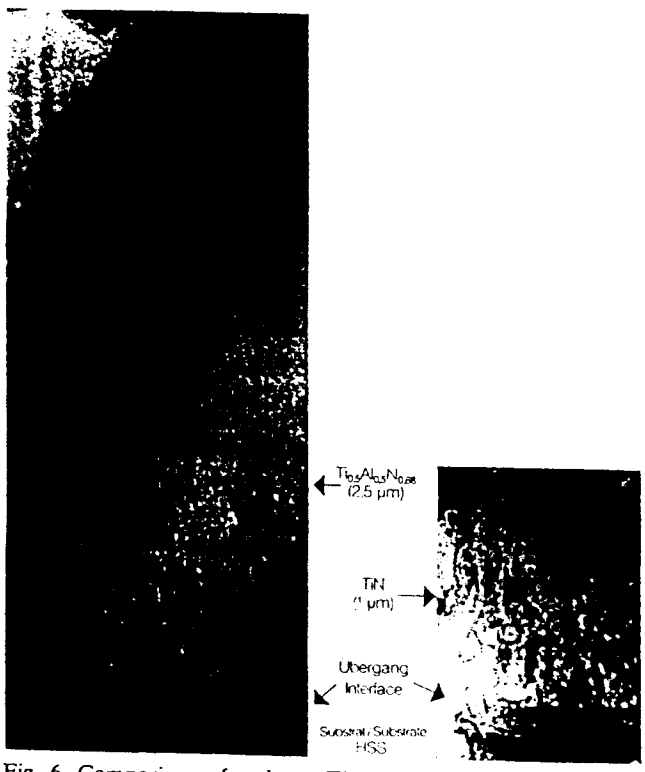

Fig. 6. Comparison of a dense $Ti_{0.5}Al_{0.5}N$ coating and a dense TiN coating. (TiAl)N: $U_B = -100$ V (2.5 μm); TiN: $U_B = -50$ V (1 μm) (transmission electron micrograph, University of Linköping, Sweden).

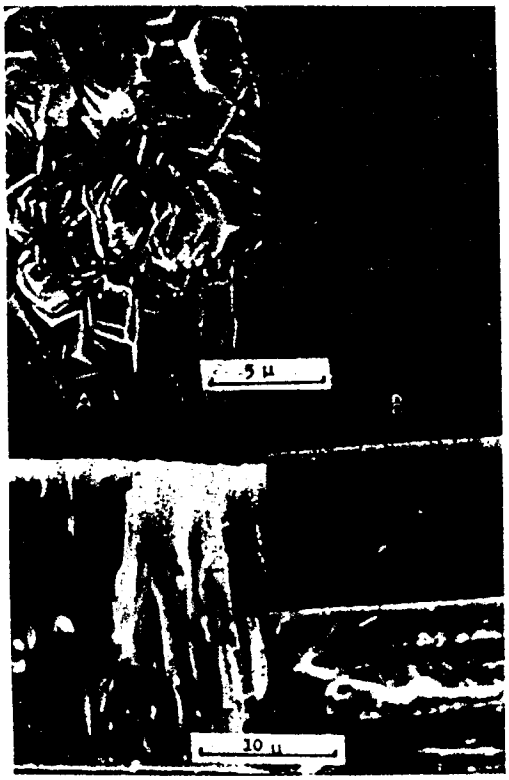
5 μ
10 μ

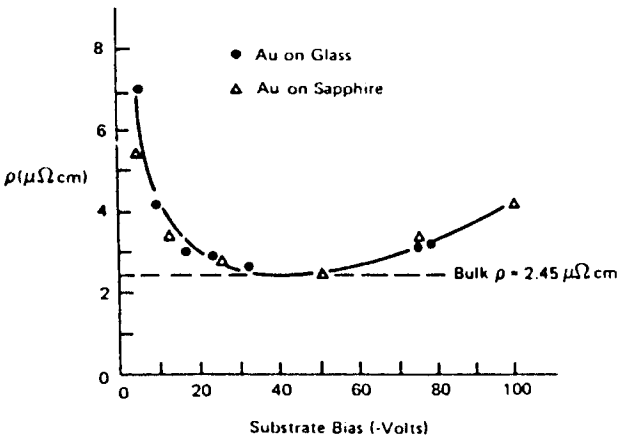
Au on Glass
Au on Sapphire
ρ(μΩcm)
Bulk ρ = 2.45 μΩcm
Substrate Bias (-Volts)
0
2
4
6
8
0
20
40
60
80
100

CONCLUSIONS

Is the simple, cylindrical magnetron sputtering the best method for cavity coating?

-low N_i/N_o
-not too high energies
-geometry

Is it possible to improve such deposition method?

-bias sputtering
-unbalanced magnetron
-sustained self-sputtering
-spherical magnetron

May be arc plasma deposition?

Exotic Superconducting Materials and Related Deposition Technologies for Coated Superconducting Cavities

E. Palmieri

S.c. properties of a material in terms of three fundamental (rather easely measurable) quantities

$T_c \longleftrightarrow \Delta$ $\qquad \Delta = \frac{5}{2} K \underline{T_c}$

$\gamma \longleftrightarrow N(E_F)$ $\qquad \gamma = \frac{2}{3} \pi^2 K^2 \underline{N(E_F)}$

$\rho_0 \longleftrightarrow l_0$ $\qquad \rho_0 = \dfrac{1}{\frac{2}{3} l^2 \underline{N(E_F)} v_F \underline{l}}$

if $\quad l_0 \ll \xi_0 \;, \; T < T_c/2 \;, \; \nu \ll \Delta/h$

$H_{c1} = 1.90 \times 10^2 (T_c/\rho_0) \ln(.90 \times 10^{-2} \gamma^{\frac{1}{2}} \rho_0)$

$H_c = 2.43 \, \gamma^{\frac{1}{2}} T_c$

$H_{sh} = .75 \, H_c$

$H_{c2} \propto \gamma \rho_0 T_c$

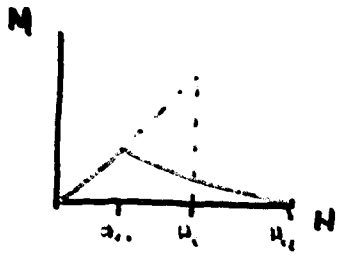

ρ_0 - $\mu\Omega \cdot cm$
γ - $erg \, cm^{-3} K^{-2}$
H - Oe

$\lambda_L [Å] = 1050 \left[\rho_0/T_c\right]^{\frac{1}{2}}$

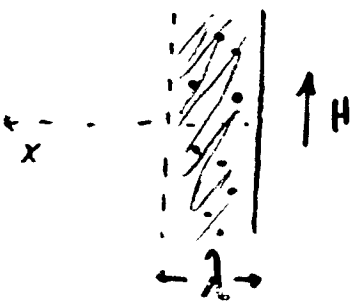

$R_s \propto \lambda \cdot \frac{m_n}{m}$

$R_s \propto \rho_0^{\frac{1}{2}} e^{-\frac{3}{2}\frac{T_c}{T}}$

The s.c material needs to be a [illegible]

According the classical theory for normal metals in the normal skin effect

$$Z_s = R_s + i X_s = (1-i) \cdot \left[\frac{\mu \omega}{2\sigma_n}\right]^{\frac{1}{2}}$$

Mattis - Bardeen $\qquad \sigma_n \longrightarrow \sigma_1 - i\sigma_2$

$$\sigma_1/\sigma_n = 2/\hbar\omega \int_{\Delta}^{\infty} \left[f(E) - f(E+\hbar\omega)\right] g^{+}(E)\, dE$$

$$\sigma_2/\sigma_n = 1/\hbar\omega \int_{\Delta-\hbar\omega}^{\Delta} \left[1 - 2f(E+\hbar\omega)\right] g^{+}(E)\, dE$$

$$f(E) = 1/(1+e^{E/kT}) \; ; \qquad g^{+}(E) = \frac{E^2 + \Delta^2 + \hbar\omega E}{[(E^2-\Delta^2)]^{\frac{1}{2}} \cdot [(E+\hbar\omega)^2 - \Delta^2]^{\frac{1}{2}}}$$

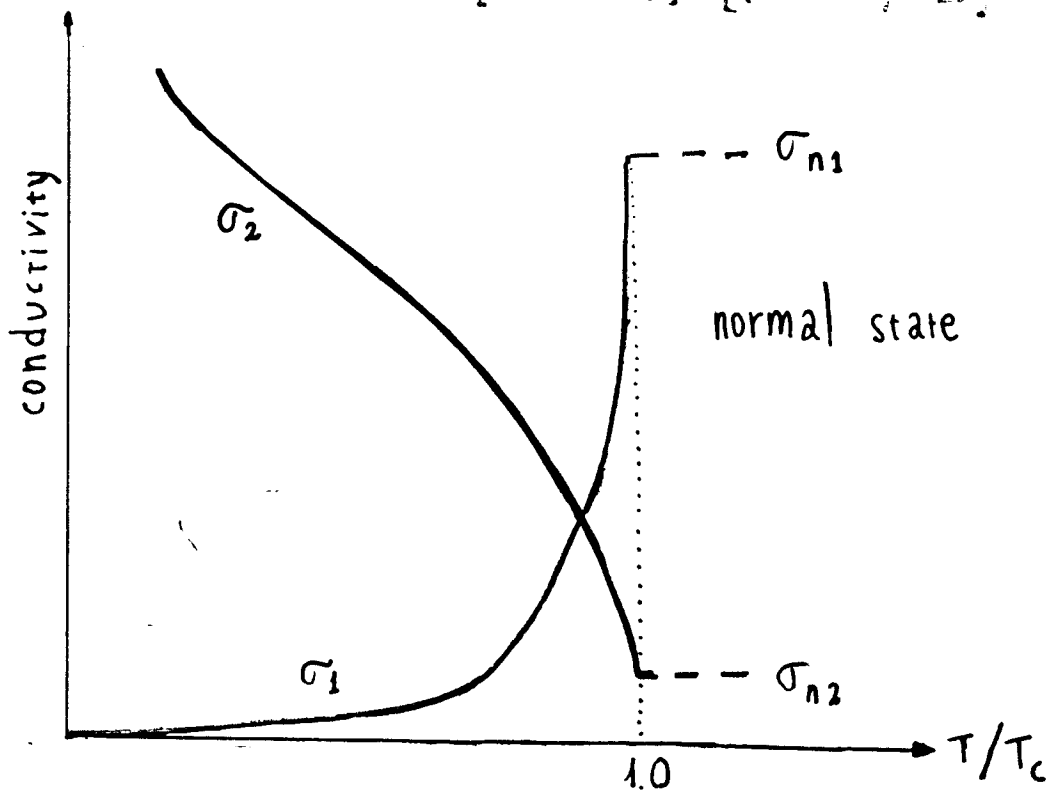

$$R_{BCS} = \frac{R_N}{\sqrt{2}} \frac{\sigma_1/\sigma_n}{(\sigma_2/\sigma_n)^{3/2}}$$

$\hbar\omega \ll \Delta$

$T < T_c/2$

London dirty limit

$$R_{BCS} \propto (\rho_n)^{\frac{1}{2}} \, \omega^{2-\alpha} \, \frac{e^{-\frac{s}{2}\frac{T_c}{T}}}{T\, T_c}$$

$$R_{BCS} = \frac{R_n}{\sqrt{2}} \cdot \frac{\sigma_1/\sigma_n}{(\sigma_2/\sigma_n)^{3/2}}$$

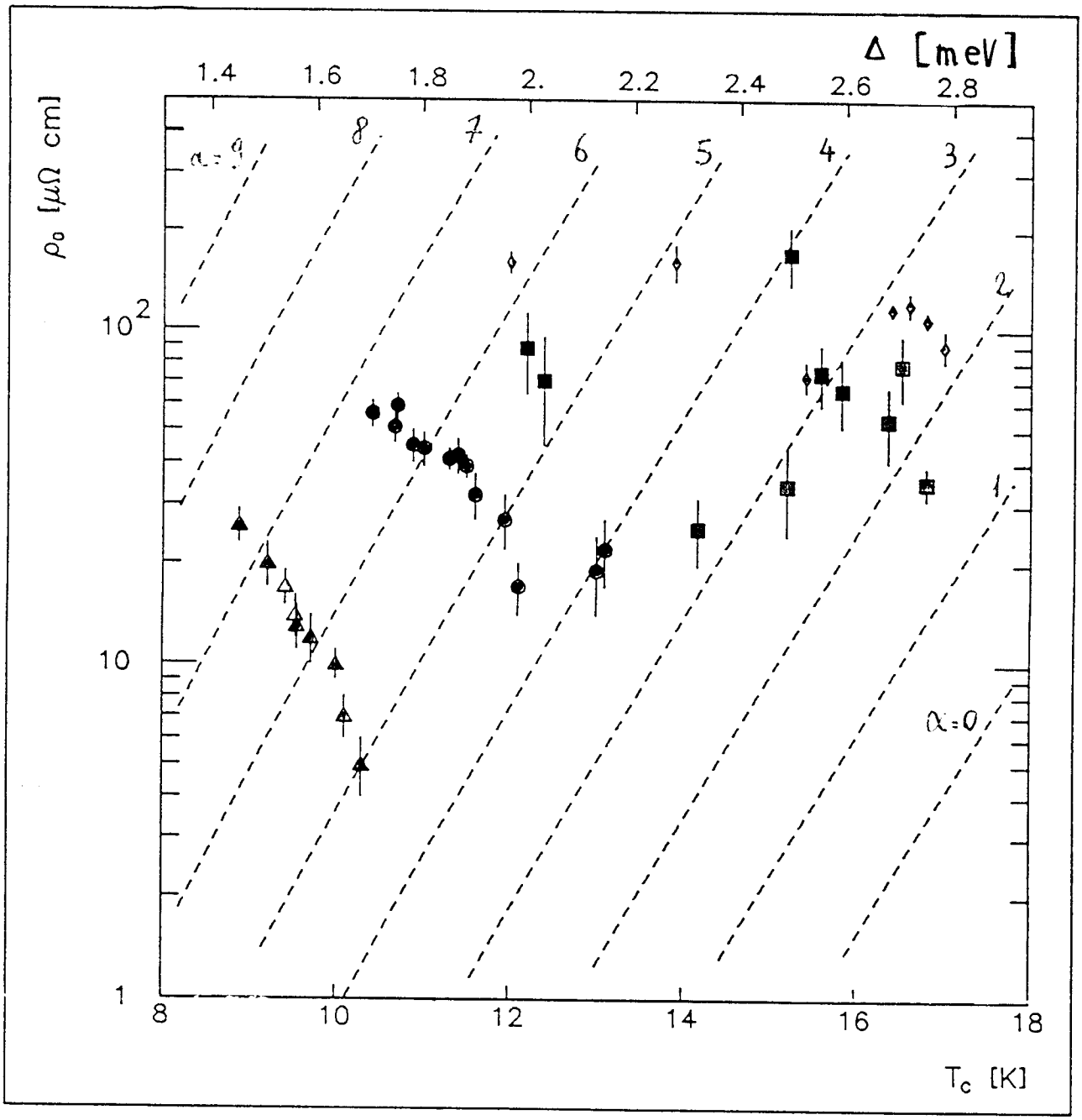

Strong Coupling factor = 3.8

ν = 500 MHz

T = 4.2 K

■ NbTiN c.s
■ NbTiN b.s
◇ NbN
▲ $Mo_{75}Re_{25}$
● $Mo_{60}Re_{40}$

$$R_{BCS} = 2^{\alpha}\ m\Omega$$

Matthias empirical rule

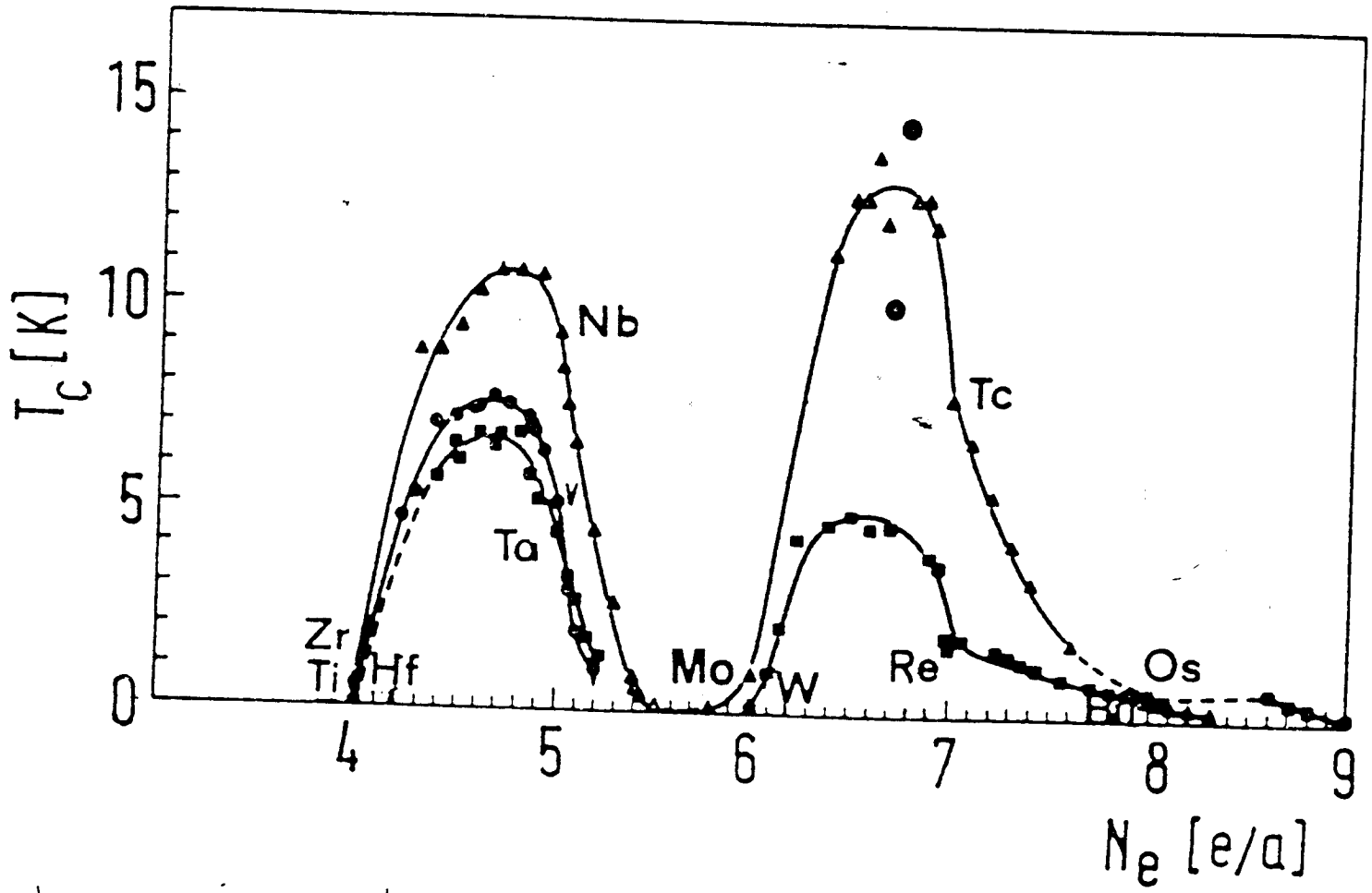

it works only for neighbourhood elements in per. t.

H																	He
Li	Be											B	C	N	O	F	Ne
Na	Mg											Al	Si	P	S	Cl	Ar
K	Ca	Sc	Ti	V	Cr	Mn	Fe	Co	Ni	Cu	Zn	Ga	Ge	As	Se	Br	Kr
Rb	Sr	Y	Zr	Nb	Mo	Tc	Ru	Rh	Pd	Ag	Cd	In	Sn	Sb	Te	I	Xe
Cs	Ba	Lu	Hf	Ta	W	Re	Os	Ir	Pt	Au	Hg	Tl	Pb	Bi	Po	At	Rn
Fr	Ra	Ac	Th	Pa	U	Np	Pu	Am	Cm	Bk	Cf	Es	Fm	Md	(No)	(Lr)	(Ku)

La	Ce	Pr	Nd	Pm	Sm	Eu	Gd	Tb	Dy	Ho	Er	Tm	Yb

Superconducting elements

Superconducting elements under pressure

Superconducting elements in thin films

Superconducting elements after irradiation

3d in 4d $T_c \downarrow$

5d in 4d $T_c \sim$

IV in V $T_c \downarrow$

$$\gamma = \frac{\pi^2}{3} k^2 N(E_F)$$

$$T_c = 1.14\, \vartheta_D \exp\left(-\frac{1}{N(E_F)V - \mu^*}\right)$$

$N(E_F) \nearrow$, $T_c \uparrow$

Nb spectrum $N(E)$ ~ to the one of other T.M.

$$E_F \propto (n_{e/a})^{3/2}$$

Different $n_{e/a}$ ⟹ shift E_F

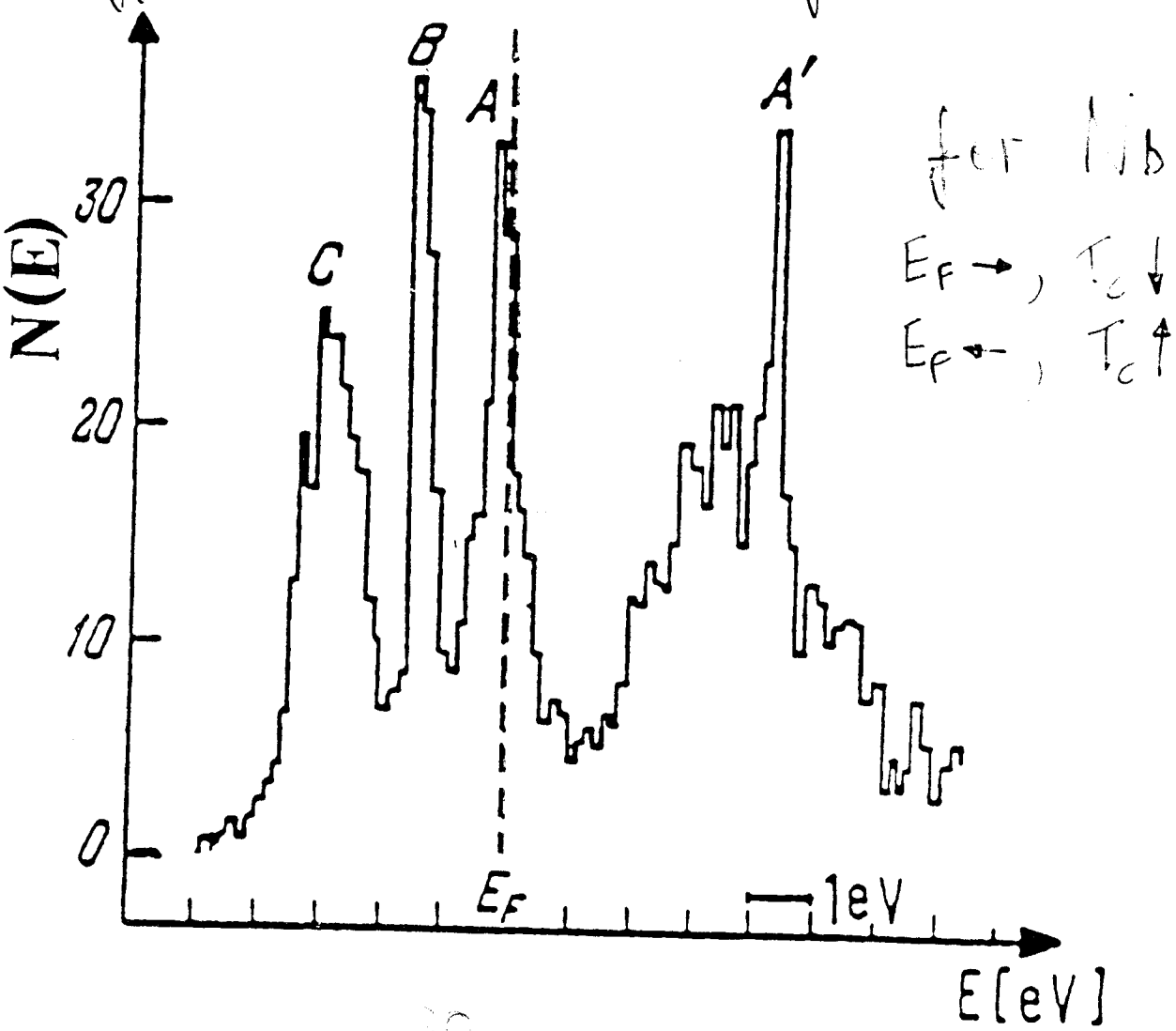

for Nb

$E_F \rightarrow$, $T_c \downarrow$

$E_F \leftarrow$, $T_c \uparrow$

for solid solutions AB

$$E_F^{3/2} = n_{e/a}(AB) = C_A\, n_{e/a}(A) + C_B\, n_{e/a}(B)$$

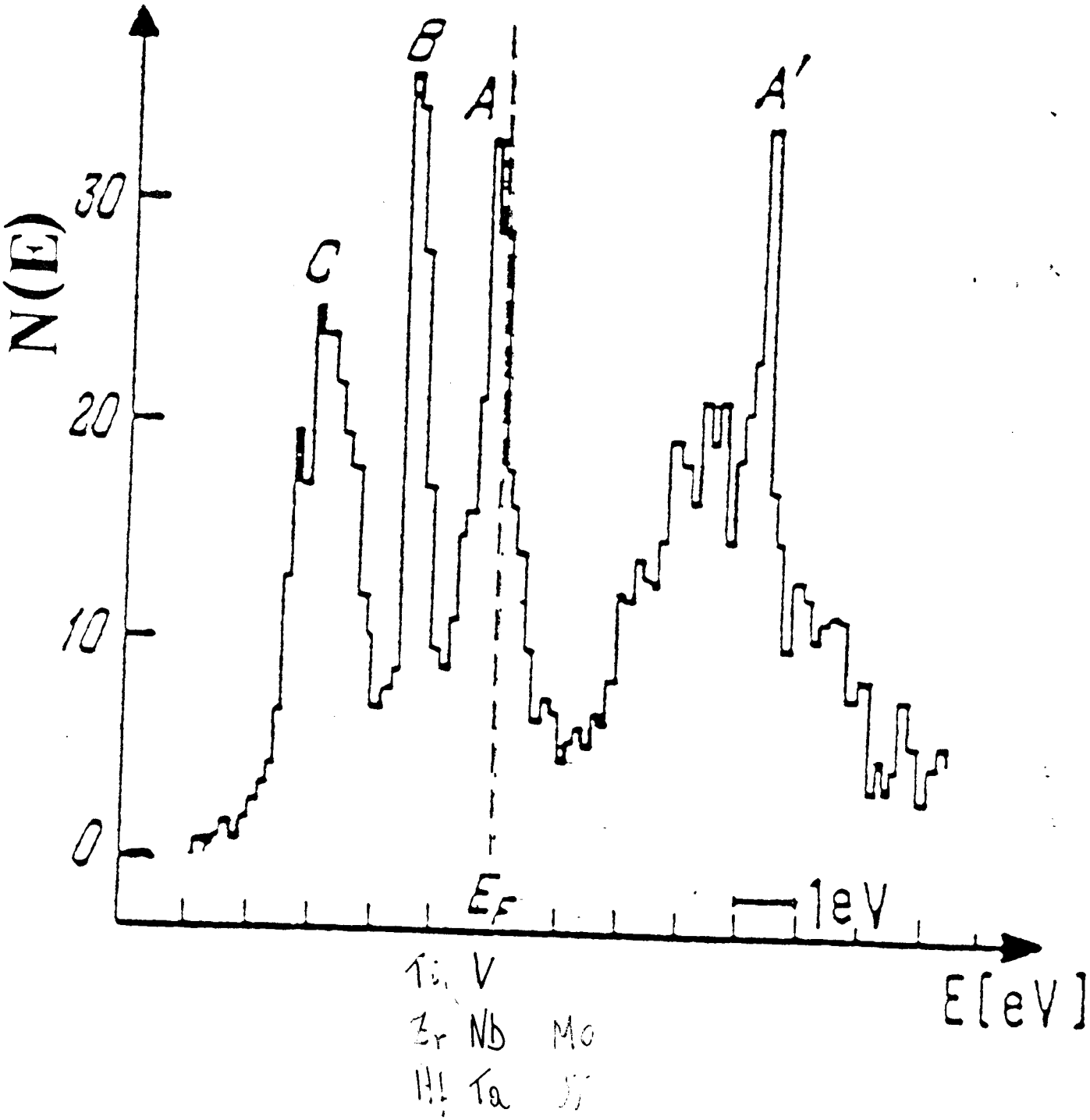

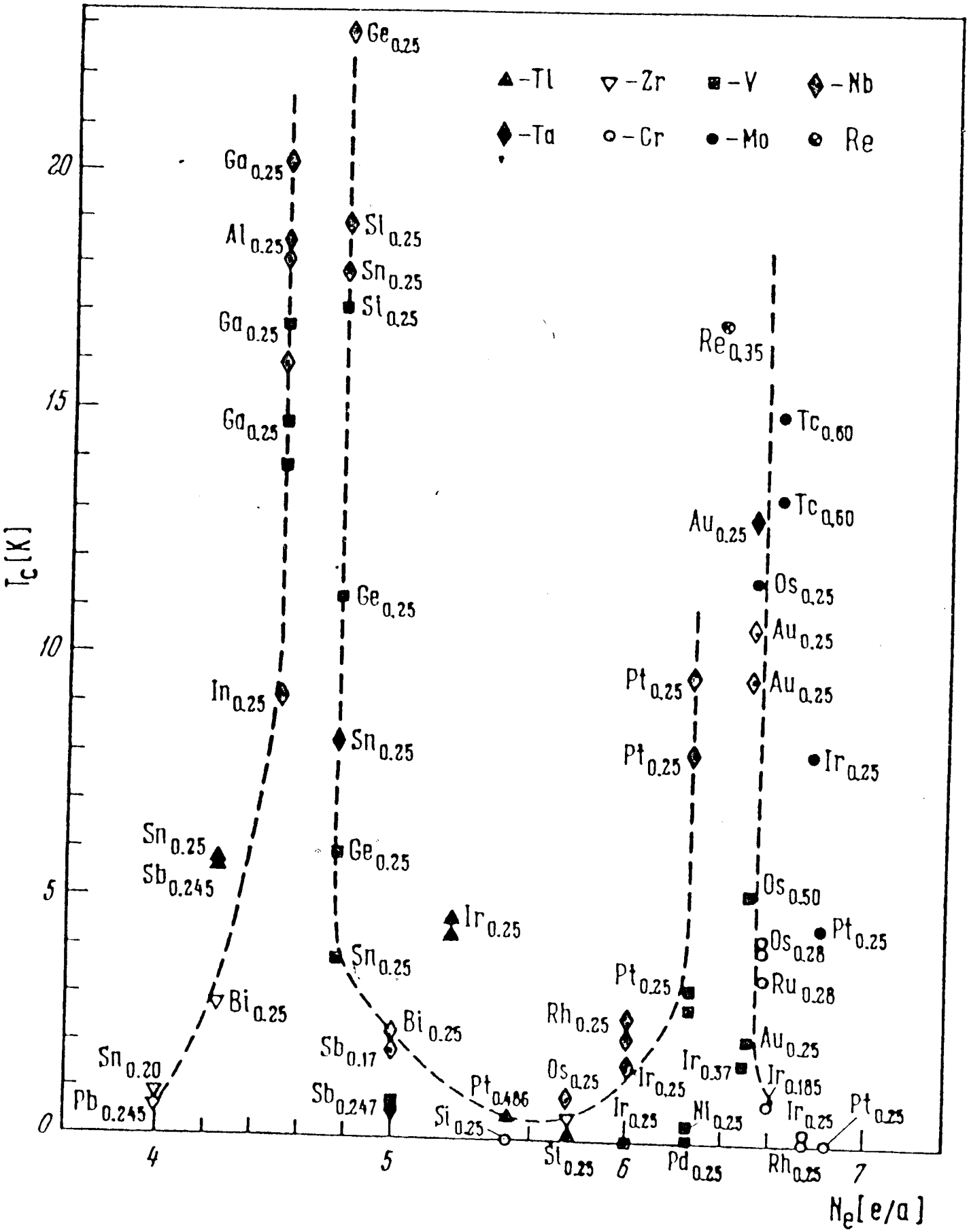

$$\xi = \frac{\hbar v_F}{K T_c}$$

$T_c \uparrow$, $\xi \downarrow$ big fluctuations

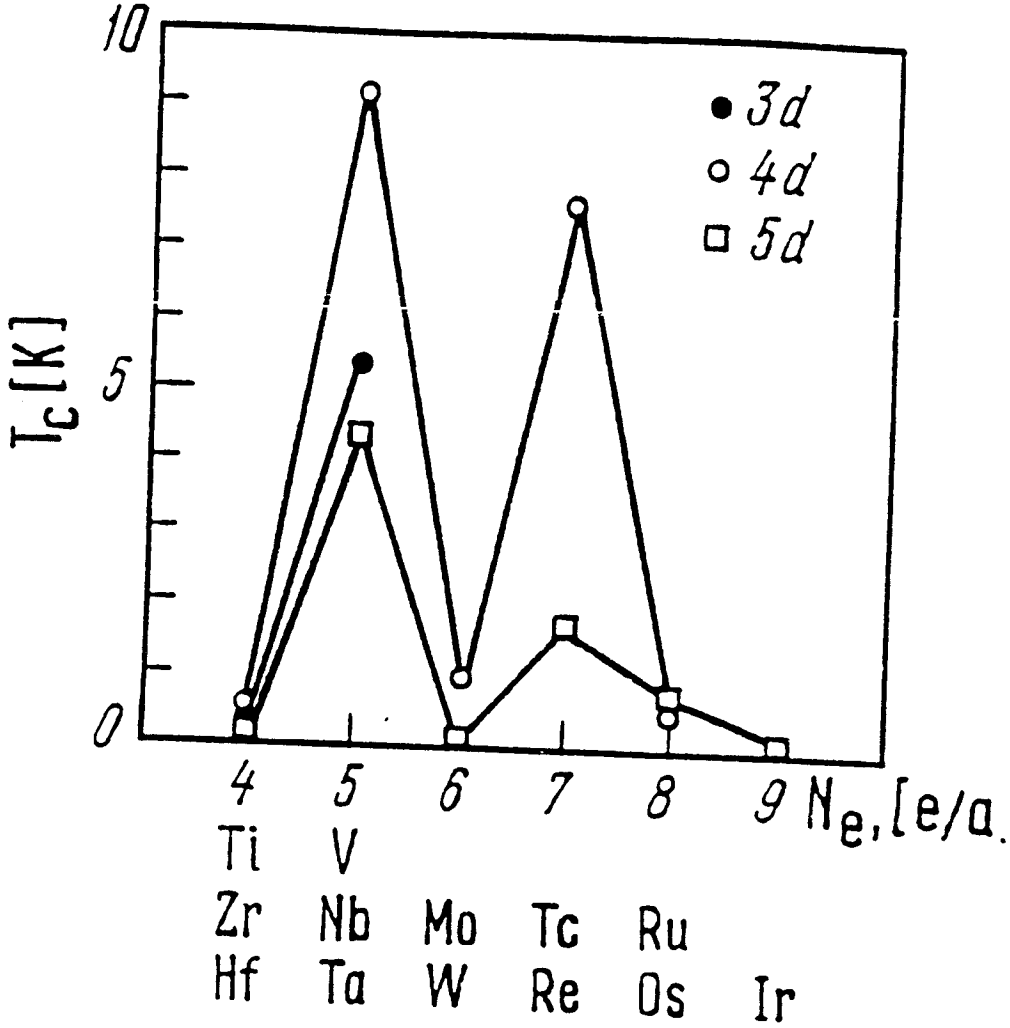
10
5
0
T_c [K]
3d
4d
5d
4 5 6 7 8 9 N_e, [e/a]
Ti V
Zr Nb Mo Tc Ru
Hf Ta W Re Os Ir

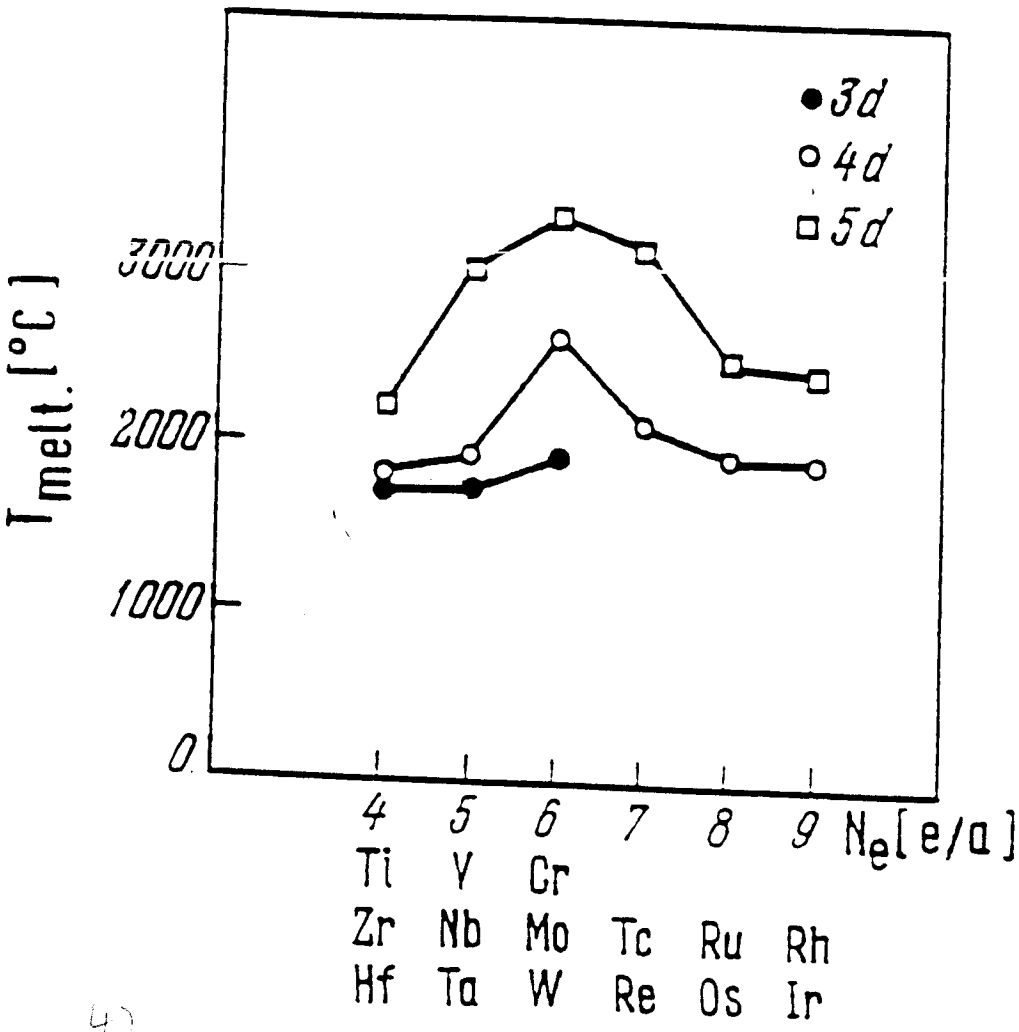
3000
2000
1000
0
$T_{melt.}$ [°C]
3d
4d
5d
4 5 6 7 8 9 N_e [e/a]
Ti V Cr
Zr Nb Mo Tc Ru Rh
Hf Ta W Re Os Ir

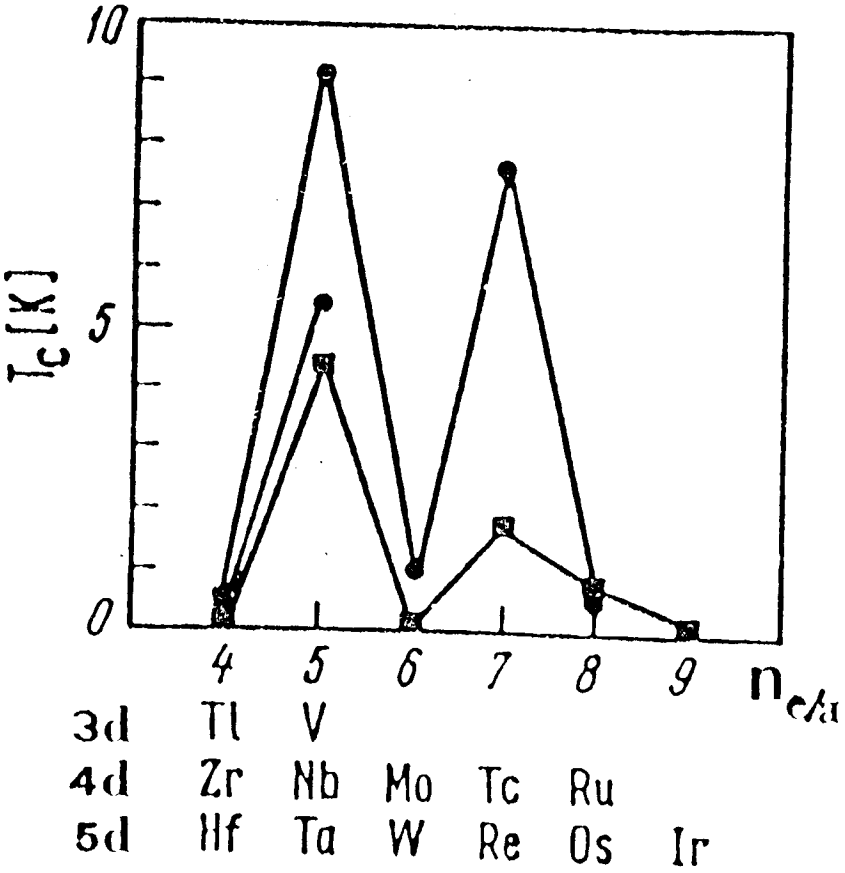
10
5
0
T_c [K]
4 5 6 7 8 9
$n_{e/a}$
3d Ti V
4d Zr Nb Mo Tc Ru
5d Hf Ta W Re Os Ir

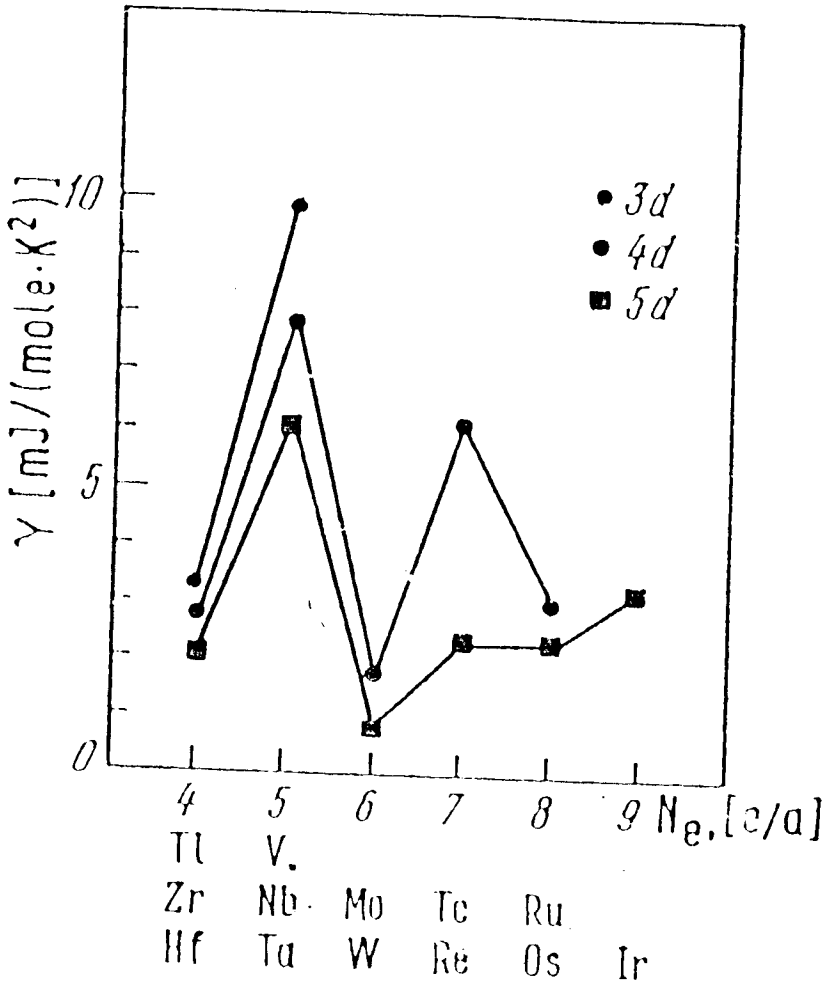
10
5
0
γ [mJ/(mole·K²)]
3d
4d
5d
4 5 6 7 8 9 N_e, [e/a]
Ti V
Zr Nb Mo Tc Ru
Hf Ta W Re Os Ir

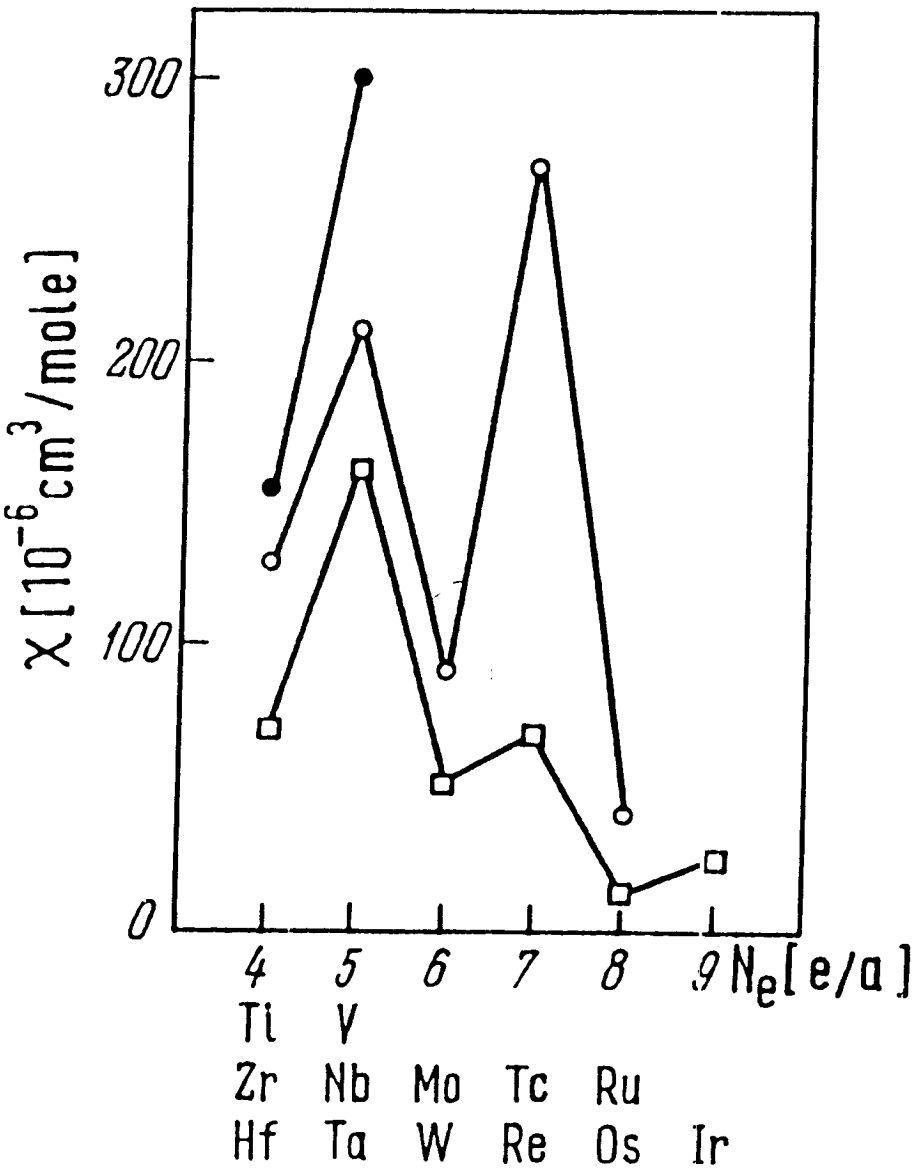
300
200
100
0
χ [10⁻⁶ cm³/mole]
4 5 6 7 8 9 Ne [e/a]
Ti V
Zr Nb Mo Tc Ru
Hf Ta W Re Os Ir

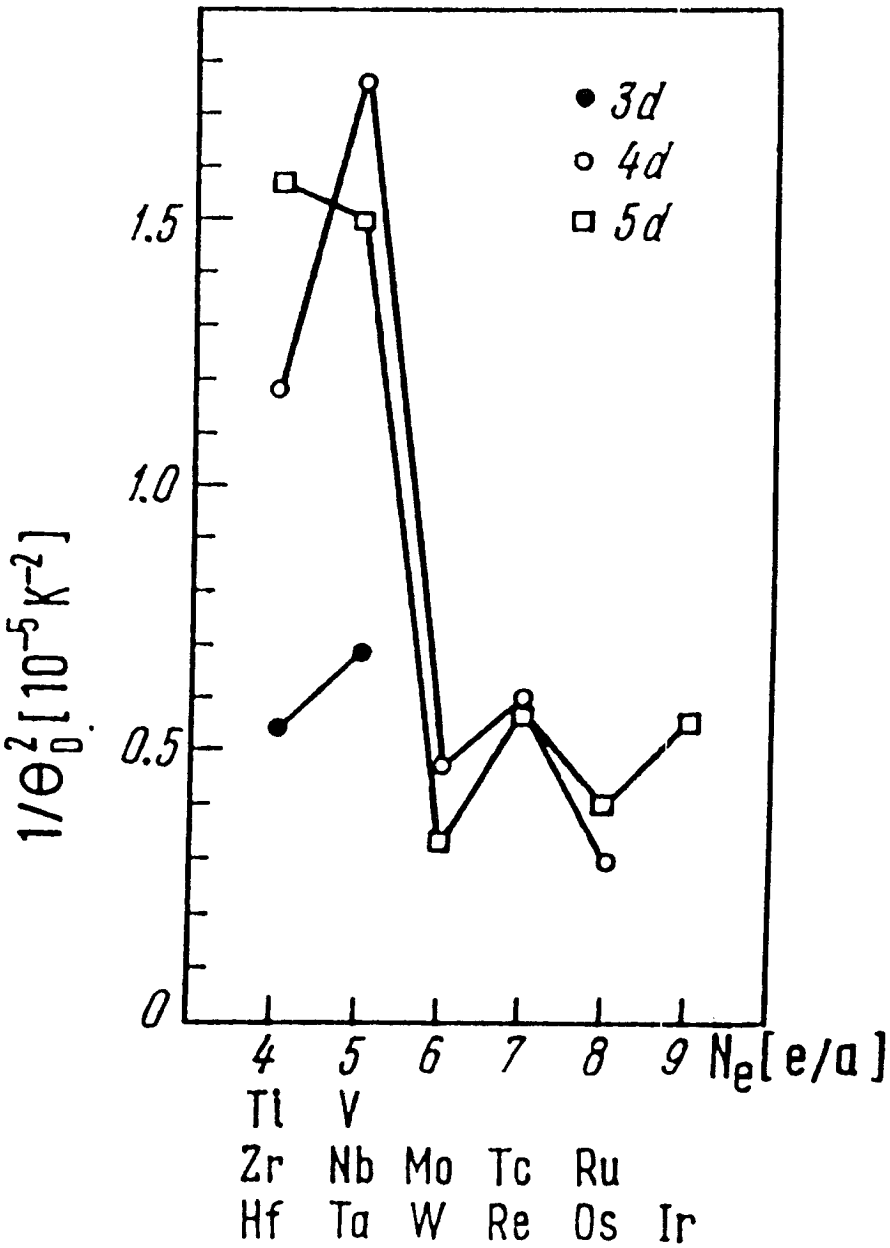
3d
4d
5d
1.5
1.0
0.5
0
1/Θ_D² [10⁻⁵ K⁻²]
4 5 6 7 8 9 Ne [e/a]
Ti V
Zr Nb Mo Tc Ru
Hf Ta W Re Os Ir

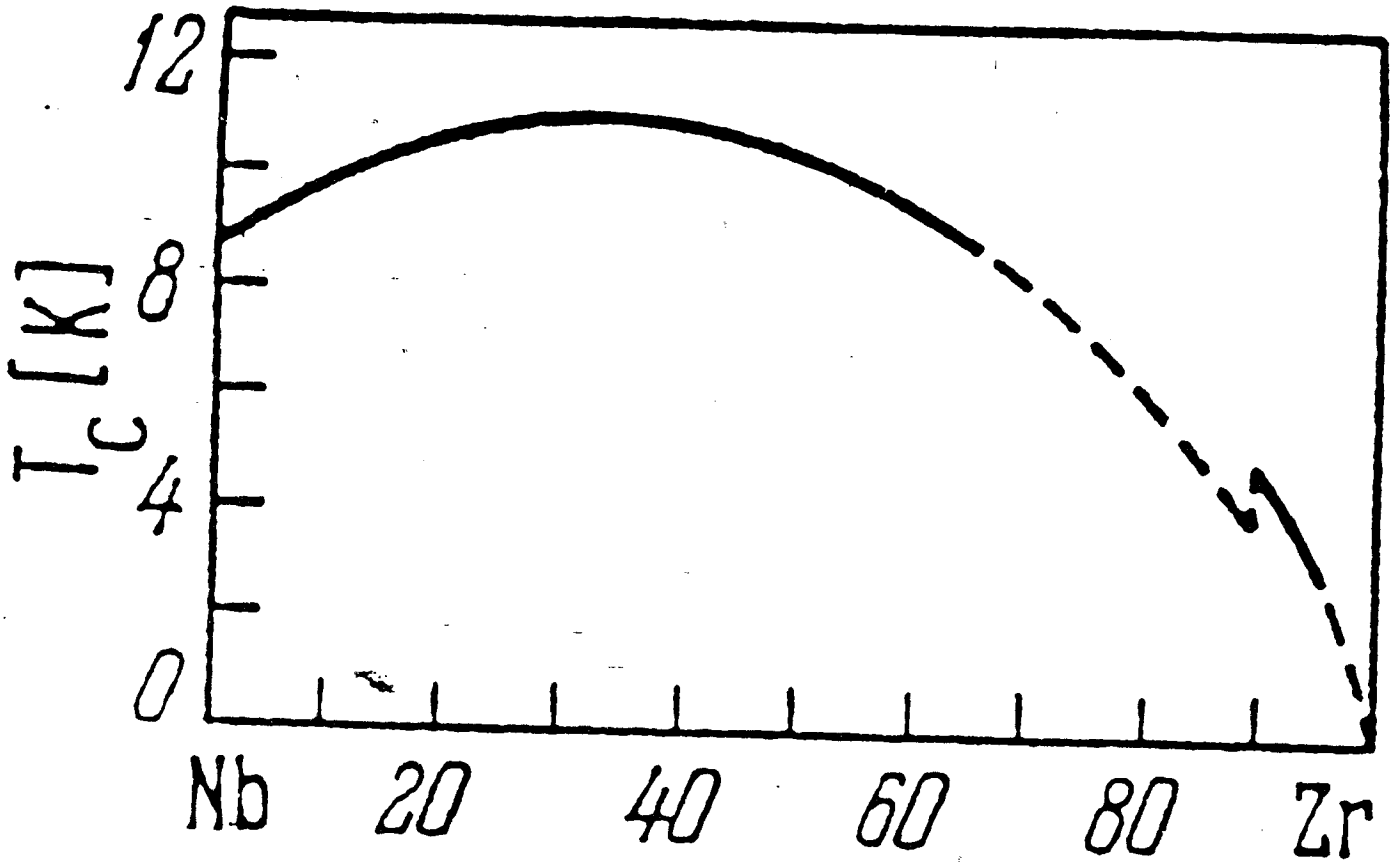
12
8
4
0
T_c [K]
Nb
20
40
60
80
Zr

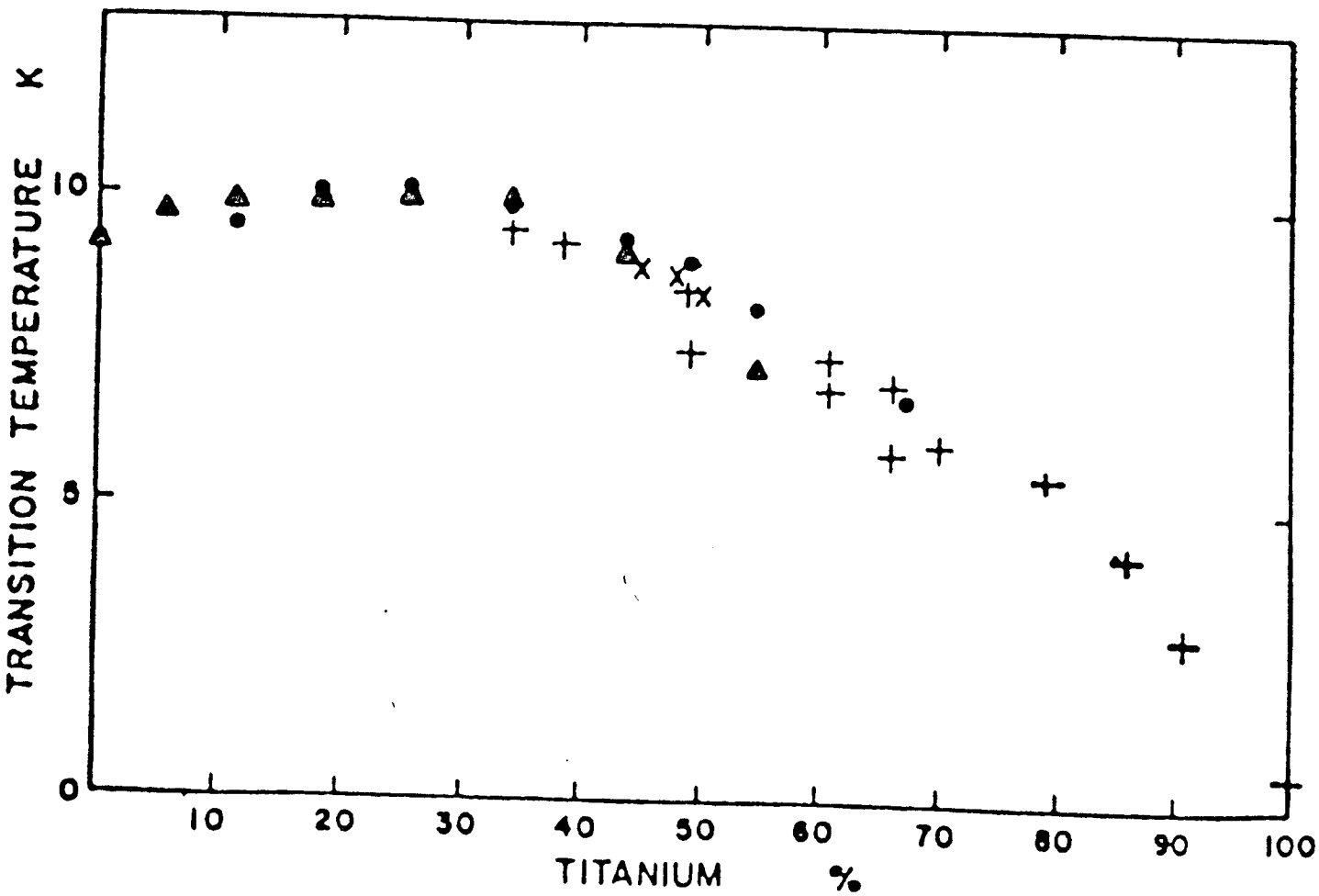
TRANSITION TEMPERATURE K
10
5
0
10
20
30
40
50
60
70
80
90
100
TITANIUM %

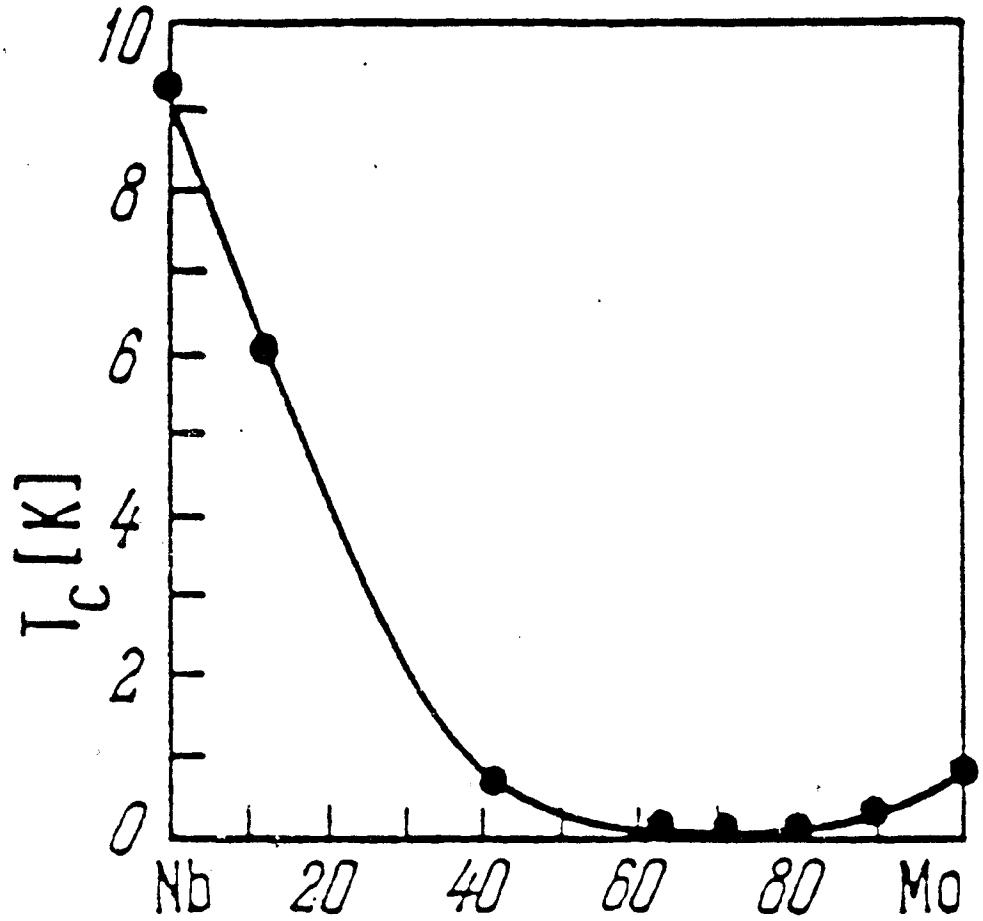
10
8
6
4
2
0
T_c [K]
Nb
20
40
60
80
Mo

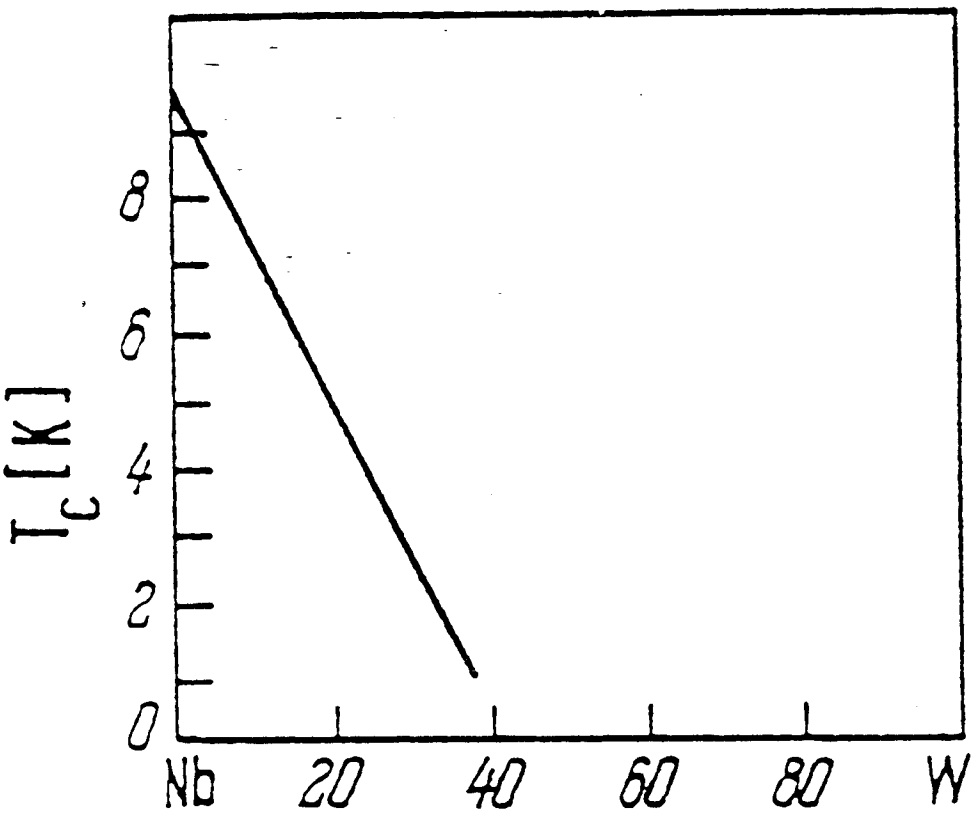
8
6
4
2
0
T_c [K]
Nb
20
40
60
80
W

CRITICAL TEMPERATURE $Mo_{75}Re_{25}$ VS. DEPOSITION TEMPERATURE

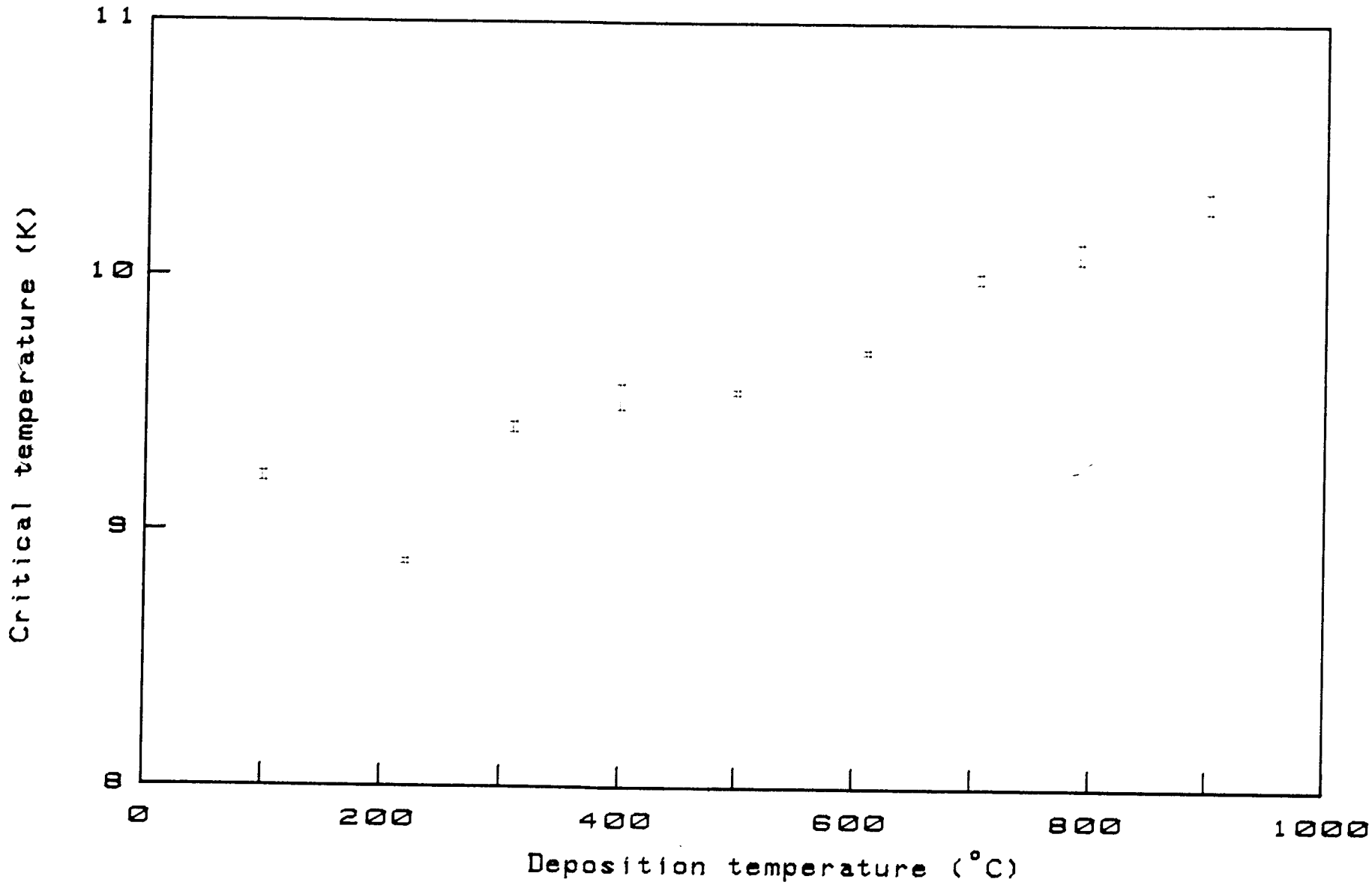

Mo60-Re40

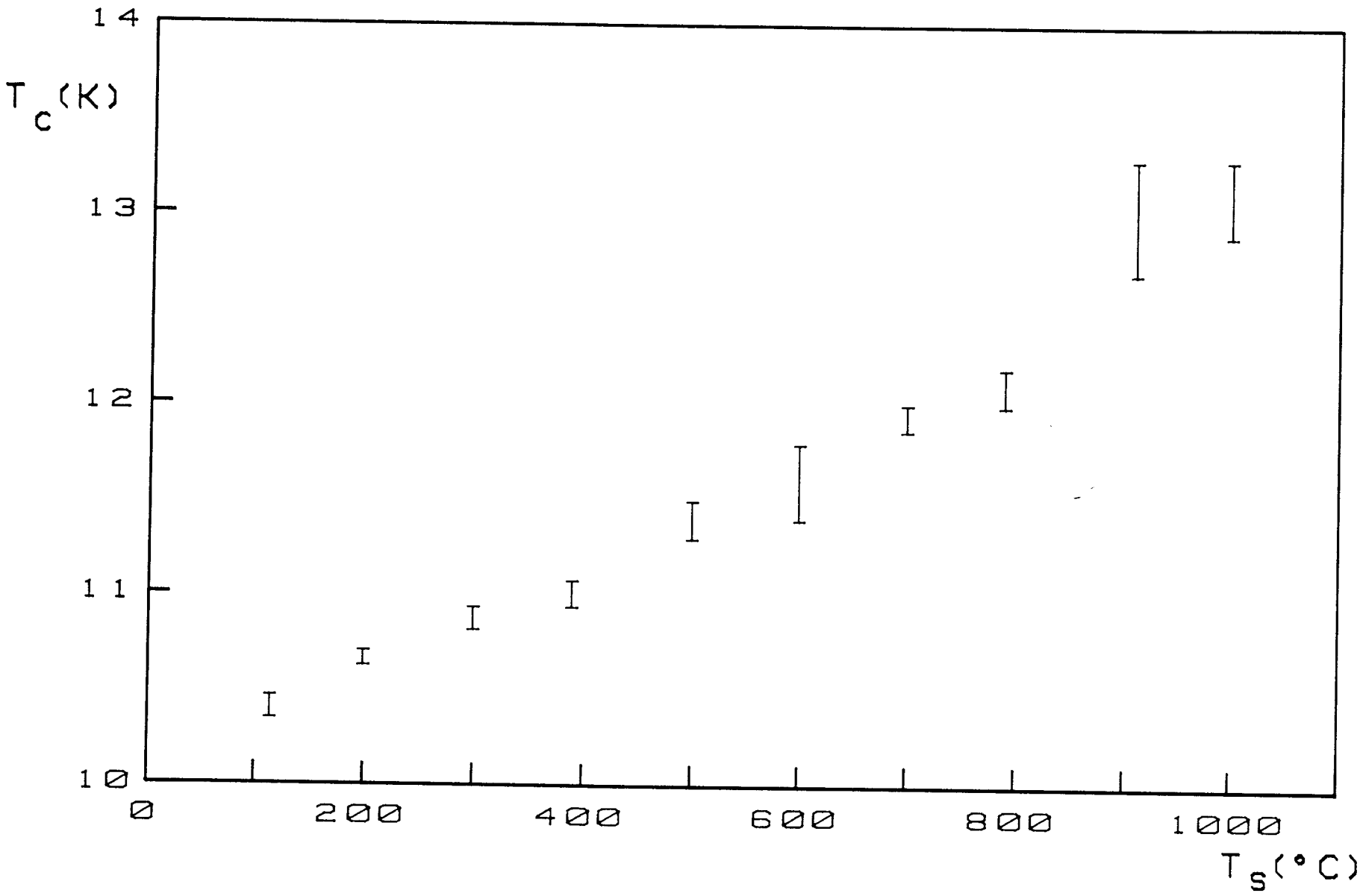

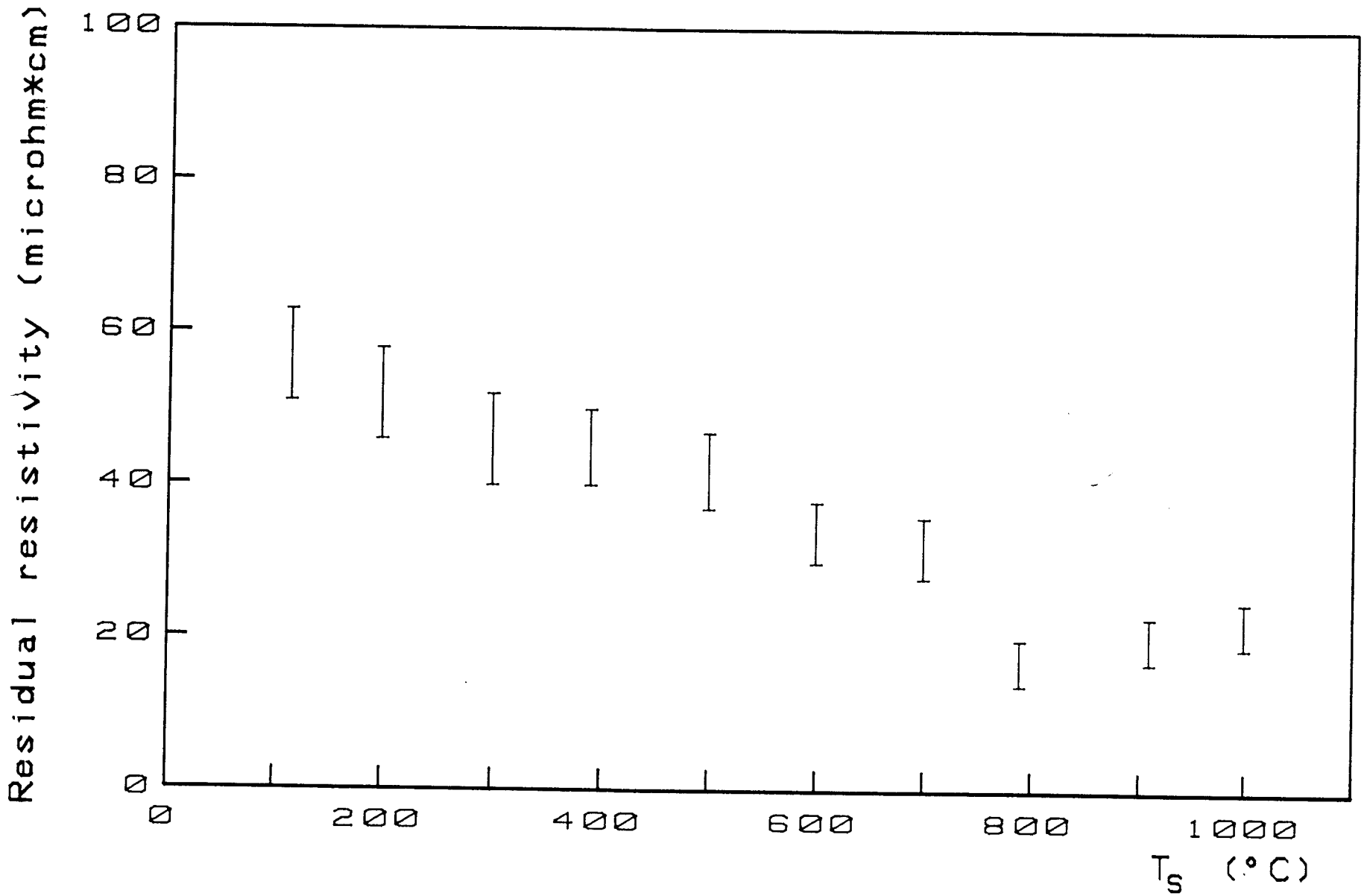
Residual resistivity (microhm*cm)
100
80
60
40
20
0
0
200
400
600
800
1000
T_S (°C)

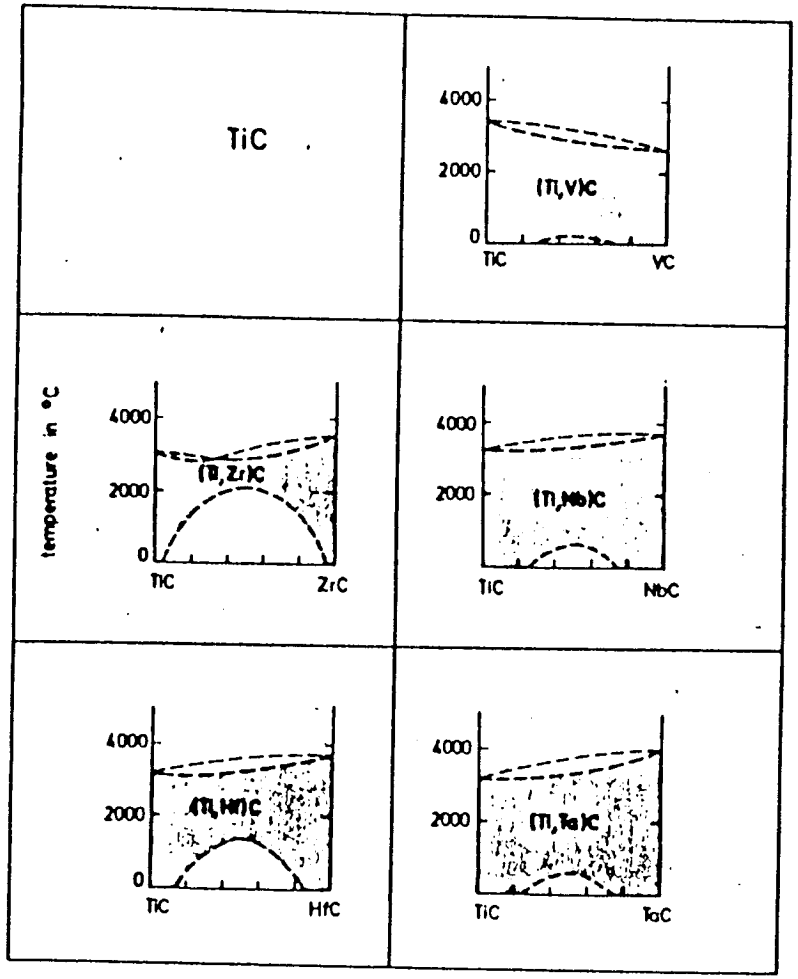

Miscibility behavior of TiC with other carbides.

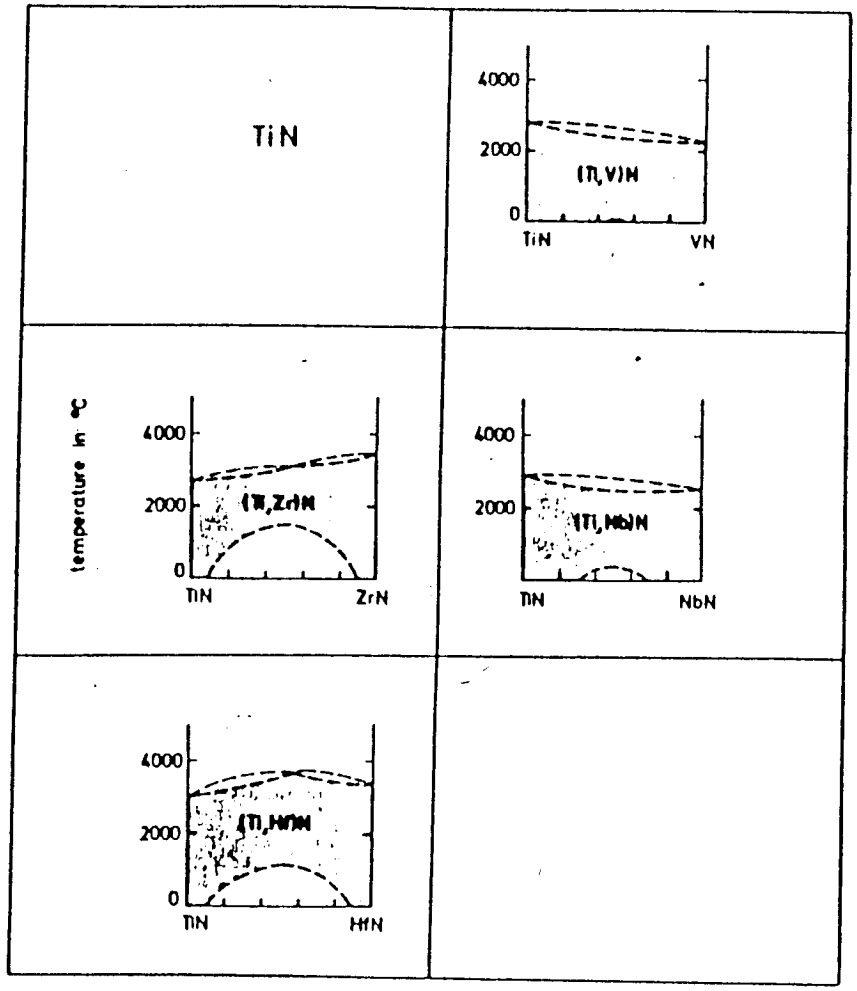

Miscibility behavior of TiN with other nitrides.

Spec. el. resistivity ($\mu\Omega\cdot$cm)

	Ti	Zr	V	Nb	Ta
N	25	21	85	58	
C	52	42	59	19	15
B_2	7	6	13	12	14

T_c (K)

	Ti	Zr	V	Nb	Ta
N	5.49	10.7	8.5	17.3	
C	3.42	<0.3	0.03	12	10.35
B_x	/	3.4	/	/	/

Ti	V	
Zr	Nb	Mo
Hf	Ta	W

For Carbo-nitrides:

3d in 4d : T_c ↓

5d in 4d : T_c ~

IV in V : T_c ↓

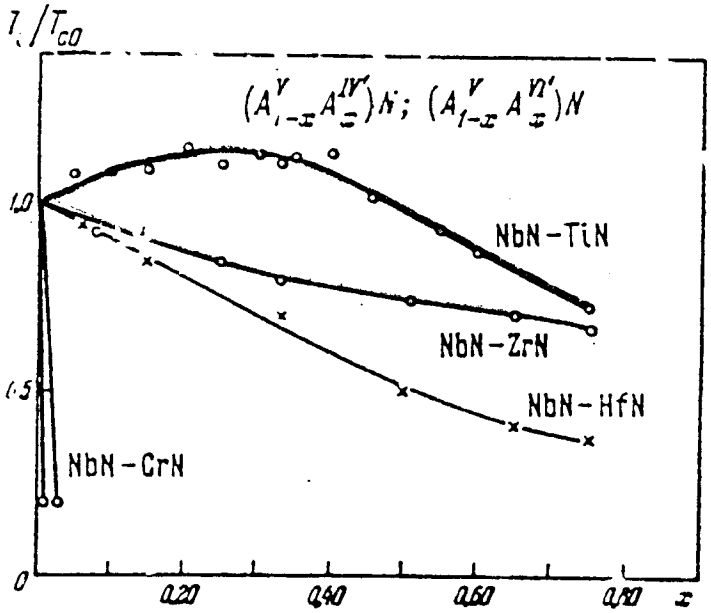

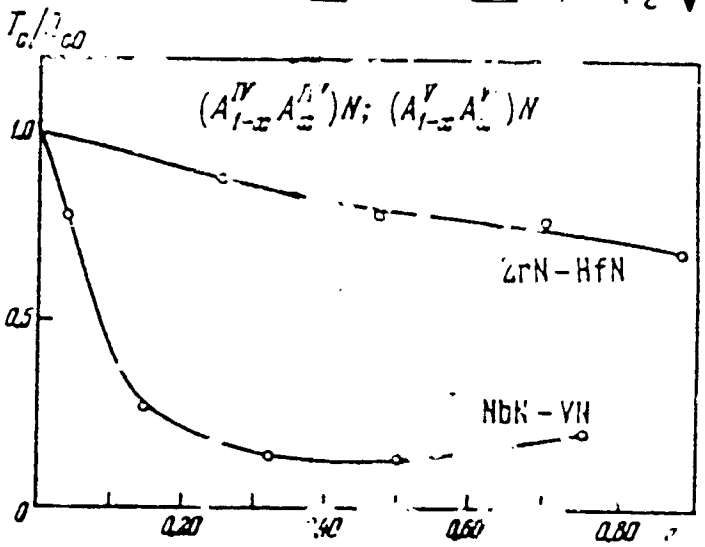

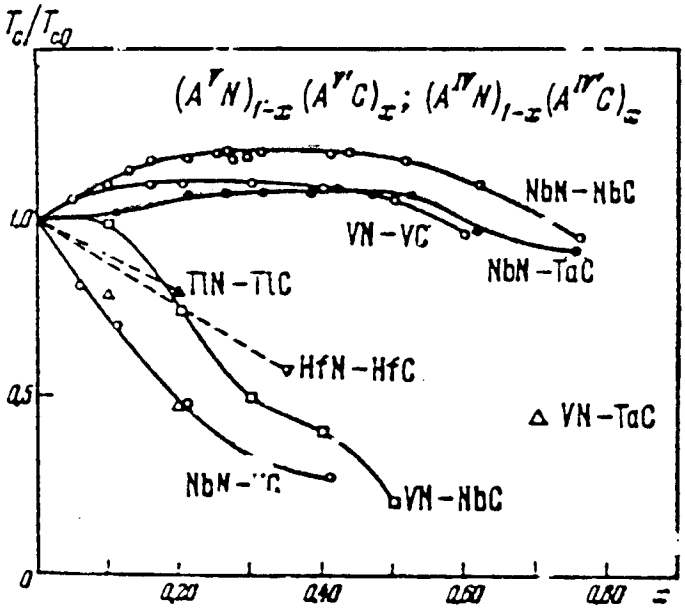

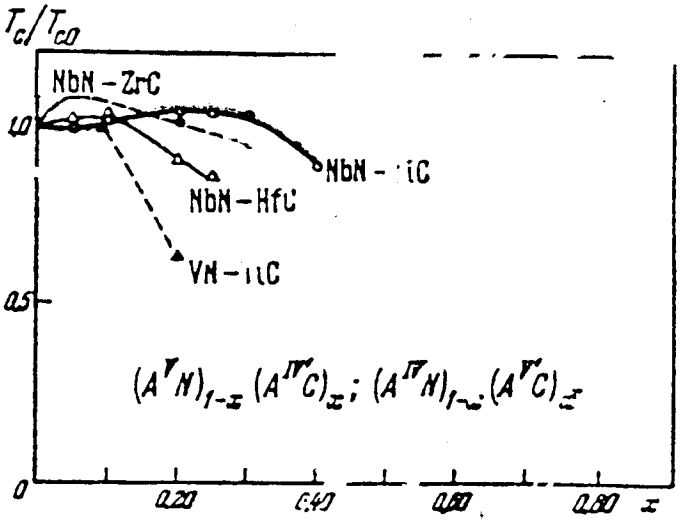

Bragg θ-2θ X-ray diffractometer

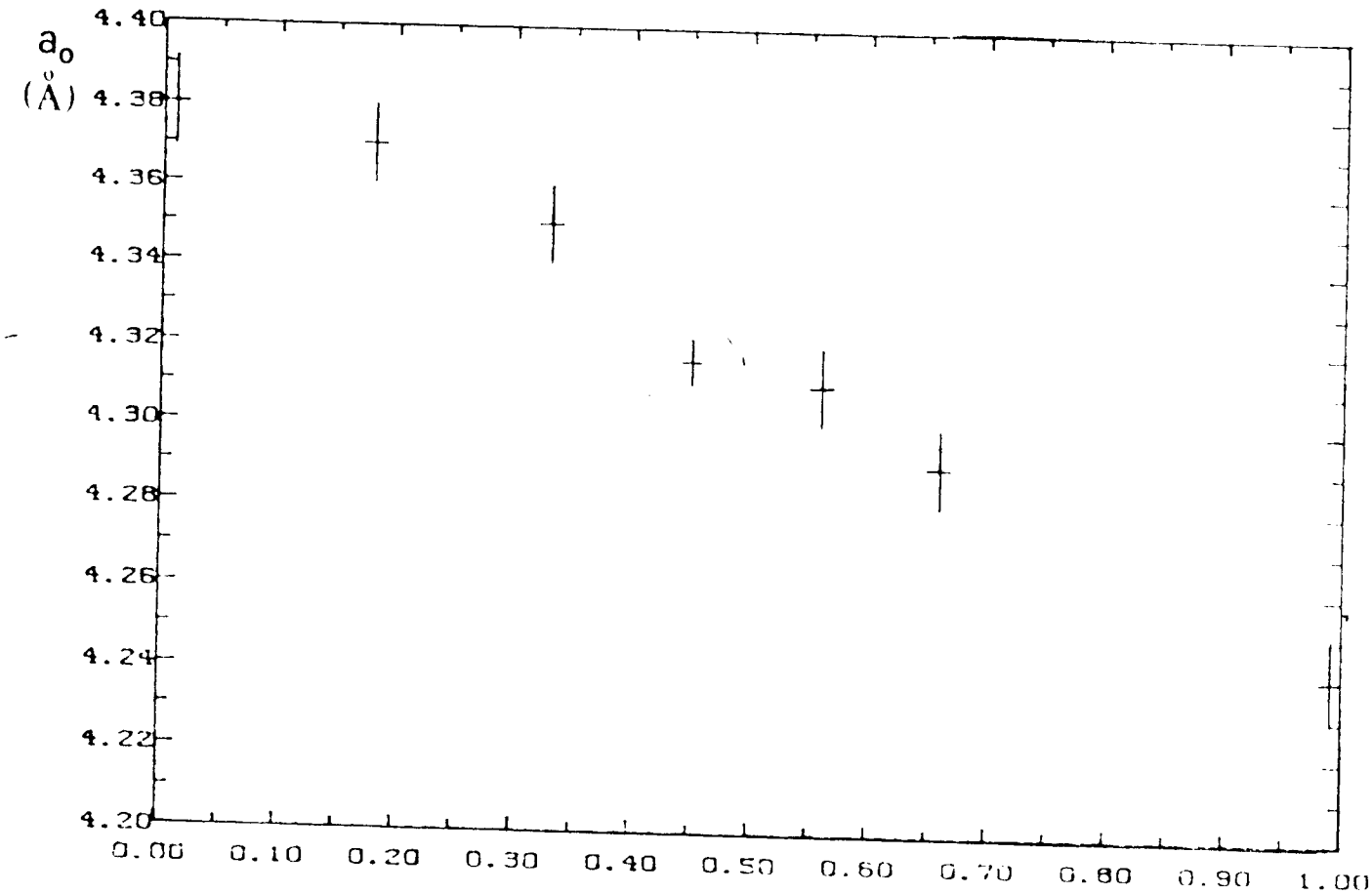

a_o (NbN) = 4.38 Å a_o (TiN) = 4.24 Å

Lattice constant a_o (in Å) as a function of the composition (x) for our $(Nb_{1-x}Ti_x)N$ films

metal-gold coloured (shift to the golden side if Ti ≥ 1)

same Nb/Ti atomic ratio of the target (averaged E.D.S)

single intense peak: [200] direction ⊥ substrate

⇓

High degree of preferential orientation

grain size = 200 ÷ 300 Å

A-15 materials

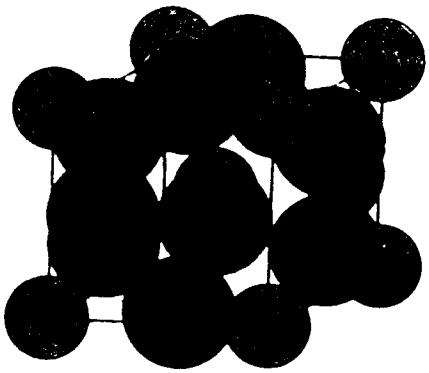

A-15 (OR β-W)
A_3B

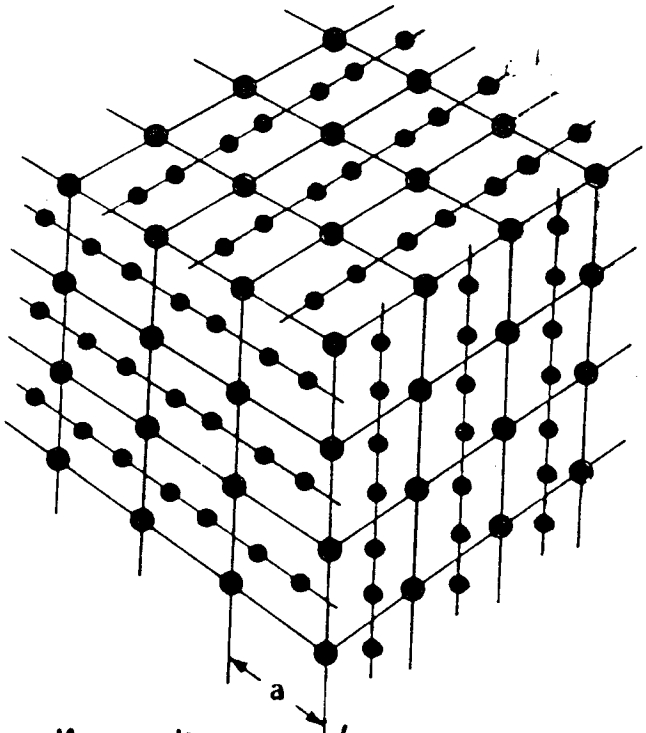

A_3B · A = Transition metal
B = metal or semiconductor

A15	T_c(K)	A15	T_c(K)	A15	T_c(K)
V_3Os	5.15	V_3Si	17.1	Nb_3Pt	10
V_3Rh	0.38	V_3Ge	7.0	Nb_3Au	11
V_3Ir	1.39	V_3Sn	4.3	Nb_3Al	18.9
V_3Ni	0.57	V_3Pb	3.7	Nb_3Ga	20.3
V_3Pd	0.08	V_3Sb	0.8	Nb_3In	8
V_3Au	3.2			Nb_3Si	18
V_3Al	9.6	Nb_3Os	0.94	Nb_3Ge	23
V_3Ga	15.4	Nb_3Rh	2.5	Nb_3Sn	18.3
V_3In	13.9	Nb_3Ir	1.76	Nb_3Bi	2.25

A15	T_c(K)	A15	T_c(K)	A15	T_c(K)
V_3Os	5.15	V_3Si	17.1	Nb_3Pt	10
V_3Rh	0.38	V_3Ge	7.0	Nb_3Au	11
V_3Ir	1.39	V_3Sn	4.3	Nb_3Al	18.9
V_3Ni	0.57	V_3Pb	3.7	Nb_3Ga	20.3
V_3Pd	0.08	V_3Sb	0.8	Nb_3In	8
V_3Au	3.2			Nb_3Si	18
V_3Al	9.6	Nb_3Os	0.94	Nb_3Ge	23
V_3Ga	15.4	Nb_3Rh	2.5	Nb_3Sn	18.3
V_3In	13.9	Nb_3Ir	1.76	Nb_3Bi	2.25

	T_c,K	ρ_0, $\mu\Omega\cdot$cm	RRR	λ, Å
V_3Si	16.5	4-6	20-30	1100
Nb_3Sn	18	20	3-10	1100
Nb_3Al	17	50	> 3	1830
Nb_3Ge	22-23	30	<2	1150

SPUTTERING CONDITIONS FOR DC DIOD and MAGNETRON SPUTTERED A15 THIN FILMS

SUBSTRATES : supphire, SiO_2 /Si

T_S = 700 - 900 °C

P =10 - 50 Pa

Deposition rate 1 - 5 Å/c

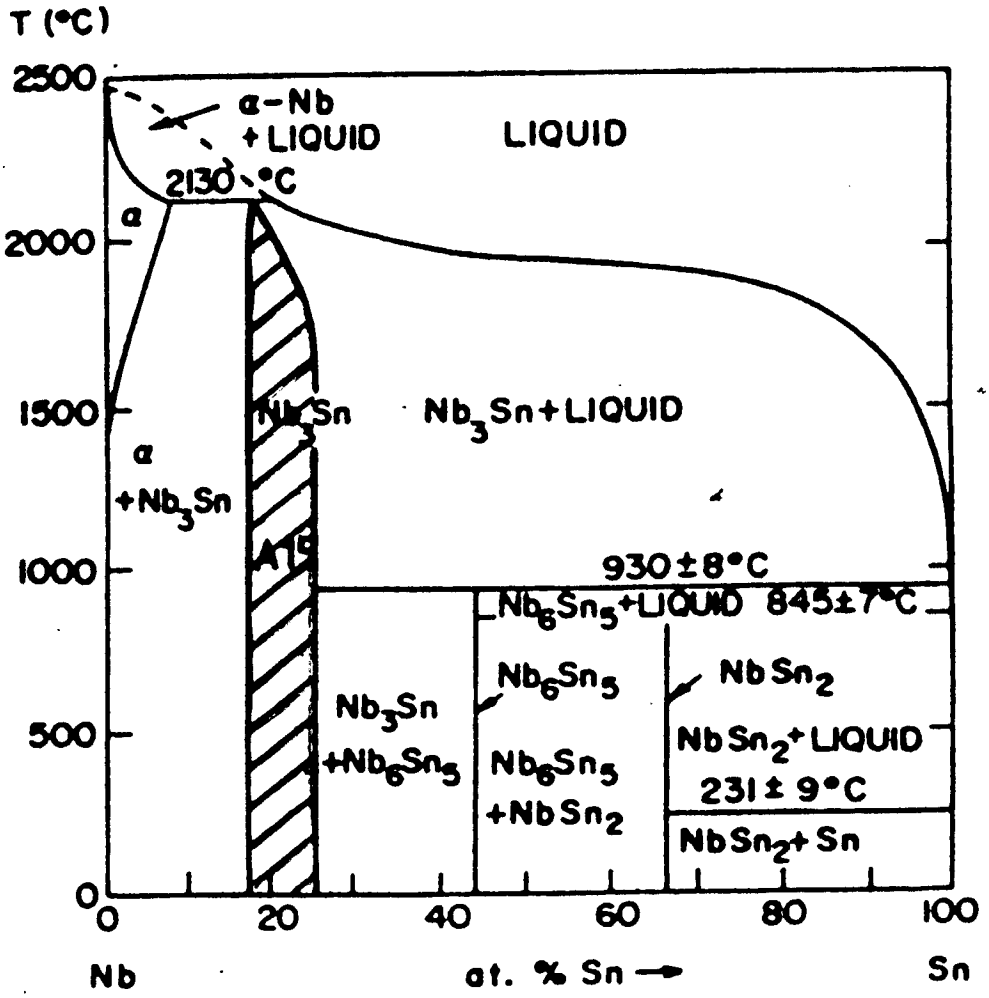
T (°C)
2500
2000
1500
1000
500
0
α-Nb
+ LIQUID
LIQUID
2130 °C
α
α
+Nb3Sn
Nb3Sn
Nb3Sn+LIQUID
A15
930±8°C
Nb6Sn5+LIQUID 845±7°C
Nb3Sn
+Nb6Sn5
Nb6Sn5
Nb6Sn5
+NbSn2
NbSn2
NbSn2+LIQUID
231 ± 9°C
NbSn2+Sn
0
20
40
60
80
100
Nb
at. % Sn →
Sn

c)

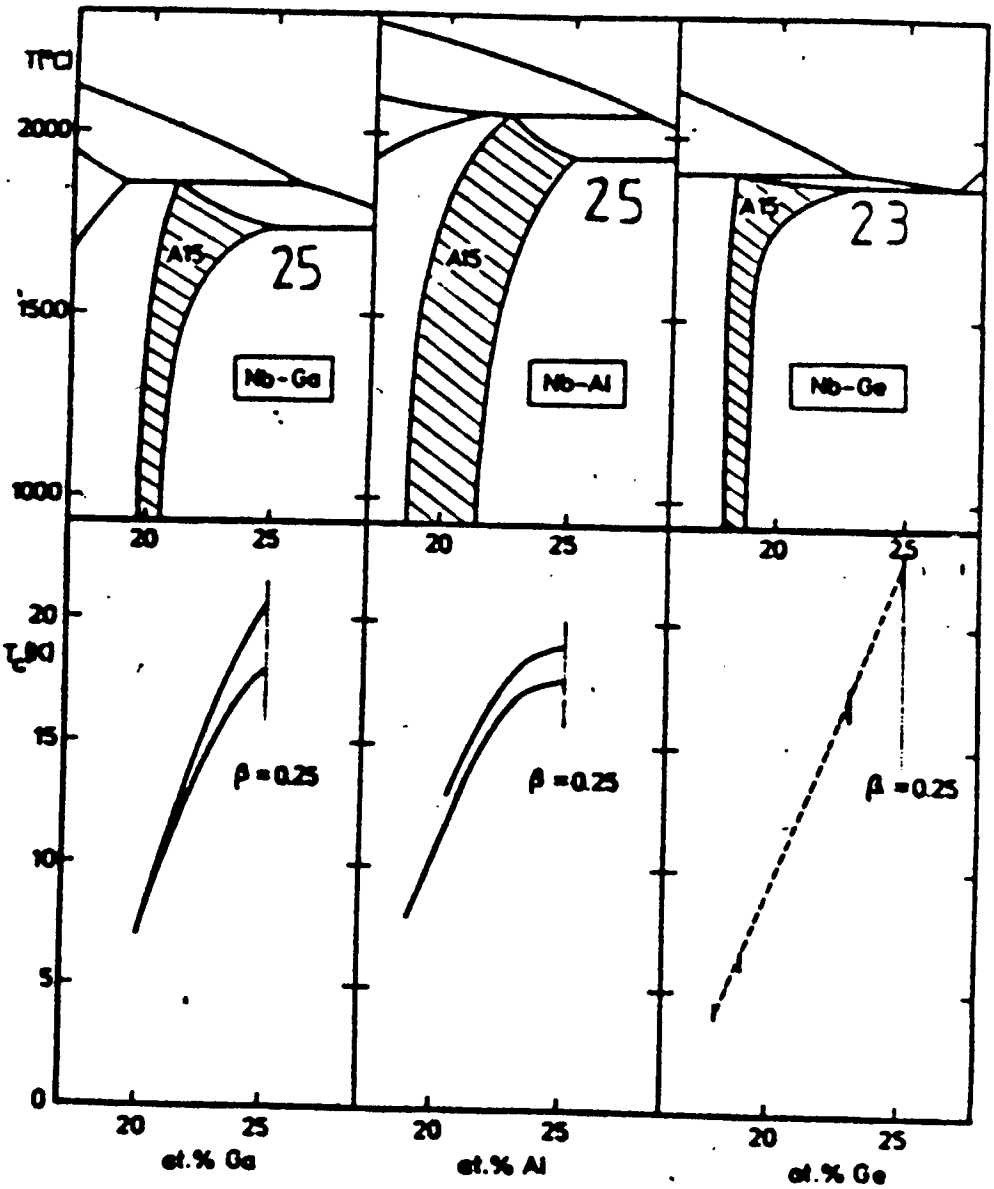
T[°C]
2000
1500
1000
A15
25
Nb-Ga
A15
25
Nb-Al
A15
23
Nb-Ge
20
25
T_c[K]
20
15
10
5
0
β = 0.25
β = 0.25
β = 0.25
at.% Ga
at.% Al
at.% Ge

b)

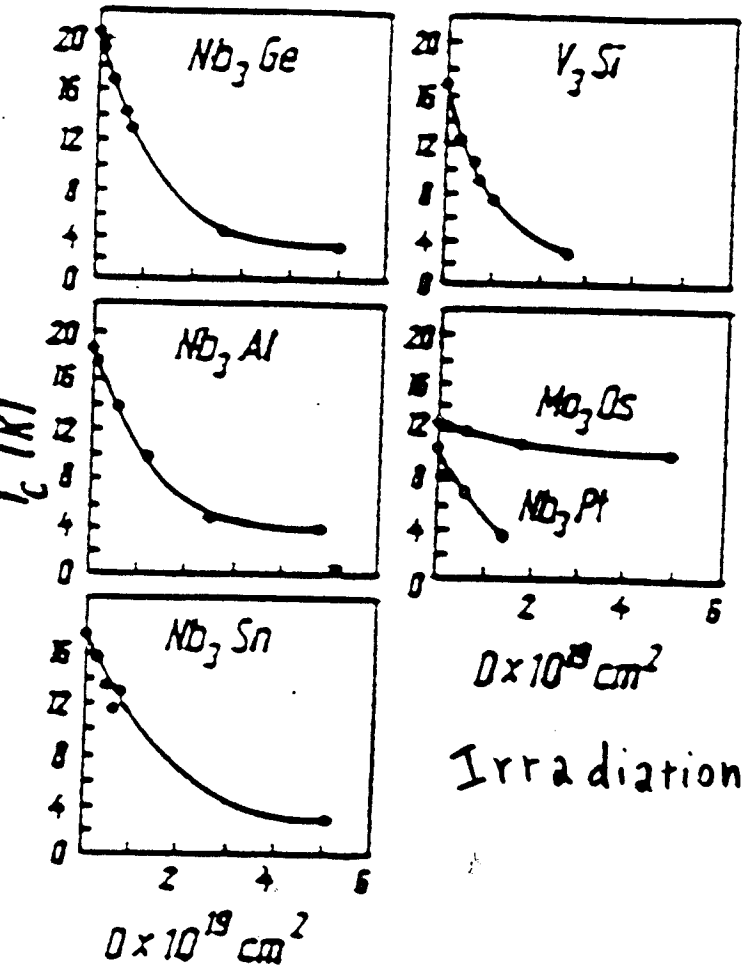

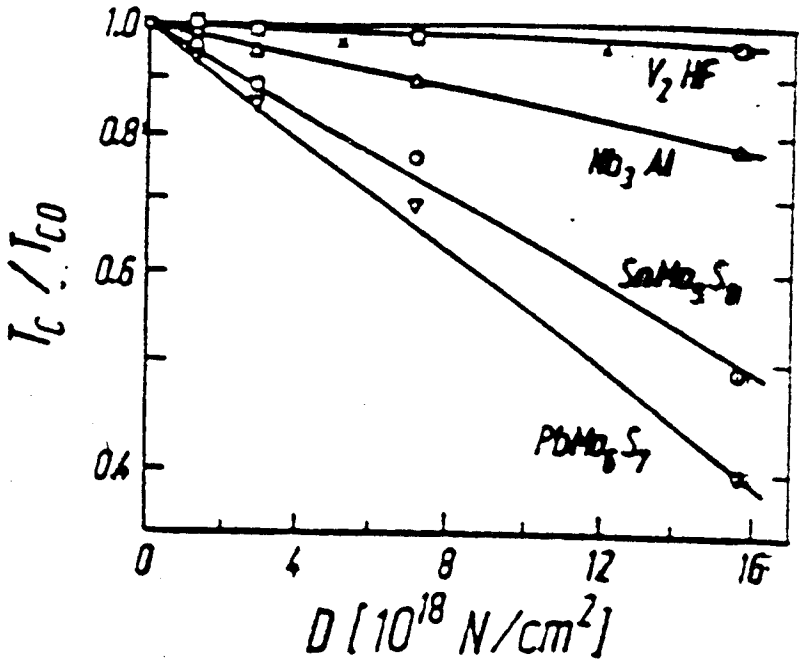

Irradiation by fast neutrons (E > 1 MeV)

Nitrides, Carbides and Nitrocarbides of TM are for radiation damage hard materials

The T_c onset of NbN after a dose of 1.5×10^{18} N/cm^2 at E > 1 MeV decreases only by [illegible]

Even for NbC at $5 \cdot 10^{18}$ N/cm^2 at [illegible]
$T_c \downarrow \sim 15\%$ but H_{c2} [illegible]

B \ A	Sc	Y	La	Ti	Zr	Hf	V	Nb	Ta	Cr	Mo	W	Re
B					3.4	3.1							
C	<1.38	<1.38		3.42	<0.3	<1.20	0.03 3.2*	12	10.35		14.3	10.0	3.4
N	<1.38	<1.4	1.35	5.49	10.7	8.83	8.5	17.3	6.5	<1.28	5.0	<1.38	
P			<1.68										
Sb		<1.02	<1.02										
O				2.0			<0.3	1.39					
S	<0.33	1.9	0.87		3.3								
Se	<0.33	2.5	1.02										
Te		2.05	1.48										

* T_c = 3.2 K was registered in vanadium carbide after implantation of C^+ ions

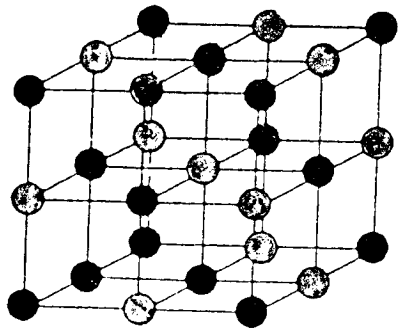

Nb

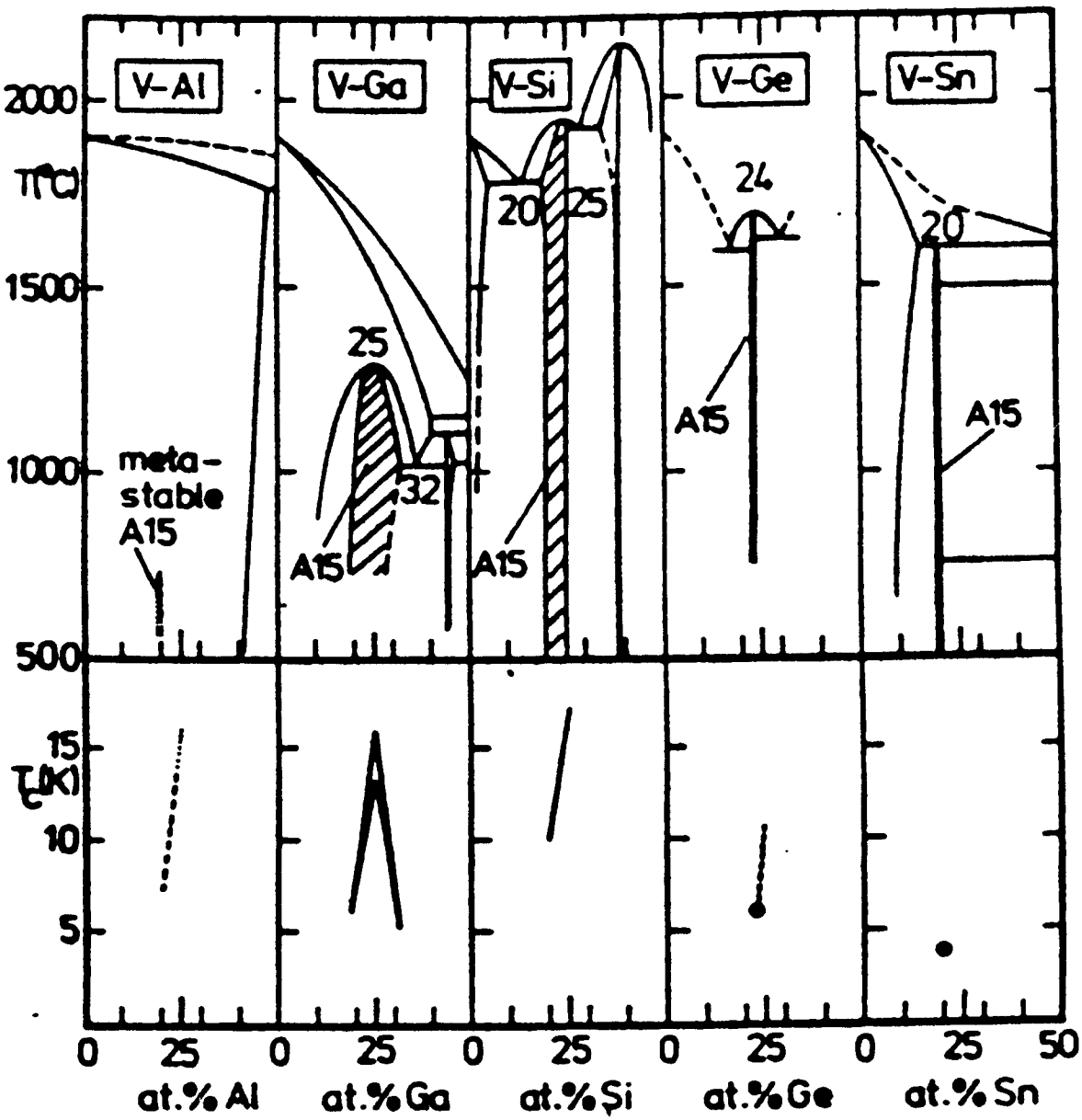
V-Al
V-Ga
V-Si
V-Ge
V-Sn
2000
T(°C)
1500
1000
500
meta-
stable
A15
25
32
A15
20
25
A15
24
A15
20
A15
15
T_c(K)
10
5
0
25
0
25
0
25
0
25
0
25
50
at.% Al
at.% Ga
at.% Si
at.% Ge
at.% Sn

a)

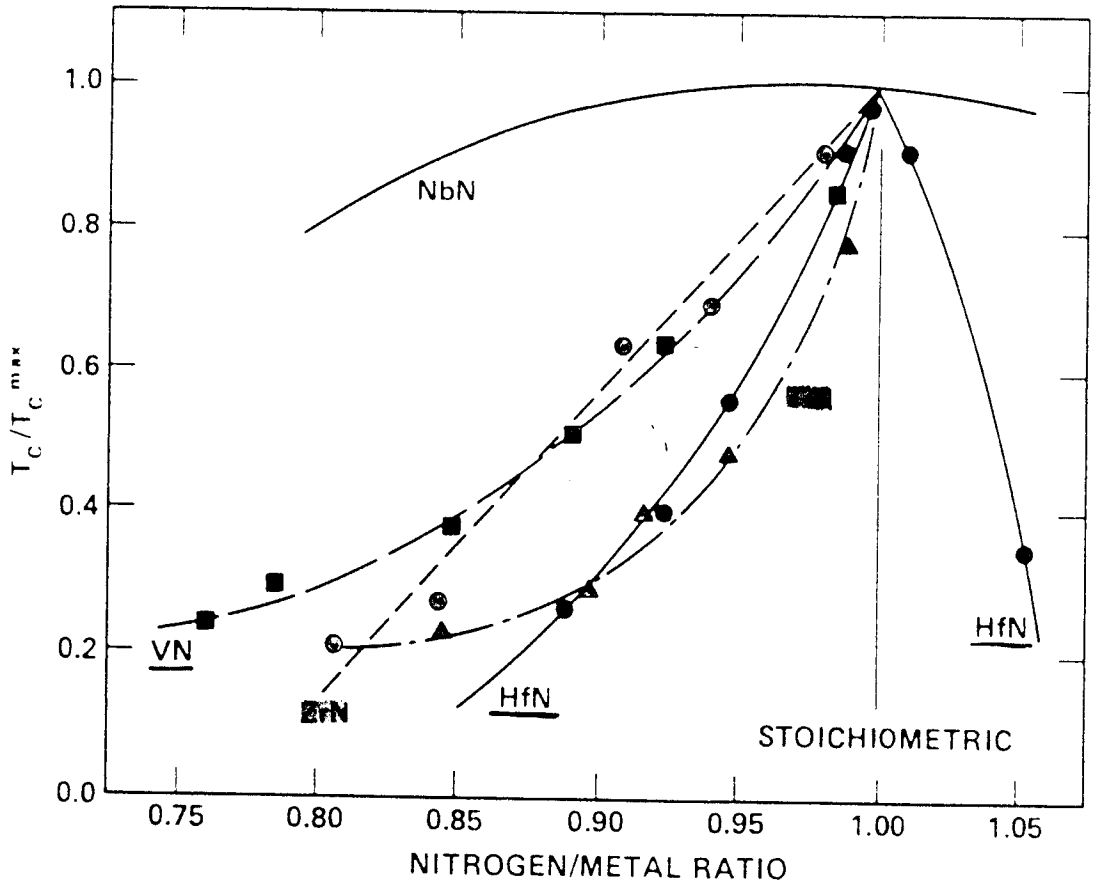
1.0
0.8
0.6
0.4
0.2
0.0
T_c/T_c^{max}
NbN
VN
ZrN
HfN
HfN
STOICHIOMETRIC
0.75
0.80
0.85
0.90
0.95
1.00
1.05
NITROGEN/METAL RATIO

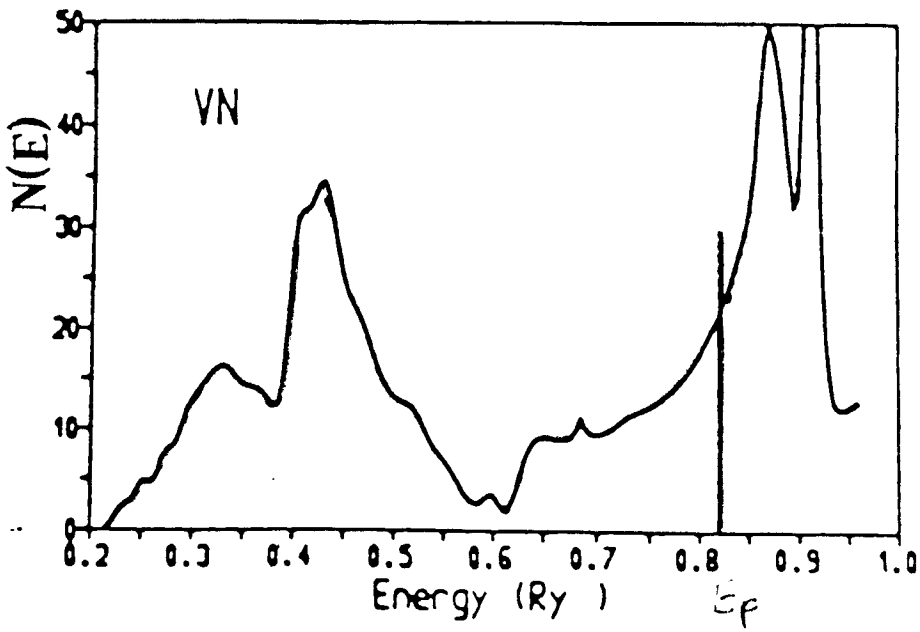
VN
N(E)
50
40
30
20
10
0
0.2
0.3
0.4
0.5
0.6
0.7
0.8
0.9
1.0
Energy (Ry)
E_F

Chevrel Phasis

$A_x Mo_6 Y_8$

$Y = S, Se, Te$

A = almost any

Formula	T_c(K)	Formula	T_c(K)
Mo_6S_8	1.7	Mo_6Se_8	6.3
$Cu_2Mo_6S_8$	10.6	$Cu_{1.4}Mo_6Se_8$	5.8
		$Cu_{2.6}Mo_6Se_8$	4.6
$AgMo_6S_8$	8.5	$AgMo_6Se_8$	5.8
$SnMo_6S_8$	11.8–14.5	$SnMo_6Se_8$	4.8
$PbMo_6S_8$	12.5–14.7	$PbMo_6Se_8$	3.6
$NaMo_6S_8$	8.5		
$LaMo_6S_8$	7.0	$LaMo_6Se_8$	11.2
$PrMo_6S_8$	2.6	$PrMo_6Se_8$	8.9
$NdMo_6S_8$	3.5	$NdMo_6Se_8$	8.0
$SmMo_6S_8$	2.4	$SmMo_6Se_8$	6.6
$GdMo_6S_8$	1.4	$GdMo_6Se_8$	5.4
$YbMo_6S_8$	8.5	$YbMo_6Se_8$	5.2

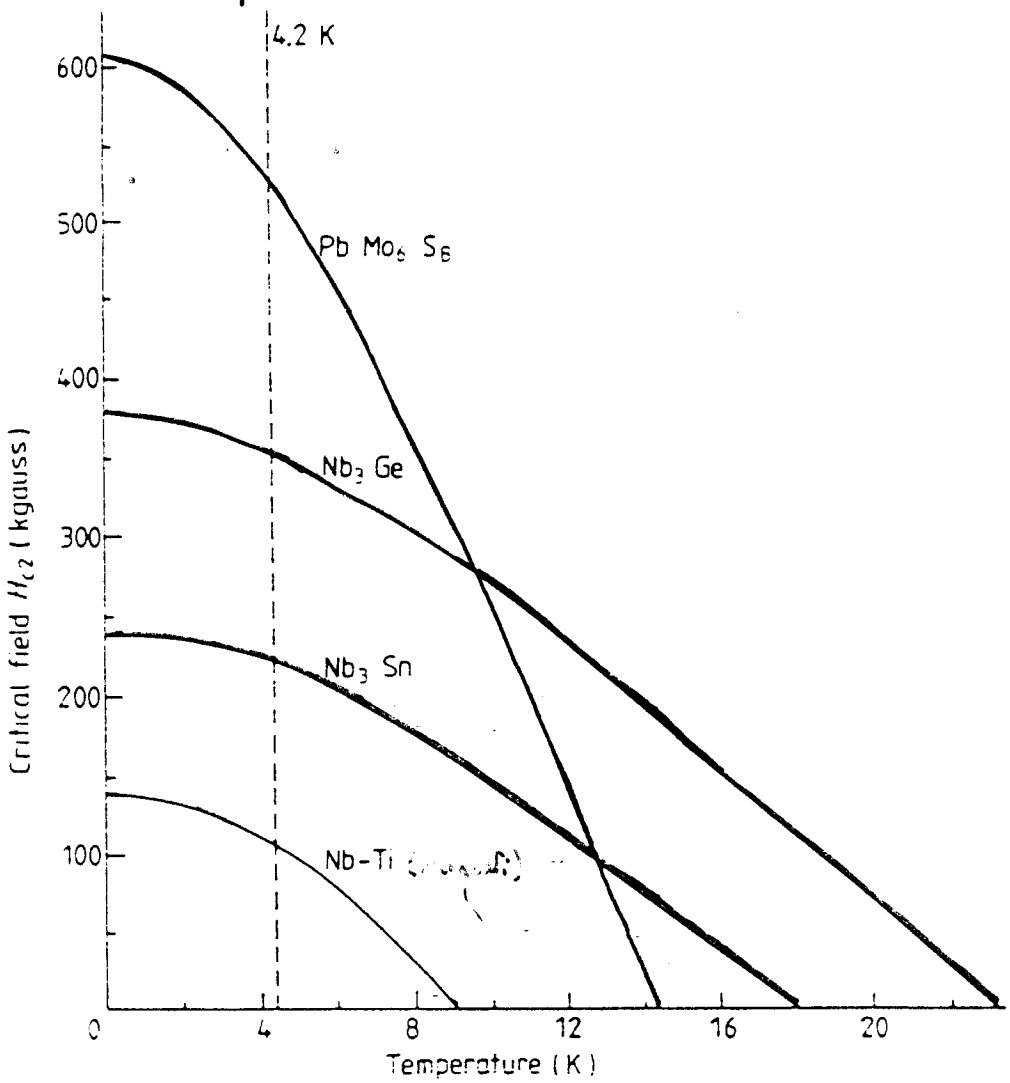

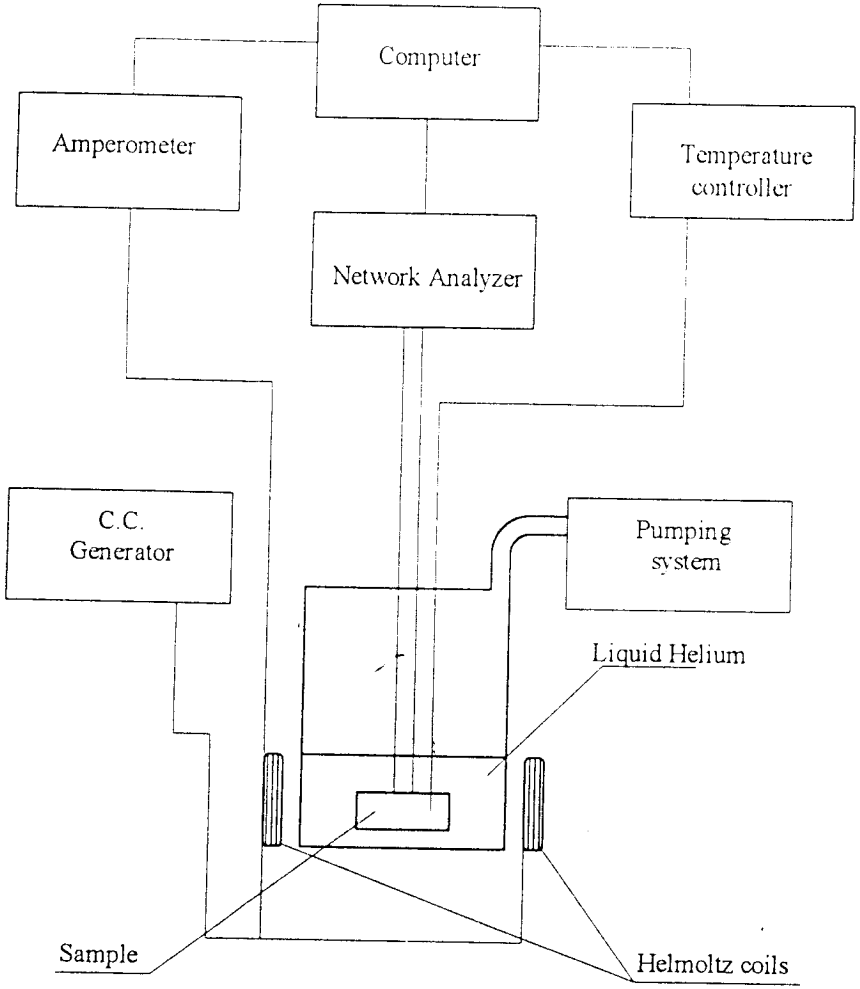

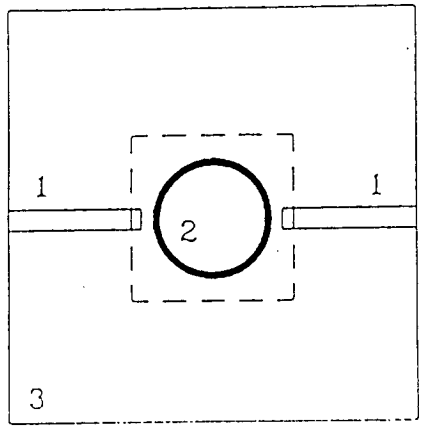

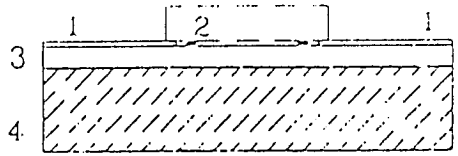

Dipendenza dell' impedenza superficiale da:

Temperatura

Frequenza

Campo r.f.

Campo d.c. con diverse applicazioni

T> 1.3 K

f=1-18 GHz

$E_{acc} \leq 25$MV/m

H$\leq$ 400 Oe

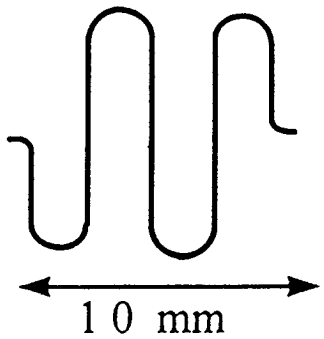

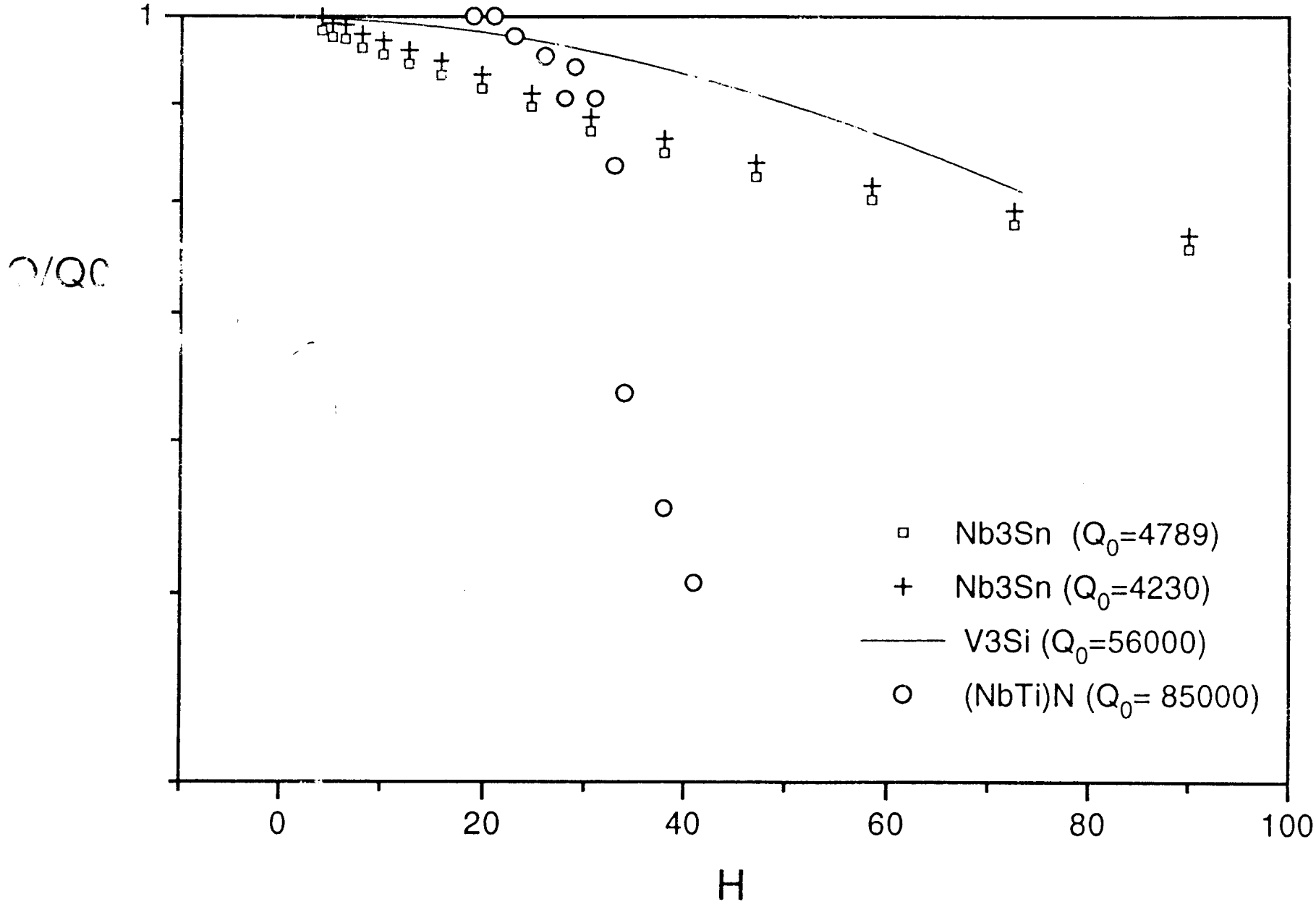
1
0
20
40
60
80
100
H
Nb3Sn (Q0=4789)
Nb3Sn (Q0=4230)
V3Si (Q0=56000)
(NbTi)N (Q0= 85000)

Surface resistance of a $(Nb_{0.55}Ti_{0.45})N/Cu$ film (*4 GHz*)

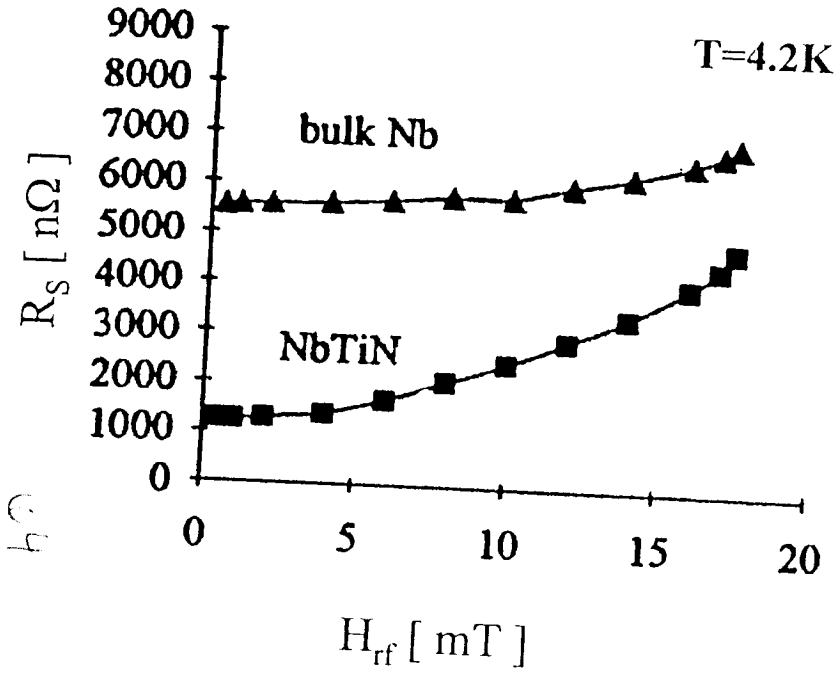

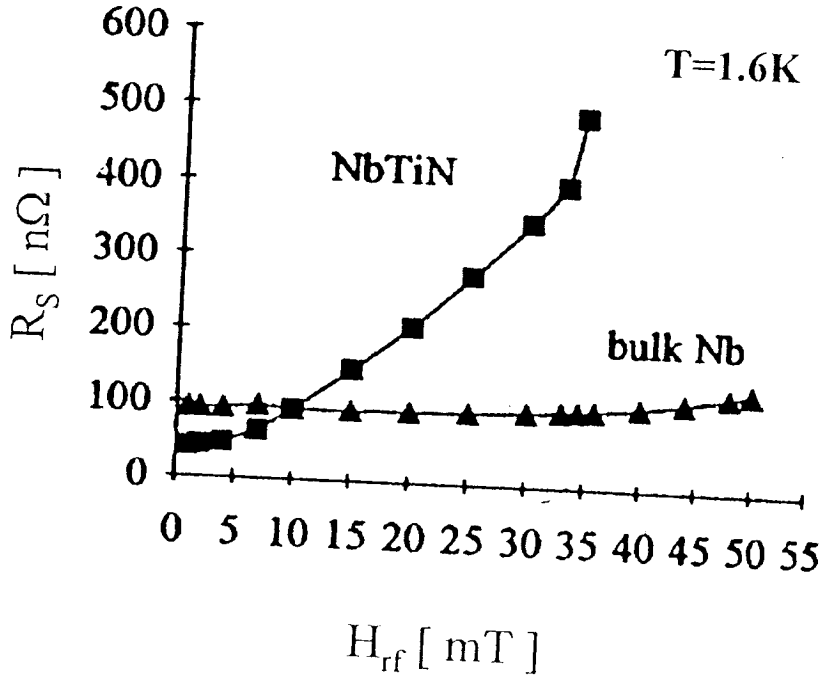

Mo-Re SUPERCONDUCTING THIN FILMS BY SINGLE TARGET MAGNETRON SPUTTERING

A. Andreone°, A. Barone°", A. Di Chiara°, G. Mascolo*, V. Palmieri', G. Peluso° and U.Scotti di Uccio°
° Dipartimento di Scienze Fisiche Università di Napoli and INFN, Napoli, Italy
* Dipartimento di Ingegneria dei materiali e della produzione, Università di Napoli, Italy
' Laboratori Nazionali di Legnaro, INFN Legnaro (Pd), Italy
" Istituto di Cibernetica, CNR Arcofelice (Na), Italy

Over the last decade a Mo-Re alloy system in the bulk form was proposed as a suitable low-loss material to be studied in cavities prototypes (Yasaitis, Rose, IEEE Trans. on Magn. Mag-11, 434, 1975). The reasons behind that were:

- T_c in bulk bcc $Mo_{1-x}Re_x$ rises from 0.92K for pure Molybdenum up to 12 K at $x \simeq 35$
- The solubility of interstitial elements, particularly Oxygen is low in Mo-Re alloys.
- If compared with other alloys Mo-Re shows low values of the GL parameter κ

Our interest is originated by the circumstance that metastable Mo-Re phases having T_c up to 15 K, not observed in bulk, can be grown in thin films by c.v.d.

	$Mo_{32}Re_{68}$	$Mo_{70}Re_{30}$	$Mo_{60}Re_{40}$
films	$T_c = 15$ K ($T_s = 1250°C$)	$T_c = 15$ K ($T_s = 1000°C$)	$T_c = 11$ K ($T_s = 300°C$)
bulk	$T_c = 6$ K Testardi et al.	$T_c = 12$ K Gavaler et al.	$T_c = 12$ K Tarutani et al.

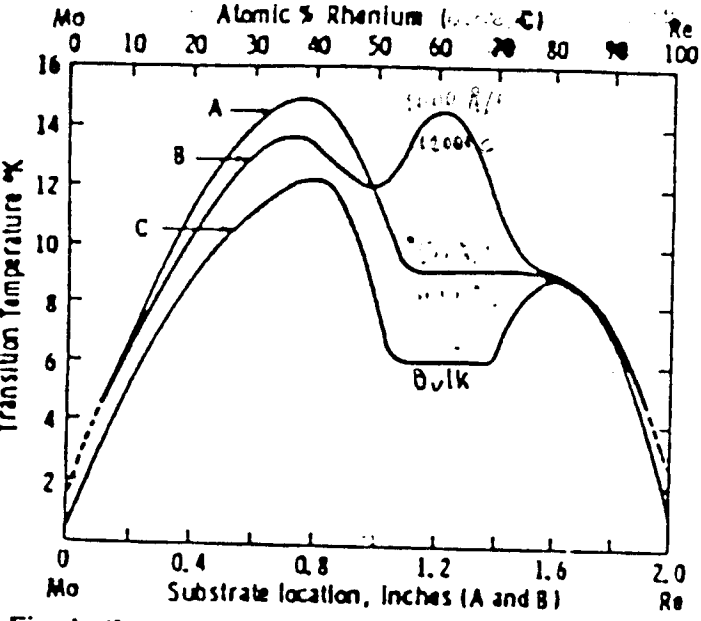

Fig. 1. Curve A—T_c vs. substrate location for Mo Re films sputtered at ~ 500 Å/min onto 1000°C substrates. Curve B—T_c vs. location for films sputtered at ~ 1000 Å/min onto 1200°C substrates. Curve C—T_c vs. composition for bulk Mo–Re samples (curve drawn from data of Blaugher *et al.*[4]).

Gavaler et al.

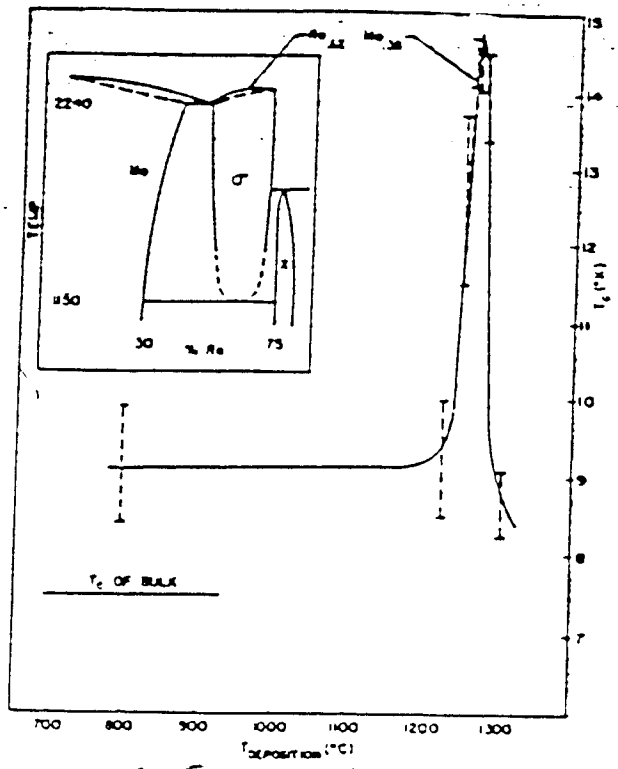

Testardi et al.

The presence of A15 phases was ruled out. Thus the crystallization of this metastable A15 structure was assumed to be responsable for the higher T_c's of the sputtered films compared to the bulk.

A-15-type phases in Mo-Re system differ from the typical Nb- or V- based with the same structure. Indeed the maximum T_c does not occur at the ideal 3:1 stoichiometric composition.

Mo-Re should be an A15 weakly radiation-damage resistant

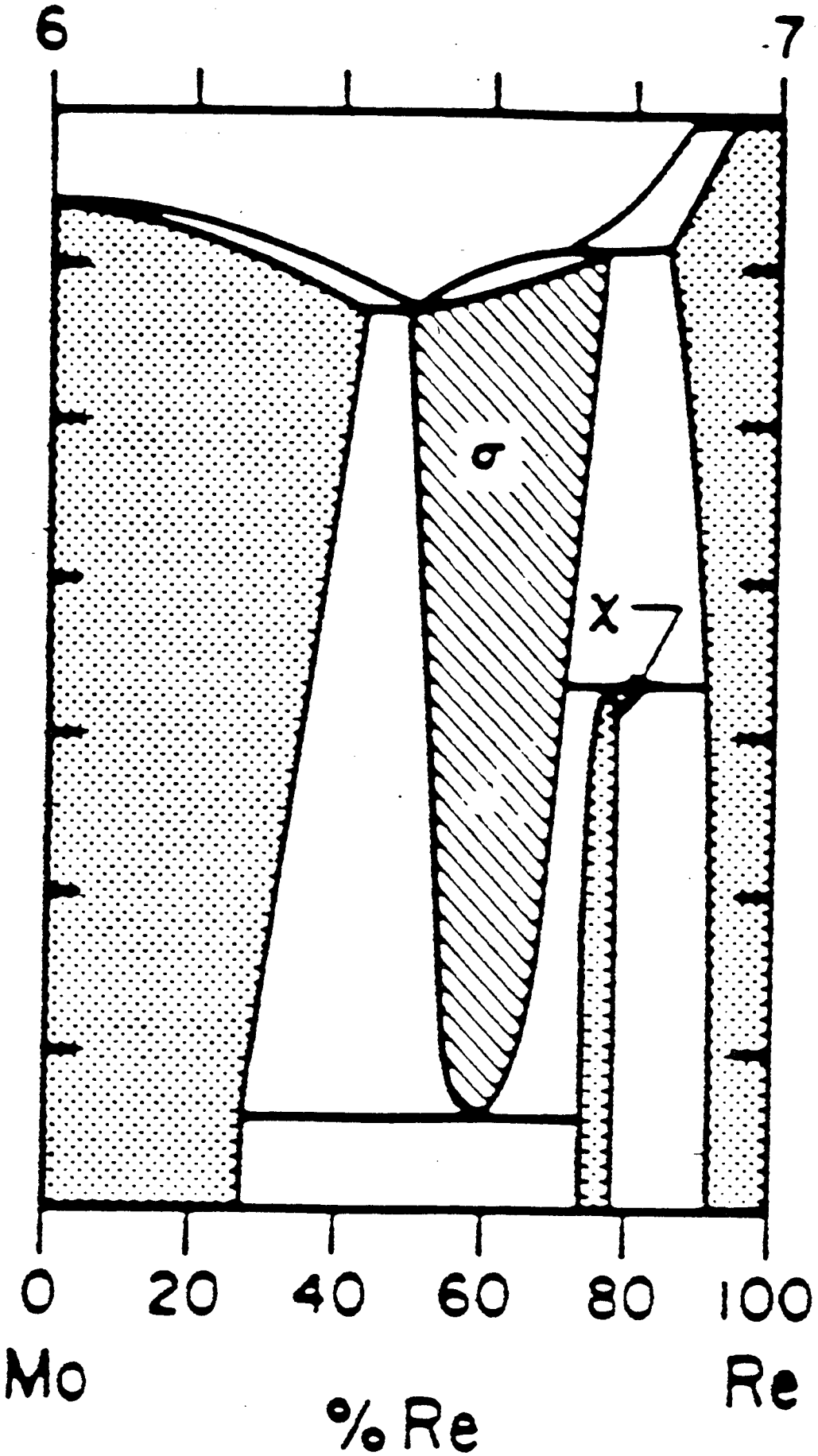
6
7
σ
χ
0
20
40
60
80
100
Mo
Re
% Re

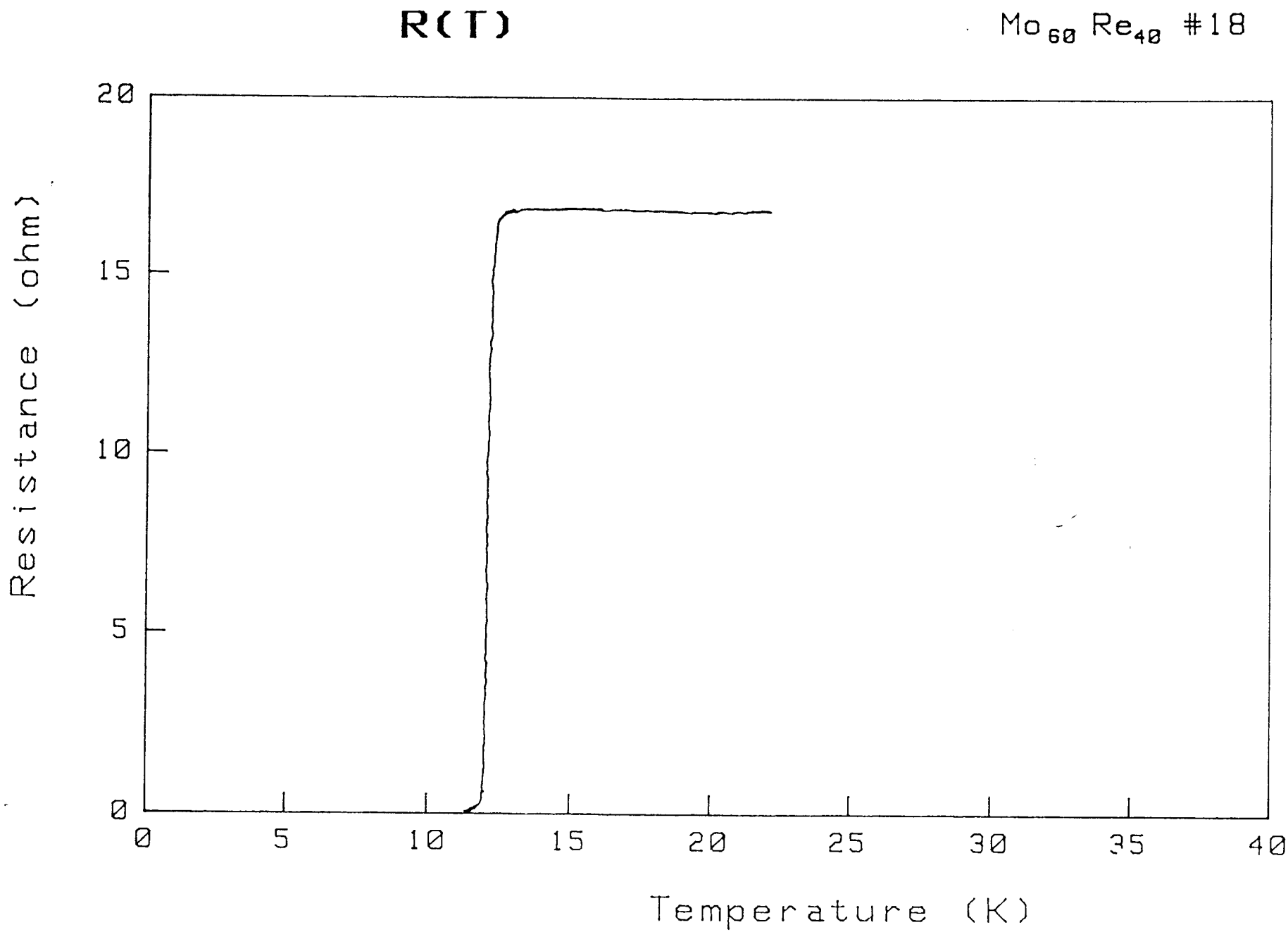
R(T)
Mo60 Re40 #18
Resistance (ohm)
20
15
10
5
0
0
5
10
15
20
25
30
35
40
Temperature (K)

Mo_{60}-Re_{40}

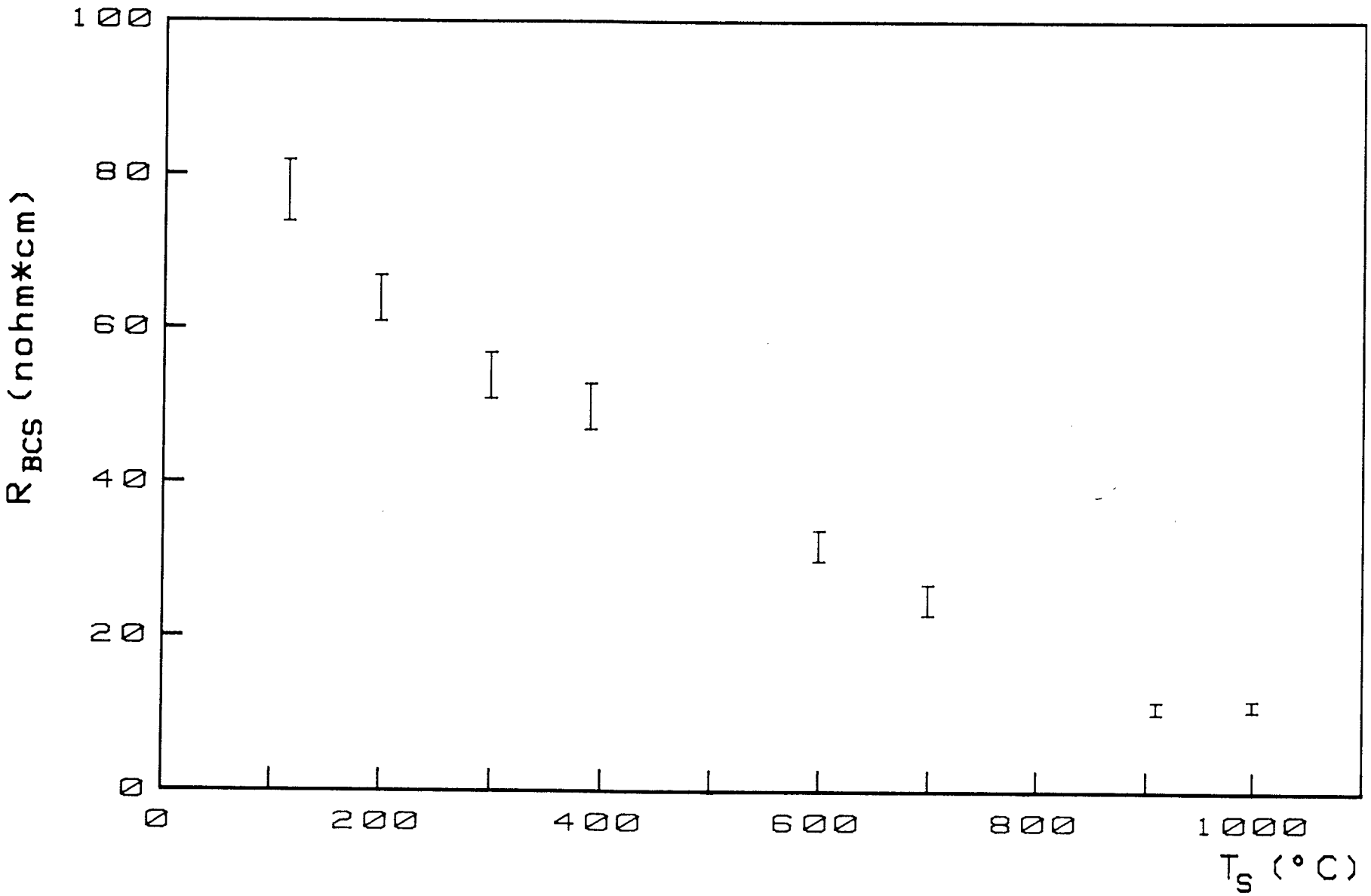

NbN has been considered as a promising material for superconductive cavities

T_c up to 17.3 K H_{c2} = 150 KG δ-NbN phase

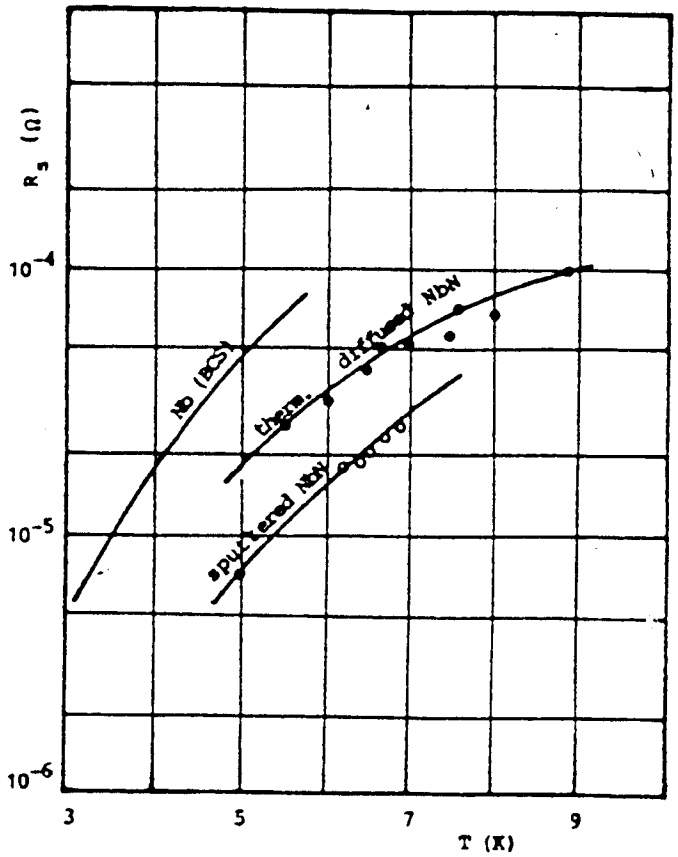

Mbaye, Pham Tu, Viet, Wartski, Villegier, Rev. Phys. Appl. 20, 457 (1985)

- Low secondary emission coefficent
- It can be easely fabricated in thin film form by reactive sputtering techniques with a good adherence on various substrates
- As all the carbides and Nitrides of transition metals, NbN is quite insensitive to disorder effects that means also scarcely sensitive to radiation

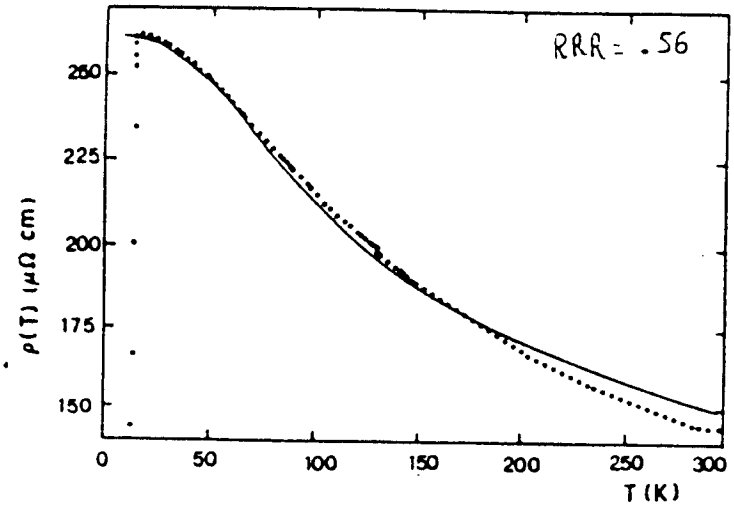

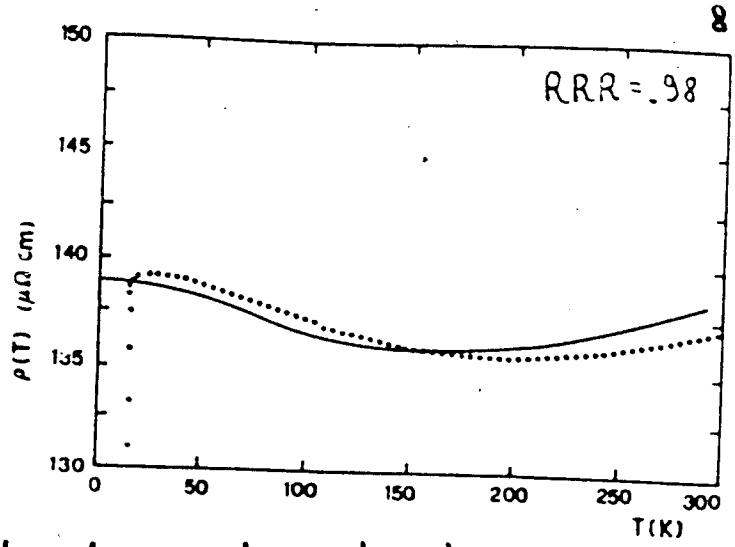

NbN grains surrounded by voids of very disordered intergranular regions

High ρ_0, low RRR negative TCR, minima in R(T) plot $\Longrightarrow$ Tunneling occurring between rather low resistivity grains separated by a semiconductive medium

single crystal: $\sigma = \frac{n e^2 \ell_\infty}{m v_F}$; Polycrystalline media: $\sigma = \frac{n e^2 \ell_\infty}{m v_F} G(\ell_\infty, D, \Gamma)$

Reiss, Vancea, Hoffman, Phys. Rev. Lett. 56, 2100 (1986)

$$G(\ell_\infty, D, \Gamma) = \Gamma^{\ell_\infty / D} \Rightarrow \ell_{eff} = \ell_\infty \Gamma^{\ell_\infty / D}$$

$$RRR = RRR_\infty \cdot \left[\frac{\rho(300)}{\rho_\infty(300)}\right]^{(1 - RRR_\infty)}$$

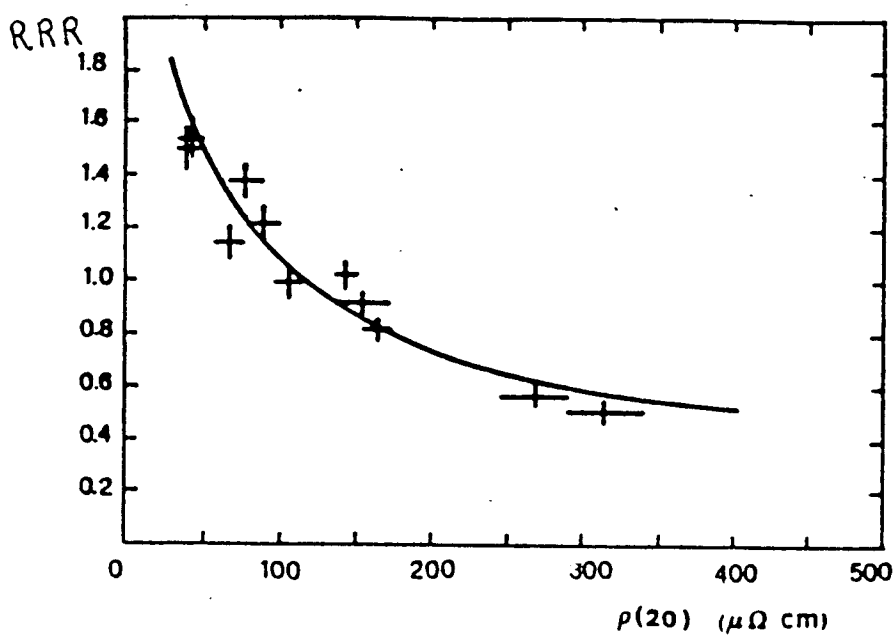

$\rho_\infty(300) = 57\,\mu\Omega \cdot cm$

$RRR_\infty = 2.2$

$(\rho_0)_\infty = 26\,\mu\Omega \cdot cm$

vacancies in the lattice

TiN $\begin{cases} RRR \text{ up to } 6 \\ \rho_0 \simeq 3\,\mu\Omega\,cm \end{cases}$

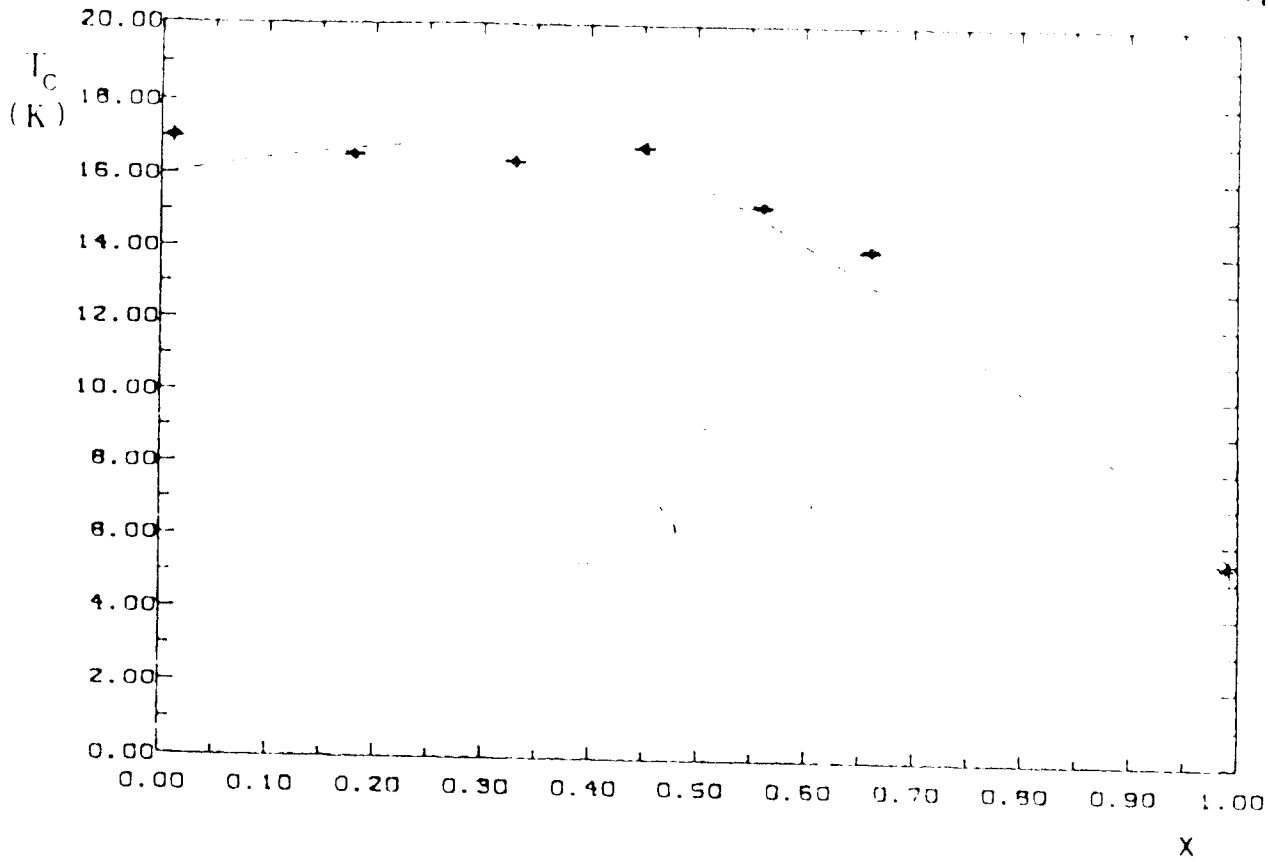

Fig. 2. Superconducting critical temperature Tc as a function of the composition (x) for our $(Nb_{1-x}Ti_x)N$ films. The dashed line represents the bulk results.

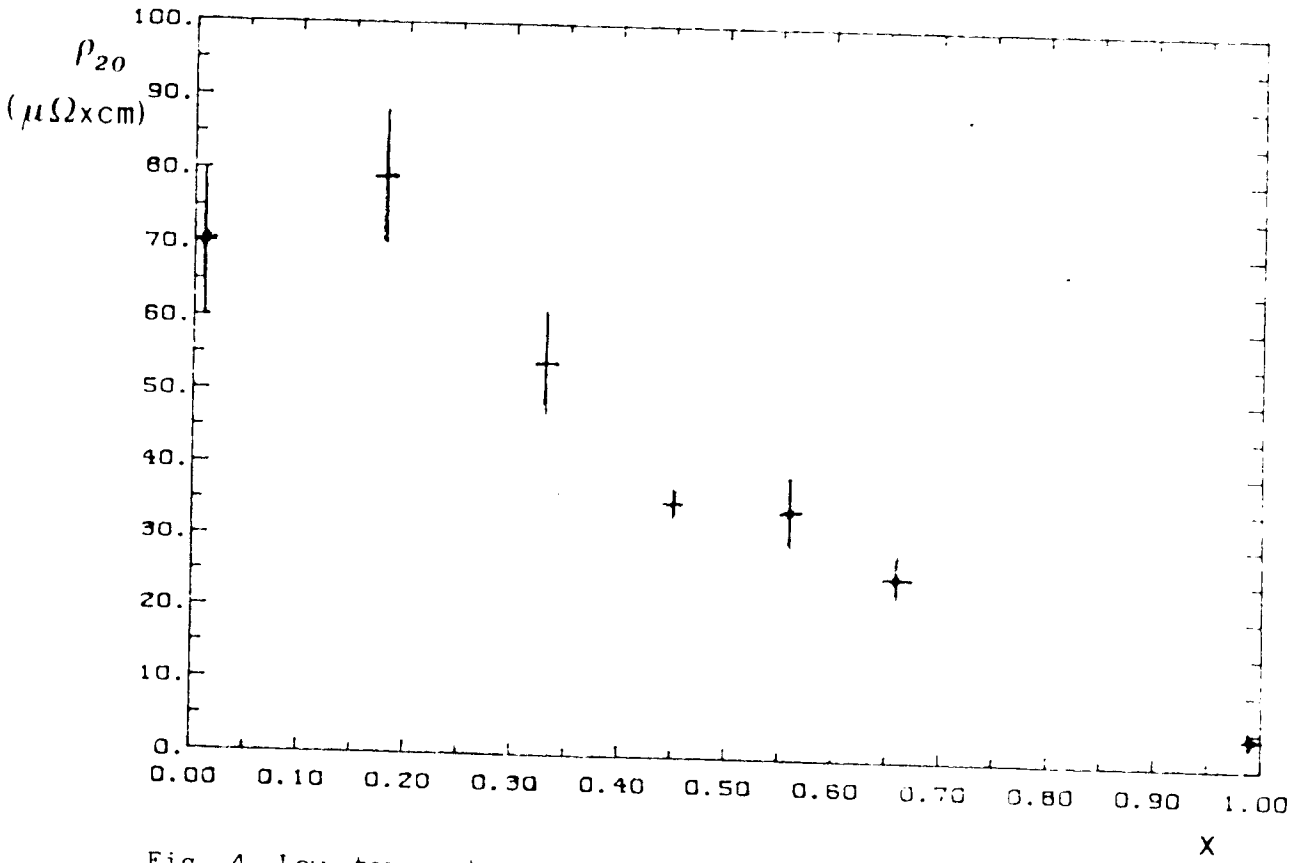

Fig. 4. Low temperature normal state resistivity ρ_{20} as a function of the composition (x) for our $(Nb_{1-x}Ti_x)N$ films.

72

	Ts (°C)	Tc (K)	ρ_n (μΩcm)	H_{c1} (Oe)	H_{sh} (Oe)	λ_o (Å)	R_s(BCS) (nΩ)
NbN	600	17	70	175	2100	2130	0.85
$(Nb_{0.54}Ti_{0.46})N$	600	16.8	35	280	2080	1515	0.67
NbN	200	15.3	170	78	1770	3500	5.4
$(Nb_{.77}Ti_{.33})N$	200	15.8	62	175	1860	2080	2.1

NbTi and NbZr largely used in magnet technology do not represent the best choice for rf cavities.

	Tc (K)	ρ_n ($\mu\Omega$ cm)	H_{cl} (Oe)	H_{sh} (Oe)	λ_o (Å)	R_s (BCS) (nΩ)
$Nb_{0.6}Ti_{0.4}$	9.8	40	165	1750	2120	50
$Nb_{0.75}Zr_{0.25}$	10.4	30	220	1930	1780	30
Nb_3Sn	18.2	20	535	4050	1100	0.27
NbN	17	70	175	2100	2130	0.85
Nb	9.25	2	1750	2400	400	33

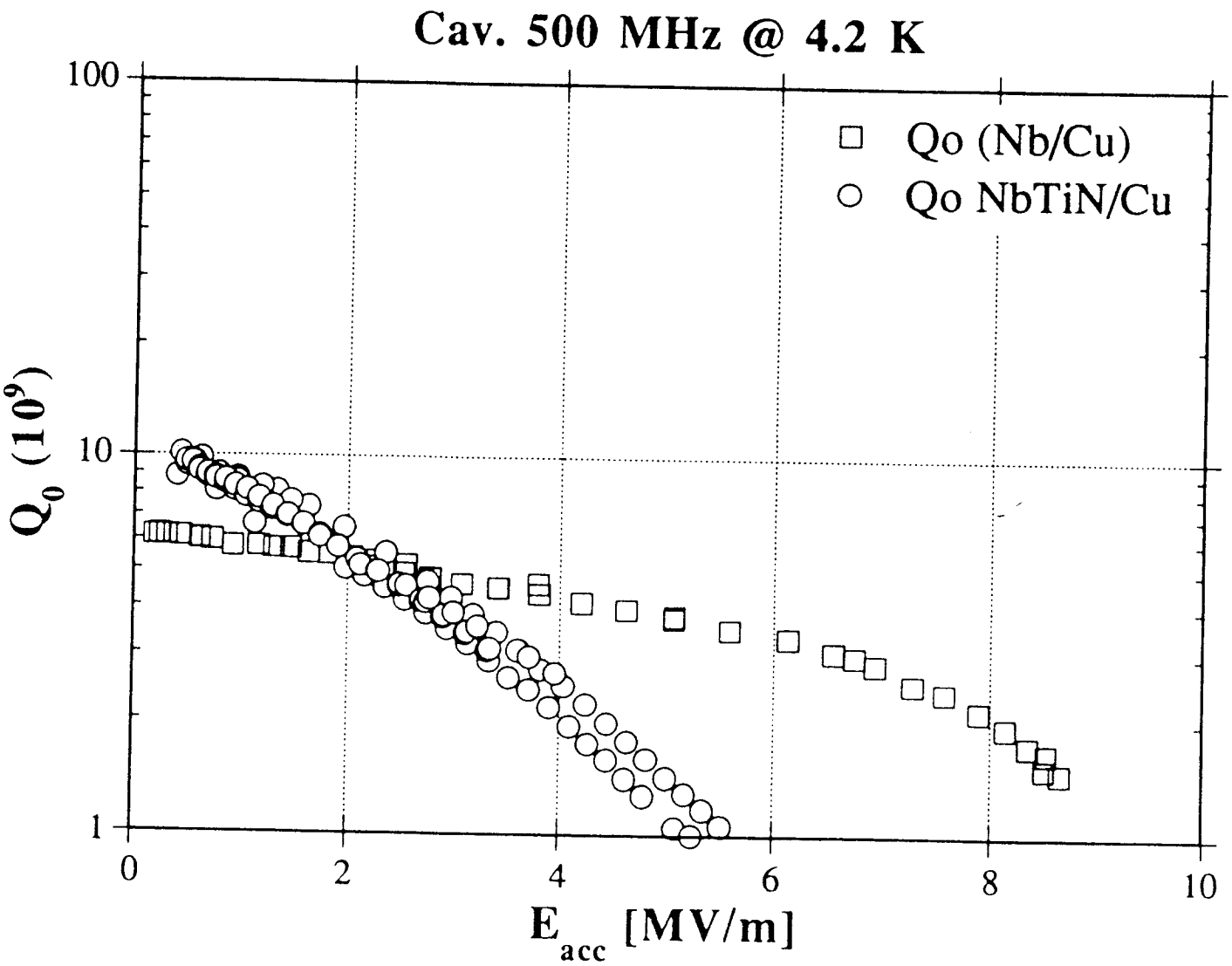
Cav. 500 MHz @ 4.2 K
Qo (Nb/Cu)
Qo NbTiN/Cu
Q_0 (10^9)
100
10
1
0
2
4
6
8
10
E_{acc} [MV/m]

Sputtering parameters common to all $(Nb_{1-x}Ti_x)N$ depositions.

Ultimate system pressure	:	$\lesssim 1\times10^{-7}$ mbar
Pressure before sputtering (heater on, main valve throttled)	:	$1\div2\times10^{-7}$ mbar
Argon Pressure	:	8×10^{-3} mbar
Substrate temperature Ts [a]	:	600 °C
Anode voltage	:	65 V
Anode current	:	6 A
Target voltage	:	400 V
Target current	:	1 A
Nitrogen Pressure ($P(N_2)$)	:	$3\div7\times10^{-3}$ mbar
Sputtering rate	:	4÷5 Å/sec
Film thickness	:	4000÷5000 Å

Status and Prospects of Nb_3Sn Cavities for Superconducting Linacs

Günter Müller, H. Piel, J. Pouryamout
Physics Department, University of Wuppertal, Germany

P. Boccard, P. Kneisel
TJNAF, Newport News, Virginia

17. September 1998

Part A

1. Motivation
2. Fabrication and microscopic quality of Nb_3Sn layers on high purity Nb cavities
3. Results of Nb_3Sn cavity tests
4. Conclusions

Acknowledgements:
A. Matheisen and D. Proch for RRR measurements

Part B + M. Perpeet, M. Weich

- Nb_3Sn-Films on sapphire substrates
- Influence of granularity
- H_{c1} measurements

Die Kristallstruktur von Nb_3Sn

A15 - Gitter

- kubisches Grundgitter (Sn)
- orthogonale Kettenpaare (Nb) → **1-dim. Modell** (J. Labbé, J. Friedel (1966))

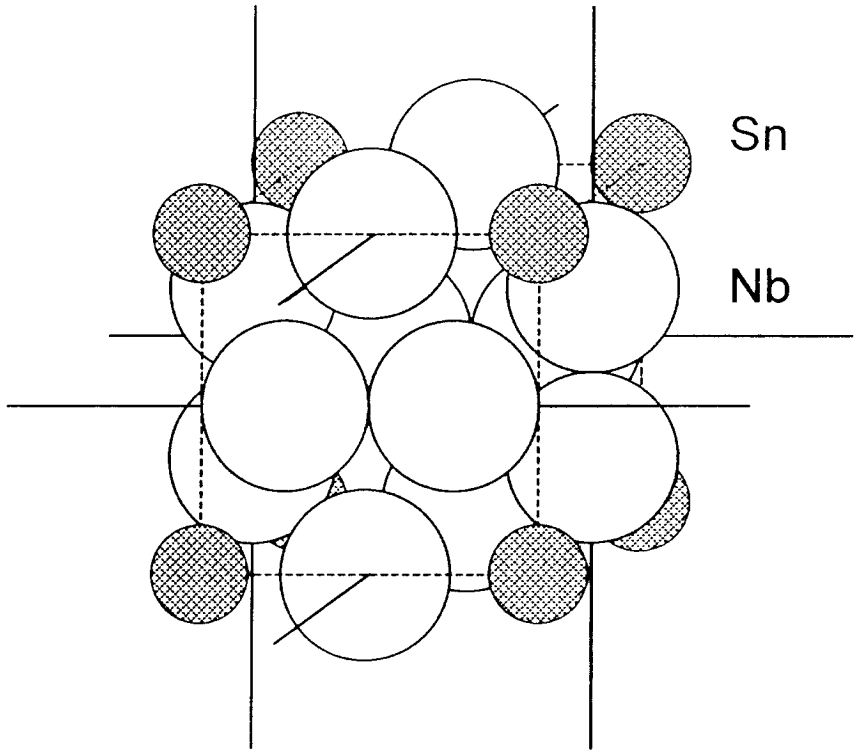

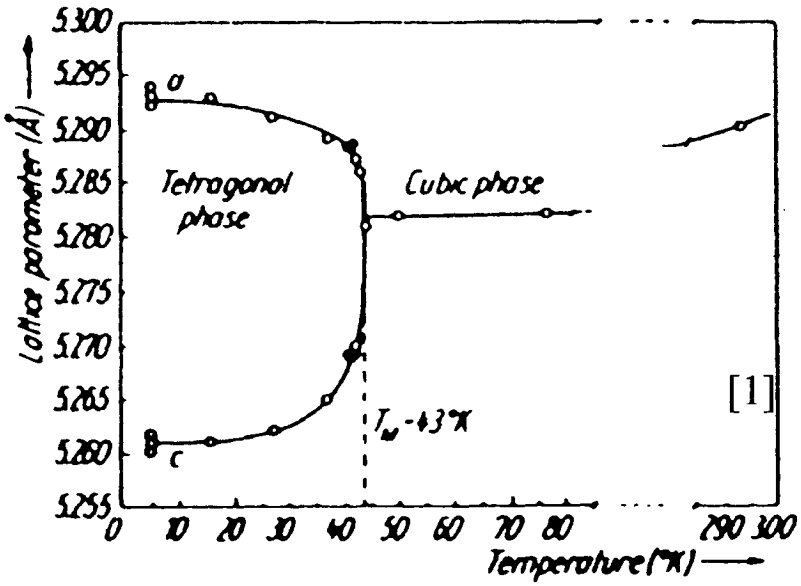

⇒ struktureller Phasenübergang (T_M = 43 K)

⇒ Supraleitung (T_c = 18 K, ...)

[1] J. Muller, *Rep. Prog. Phys.* **43**, 641 (1980)

Phasendiagramme der Nb-A15-Verb.-SL

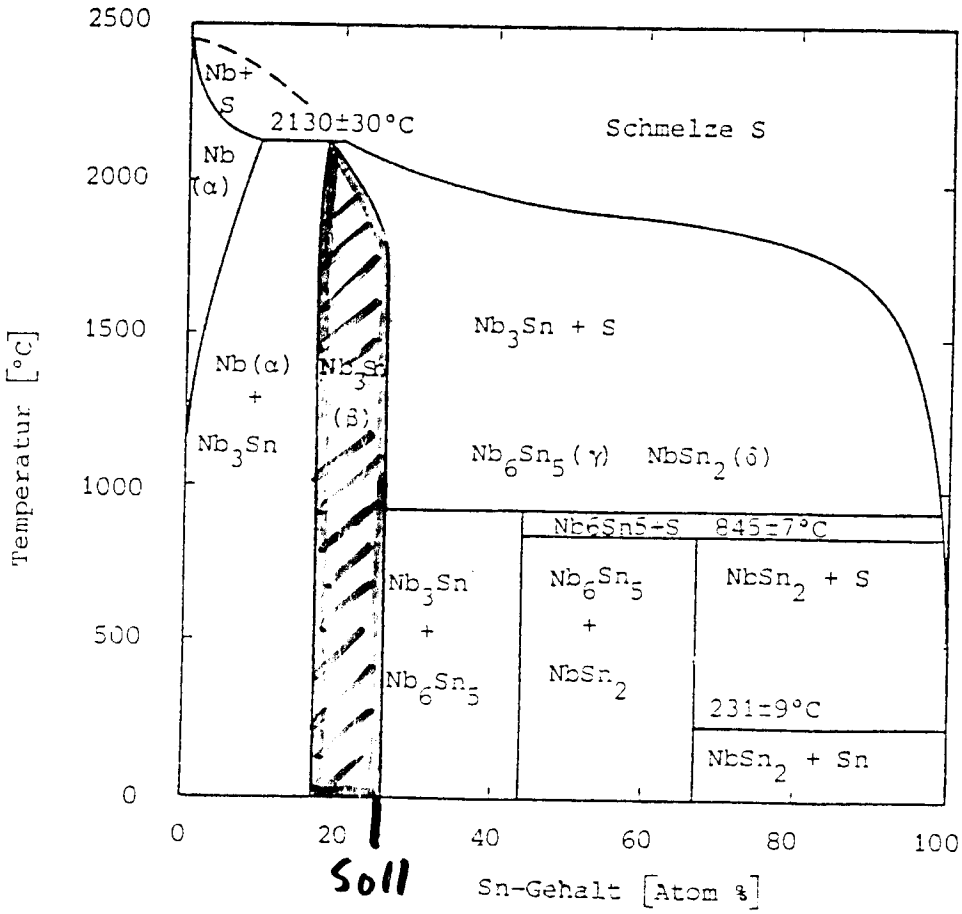

Nb-Sn

⇒ thermodynamisch stabil herstellbar

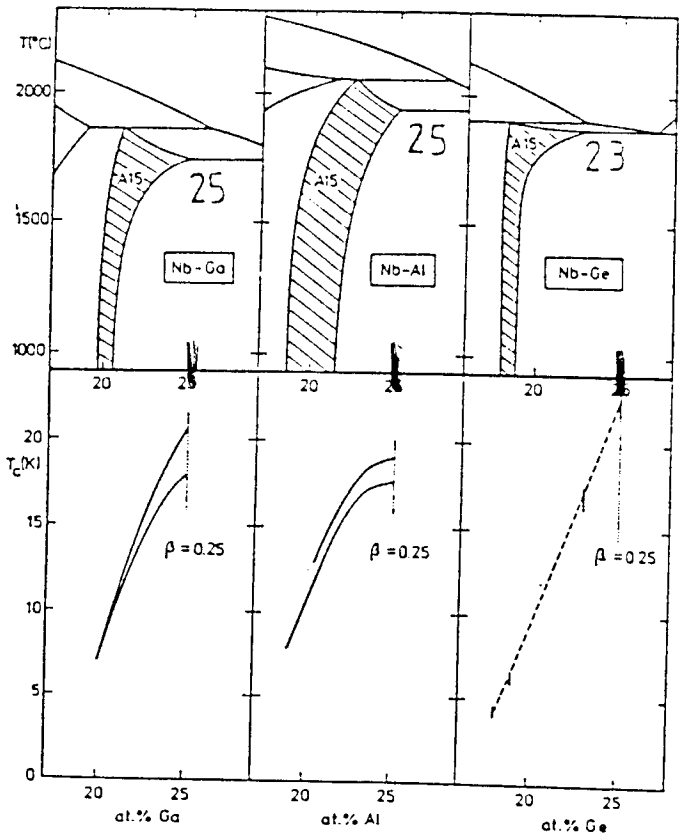

Nb-Ga Nb-Al Nb-Ge

⇒ thermodynamisch instabil
⇓
Zersetzung oder T_c-Abnahme

PREPARATION AND MICROSTRUCTURE OF Nb_3Sn-FILMS

Two – Step – Process

1. Nb-magnetron-sputtering onto sapphire substrate ($\varnothing \leq 1''$)
2. Sn-vapour-diffusion inside a Nb-tube (at $p_{Sn} = 6 \cdot 10^{-3}$ mbar) ~12h at $T \approx 1150°C$

→ phase pure Nb_3Sn-Films with columnar grain structure

→ avg. grain size d_G is correlated with film thickness d_F

→ growth process dominated by grain boundary diffusion

columnar structure

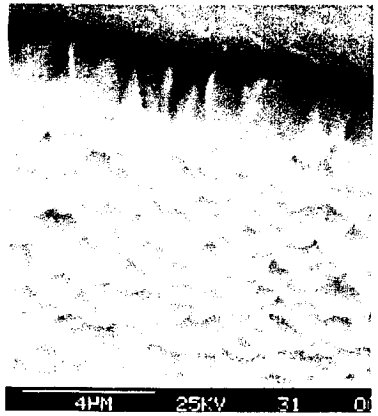

d_F = 0.5 µm

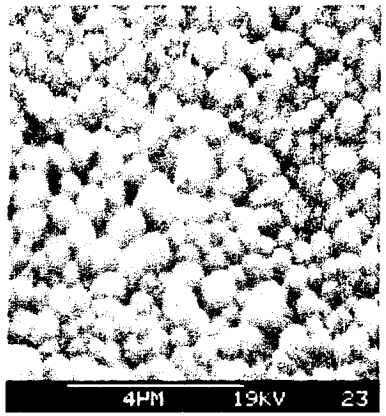

d_F = 2.2 µm

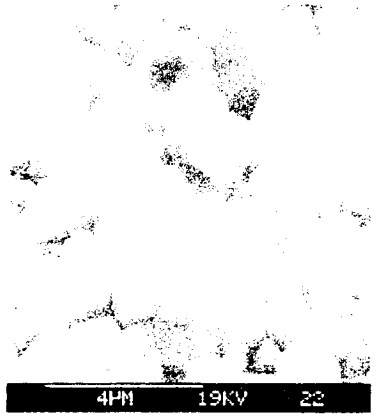

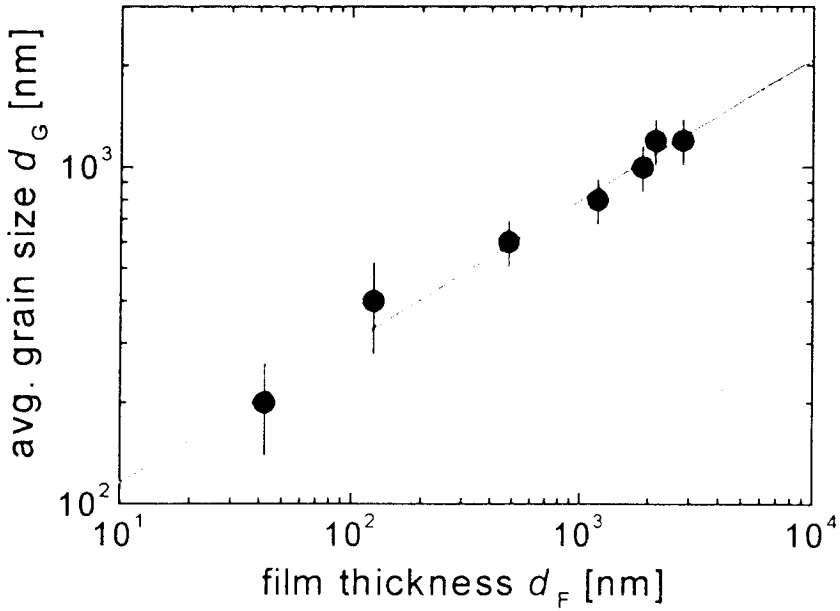

Universität Wuppertal Physics Department (Germany)
M. Perpeet

SURFACE IMPEDANCE AND CHARACTERISTIC PARAMETERS (d_F = 3 µm)

ω^2-scaled

1.5 GHz:

R_S (4K) = 3 nΩ

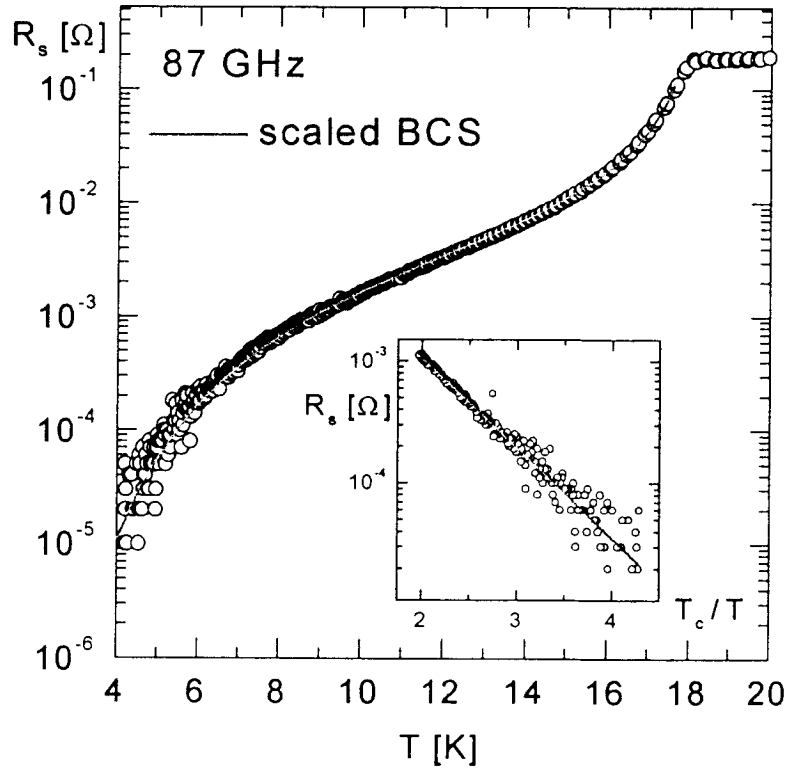

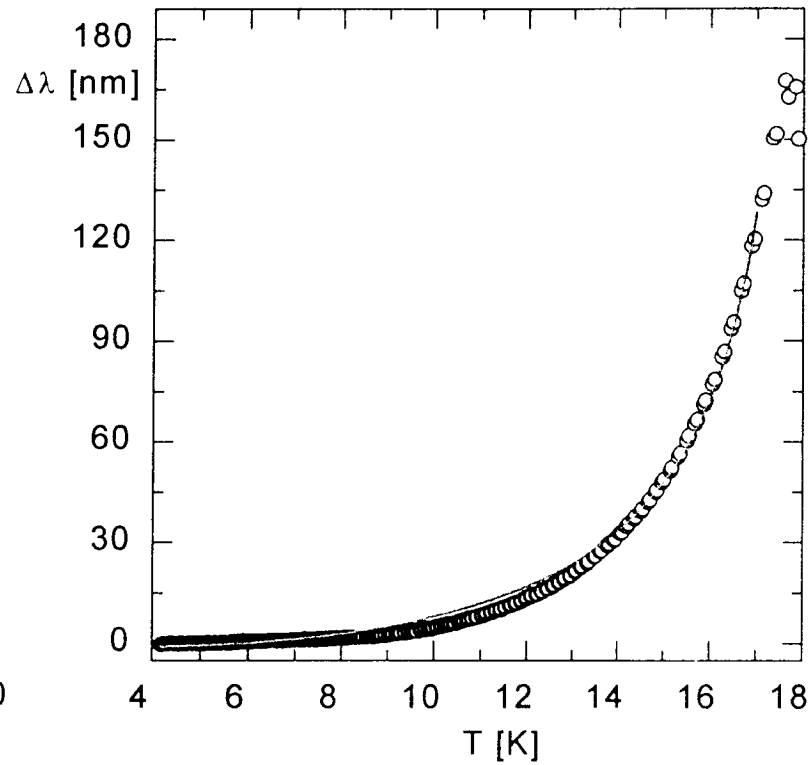

T_c [K]	Δ/kT_c	$\rho(T_c)$ [µΩcm]	λ_L [nm]	l [nm]	ξ_0 [nm]
18	2.1	7	91	15	7

Quality of Nb_3Sn-Films is similar to that of Nb_3Sn on bulk Nb-cavity

INFLUENCE OF GRANULARITY

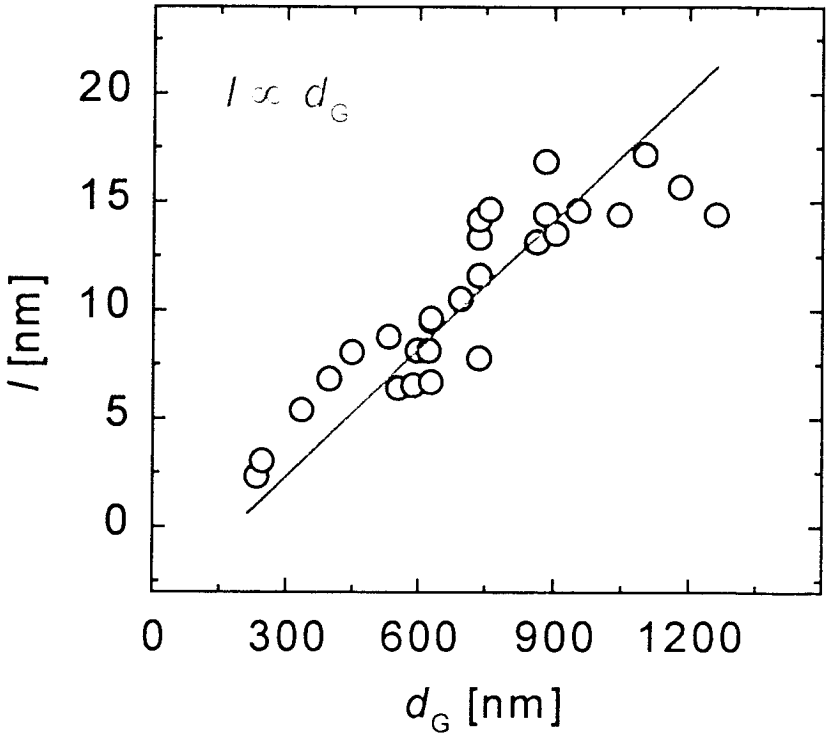

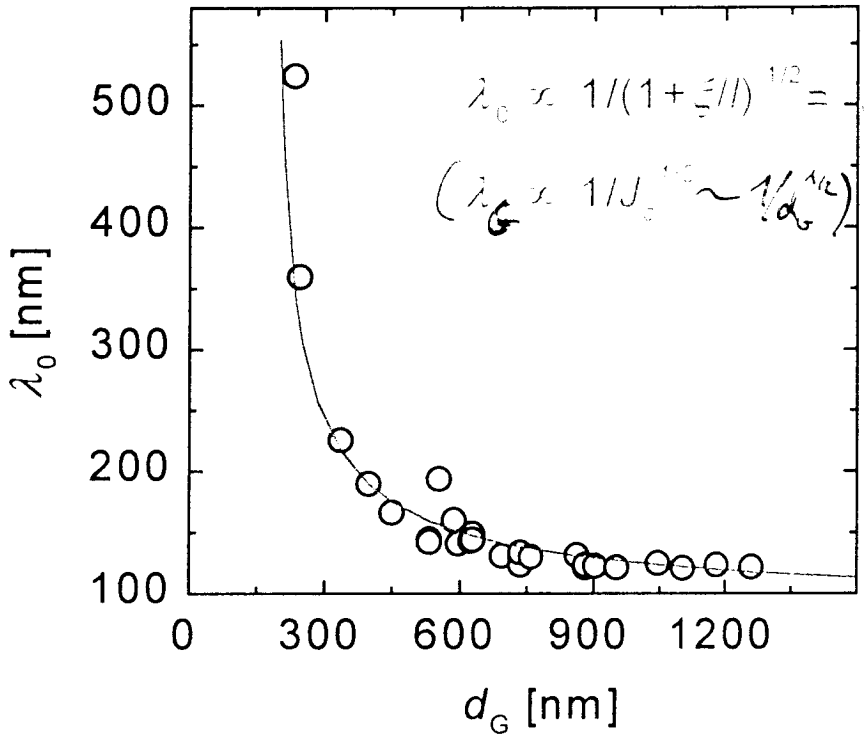

$\Downarrow$

grain boundary scattering dominates $\rho(T_c) \sim \frac{1}{e}$

$\Downarrow$

l dominates λ_0 and j_c

polycrystalline Nb_3Sn-Films are granular superconductors with weak links

MICROWAVE FIELD LIMITATION OF NB_3SN-FILMS

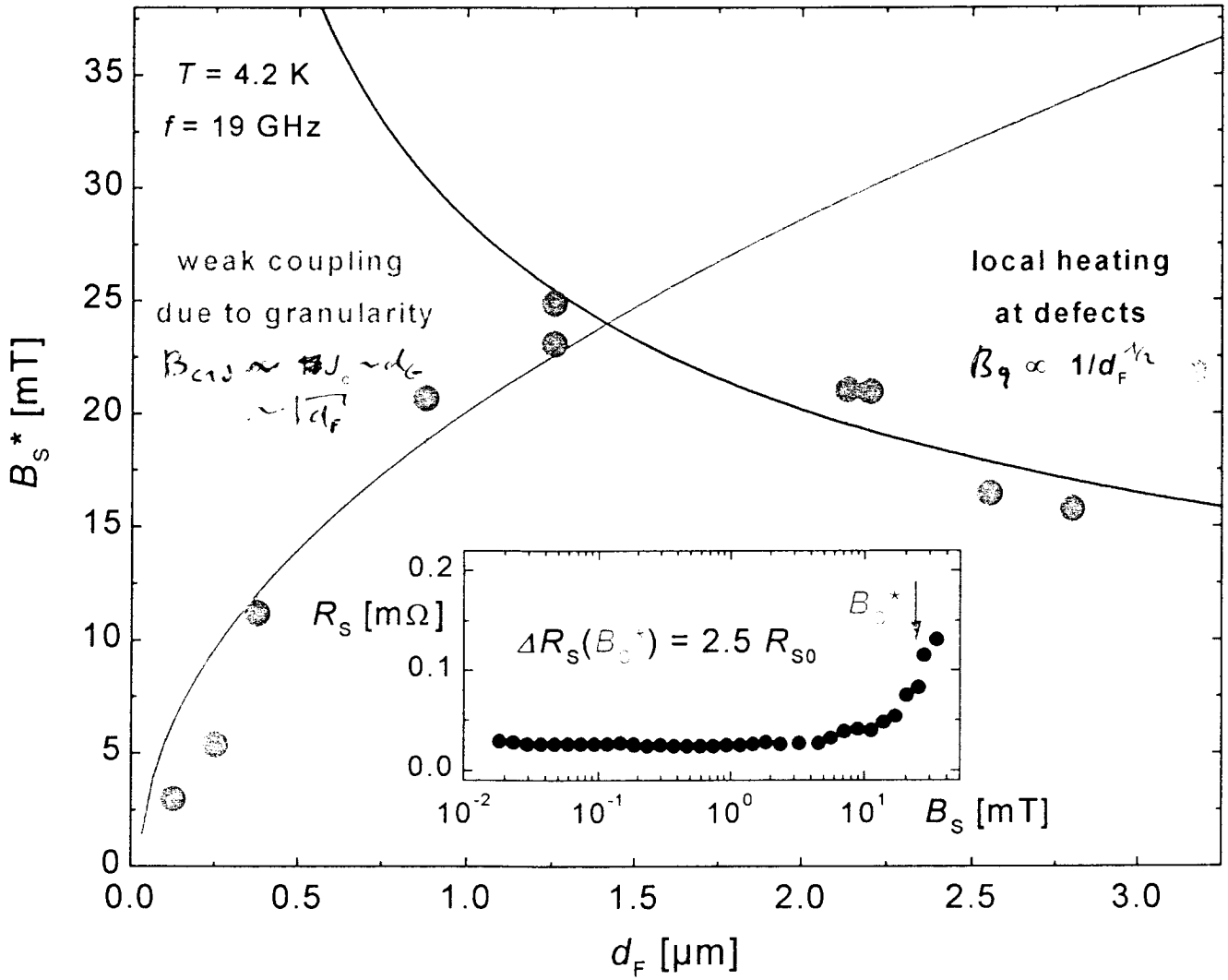

B_{c1} (≅ 140 mT) and B_c / B_{sh} can not be reached because of granularity

Universität Wuppertal
Fachbereich Physik

Z_S im DC - Magnetfeld

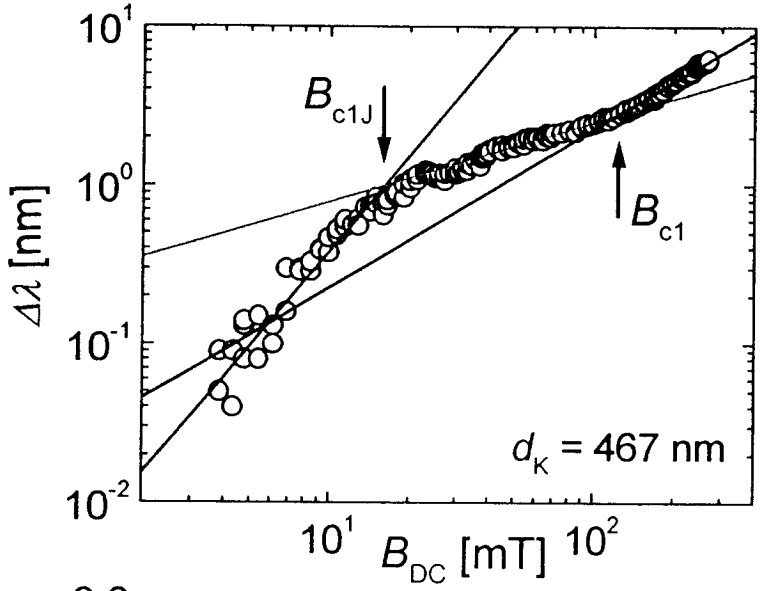

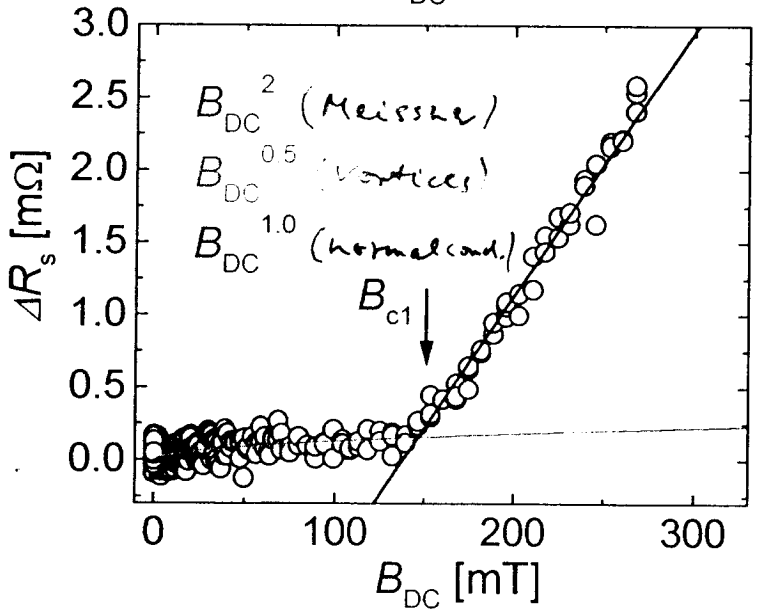

B_{c1}	aus $\Delta\lambda$	**133 ± 17 mT**
	aus ΔR_S	**146 ± 20 mT**
	(induktiv $(dB_{c2}/dT\|_{Tc})$	137 ± 20 mT)

- $B_{c1} >> B_S^*$

B_{c1J}

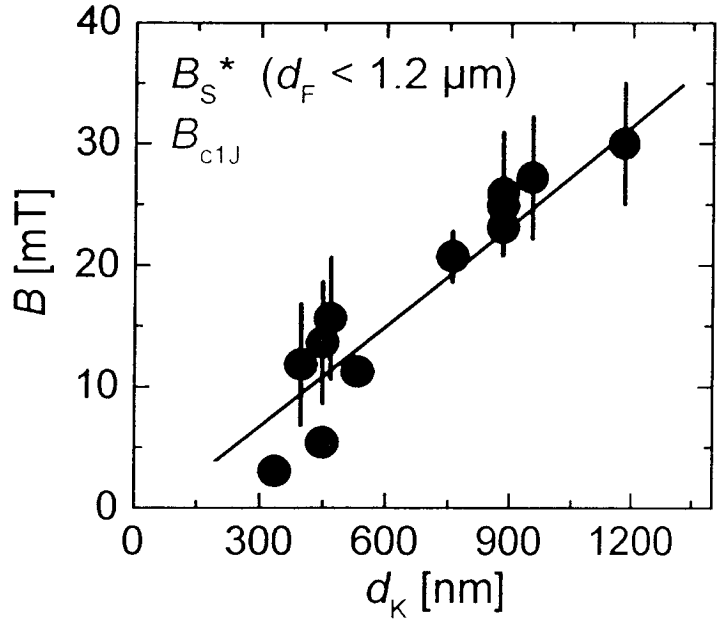

- **d_F < 1.2 µm: HF-Feldstärkebegrenzung durch Granularität — Korngrenzen als „weak links“.**

Fabrication of Nb_3Sn Layers on Bulk Nb Cavities by means of the Vapour Diffusion Technique

Nb_3Sn coating furnace for accelerator cavities (f≥1Ghz, L≤1m) with seperate heaters for cavity and Sn source (T≤1200°C)

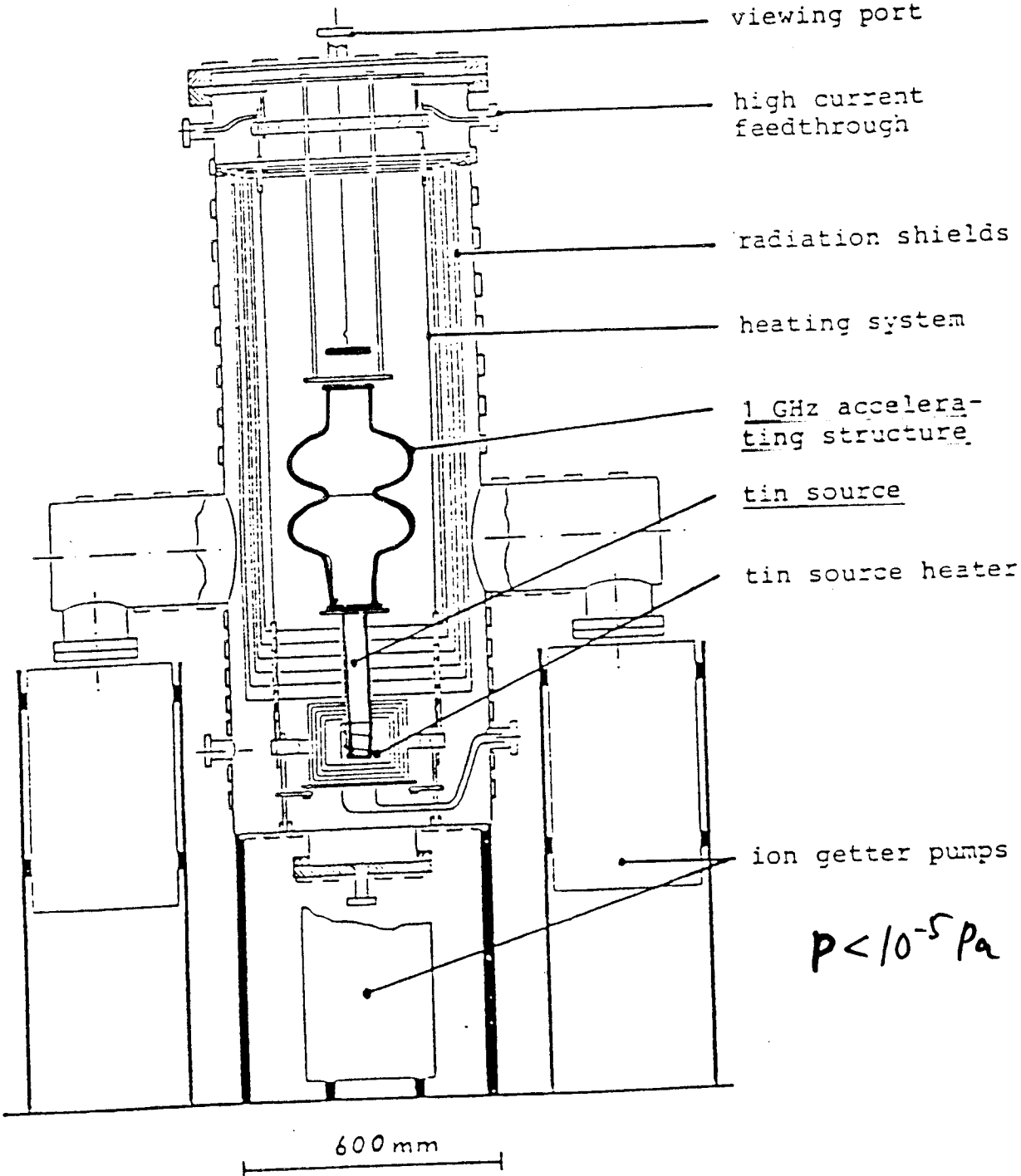

⇒ Improved nucleation of Nb_3Sn especially on high purity Nb by $SnCl_2$ (at T≥200°C) and oversaturated Sn pressure (1Pa)

Typical temperature settings to grow Nb_3Sn by vapour diffusion

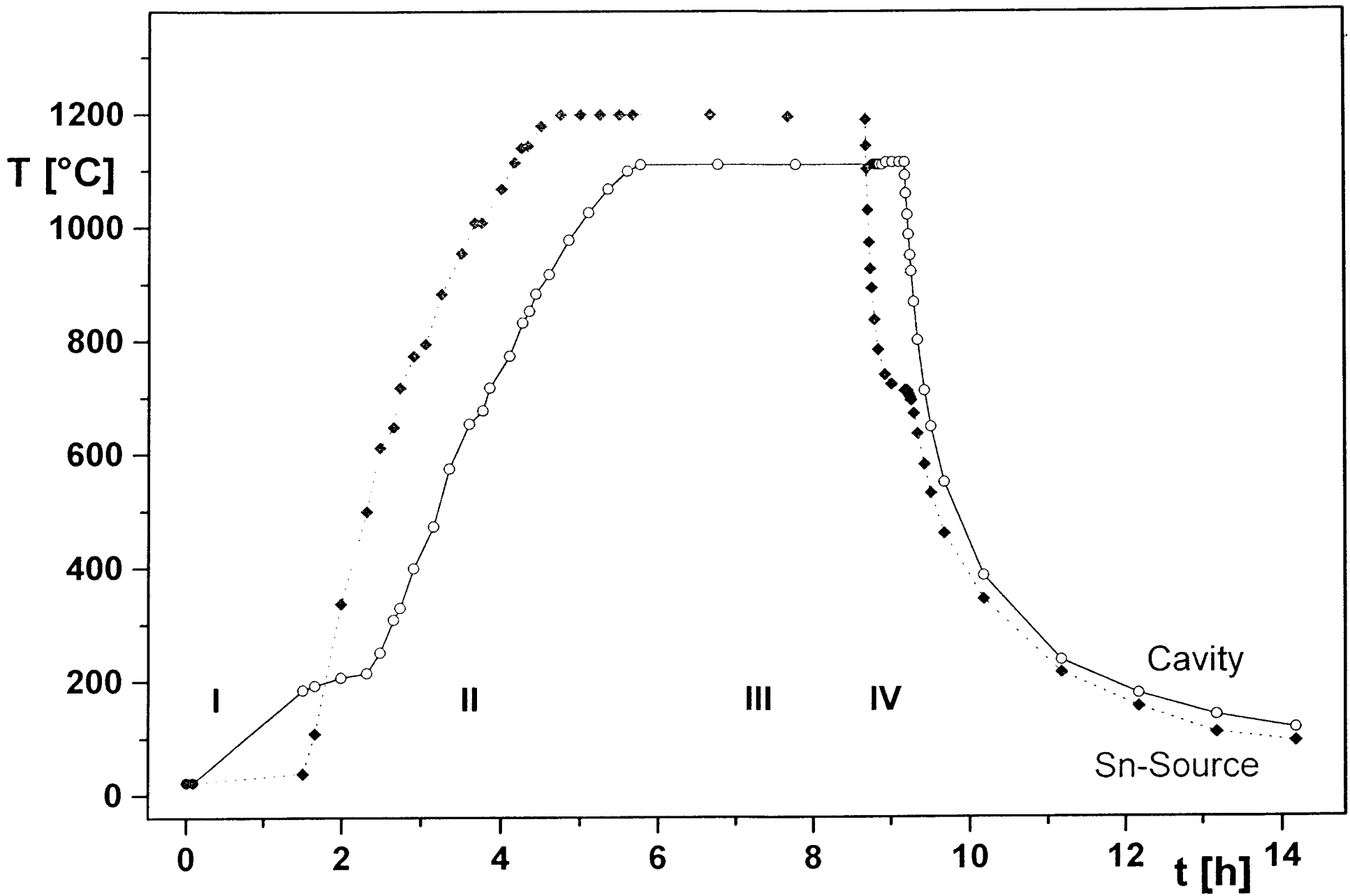

Sn nucleation on high purity Nb by $SnCl_2$ at 200°C

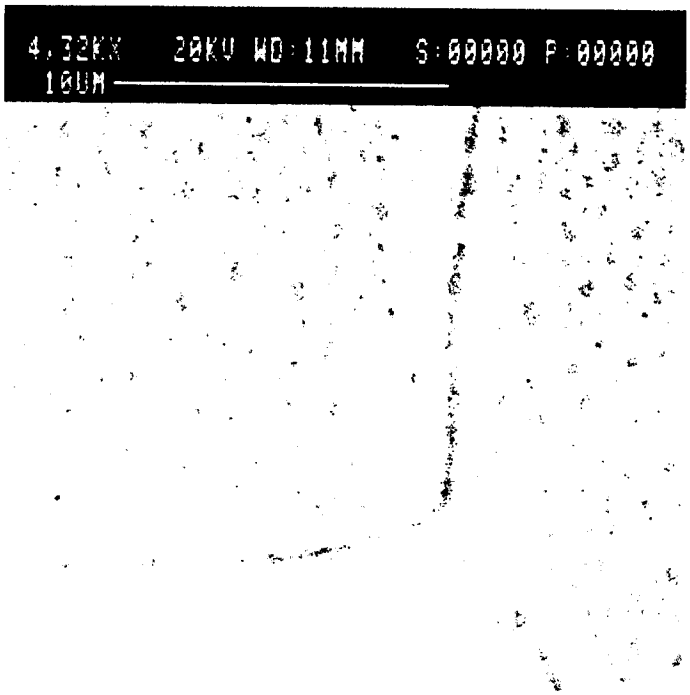

Nb_3Sn layer grown for 3h at 1100°C and P_{sn}=1Pa

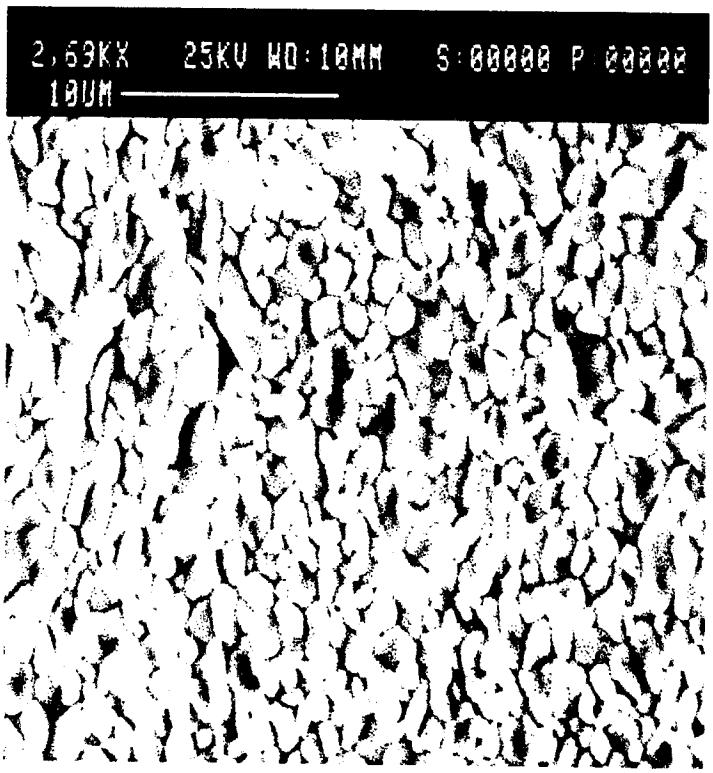

Depth profile of typical Nb_3Sn film (measured by EDX)

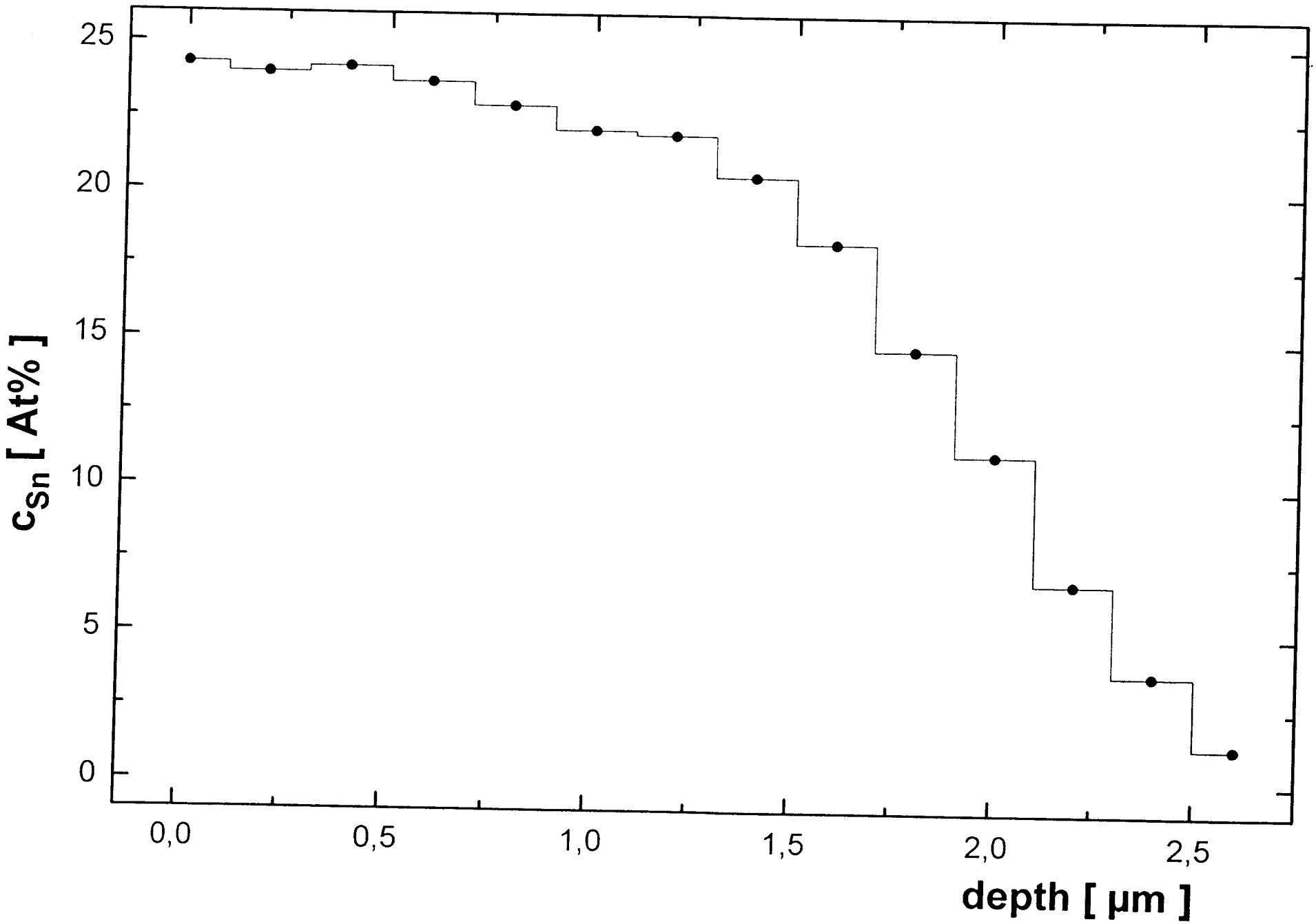

Conservation of high bulk RRR after optimizing the Nb_3Sn-coating procedure

by means of Ti-Liner around cavity

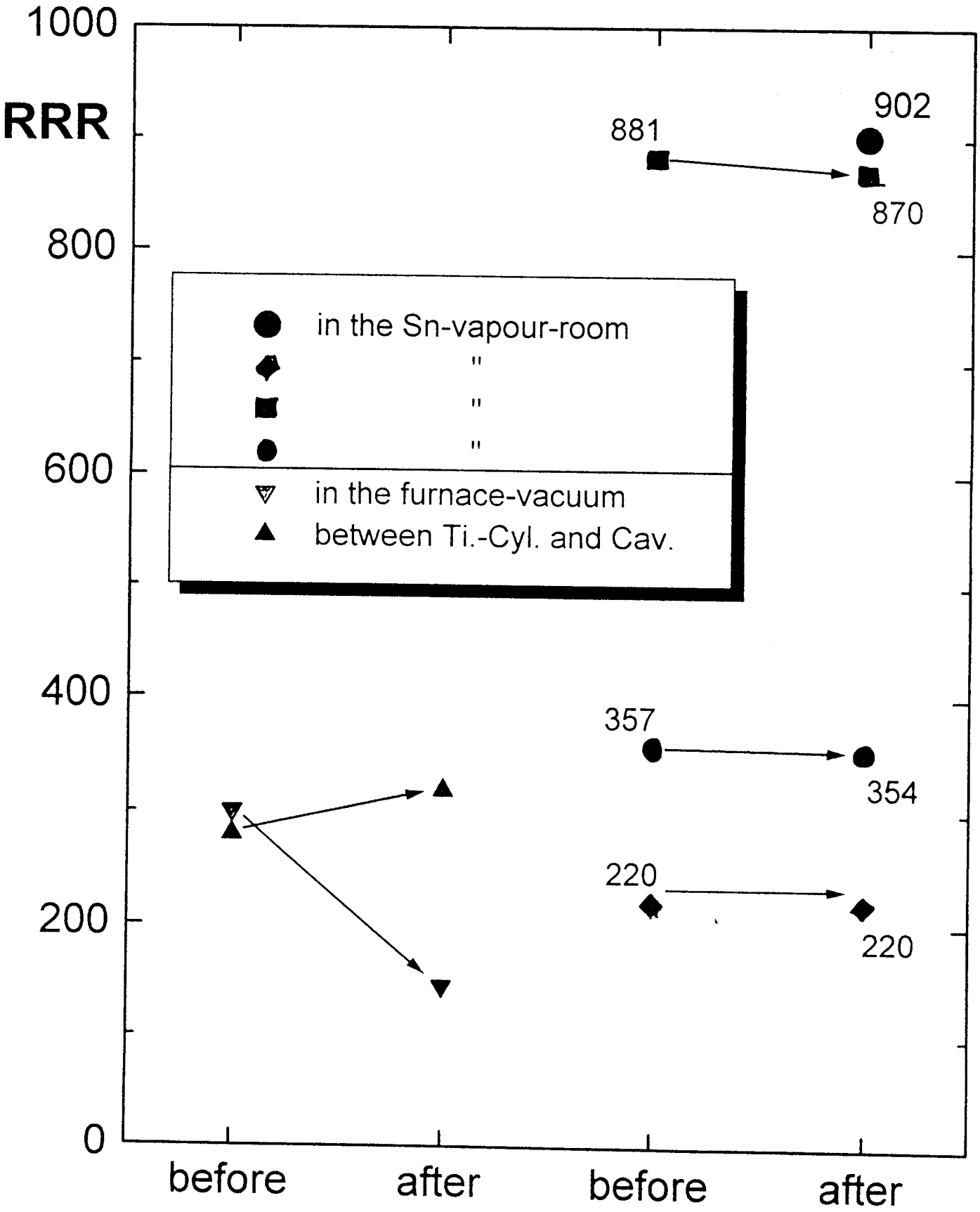

Q(E)-performance of the first two Nb_3Sn-coated 1.5*GHz* singel-cell cavities

in comparison to pure Nb at 4.2*K* and 2*K*

measured by Peter Kneisel and CEBAF

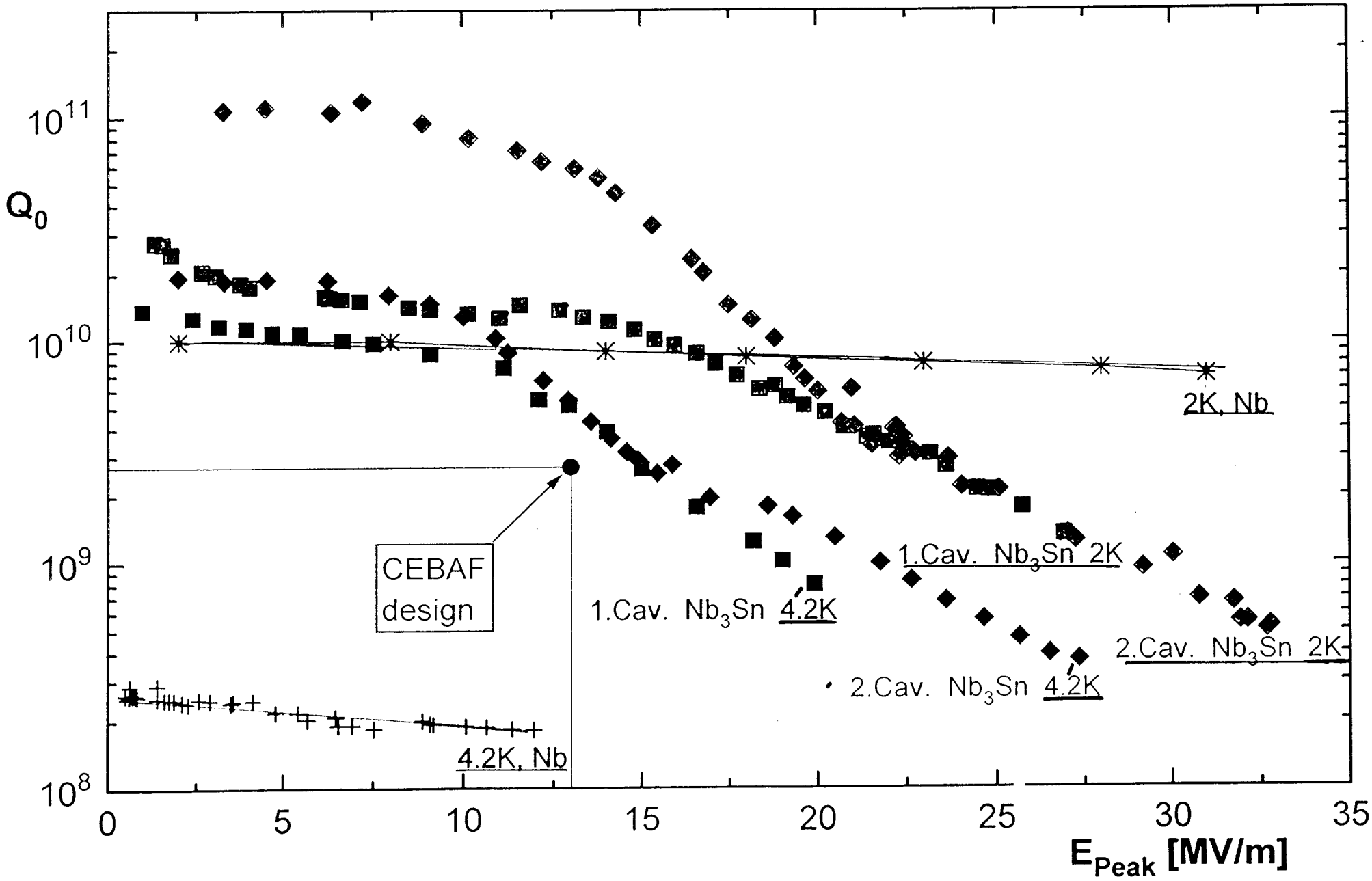

First Results of Nb_3Sn 5-cell Cavity at 1.5 GHz

CEBAF model structure without waveguide couplers

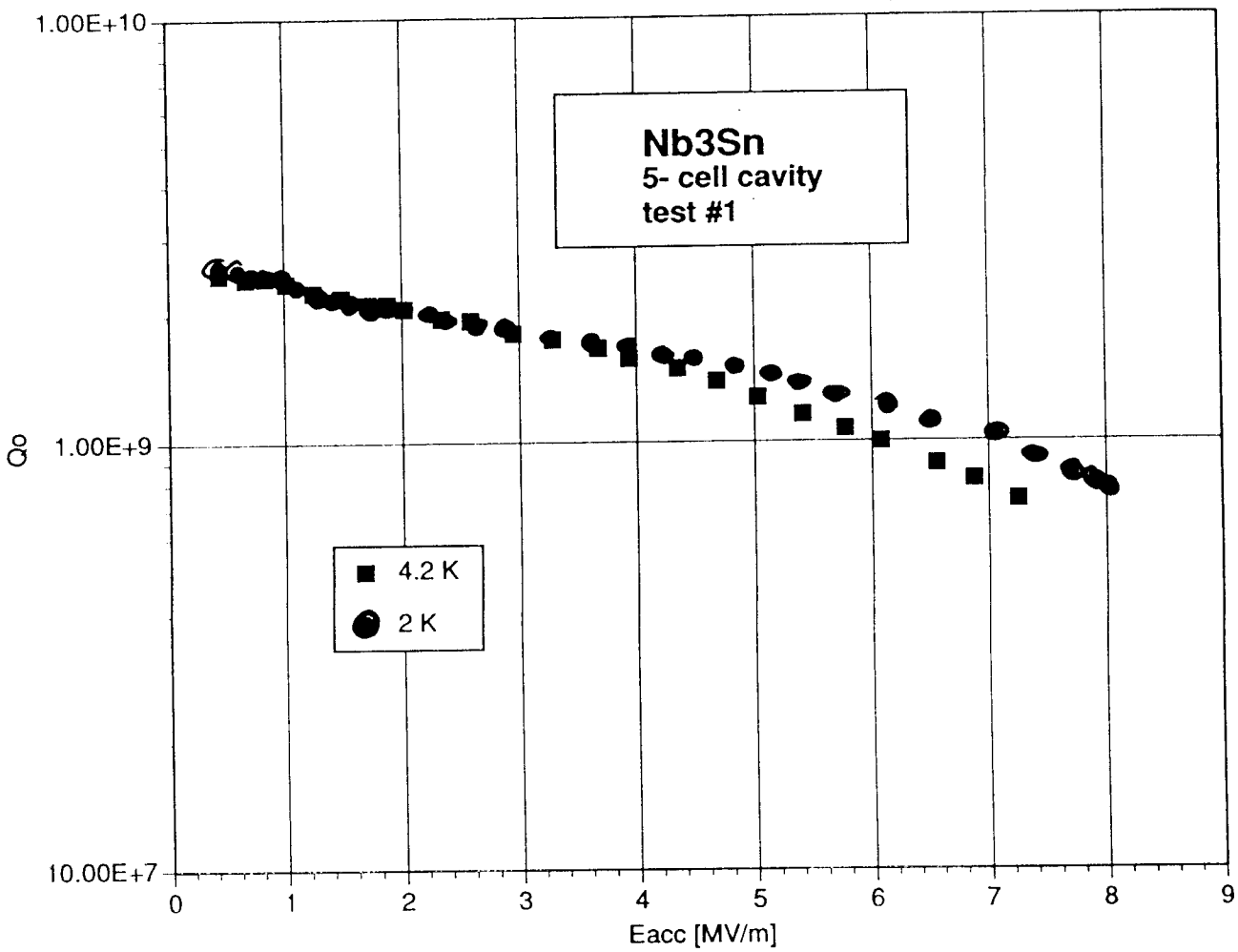

⇒ after HPWR Eacc= 7 MV/m (Ep= 16 MV/m) achieved at 4.2K

⇒ no improvement but quenches after oxypolishing

⇒ transfer of 1-cell results to 5-cell structures challenging

Cavity #1

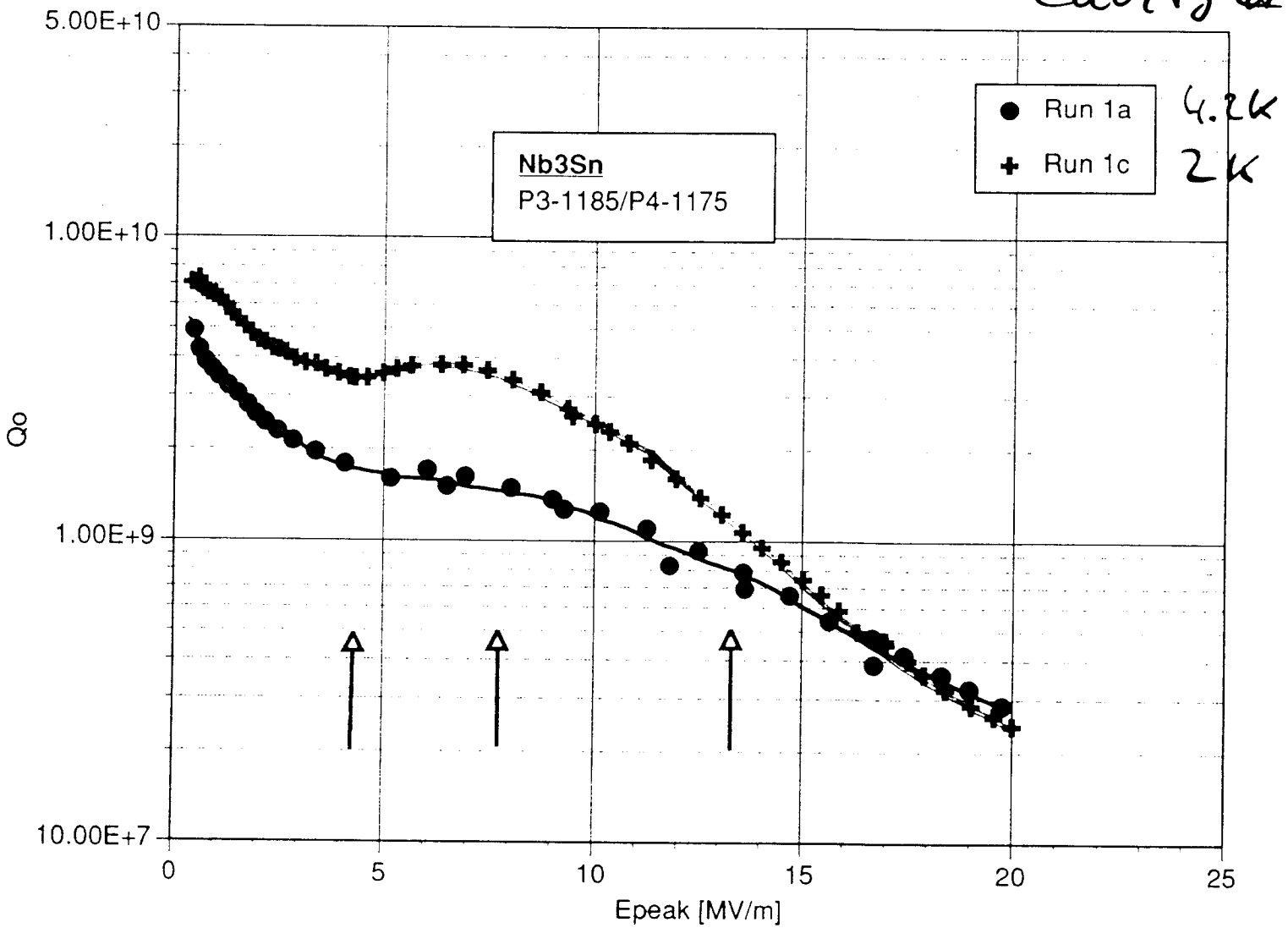

Qo vs Epeak after Oxipolishing ⇒ Degradation

Surface Resistance of two Nb_3Sn Coated 1.5 GHz Single-Cell Cavities (Nb RRR=300)

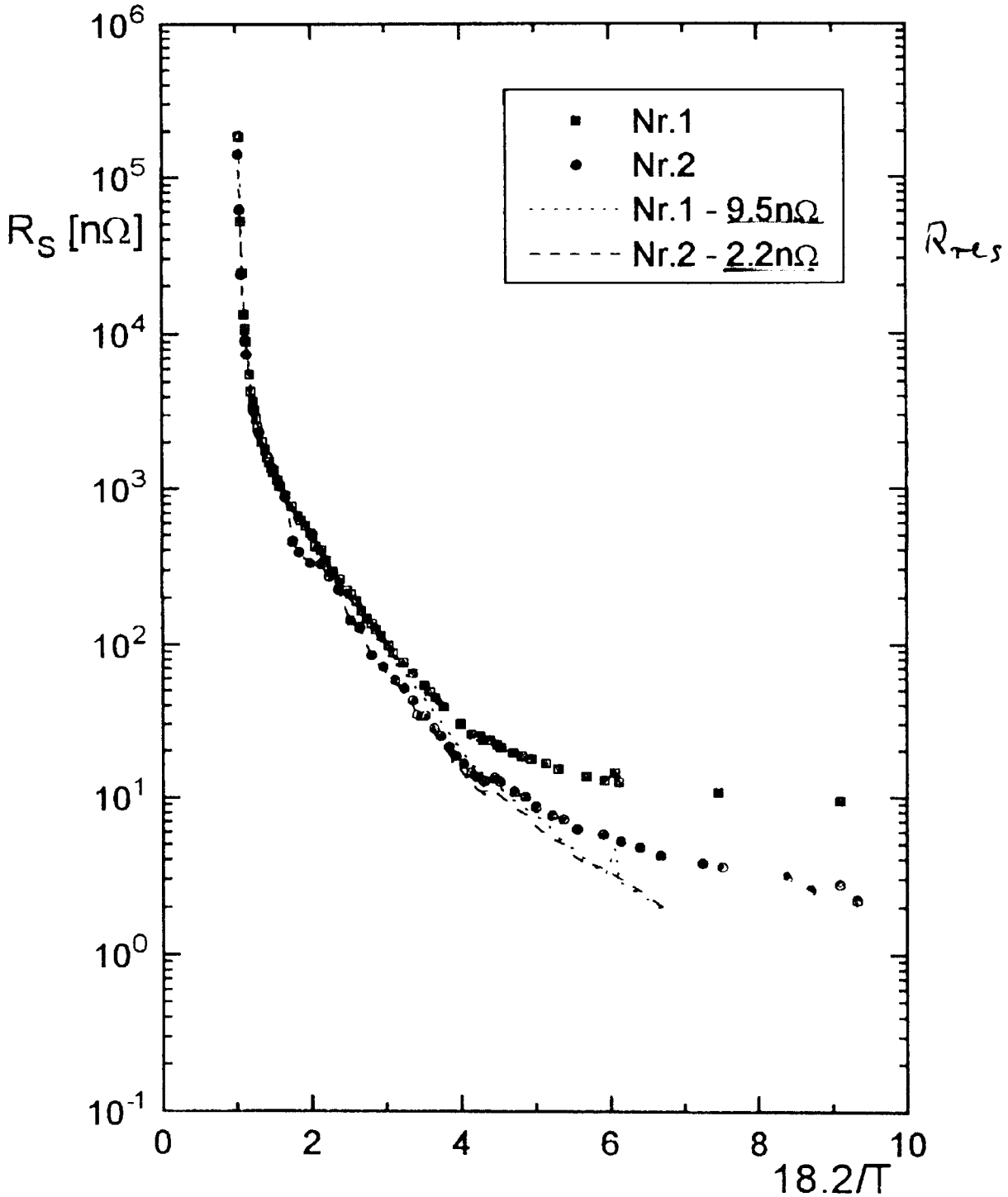

⇒ Extremely low Rres < 10 nΩ possible
for optimized fabrication parameters and surface cleaning (HPWR) and slow cooling rates (1K/6min) in the supercond. transition range

Temperature Mapping of Nb_3Sn Cavities in Subcooled Helium ($T \geq 2.2K$)

Rotating arm with 16 Allen Bradley resistors (100Ω, 1/8W)

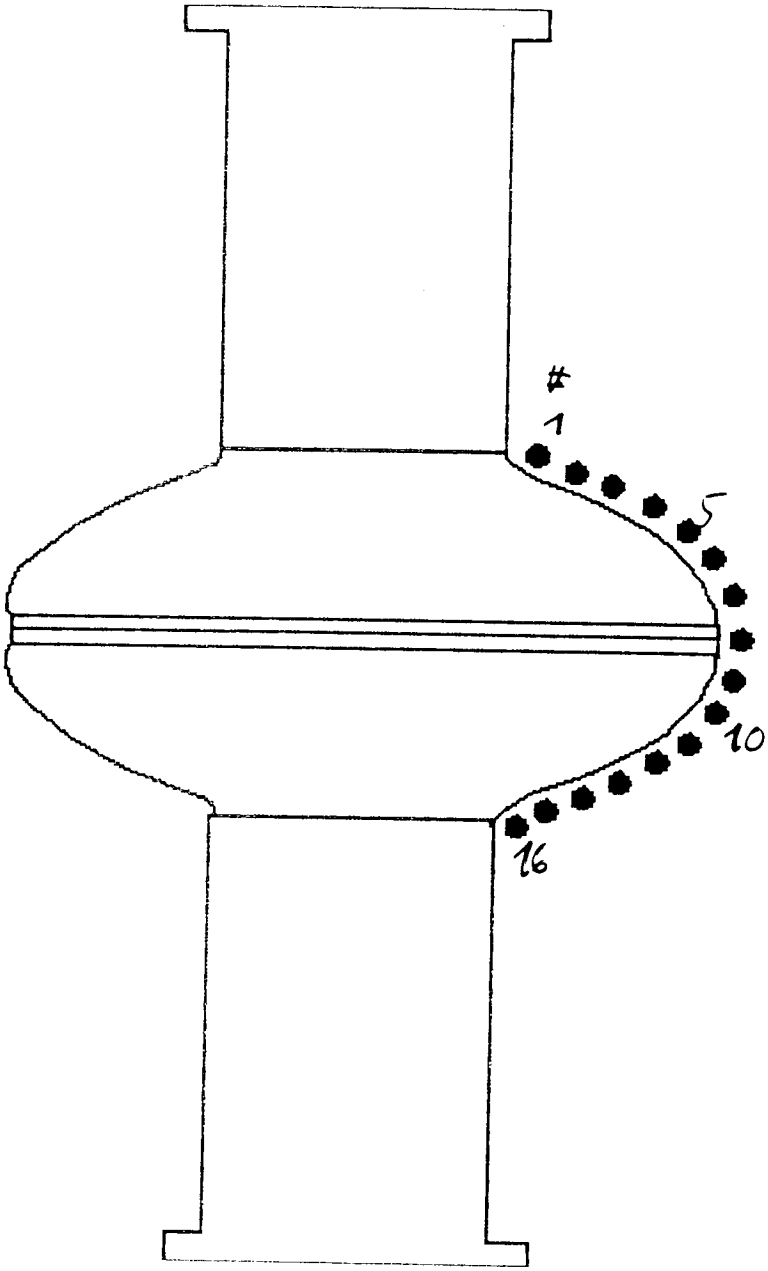

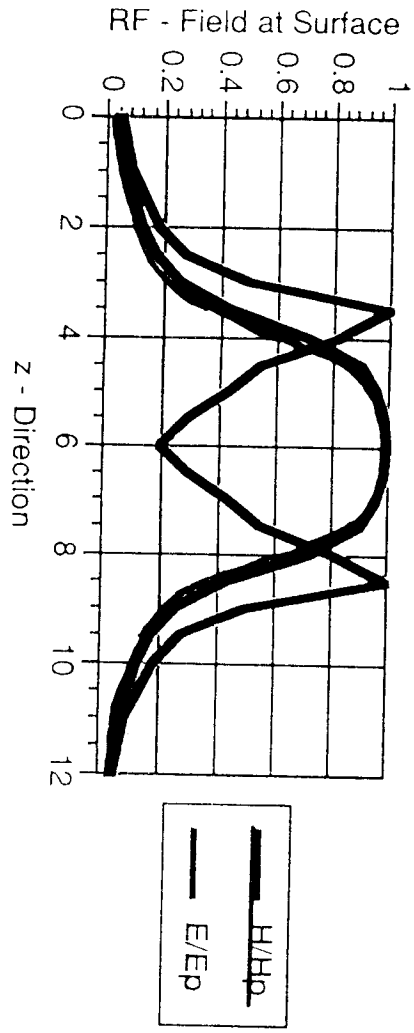

→ Temperature maps of entire cavity surface at constant power
→ Temperature increase of the 16 resistors with field at fixed ϕ

CAVITY TEST SYSTEM WITH THERMOMETRY

at TJNAF

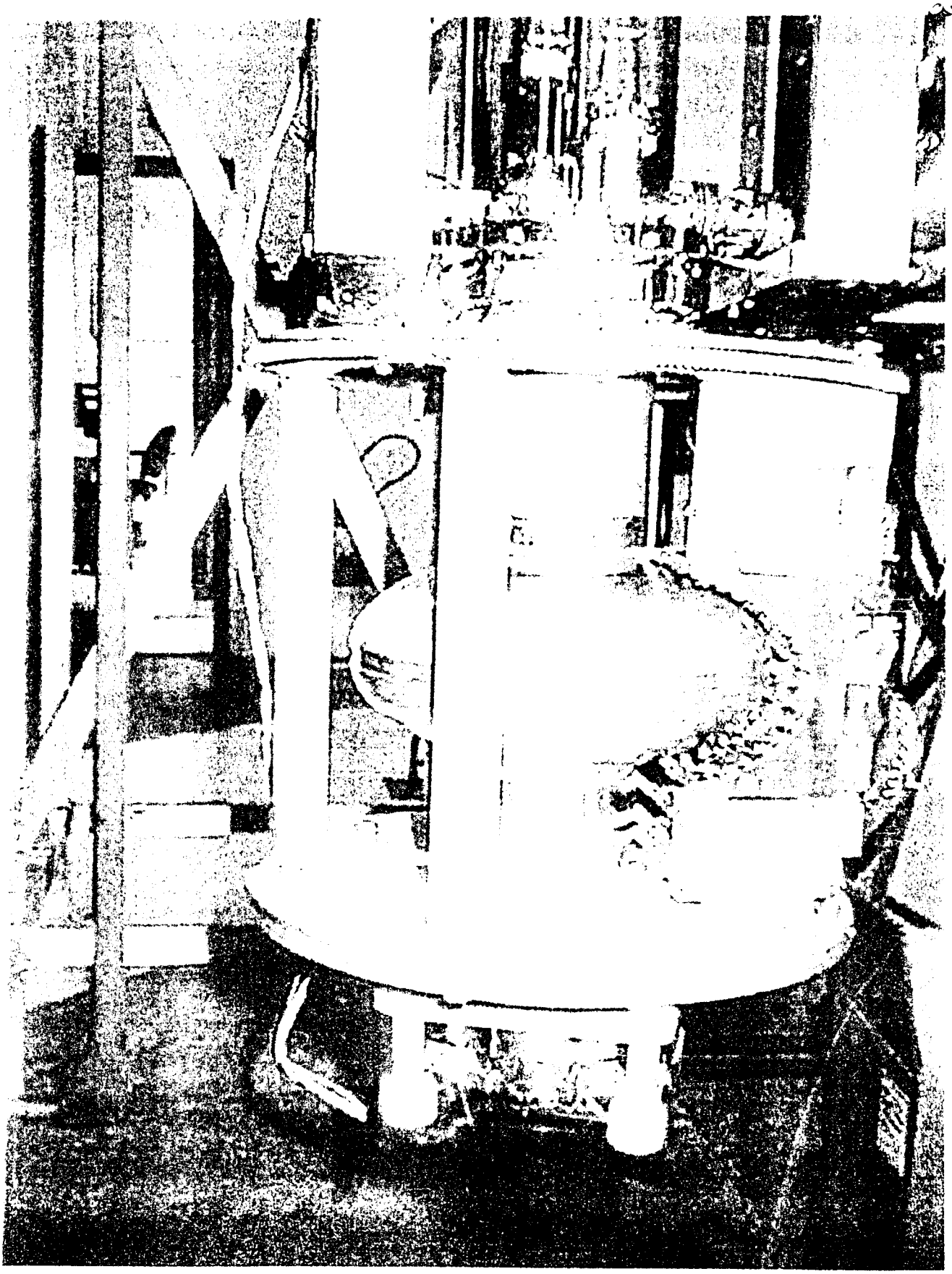

T-Map of the best Nb_3Sn Cavity before Quenches

at $E_p = 18$ MV/m

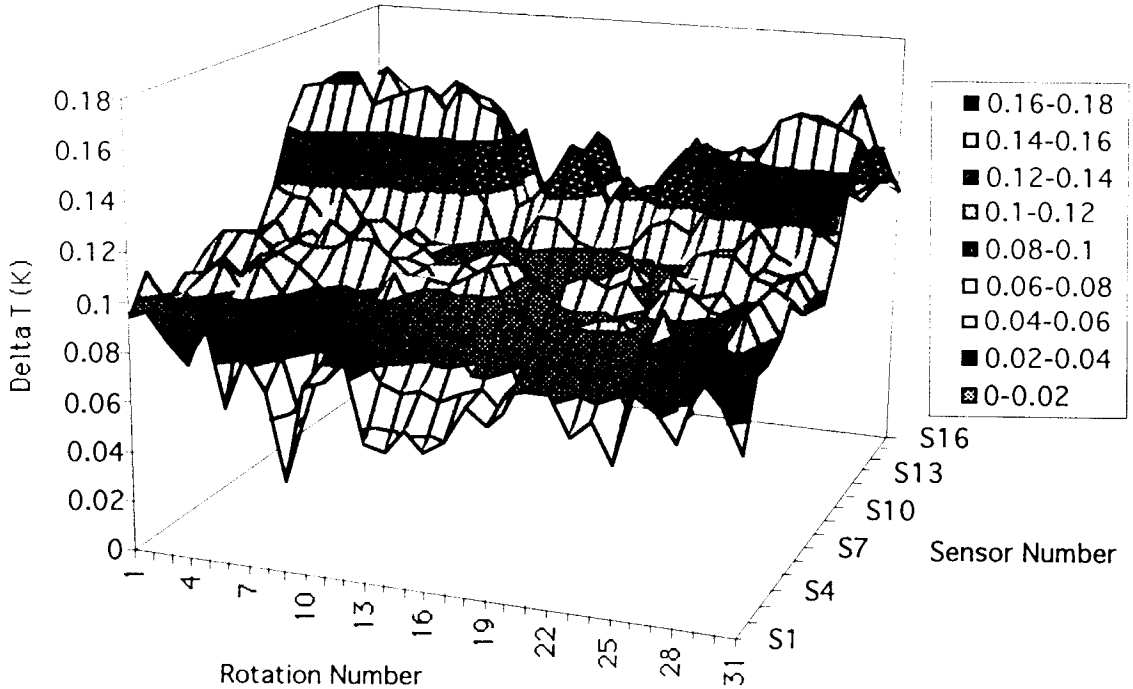

nearly uniform H^2 heating, more at cavity bottom ⇒ cooling?

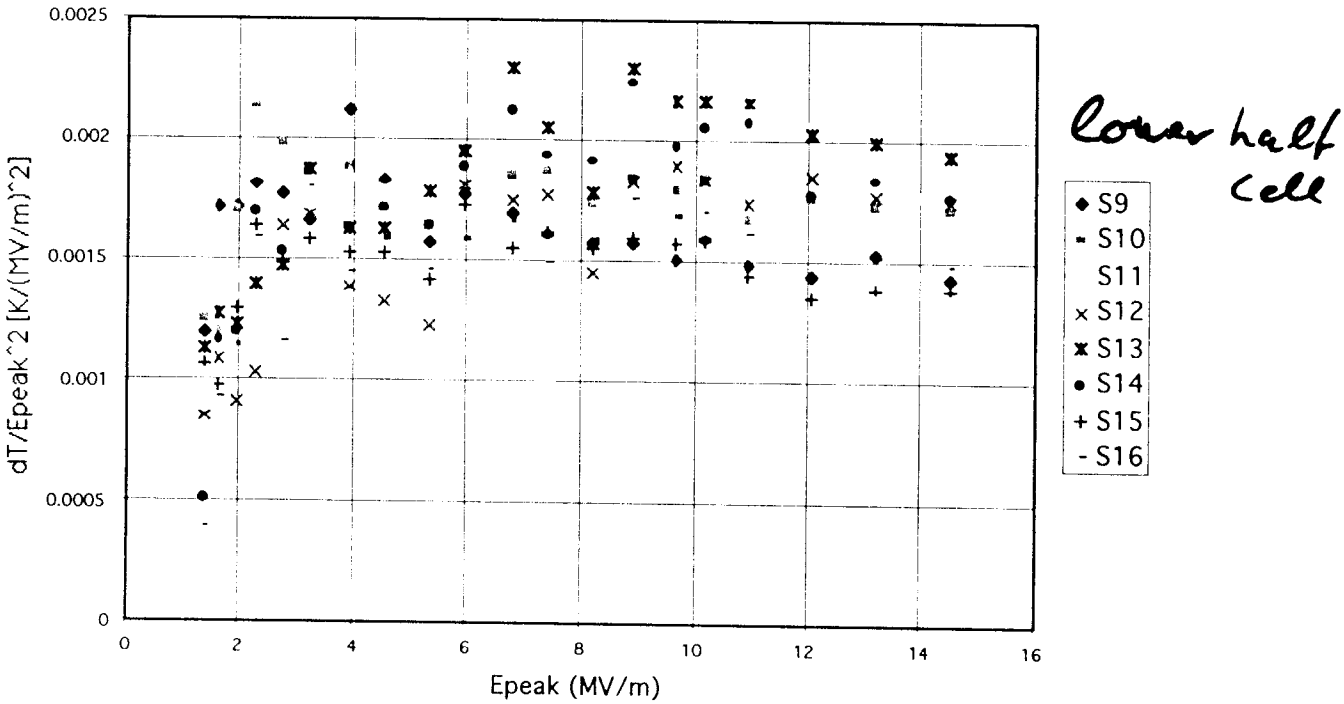

lower half cell

⇒ normalized data show quadratic heating up to Ep= 15MV/m

T-Map of an oxipolished Nb_3Sn Cavity at 4 MV/m (E_p)

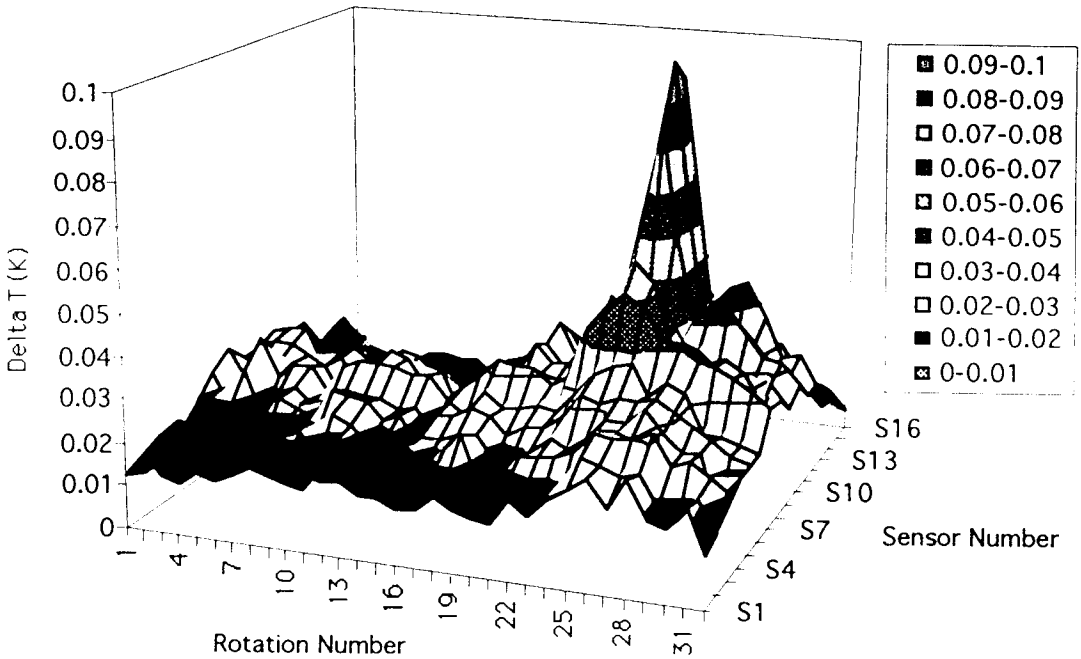

⇒ local defect (at S11) above uniform H^2 background heating

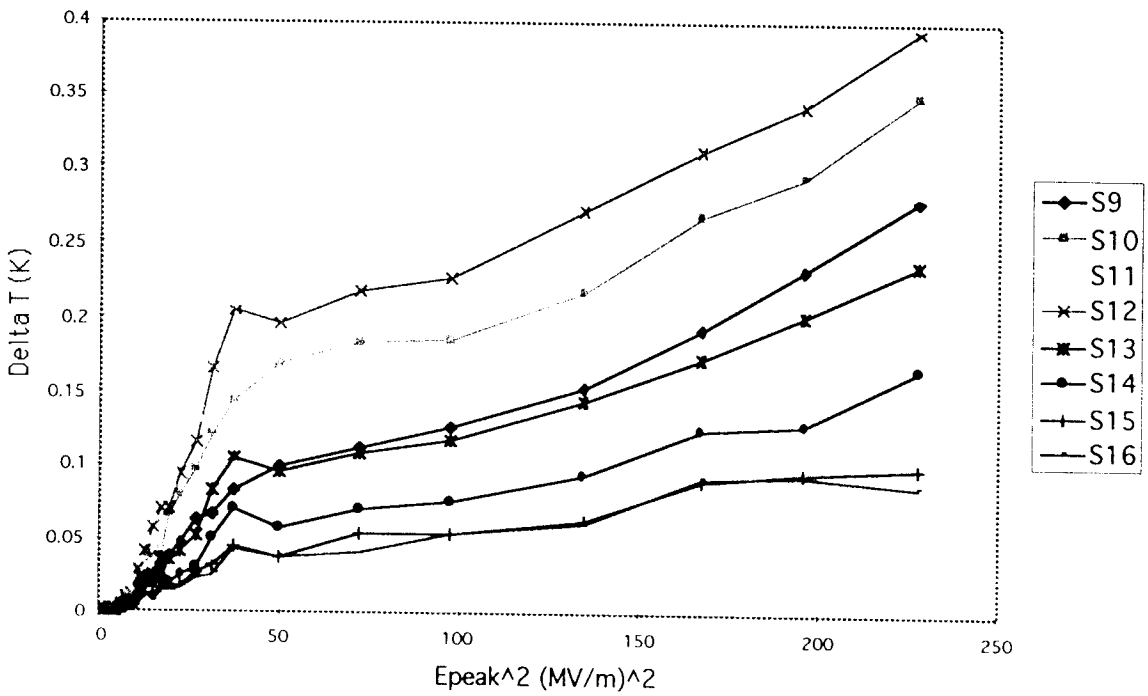

⇒ defect dominates nonlinear losses (Q drop) for Ep < 5MV/m
⇒ background heating quadratic (stronger) for Ep<(>)10MV/m

Typical T-map at Ep = 8 MV/m after occurence of quenches (#1)

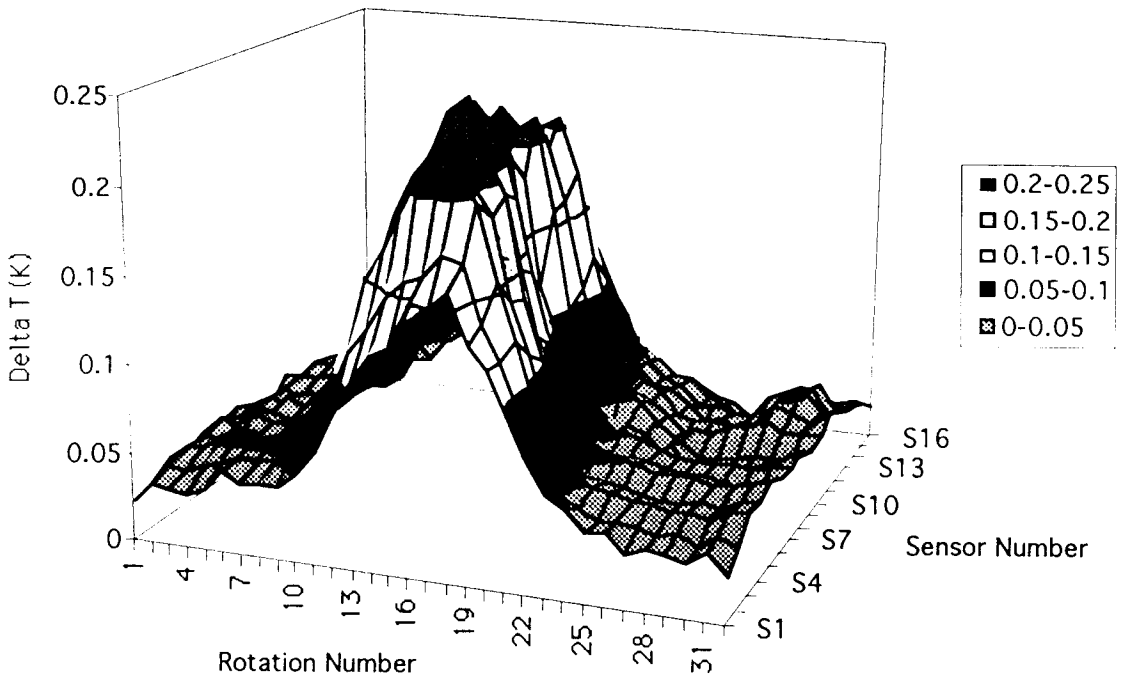

ΔT(Ep)-Increase of 8 resistors at ϕ_{max}

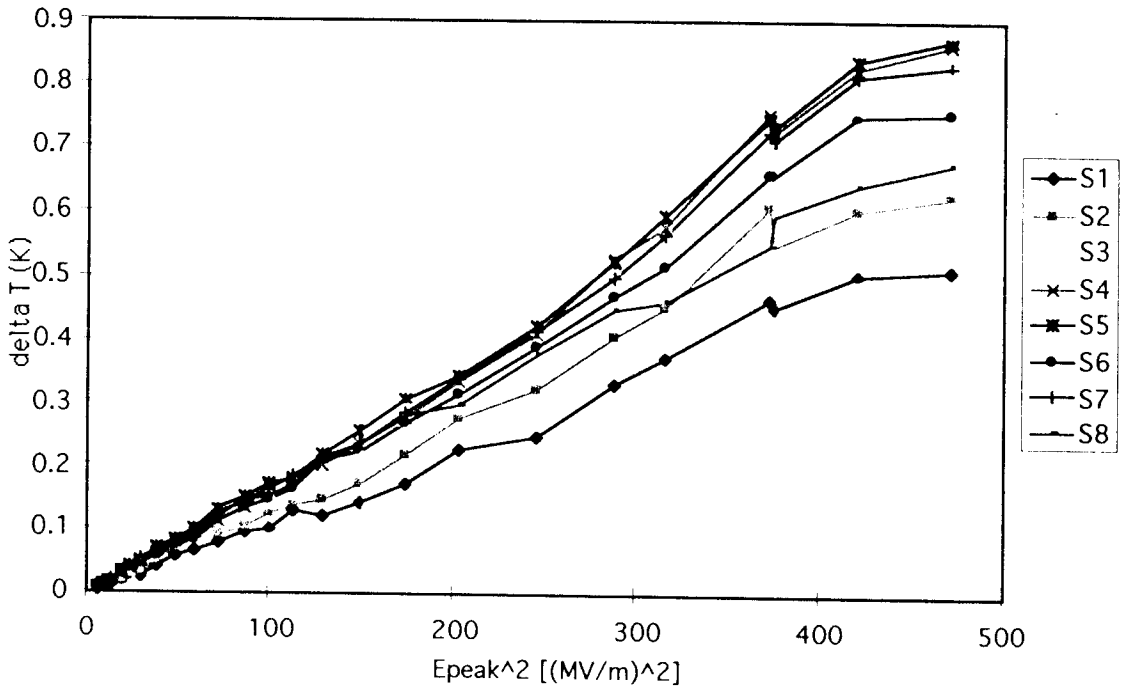

Quadratic heating $\Delta T \sim E_p^2$ up to saturation $\Rightarrow$ frozen in flux

Q Degradation of Nb_3Sn Cavities after Quenches

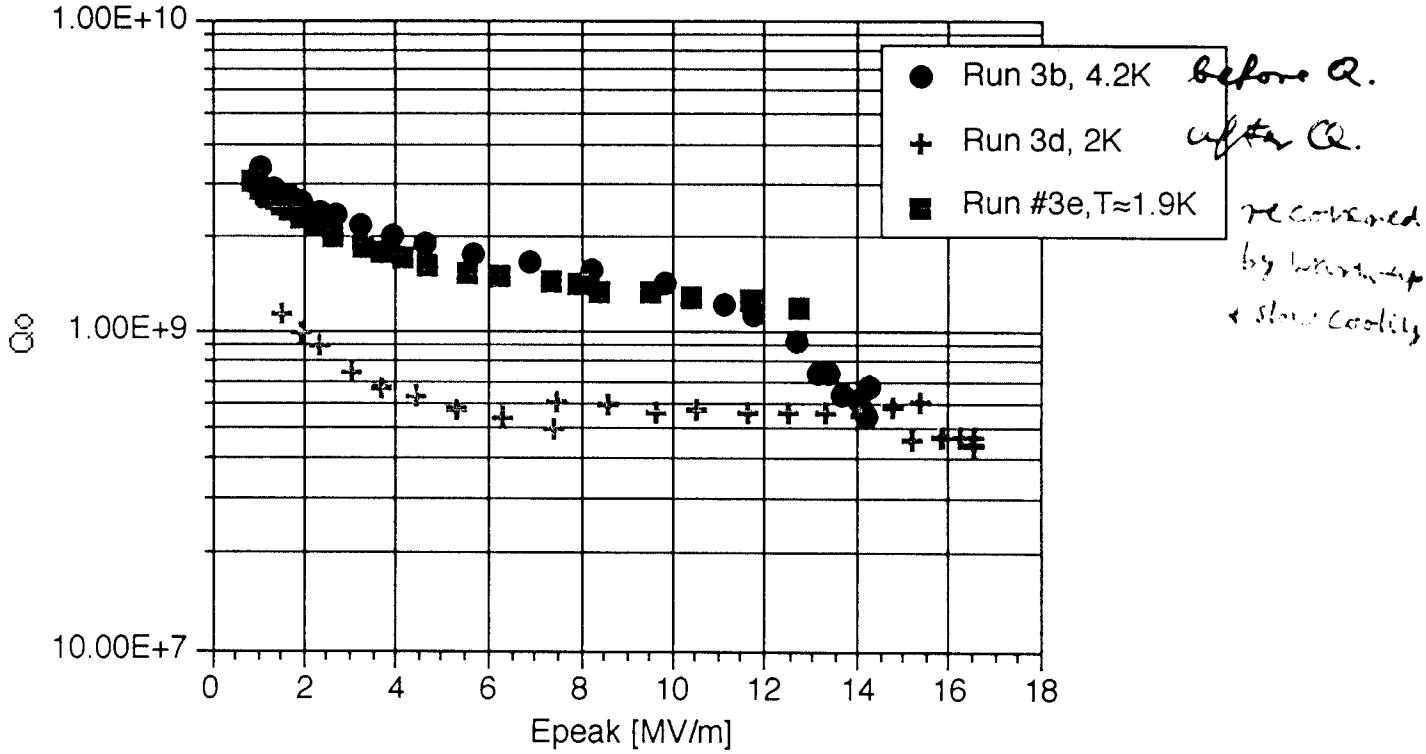

Typical T-map at Ep = 15 MV/m after several quenches

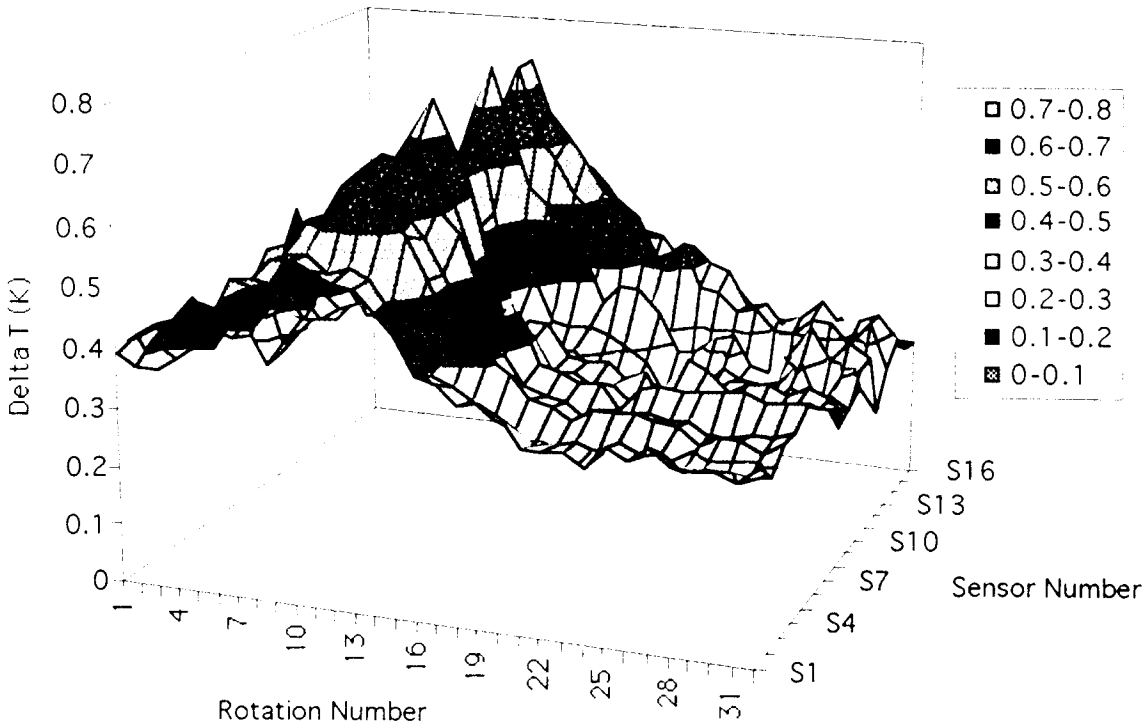

Broad-area heating along an azimuth ϕ $\Rightarrow$ Thermocurrents

due to Quenches

Conclusions

Uniform Nb_3Sn coatings have been obtained on high purity Nb cavities with an optimized vapour diffusion technique without Nb-RRR degradation

Extremely low Rres<10nΩ and Ep up to 35 MV/m were achieved for 1.5 GHz 1-cell Nb_3Sn cavities after HPWR, resulting in Q`s above 10^{10} at 4.2K

An exponential Q degradation was reproducibly seen for Ep>10MV/m, but its origin is still unclear

Temperature maps in subcooled Helium revealed:
nearly uniform quadratic losses for Ep≤15MV/m
nonlinear losses by defects after oxypolishing
thermocurrent-induced losses after quenches

First results of a 1.5 GHz 5-cell Nb_3Sn cavity showed less performance, but are promising for applications in medium-gradient high-efficiency superconducting linacs with CW operation at 4K

A short summary of the R&D activity carried out at CERN in the past five years and Ideas for further R&D based on the present state of the art

Present core team:
C. Benvenuti, S. Calatroni, H. Neupert, M. Prada, A.-M. Valente

1- Coating optimisation at low field

- "Historical" background: 5-year wide spectrum R&D with the collaboration of Pierre Darriulat to identify the physical basis of the RF behaviour of films
- Choice of the copper treatment: spun cavities showed a better R_{res} compared to hydroformed cavities. Evidence that the roughness was improved, thus the choice of studying electropolishing. As a standard procedure it has replaced chemical polishing at the beginning of 1999
- Choice of [1] the sputter gas and of [2] the coating conditions: [1] mainly dictated by the wish of reducing the effect of stray magnetic fields (trapped fluxons), best with Kr. [2] In-situ sputter etching of the copper oxide prior to coating resulted in worse average R_{res} than for films coated onto the passivated copper. Huge differences have been identified between films coated in the two different conditions.
- Rinsing: HPWR has always been performed (before and after coating), but not in clean enough conditions. Average field limit was 8÷10 MV/m. Upgraded to closed cycle rinsing in summer 1999
- Results presented at Santa Fe

Cavity manufacturing techniques

Spinning
Palmieri (LNL)
technology

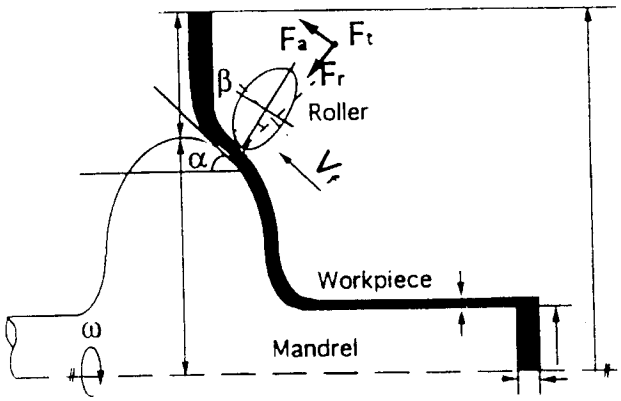

Hydroforming
Hauviller (CERN)
technology

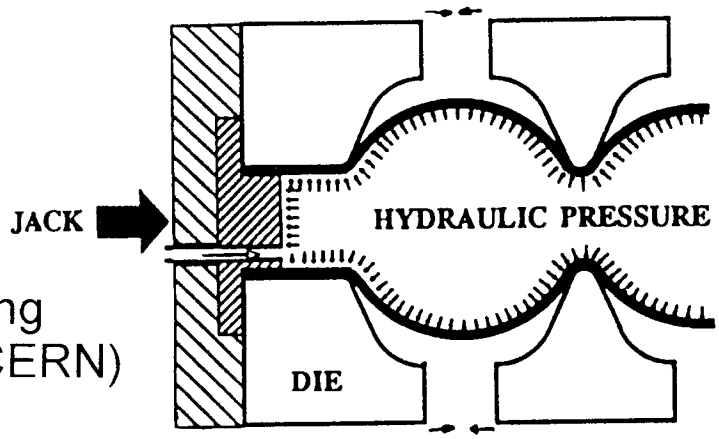

Pulsed
electroplating
on glass

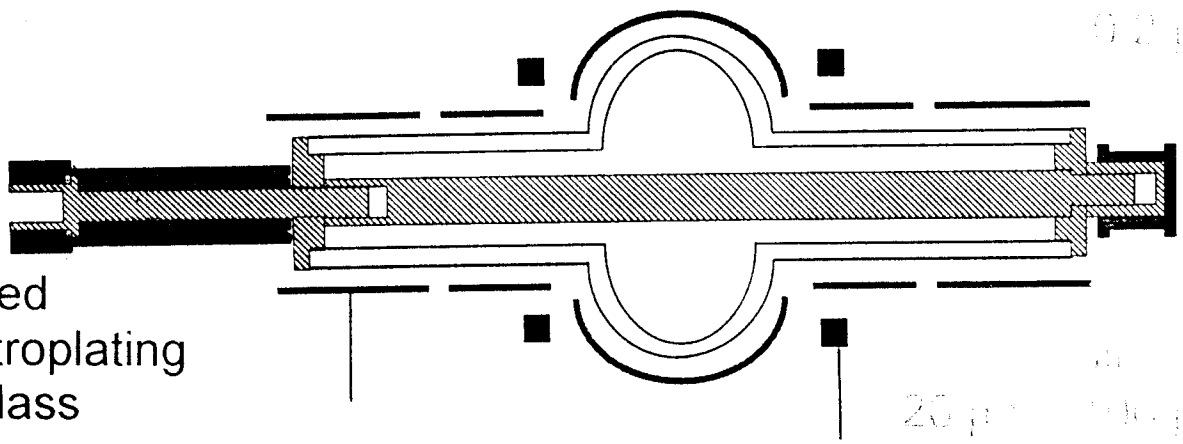

Surface quality : effect of roughness

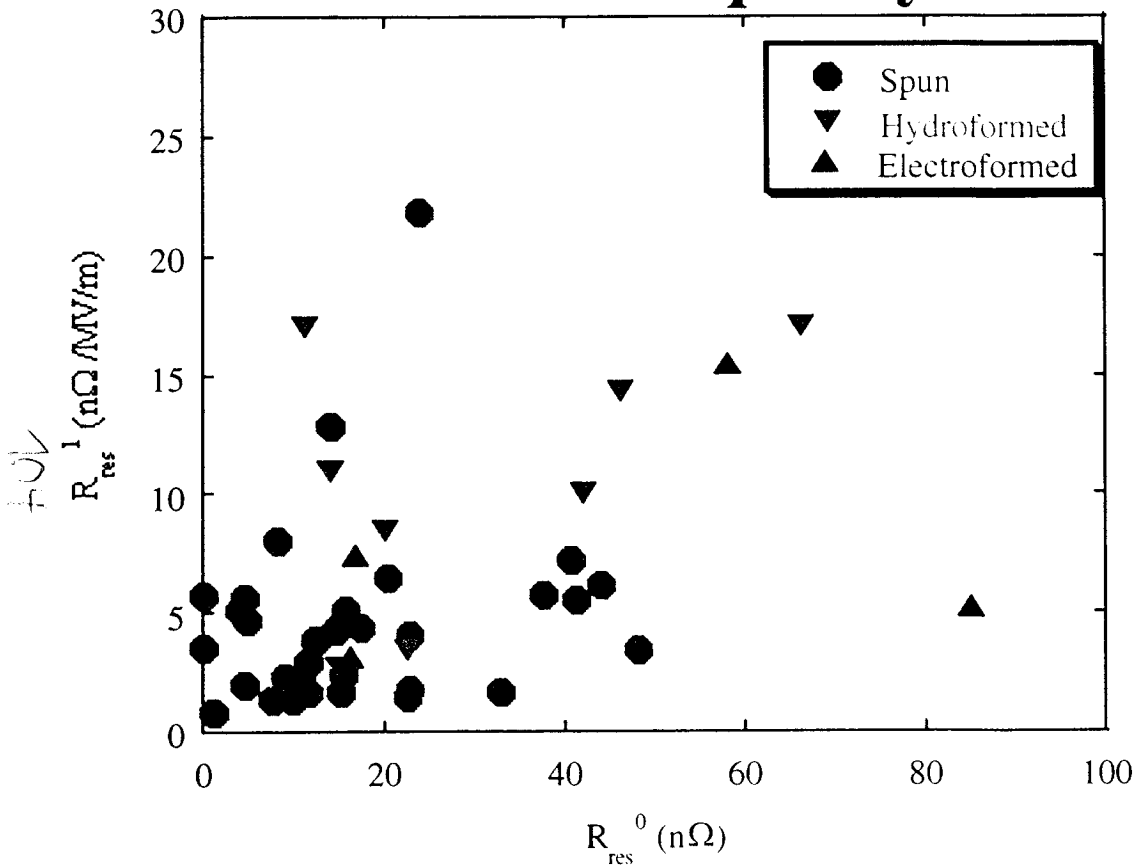

Standard coatings using argon as sputter gas

Spun cavities: 0.2 µm
Hydroformed cavities: 0.8 µm
Electroformed cavities: 0.2 µm

	Spun cavities	Hydroformed cavities
R_{res}^{0}	17±3 nΩ	28±6 nΩ
R_{res}^{1}	5±1 nΩ m MV^{-1}	10±2 nΩ m MV^{-1}

Surface quality : effect of polishing

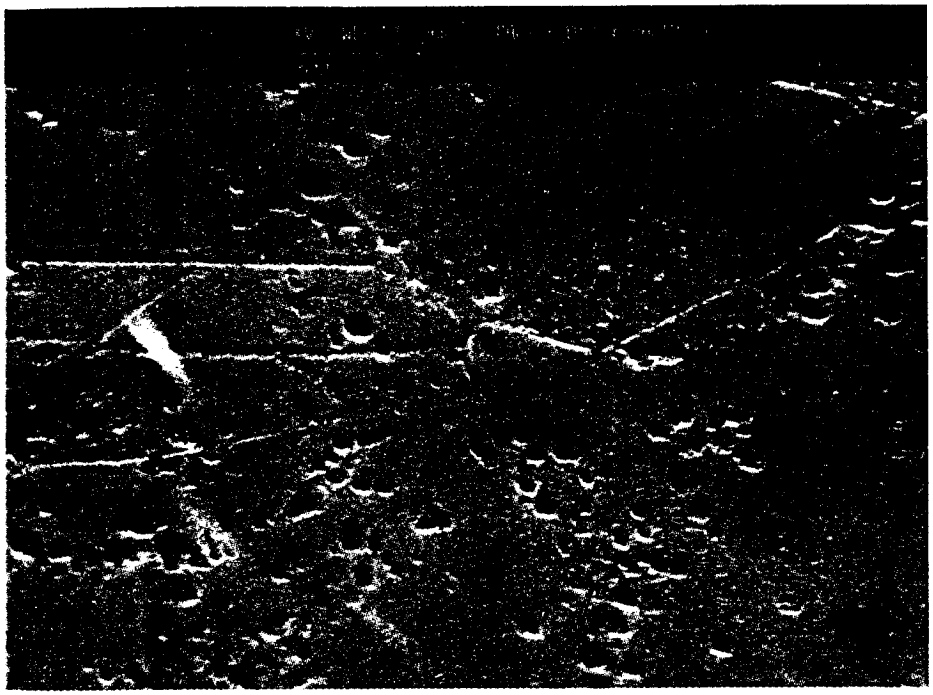

Chemically polished copper

- roughness 0.2 µm
- pinholes of 0.3 µm

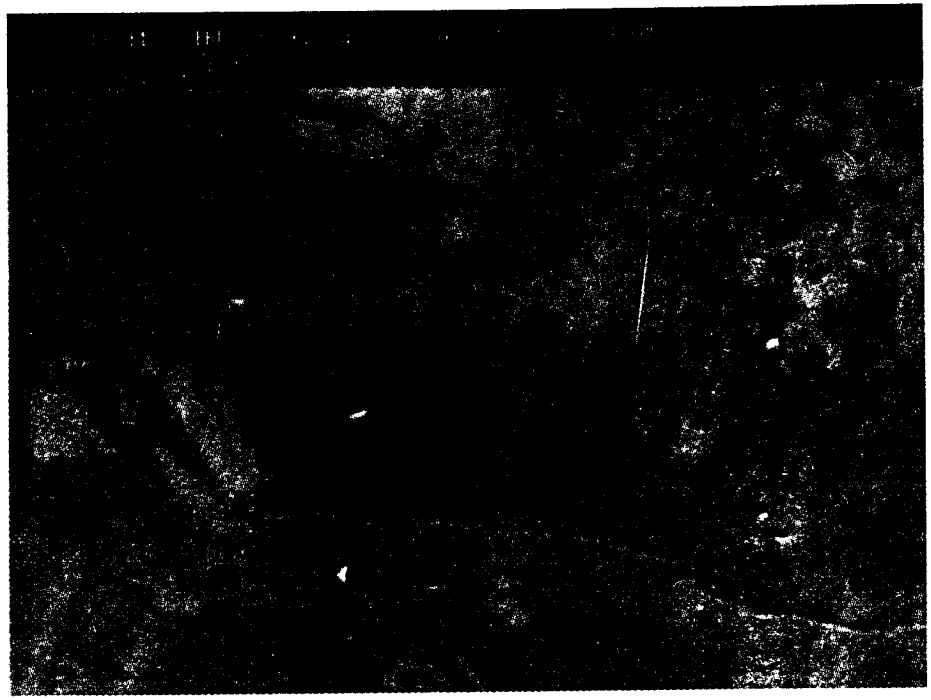

Electropolished copper

- roughness 0.04 µm
- nearly no defects

Copper surface preparation

1.5 GHz spun copper cavities have been used throughout the study. Hydroformed and electroformed cavities have also been tested.

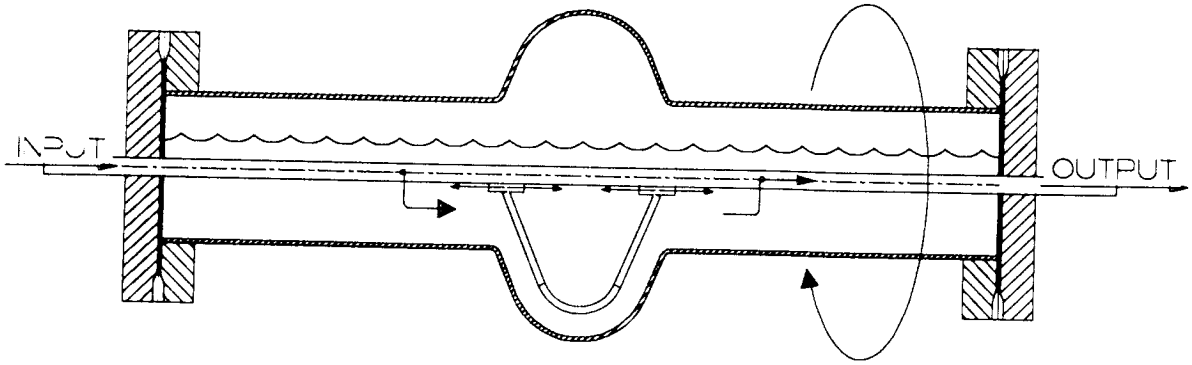

Electropolishing parameters:

- 55% vol. H_3PO_4
  45% vol. butanol
- Current density:
  $0.2 A/cm^2$
- HP water rinsing

Electropolishing has replaced chemical polishing (LEP standard) for surface preparation.

Advantages: lower roughness, absence of defects

STUDY OF THE RESIDUAL RESISTANCE OF SUPERCONDUCTING NIOBIUM FILMS AT 1.5 GHZ

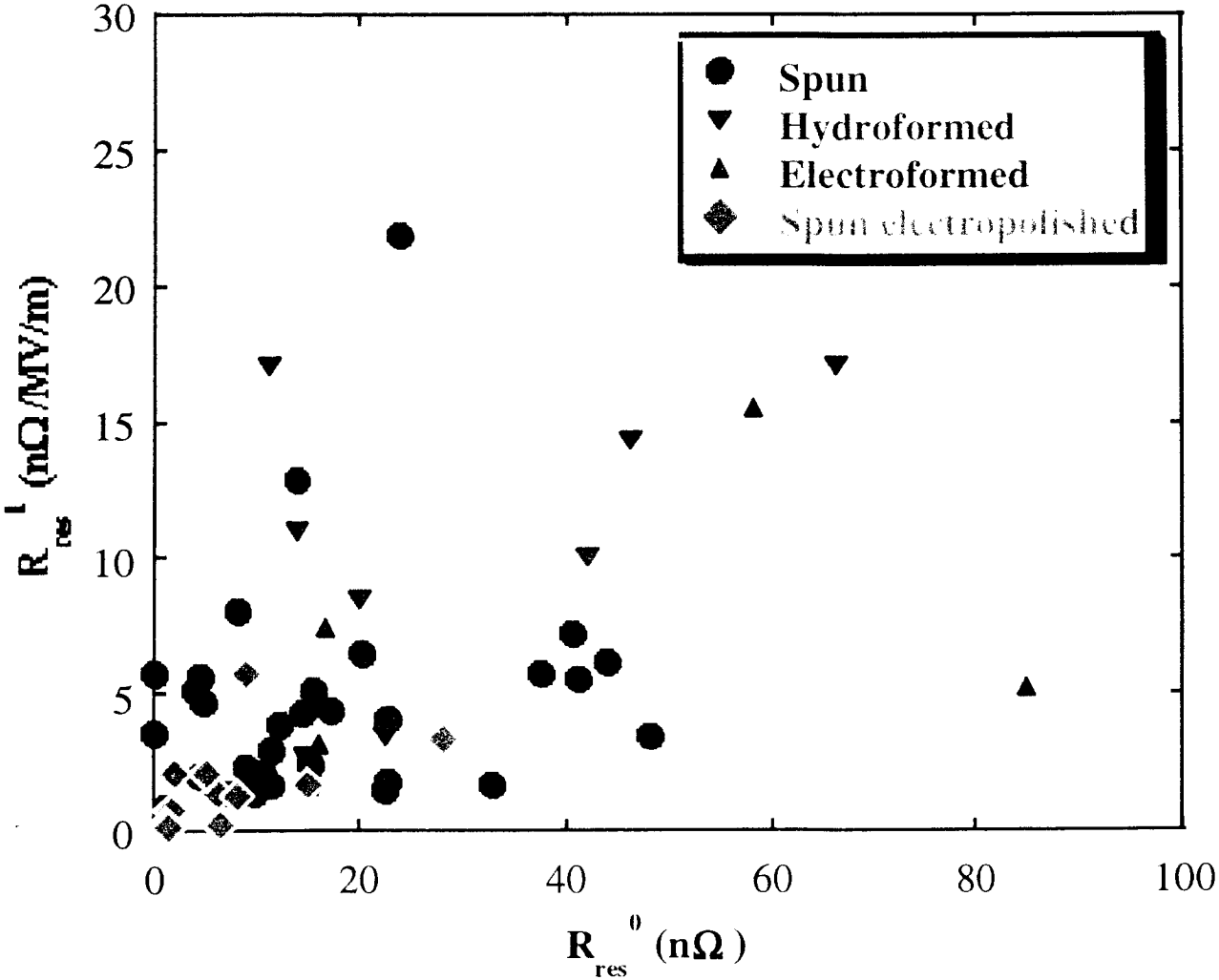

Surface treatment :
Electropolishing

R_{res}^{0}	6±6 nΩ
R_{res}^{1}	1.5±1 nΩ m MV^{-1}

Niobium sputtering

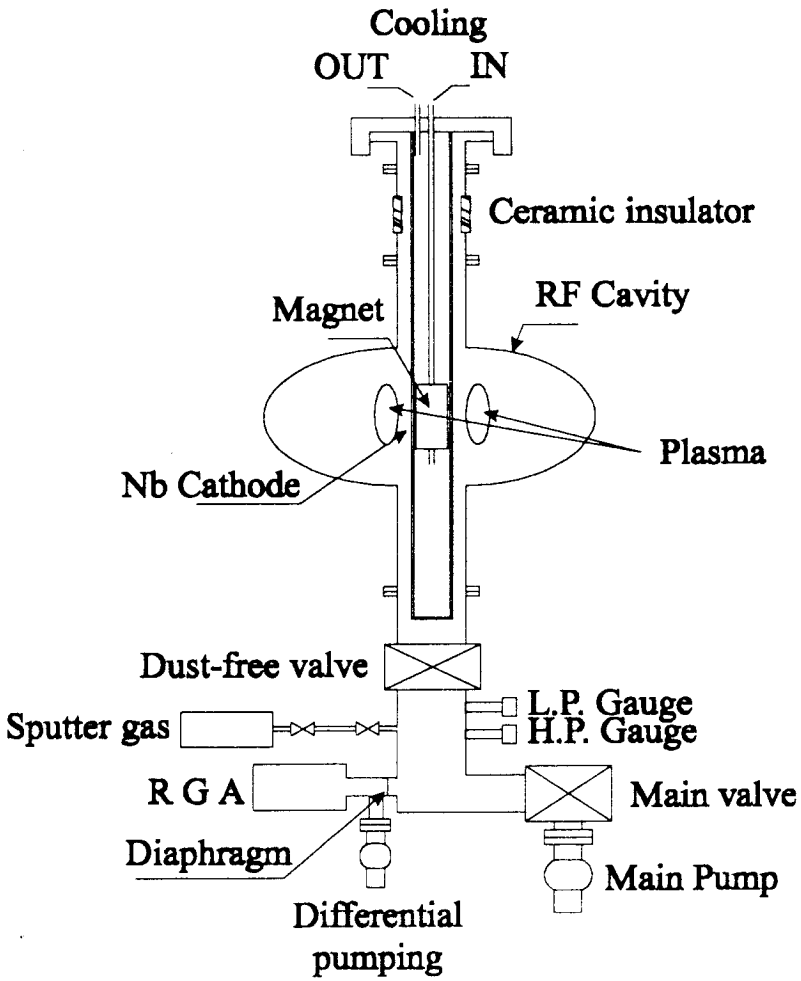

Sputtering parameters:

- Discharge current stabilized at 3 A.
- Sputter gas pressure of 1.5×10^{-3} mbar, corresponding to ~ 360 V.
- Coating temperature is 150 °C.
- Thickness: 1.5 μm

LEP "standard film" characteristics:

- RRR: 11.5 ± 0.1
- Argon content: 435 ± 70 ppm
- Grain size: 110 ± 20 nm
- Tc: 9.51 ± 0.01 K
- Strain: $\Delta a_{\perp}/a_{\perp} = 0.636 \pm 0.096$ %

Effect of the Nb/Cu oxide interface

Texture of the film

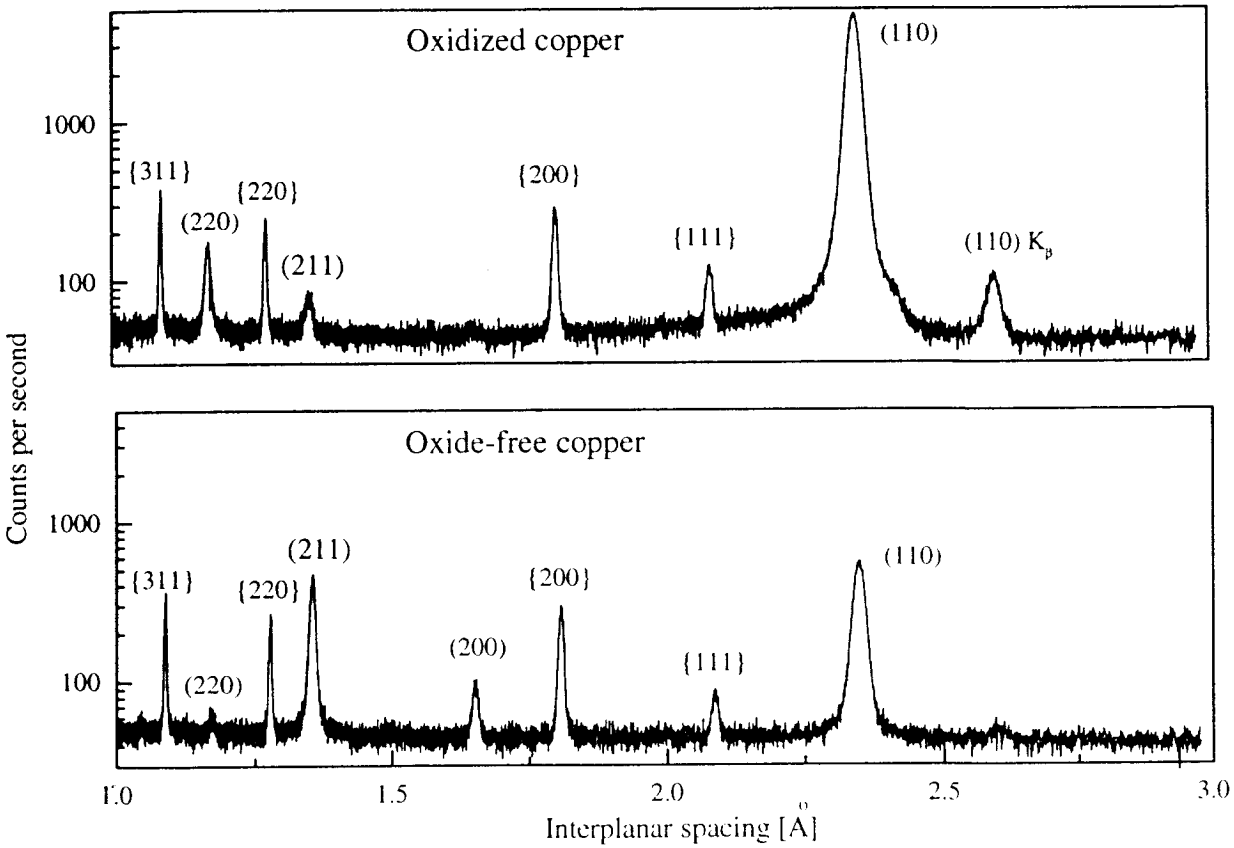

	Standard	Oxide-free
RRR	~10	~30
T_C	9.51±0.01 K	9.36±0.04 K
Ar cont.	435 ±70ppm	286 ±43ppm
Texture	(110)	(110), (211), (200)
	fibre texture	heteroepitaxy
λ/λ_{clean}	1.51 ±0.04	1.04 ±0.09
Hc_2	1.15 ±0.025 T	0.77 ±0.01 T
a_0	3.3240(10)Å	3.3184(6) Å
Stress	-706 ±56 MPa	-565 ±78 MPa
H_{c1}	31 ± 3 mT	85 ± 5 mT
Grains	110 ± 20 nm	7 µm

Effect of the Nb/Cu oxide interface

TEM micrographs in plan view

Standard

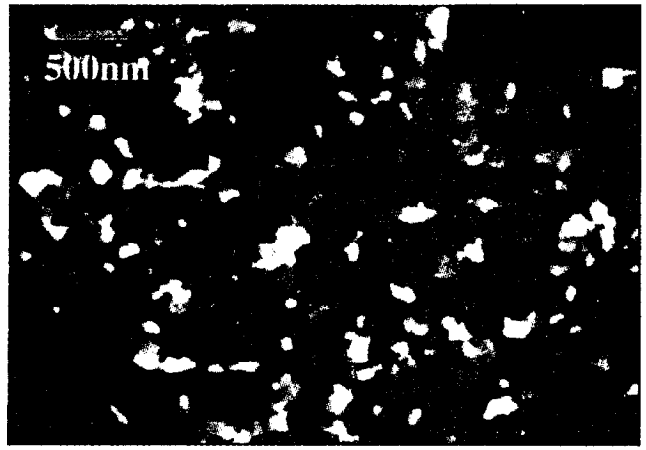

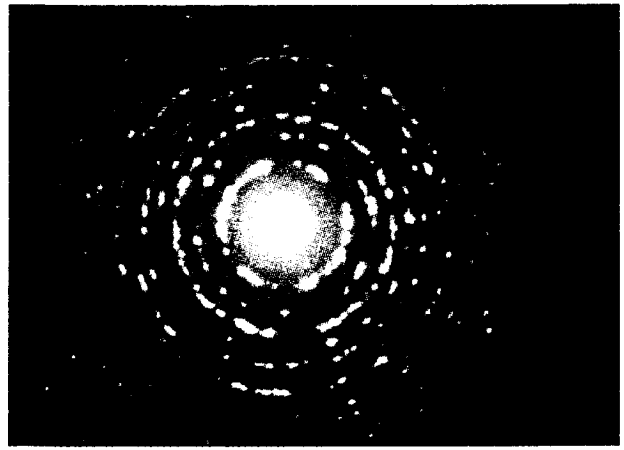

Grain size ~ 100 nm
Fibre texture
Diffraction pattern:
powder diagram

Oxide-free

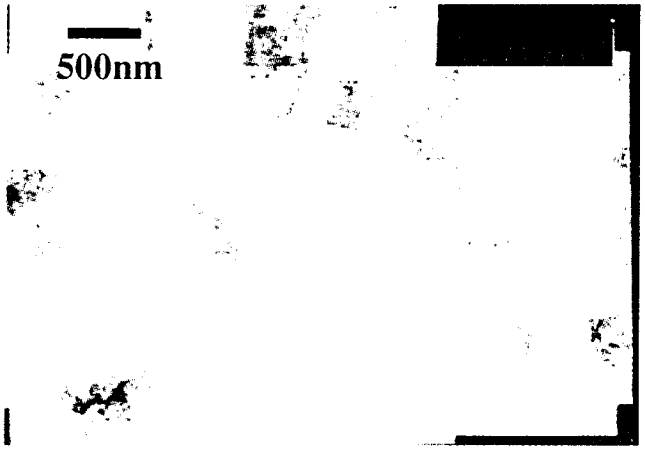

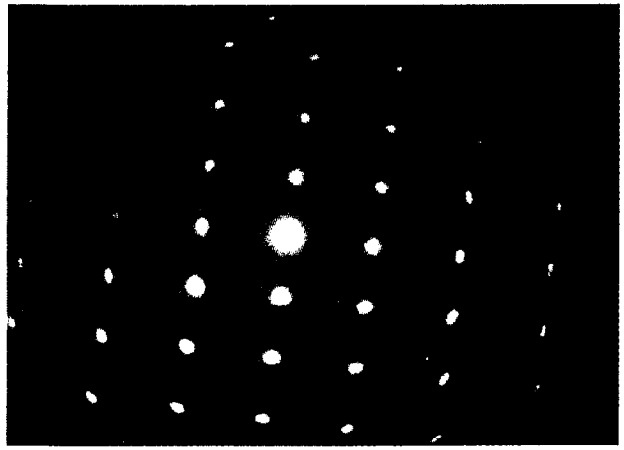

Grain size ~ 1-5µm
Heteroepitaxy
Diffraction pattern:
zone axis [110]

Nb/Cu film characterisation - Transmission Electron Microscopy

TEM micrographs in cross section

Standard

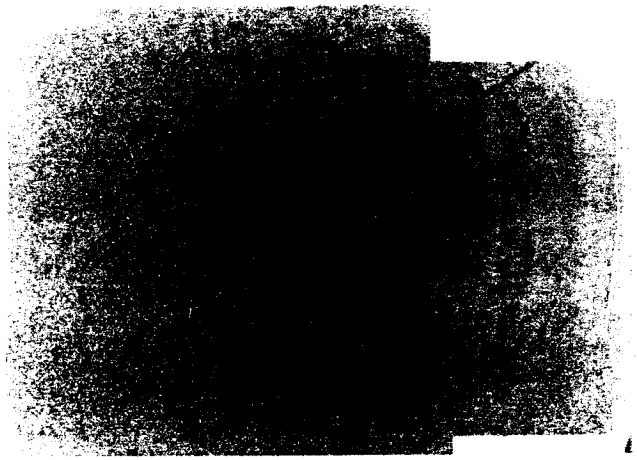

(110) fibre texture

⊥ ♈

substrate plane

Oxide-free

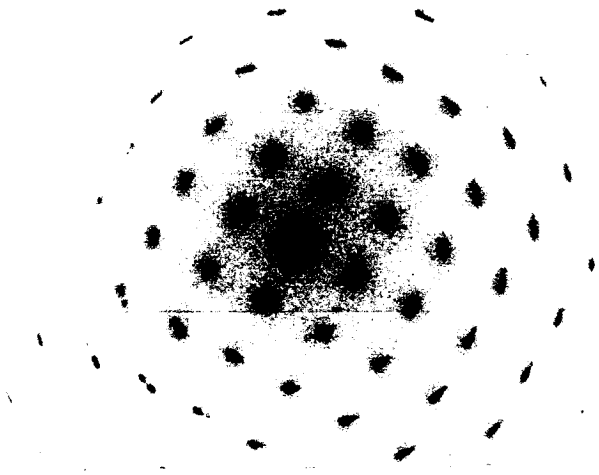

Heteroepitaxy

Nb (110) //Cu(010)

Nb (110) //Cu(111)

Nb (100) //Cu(110)

Oxide-free coating: texture correlation

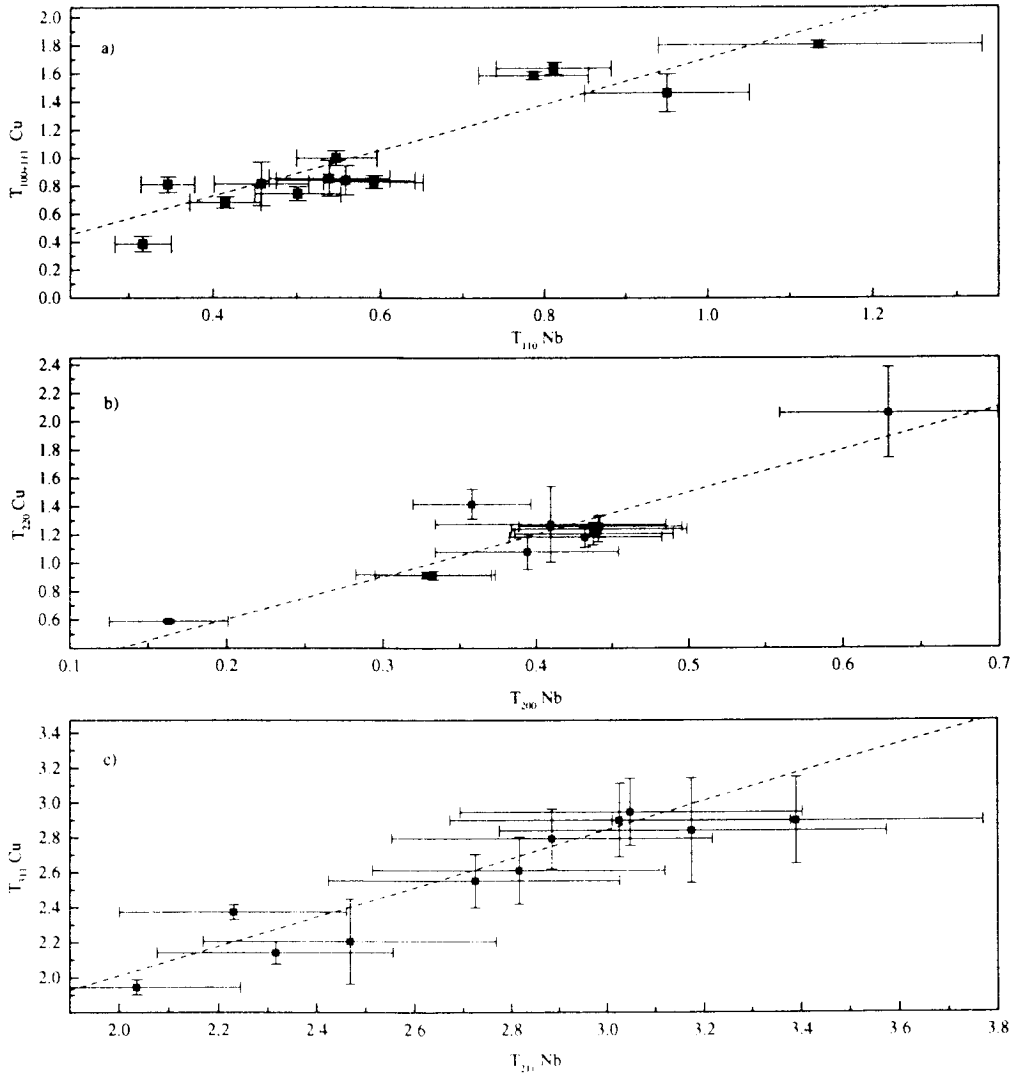

Effect of the Nb/Cu oxide interface

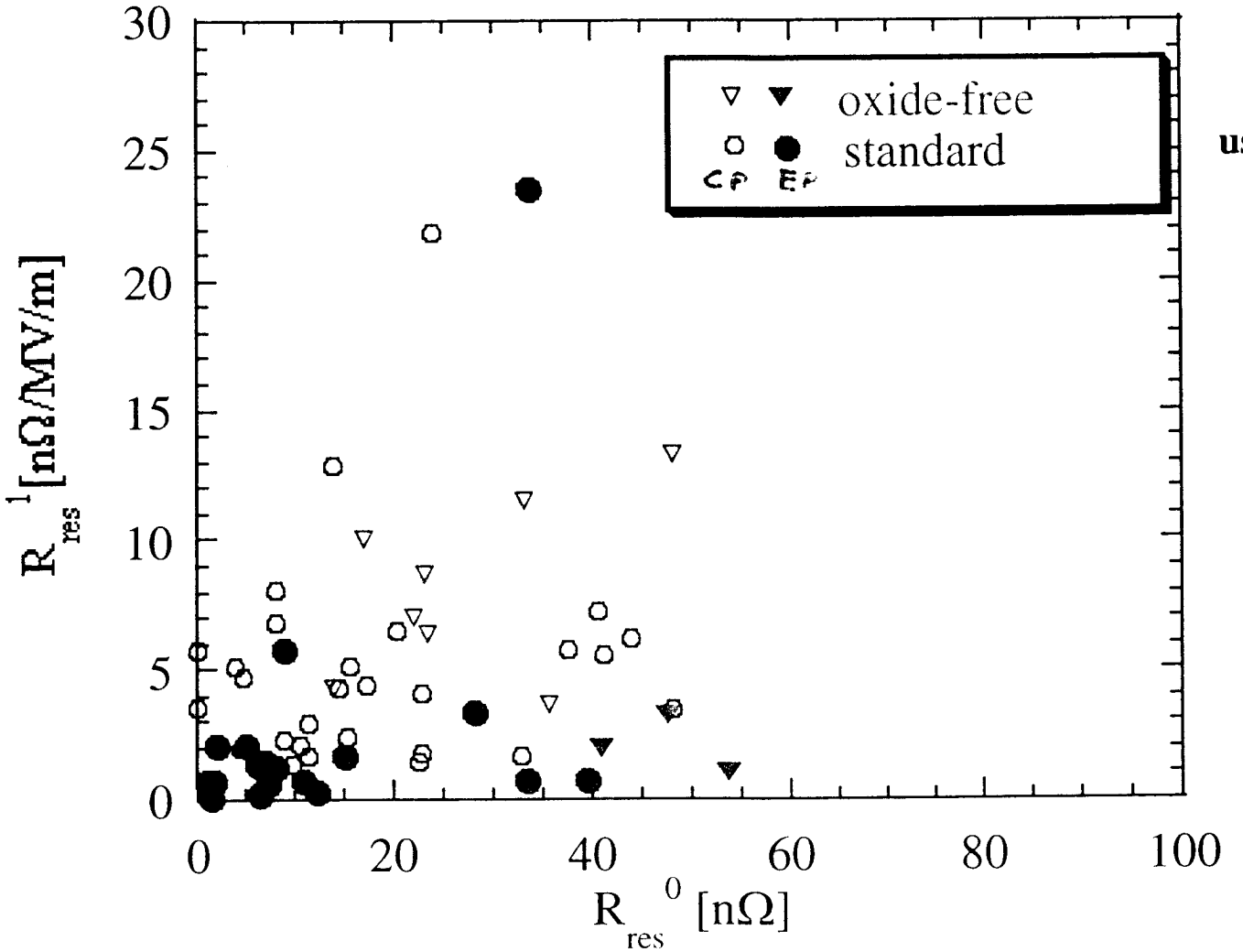

All coatings on spun cavities using argon, krypton or xenon as sputter gas

Change of substrate

Various substrates have been explored:
- Copper (covered with natural oxide)
- Oxide free copper (by sputter etching prior to coating)
- Niobium
- Oxide free niobium

And various underlayers (sputter-coated):
- Copper
- Titanium
- Gold
- Aluminium
- Oxidised aluminium

Niobium films on most substrates or underlayers behave as standard LEP films. However, some films belong to a second "family".

In the case of oxide free copper:

- RRR: 28.9 ± 0.9
- Grain size: >1 μm
- Argon content: 286 ± 43 ppm
- Tc: 9.27 ± 0.09 K
- Strain: $\Delta a_{\perp}/a_{\perp} = 0.466 \pm 0.093$ %

Theoretical and experimental BCS resistance at zero RF field

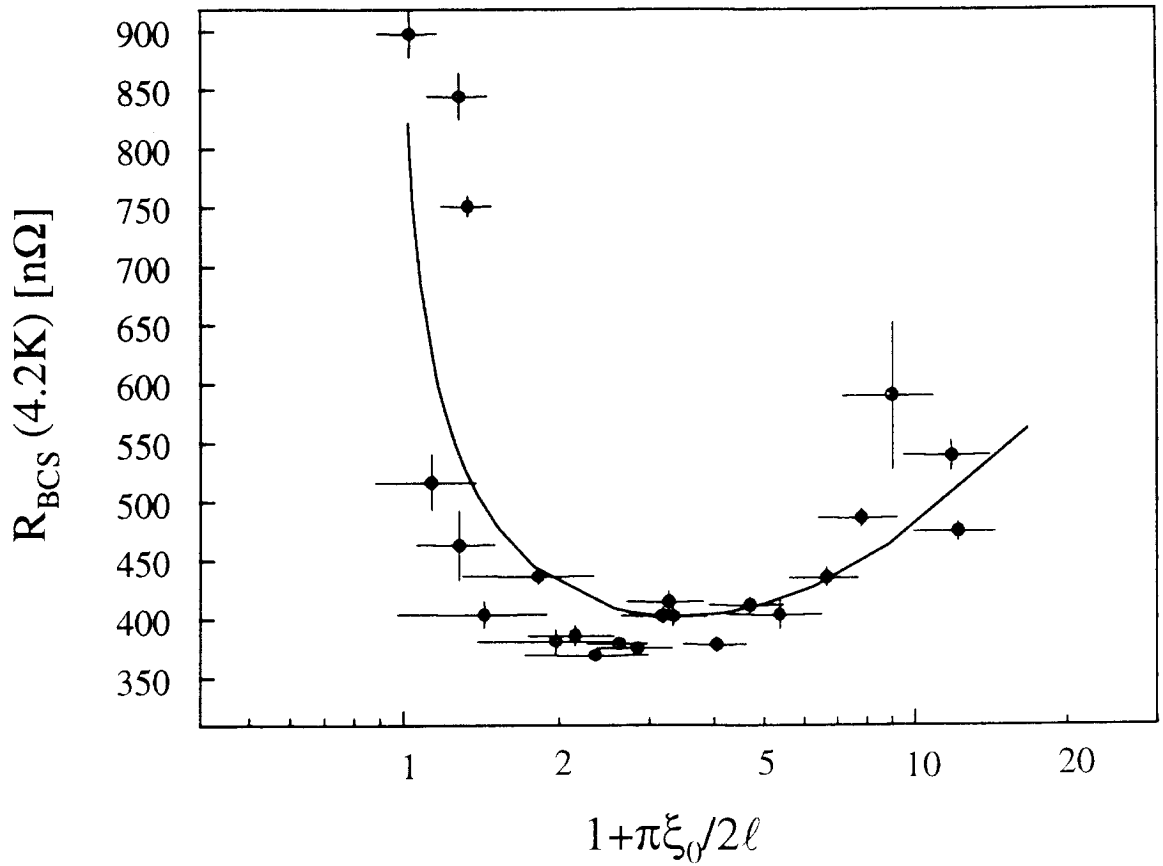

R_{BCS} at 4.2 K
Nb bulk: ~900 nΩ
Nb films: ~400 nΩ

R_{BCS} at 1.7 K
Nb bulk: ~2.5 nΩ
Nb films: ~1.5 nΩ

The RF field dependence of the BCS resistance

R_{BCS} (4.2K, H_{RF}) for film and bulk has a similar slope, and can be written as R^0_{BCS} (T)•G(H_{RF}). The G(H_{RF}) term can be approximated with a quadratic dependence on the RF field.

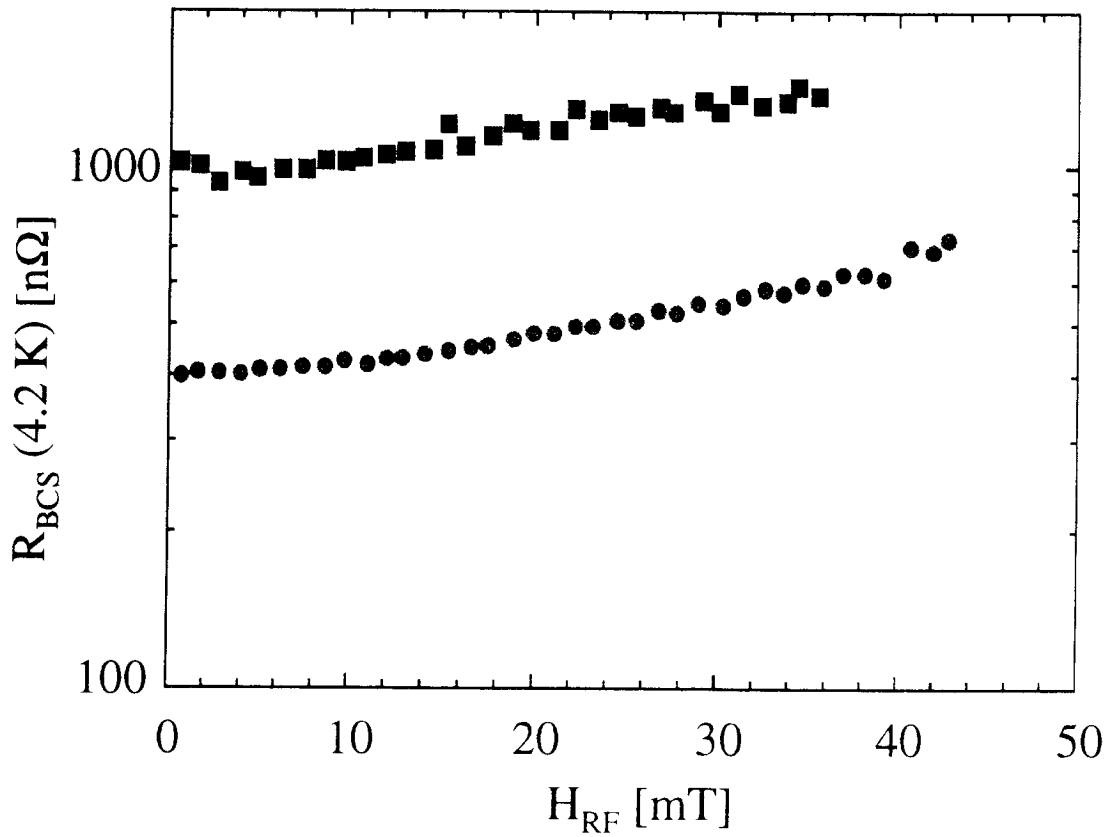

Squares: Nb bulk
Rounds: Nb films

$G(H_{RF}) \cong (1+5.10^{-4}H_{RF}^2)$
or
$G(E_{RF}) \cong (1+0.01E_{RF}^2)$

Fluxon-induced losses

Fluxon-induced losses at 1.7 K are characterized as $R_{fl} = (R_{fl}^0 + R_{fl}^1 H_{RF}) H_{ext}$

The minimum values are obtained using krypton as sputter gas:

$R_{fl}^0 = 3 n\Omega/G$ $R_{fl}^1 = 0.4\ n\Omega/G/mT$

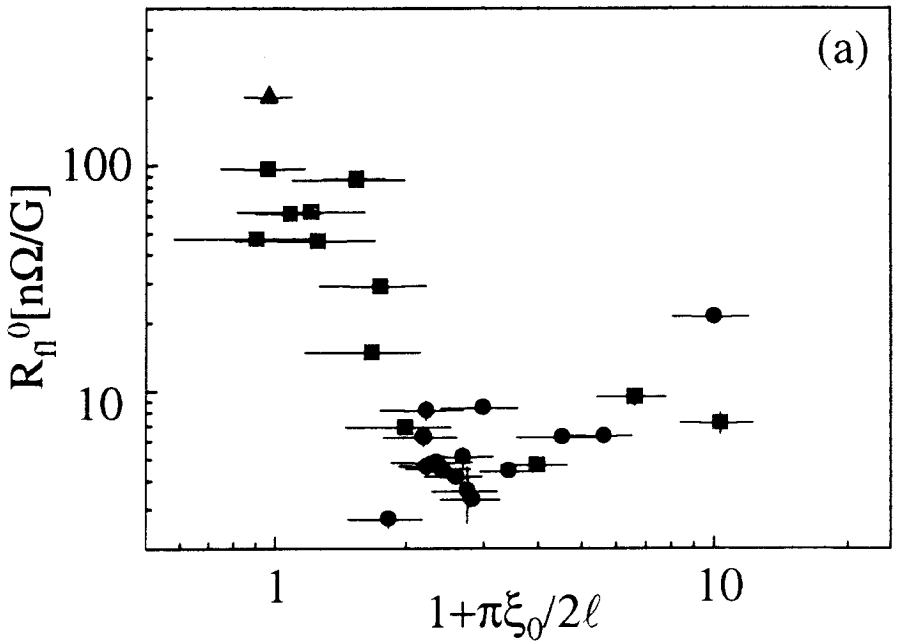

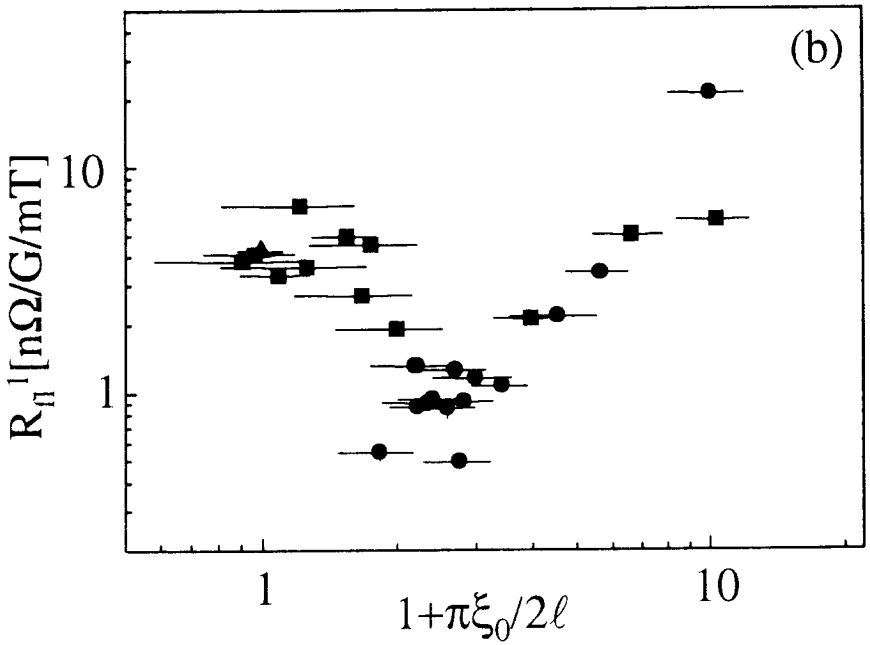

Triangles: bulk Nb

Squares: coatings on oxide-free copper

Circles: coatings on oxidized copper

Fluxon-induced losses

Fluxon-induced losses could be a limitation for high RF-field operation of film cavities, unshielded from the Earth's magnetic field.

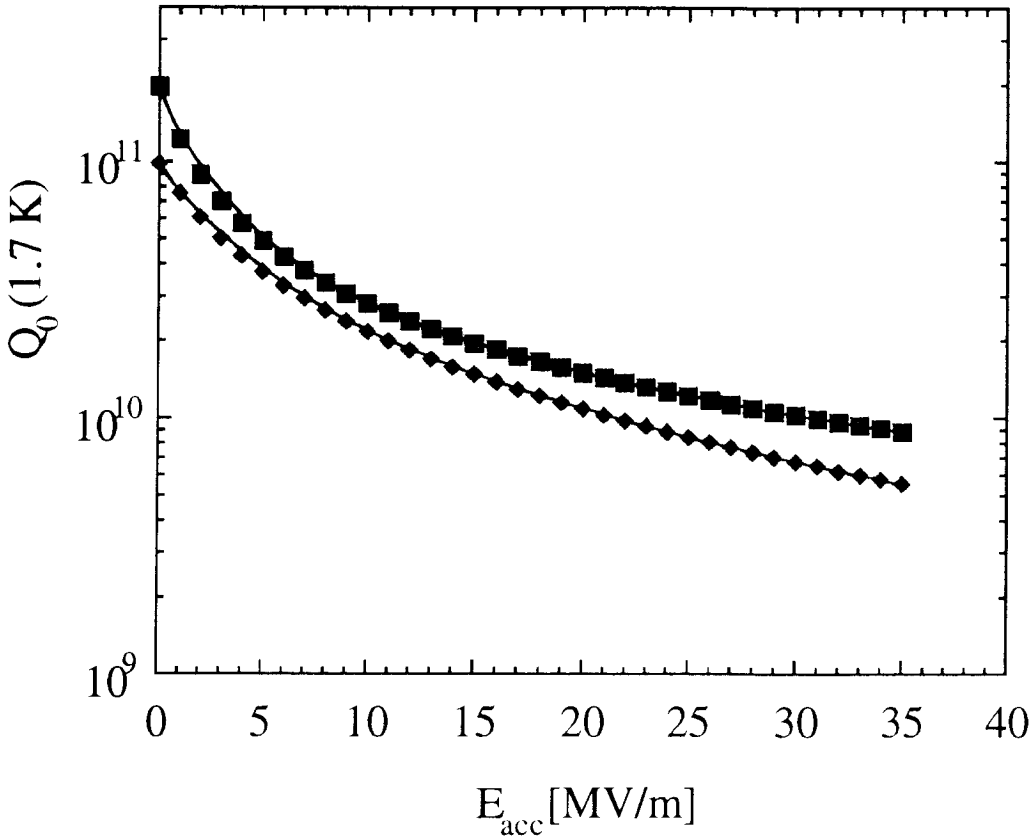

Fluxon losses for krypton calculated for $H_{ext} = 0.5$ G
~32 nΩ at 35 MV/m

BCS + Fluxon losses
~52 nΩ at 35 MV/m

The residual resistance: effect of electropolishing

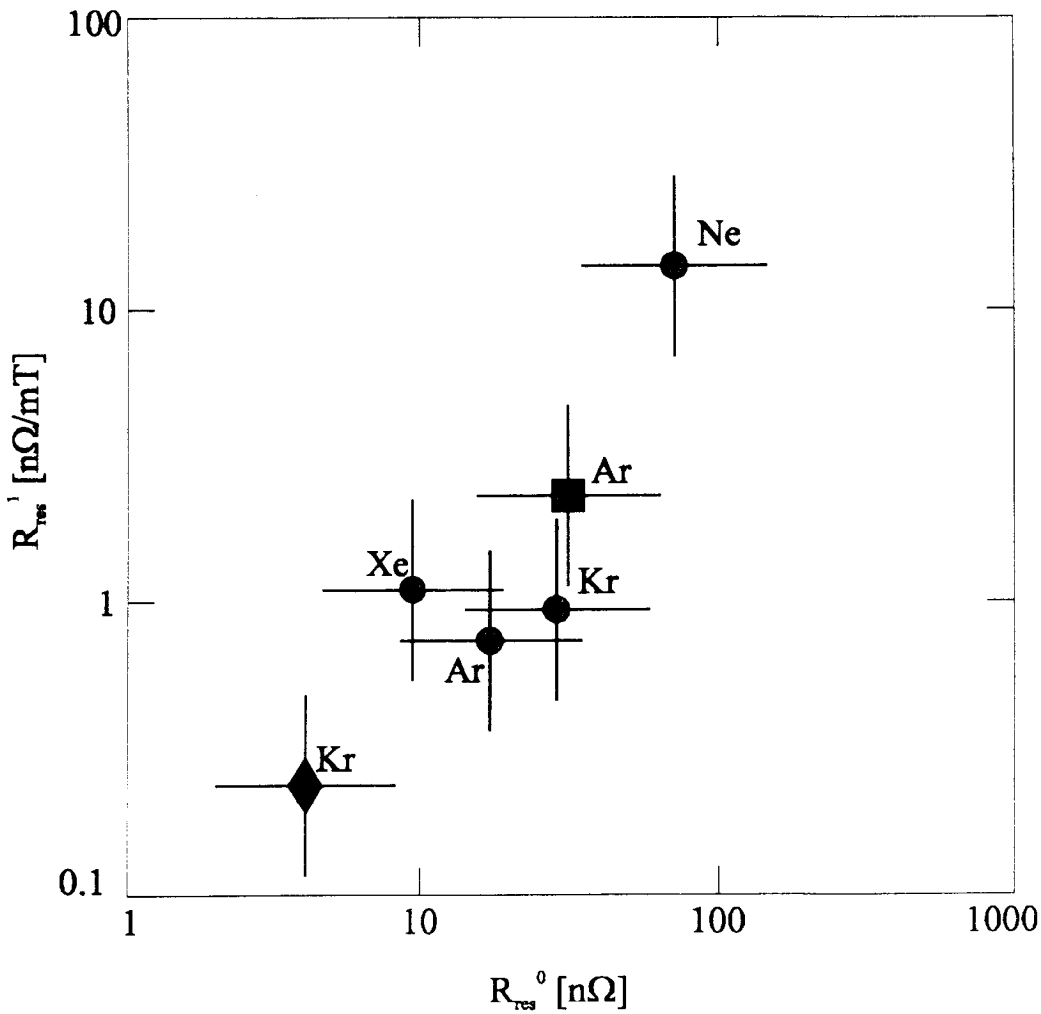

Standard coatings using Xe, Kr, Ar, Ne as sputter gas

Average roughness of chemically polished spun cavities: 0.2μm

Average roughness of chemically polished hydroformed cavities: 0.8μm

Average roughness of electropolished spun cavities: 0.04μm
Absence of defects (etching pits)

Processing :Upgrade of the rinsing system

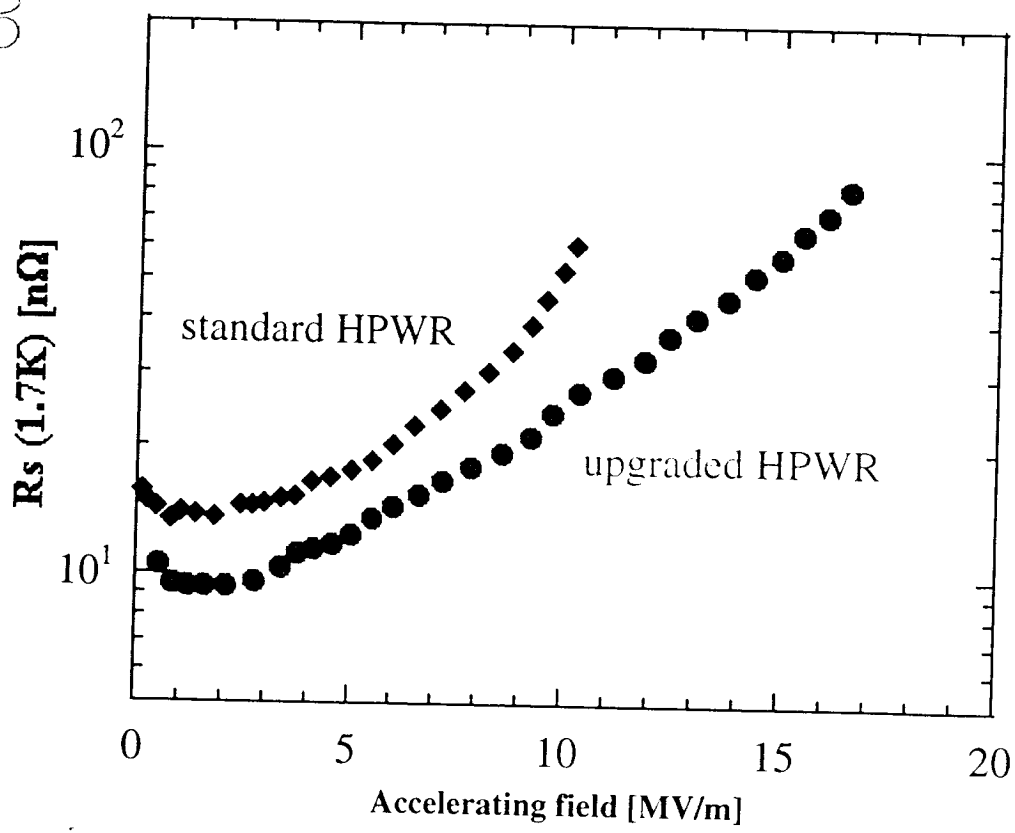

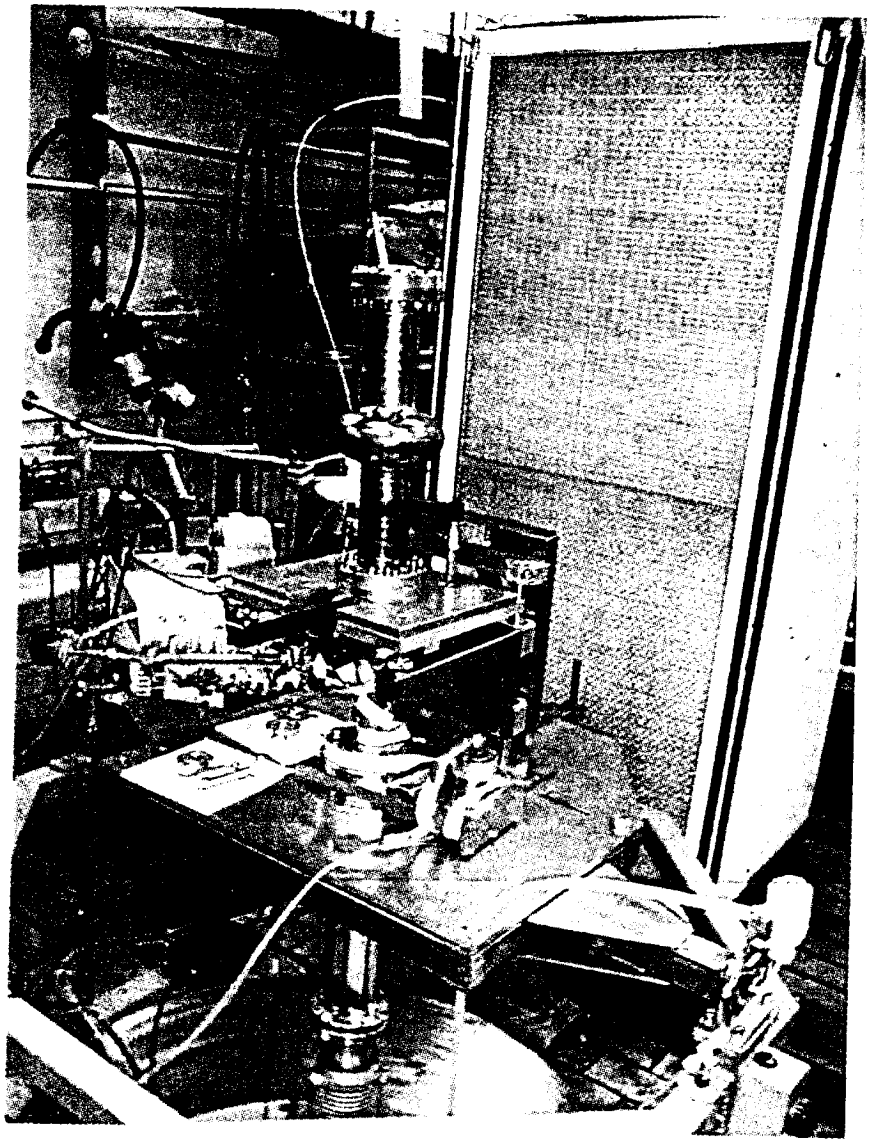

2- Needs for further R&D

An unexpected trend has been observed for all cavities , whose performance seemed to converge with a similar slope to a Q of 4×10^9 at 20 MV/m (limited by RF power).

- Instrumental effect of the RF system: helium level (only 60 litres), vacuum quality, differences between the 1st and the 2nd cool down.
- Effect of the roughness: comparison between bulk Nb and Cu, and Nb/Cu films. Is the advantage of EP due to an improvement in micro- or macro-roughness? Direct measurement of the roughness inside a cavity studying adsorbed gases.
- Thermal effect: measurement of the real temperature of the film by measuring the equilibrium He pressure inside the cavity. Measurement of the thermal impedance at the Nb/Cu interface (and eventually Nb/Nb, Nb/Al). Possible heating due to pinholes (10^{-7} of the total surface) or insufficient thickness locally.
- Grain size and RRR of the coating: has this an influence at higher fields? Is a difference in H_{c1} or in RRR important? All these can be modulated with the proper choice of coating conditions.
- Effect of hydrogen: it is present in the films, trapped by defects or impurities. Has it an effect at large fields (or at all)? Pump it with a getter underlayer.

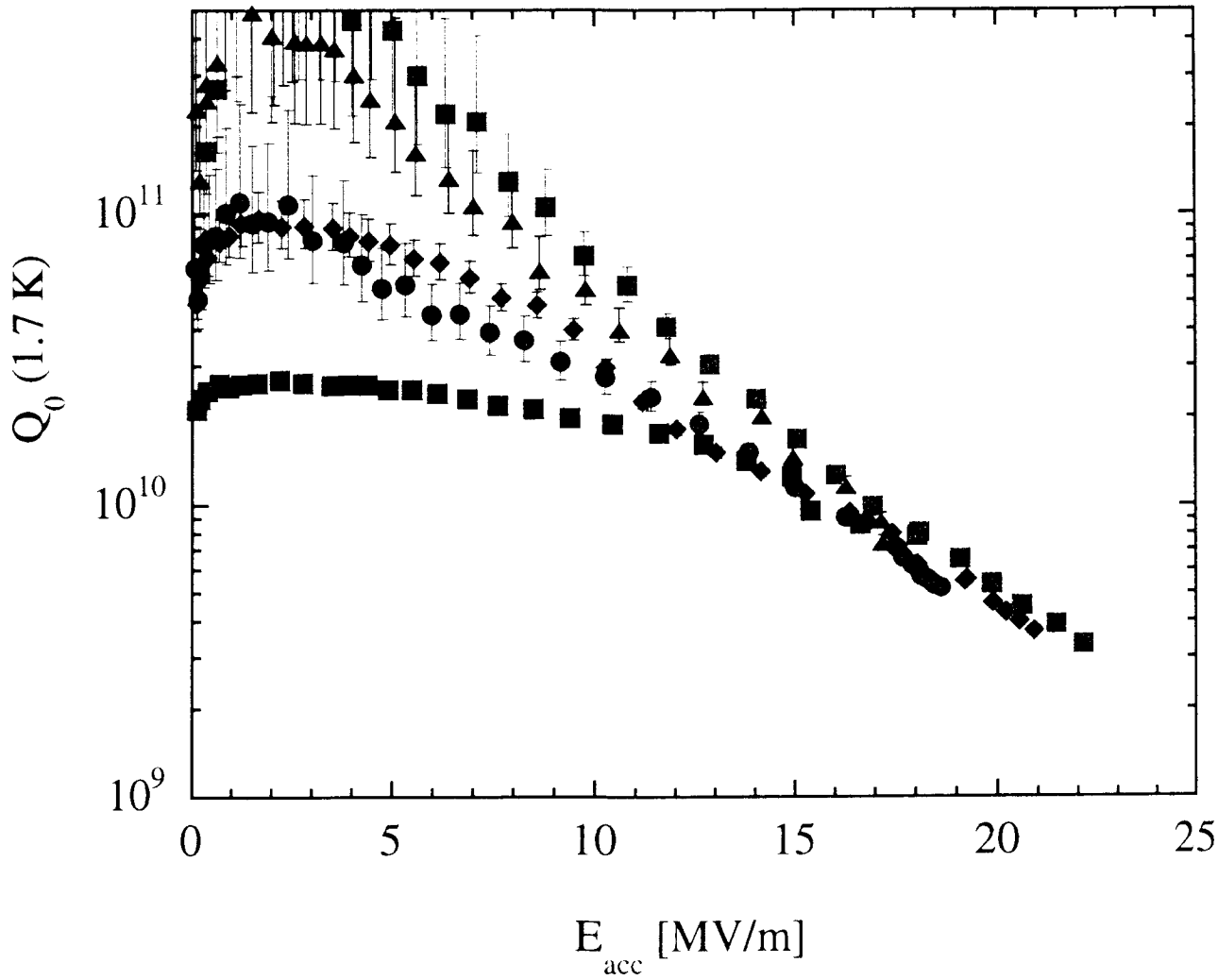
10^{11}
10^{10}
10^{9}
Q_0 (1.7 K)
0
5
10
15
20
25
E_{acc} [MV/m]

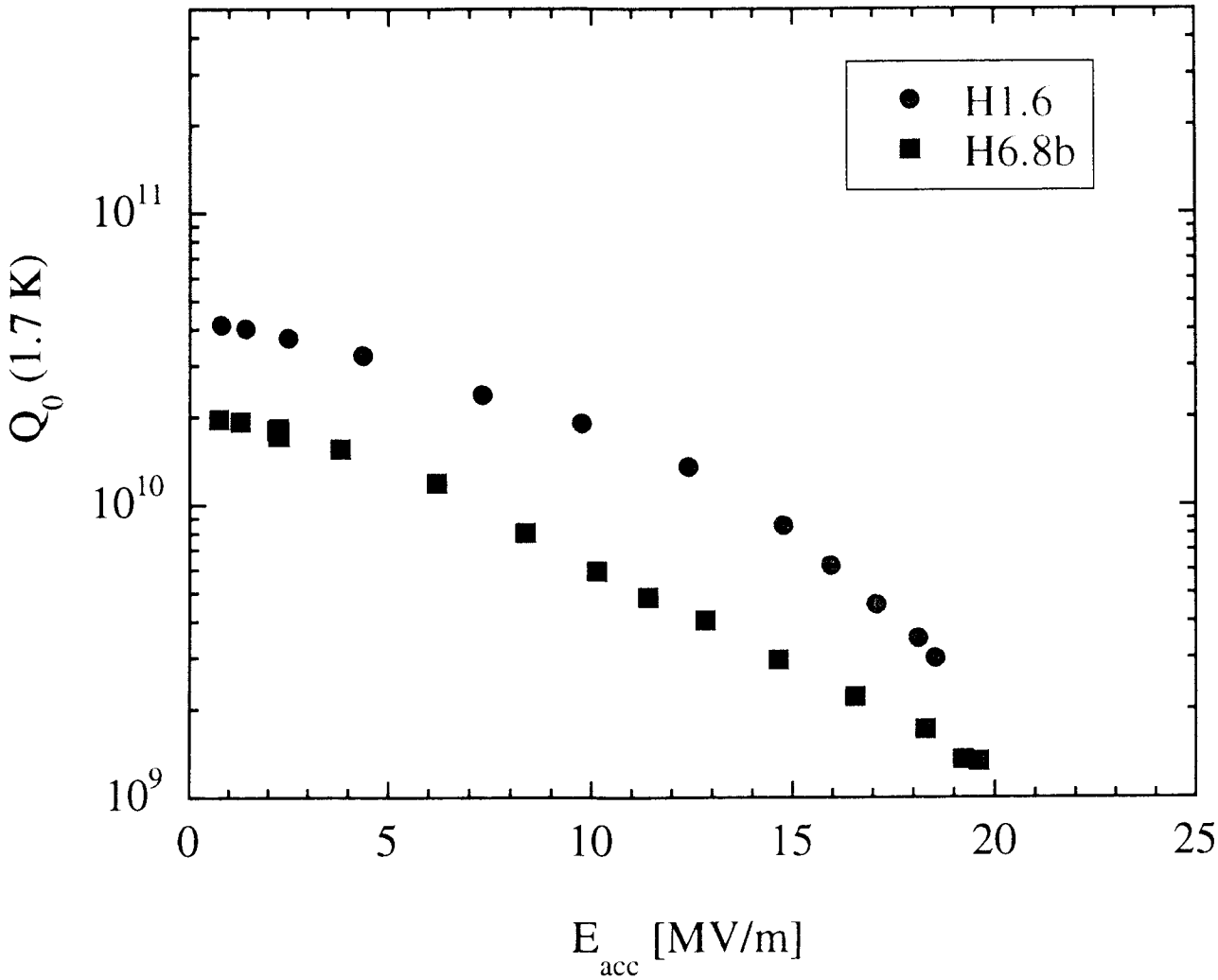
H1.6
H6.8b
10^{11}
10^{10}
10^{9}
Q_0 (1.7 K)
0
5
10
15
20
25
E_{acc} [MV/m]

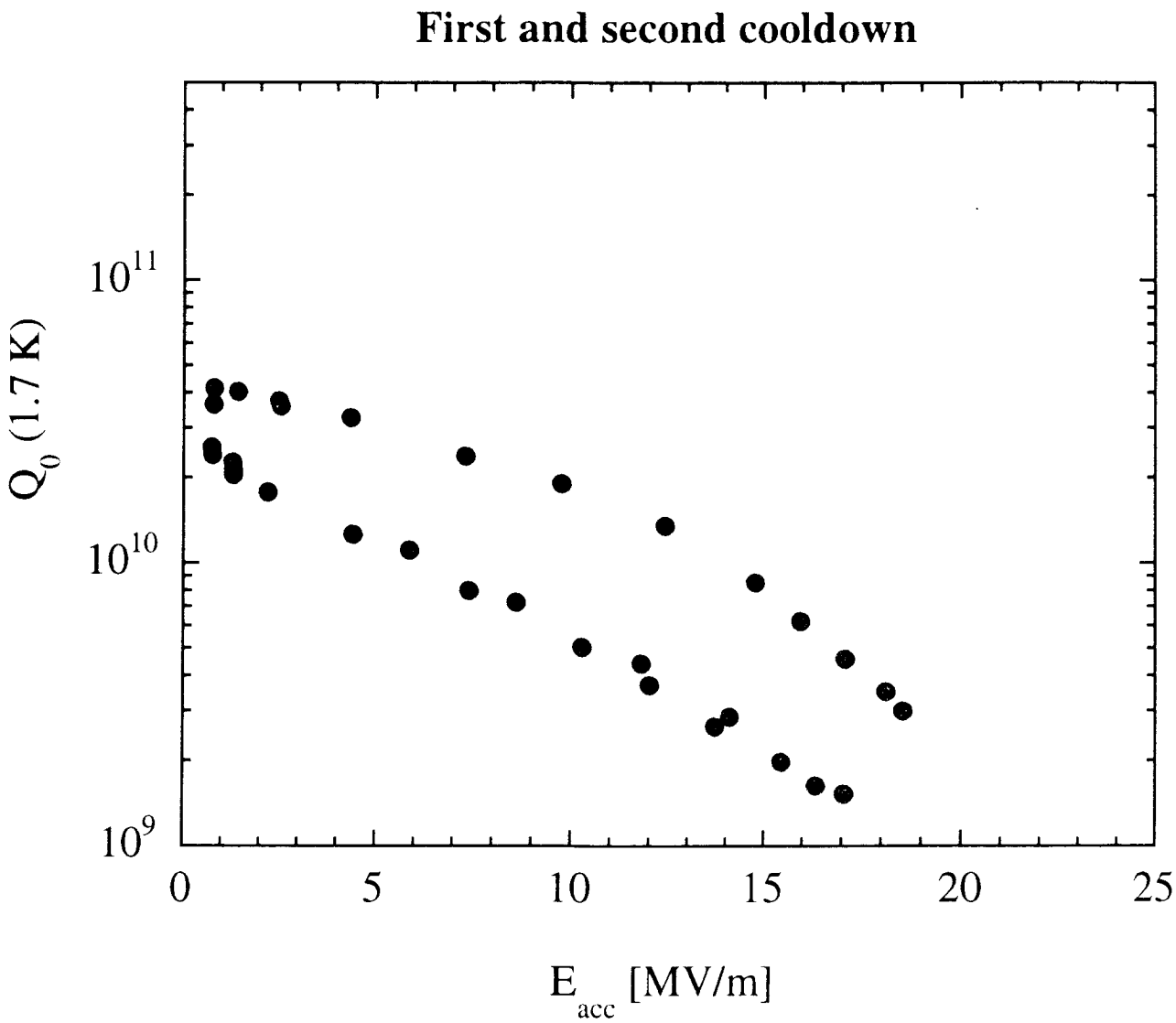
First and second cooldown
Q_0 (1.7 K)
10^{11}
10^{10}
10^{9}
0
5
10
15
20
25
E_{acc} [MV/m]

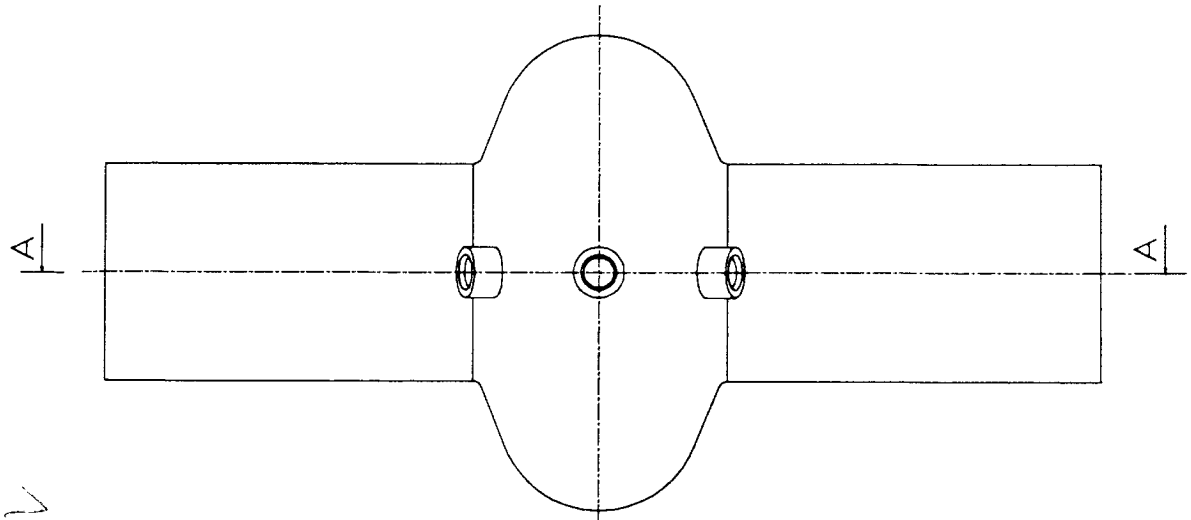

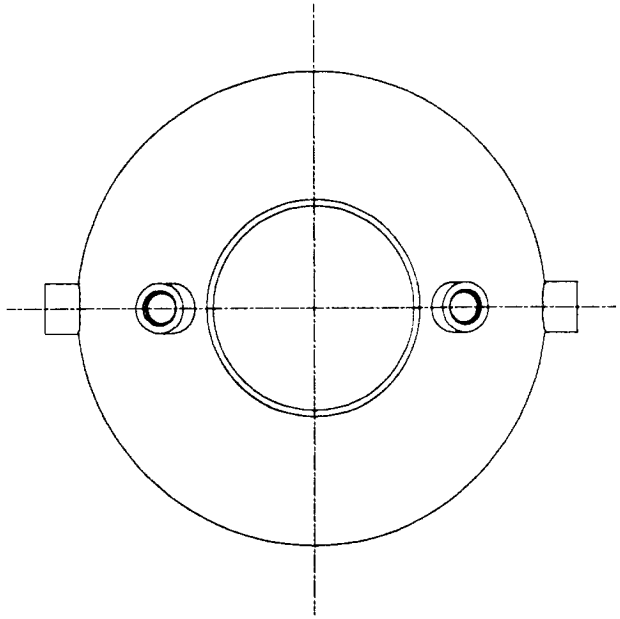

1/2 COUPE A-A

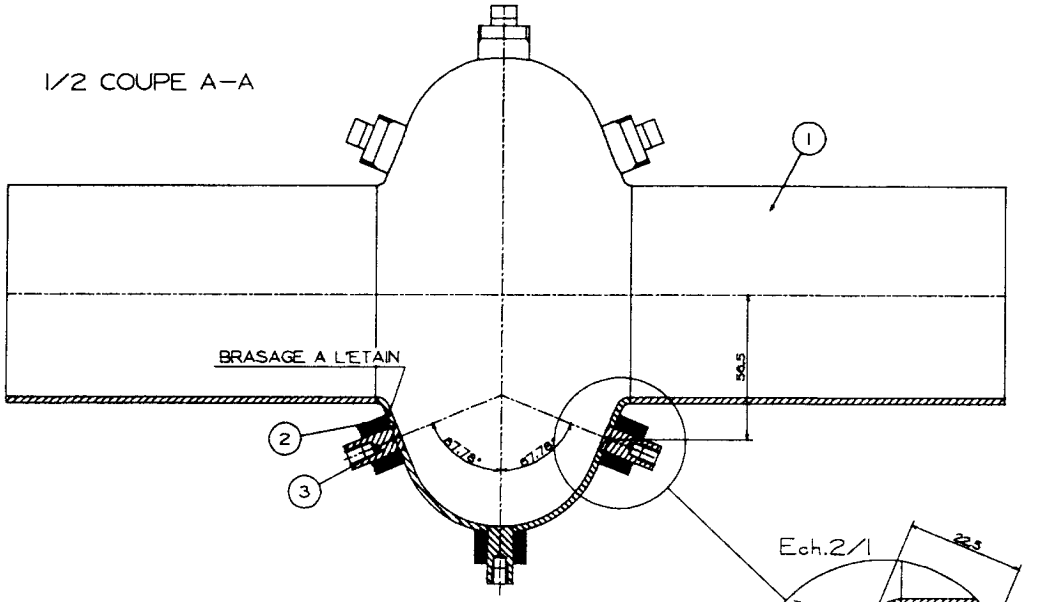

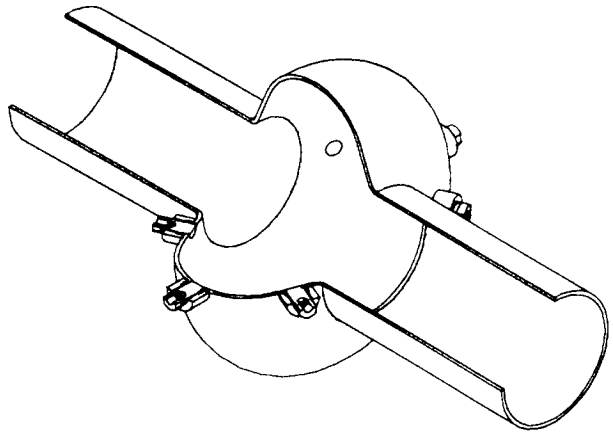

Ech.2/1

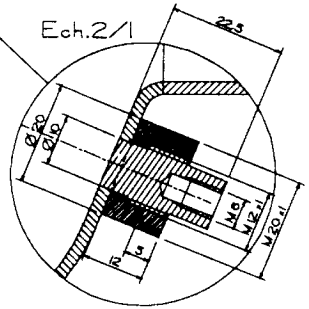

QUANT	DESIGNATION	POS	MAT.	OBSERVATIONS	REFERENCE
	ROND Ø 16	3	CUIVRE OFHC		4.4.09.A.7
					2.16.6
6	ROND Ø 28	2	A/S 304 L		4.4.57.10
					4.20.A
1	CAVITE 1.5 GHz	1		06LEPAASCT00802	

SYMB./ABBR. — SYMB./SIGNES

CAVITE SUPRA TEST	ECHELLE SCALE		NOM/NAME	DATE
CAVITE 1.5 GHZ MODIFICATION POUR TEST POLISSAGE CH - -	1/1 2/1	DESS./DRA.	G.POPPARD	1997-07-04
		CONTROL		
		APPROB.		
		UNCONTROLLED COPY		
		REPLACES/REPLACES		
NON VALABLE POUR EXECUTION NOT VALID FOR EXECUTION		06LEPAASCT059771		REV.

IND.	DATE	NOM/NAME	ZONE	MODIFICATION

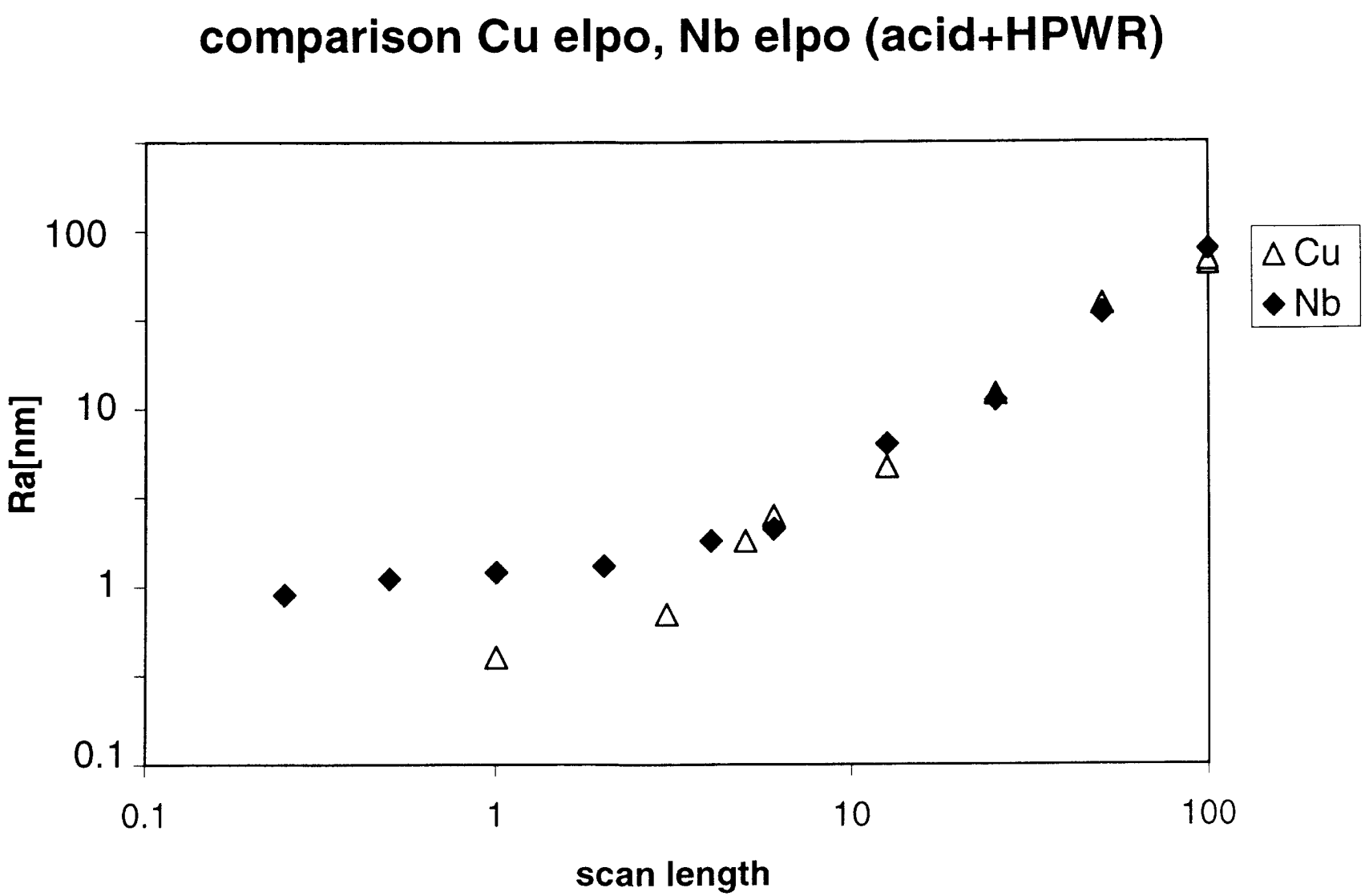
comparison Cu elpo, Nb elpo (acid+HPWR)
Ra[nm]
100
10
1
0.1
0.1
1
10
100
scan length
Cu
Nb

Effect of Nb angle of incidence

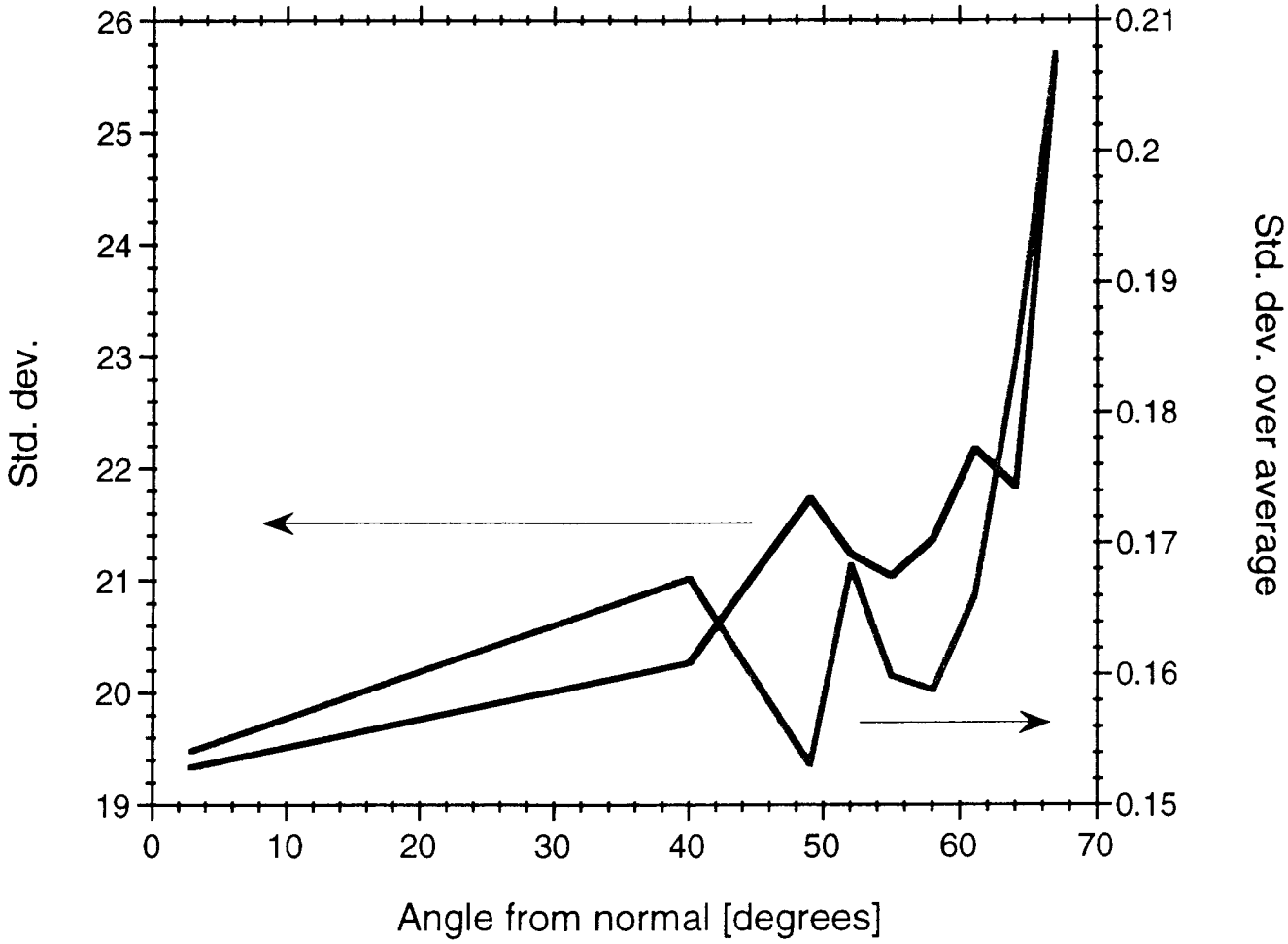

Surface quality : effect of roughness and sputtering incidence angle

Irregularities on the substrate surface ➡ shadowing effect
film inhomogeneities

He leak rate experiment (CHEMICAL POLISHING)

	$\langle\theta_{sp}\rangle$	fraction of leaky film surface
equator	9°	4.4 ppm
iris	50°	25 ppm

EQUATOR EP 0.1 ppm

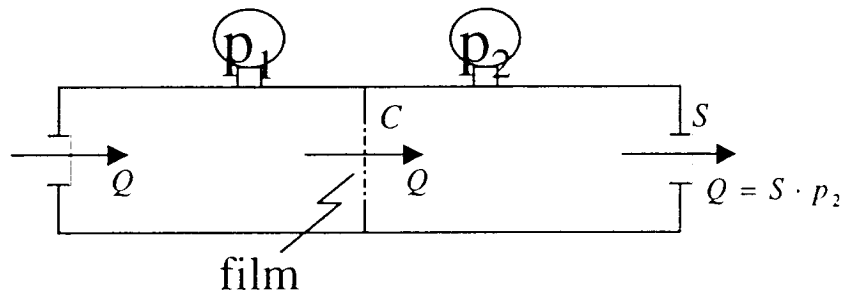

KAPITZA IMPEDANCE

Cu/He INTERFACE:

CONDUCTANCE $\simeq 800 \div 1200\, T^3$ $[W K^{-1} m^{-2}]$

$\rightarrow$ 1.8 K $\simeq 4700 \div 7000$ $[W K^{-1} m^{-2}]$

J.M. RIEUBLAND, G. VANDONI LHC REPORT 232 (1998)

Nb/He INTERFACE:

CONDUCTANCE $\simeq 500 \div 900\, T^{3 \div 4}$

$\rightarrow$ 1.8 K $\simeq 4000 \div 6500$

J. AMRIT, MX. FRANCOIS J. LOW. TEMP. PHYS 119 (2000) 27

Nb/Cu INTERFACE:

SOUND VELOCITY: Nb $\rightarrow$ $3.48 \cdot 10^3\, m s^{-1}$

Cu $\rightarrow$ $3.57 \cdot 10^3\, m s^{-1}$

$\rightarrow$ $\alpha_{CRITICAL} = \arcsin(v_1/v_2) = 77° \rightarrow 1.56\pi$

ACOUSTIC IMPEDANCE: $\rho v_{Nb} = 2.98 \times 10^7\, kg m^{-2} s^{-1}$

$\rho_{Nb} = 8.57$ $\rho_{Cu} = 8.32$ $\rho v_{Cu} = 3.18 \cdot 10^7\, Kg m^{-2} s^{-1}$

$\rightarrow$ ENERGY TRANSMISSION $\gtrsim 0.99$

THE ELECTRONIC CONTRIBUTION IS (?) NEGLIGIBLE.

The residual resistance: effect of hydrogen

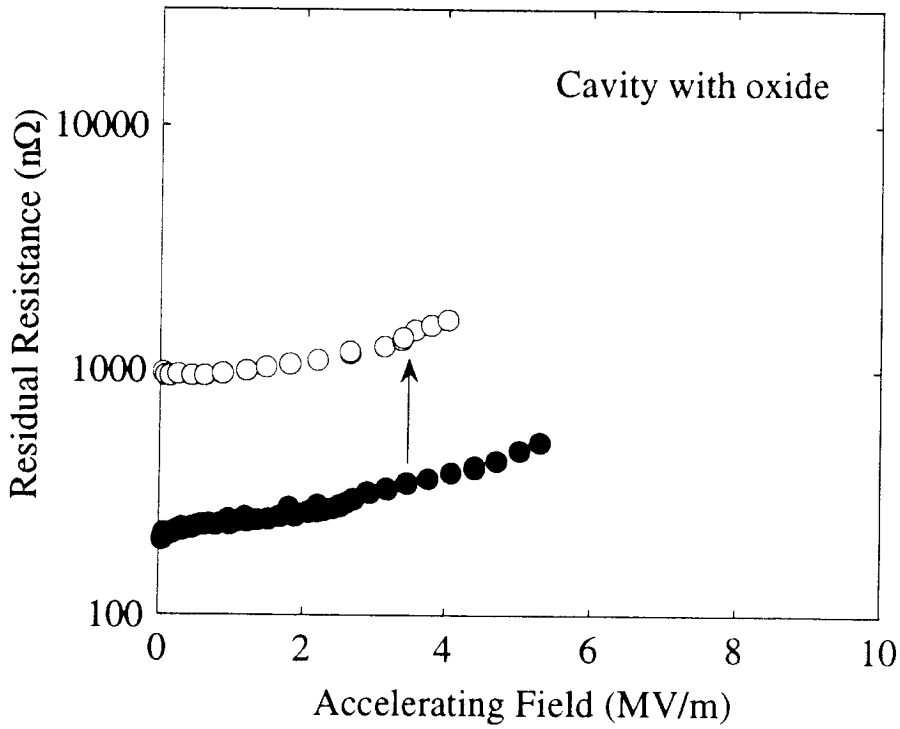

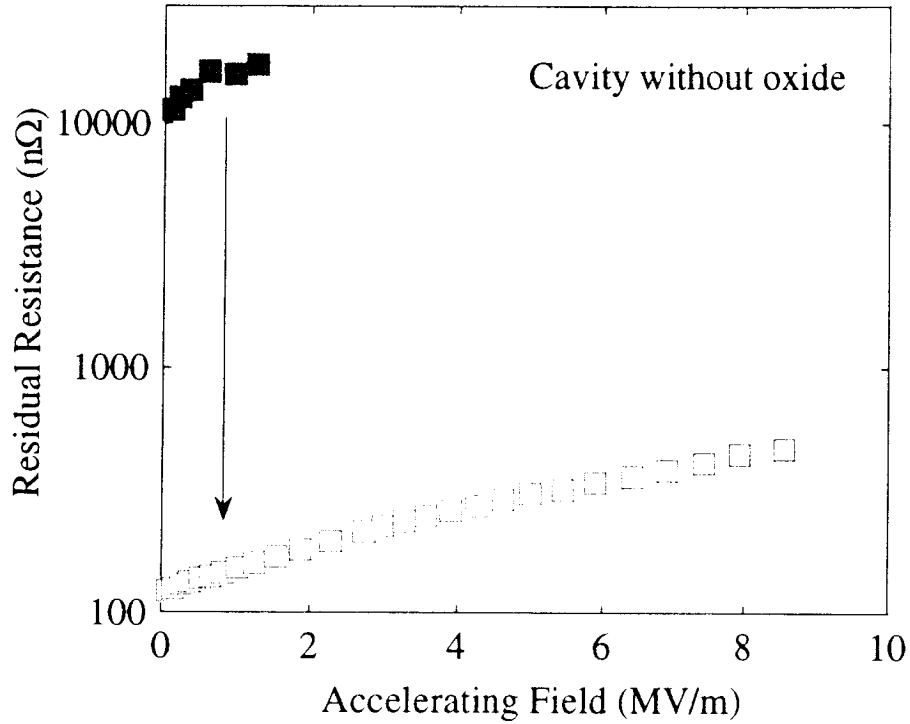

Full symbols: spun cavities coated using argon as sputter gas, loaded with 1.5% at. of hydrogen

Empty symbols: same after outgassing at 300 °C for 12 hours

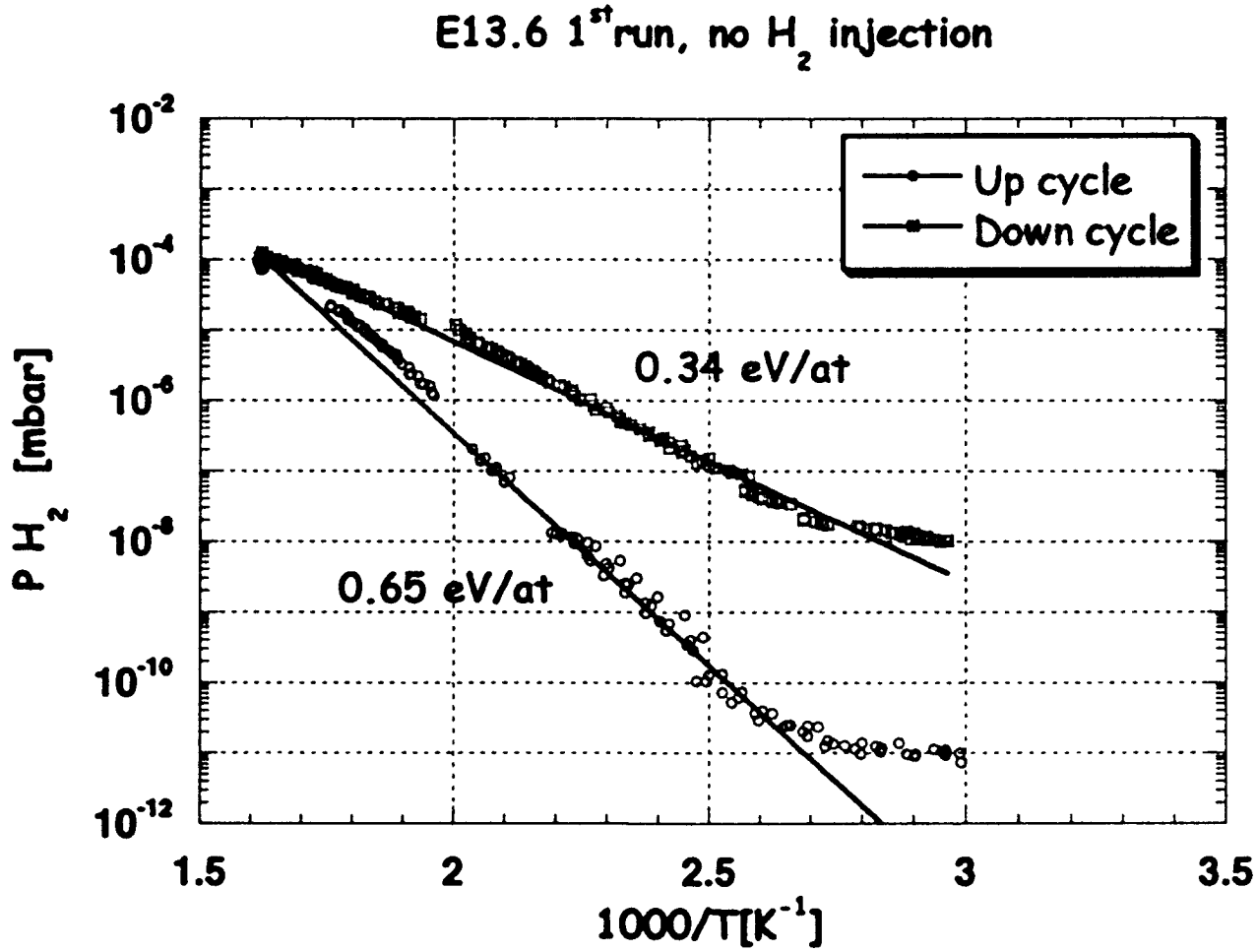
E13.6 1st run, no H2 injection
Up cycle
Down cycle
0.34 eV/at
0.65 eV/at
P H2 [mbar]
10-2
10-4
10-6
10-8
10-10
10-12
1.5
2
2.5
3
3.5
1000/T[K-1]

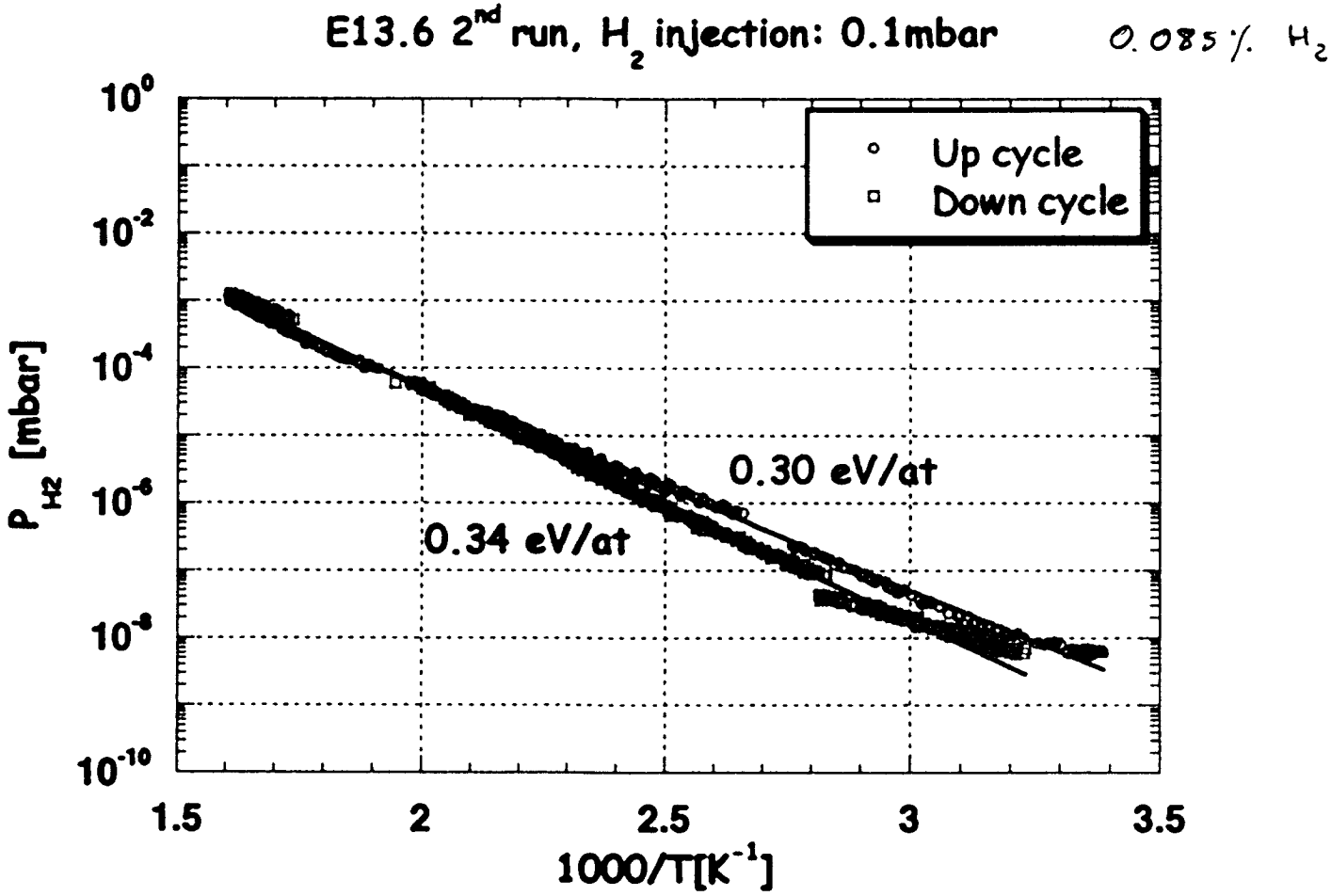
E13.6 2nd run, H2 injection: 0.1mbar
0.085% H2
Up cycle
Down cycle
0.30 eV/at
0.34 eV/at
P H2 [mbar]
1000/T[K-1]
10^0
10^-2
10^-4
10^-6
10^-8
10^-10
1.5
2
2.5
3
3.5

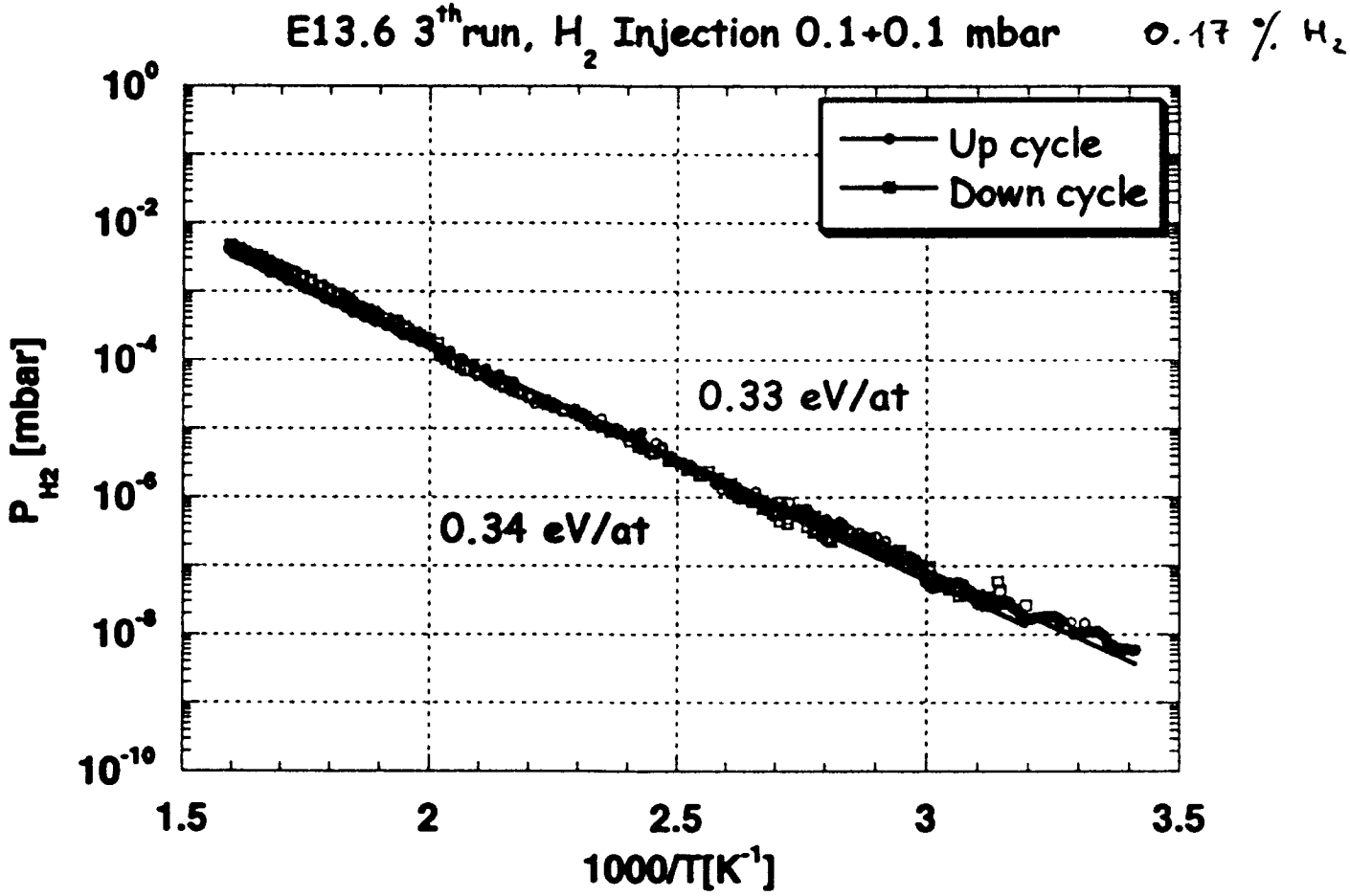
E13.6 3th run, H2 Injection 0.1+0.1 mbar
0.17 % H2
Up cycle
Down cycle
0.33 eV/at
0.34 eV/at
P H2 [mbar]
1000/T[K-1]
10^0
10^-2
10^-4
10^-6
10^-8
10^-10
1.5
2
2.5
3
3.5

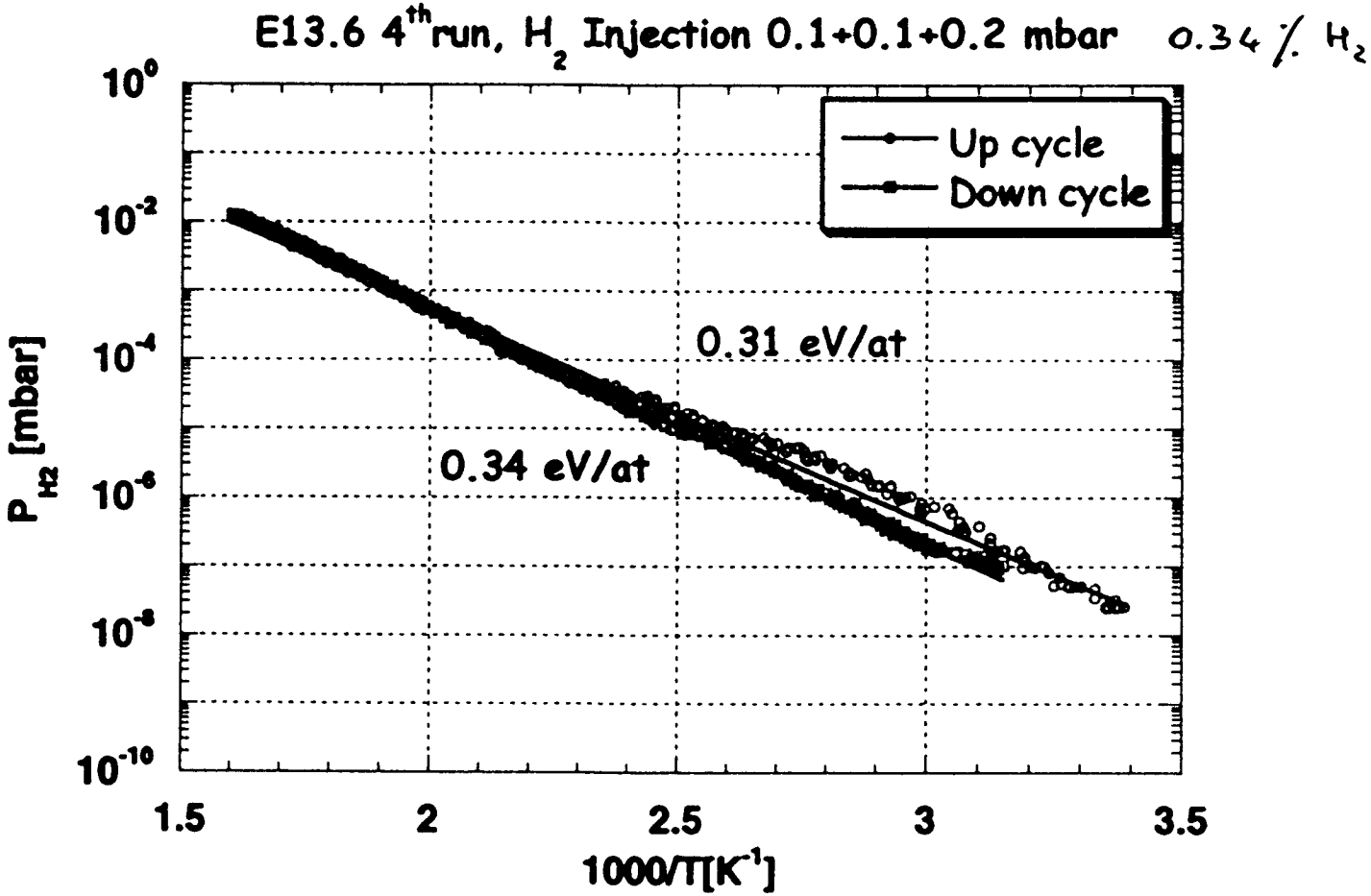
E13.6 4th run, H2 Injection 0.1+0.1+0.2 mbar 0.34 % H2
Up cycle
Down cycle
0.31 eV/at
0.34 eV/at
P H2 [mbar]
1000/T[K-1]
10^0
10^-2
10^-4
10^-6
10^-8
10^-10
1.5
2
2.5
3
3.5

154

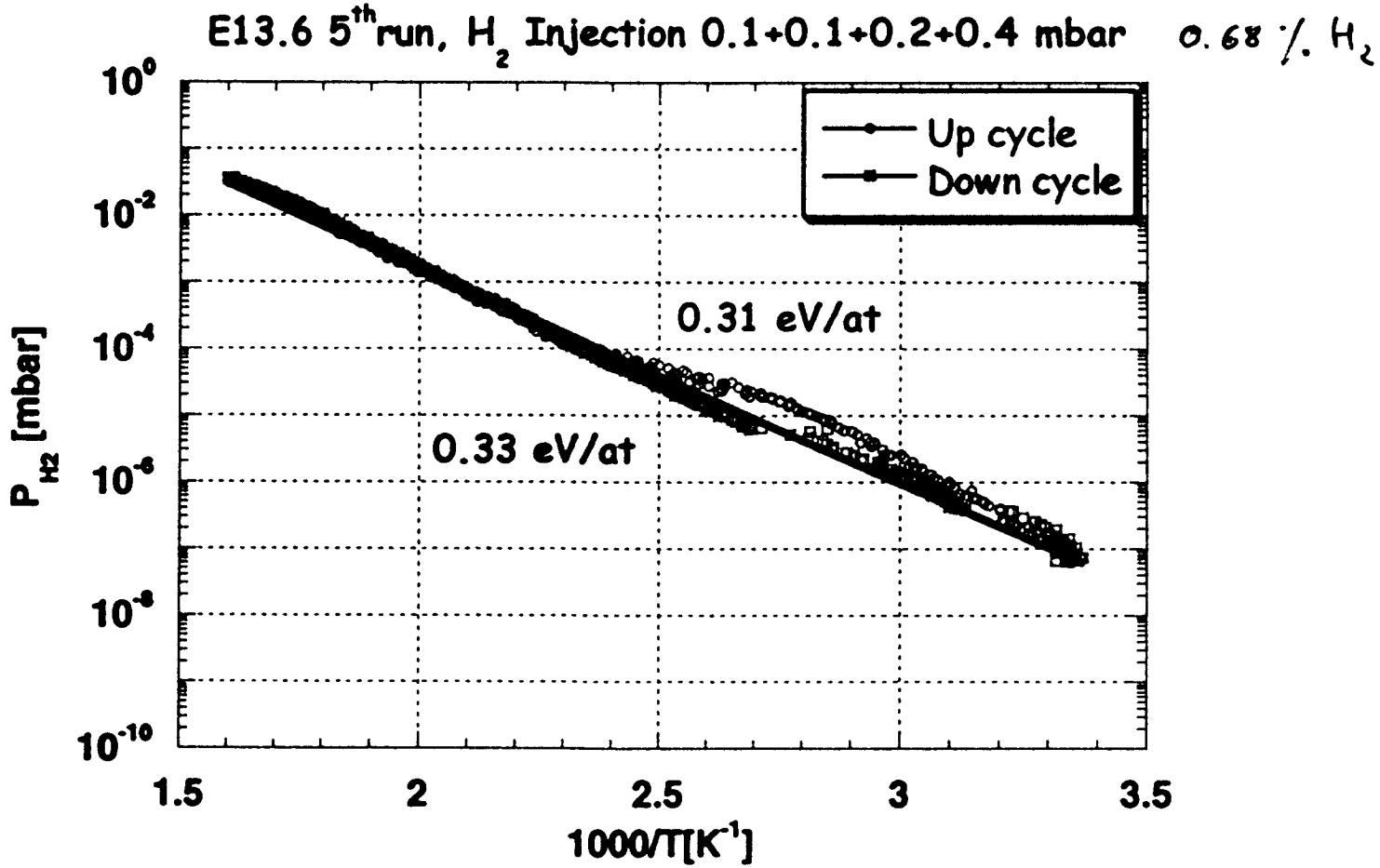
E13.6 5th run, H2 Injection 0.1+0.1+0.2+0.4 mbar
0.68 % H2
Up cycle
Down cycle
0.31 eV/at
0.33 eV/at
P H2 [mbar]
10^0
10^-2
10^-4
10^-6
10^-8
10^-10
1.5
2
2.5
3
3.5
1000/T[K^-1]

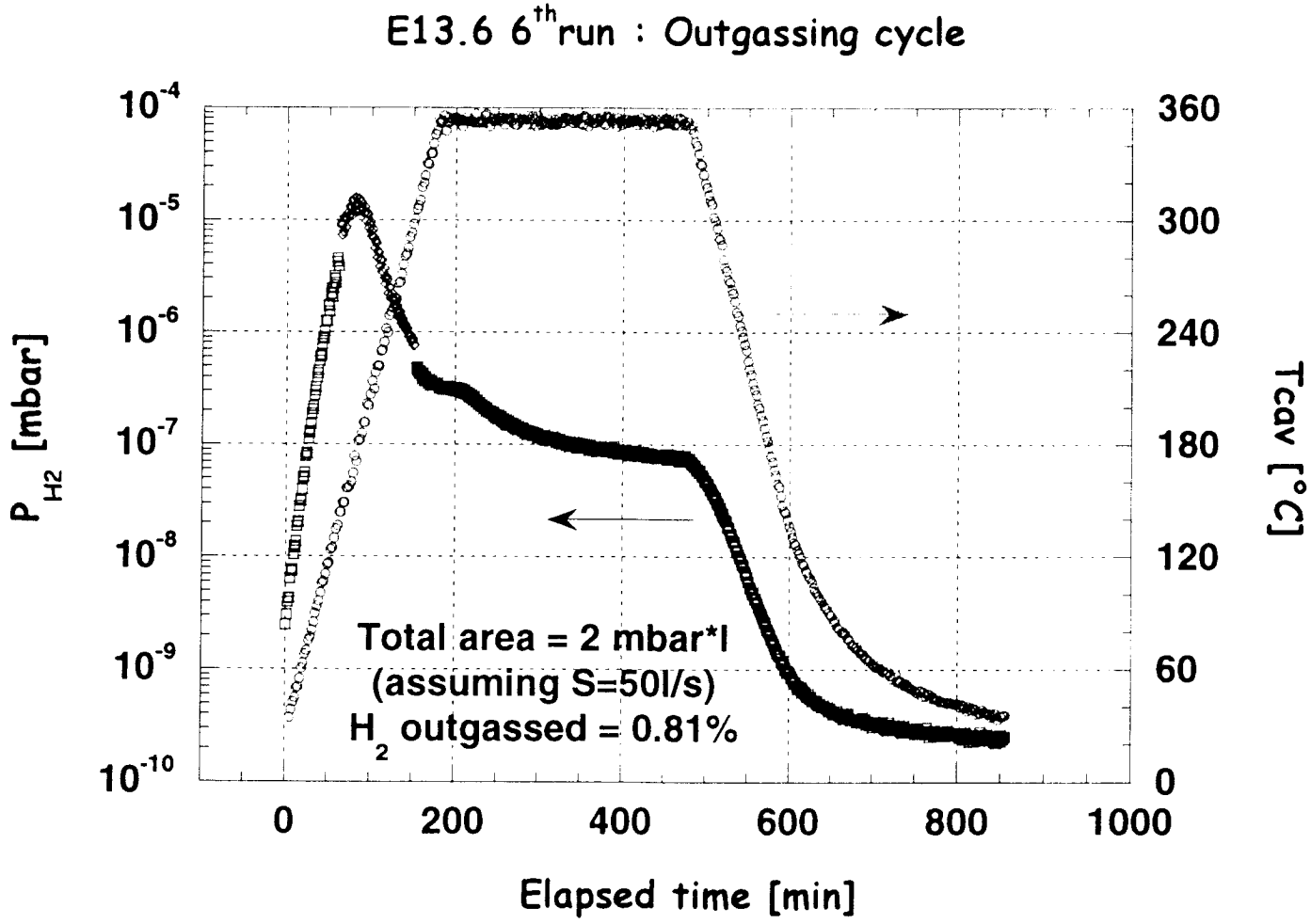
E13.6 6th run : Outgassing cycle
P_{H2} [mbar]
10^{-4}
10^{-5}
10^{-6}
10^{-7}
10^{-8}
10^{-9}
10^{-10}
Tcav [°C]
360
300
240
180
120
60
0
0
200
400
600
800
1000
Elapsed time [min]
Total area = 2 mbar*l
(assuming S=50l/s)
H_2 outgassed = 0.81%

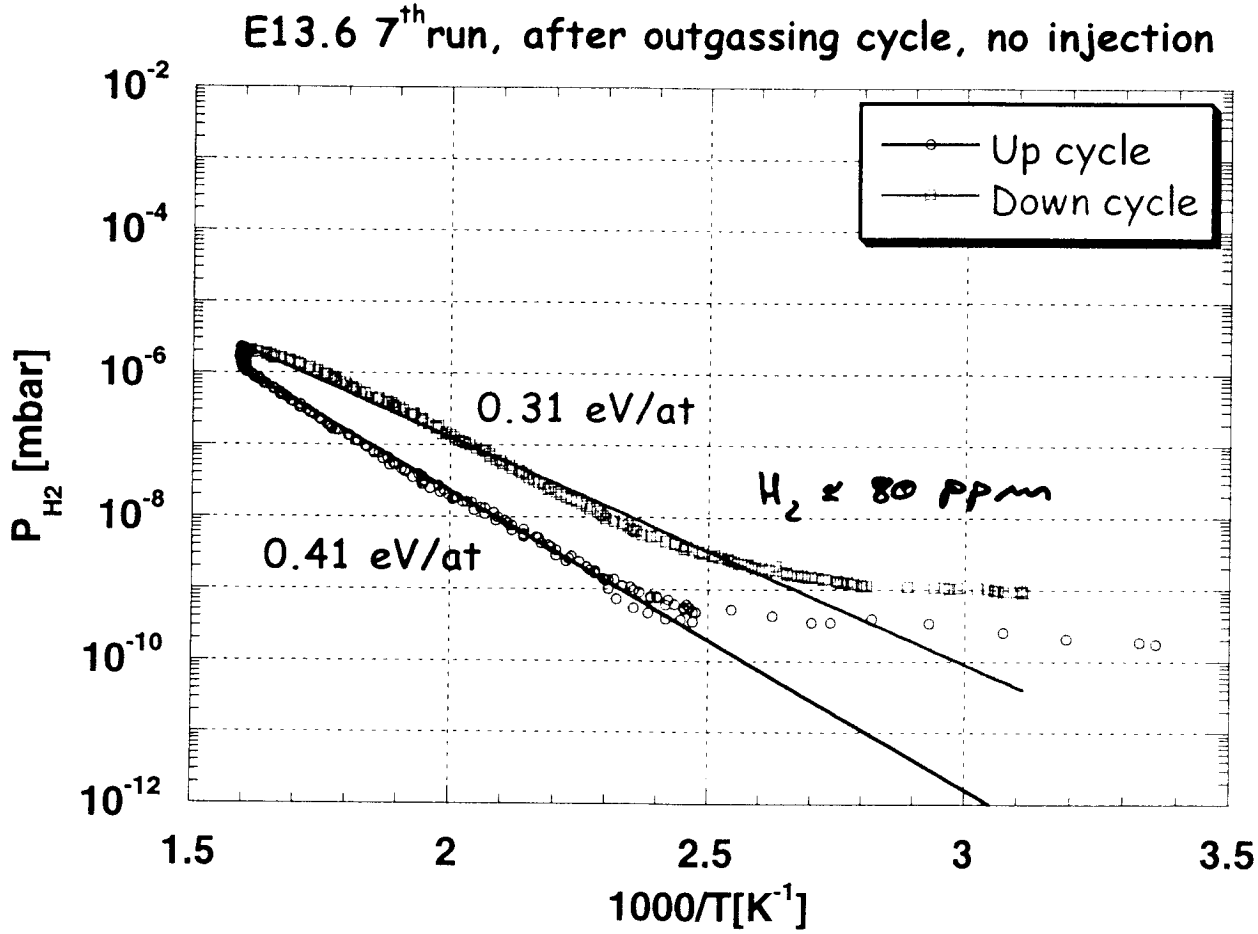
E13.6 7th run, after outgassing cycle, no injection
Up cycle
Down cycle
0.31 eV/at
0.41 eV/at
H2 ≈ 80 ppm
P H2 [mbar]
1000/T[K-1]
10-2
10-4
10-6
10-8
10-10
10-12
1.5
2
2.5
3
3.5

ASV

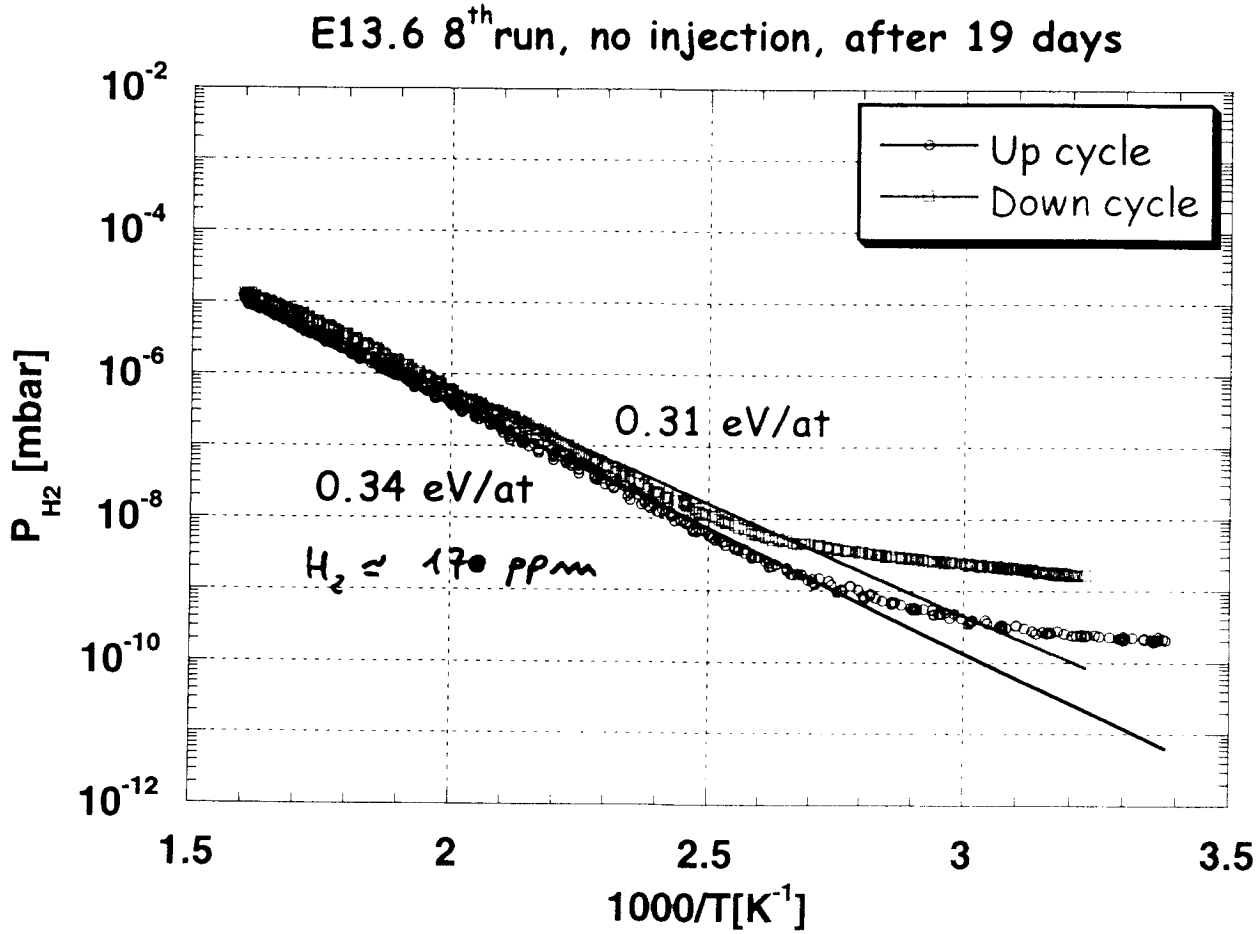
E13.6 8th run, no injection, after 19 days
Up cycle
Down cycle
0.31 eV/at
0.34 eV/at
H2 ≃ 170 ppm
P H2 [mbar]
10-2
10-4
10-6
10-8
10-10
10-12
1.5
2
2.5
3
3.5
1000/T[K-1]

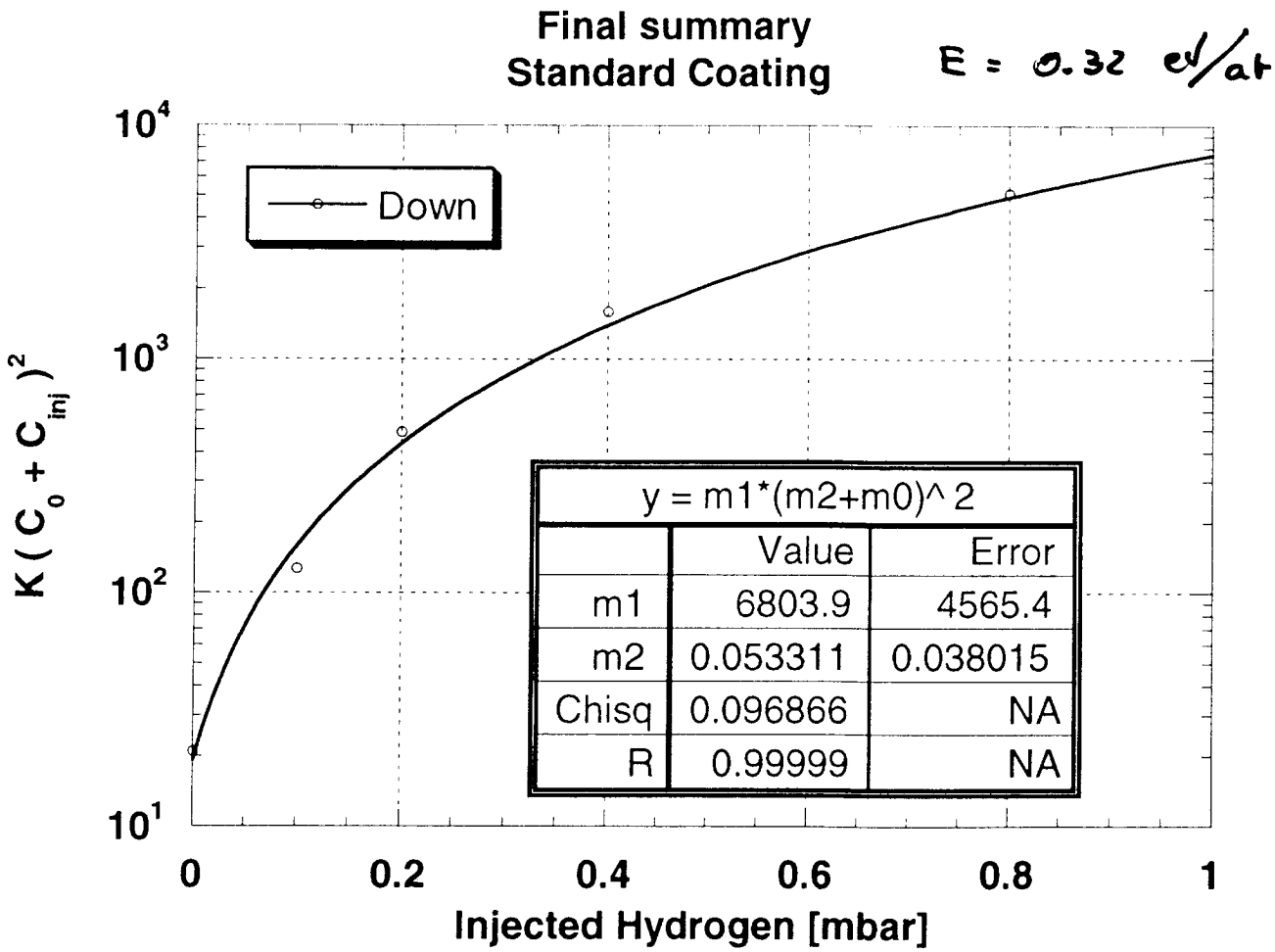
Final summary
Standard Coating
E = 0.32 eV/at
Down
$K(C_o + C_{inj})^2$
10^4
10^3
10^2
10^1
0
0.2
0.4
0.6
0.8
1
Injected Hydrogen [mbar]
y = m1*(m2+m0)^ 2
Value
Error
m1 6803.9 4565.4
m2 0.053311 0.038015
Chisq 0.096866 NA
R 0.99999 NA

C_o = 0.04 % H_2

Thin Films activities at Saclay sputtered Nb/Cu cavities

P. Bosland

Nb/Cu sample studies

Marion Ribeaudeau (thesis)

- **Optimisation of coating parameters**
- **Influence of the coating temperature**

  sputtering or heating between 400°C et 800°C

  analysis of Cu diffusion in sputtered Nb (RBS, NRS)

- **Effect of copper roughness on the niobium films**

  Different substrate roughness

  Characterisations of the deposited films:

  → SEM observations

  → RRR, critical magnetic fields and temperature

  → R_s thermometric measurements (with IPN Orsay)

Effect of copper roughness on niobium films

- **substrates**

10µm

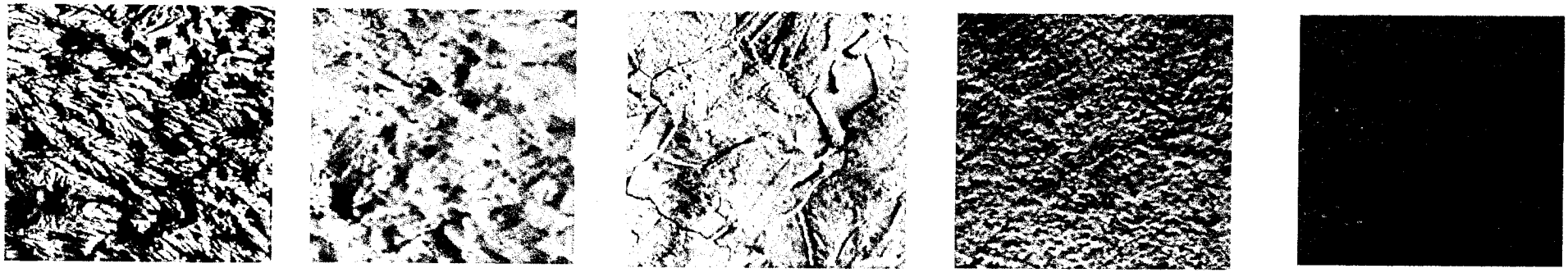

Ech1= SSCR2 Ra= 150nm

Ech2= SN6 Ra= 100nm

Ech3 =SN2 Ra= 25nm

Ech4=SSCR2+SN10 Ra= 15nm

Ech5=EL Ra= 10nm

- **coatings**

1µm

⇒ **micrometric defects on rough substrates**

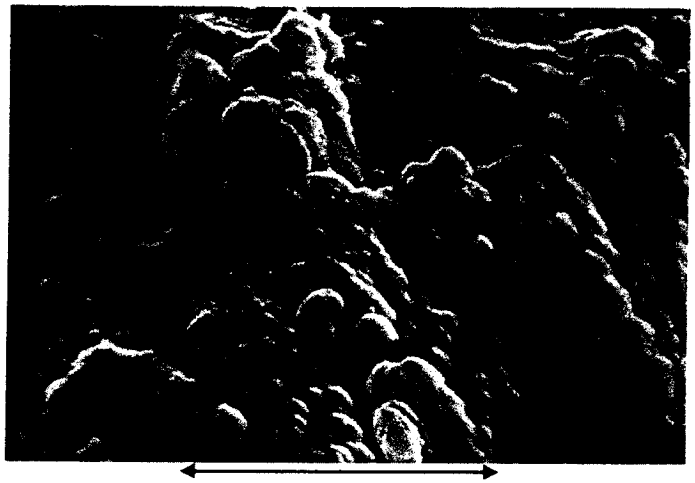

5μm

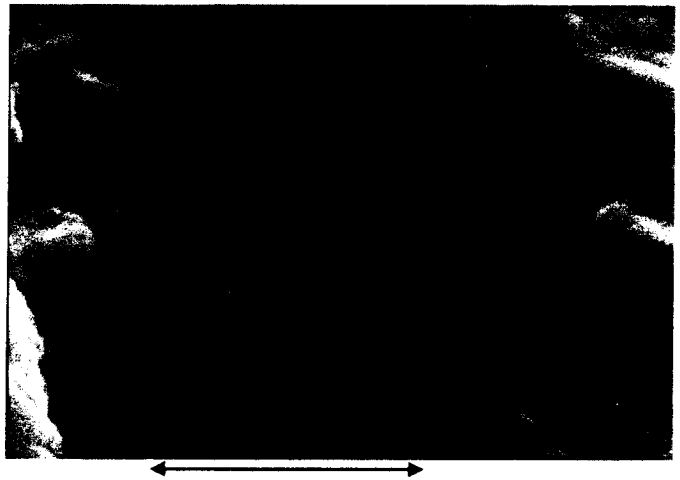

2μm

- **No effect on RRR (≈25)**

- **No effect on B_{c1} (SQUID)**

  sample 1 : $B_{c1}(0K)$=180mT T_c=9,45K

  sample 5 : $B_{c1}(0K)$= 175mT T_c=9,5K

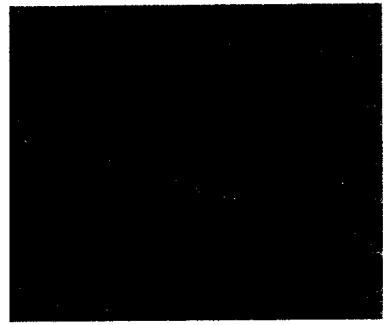

- **No effect on R_{BCS} (determined by thermometric measurements)**

$$R_{BCS} = \frac{A(\lambda,\xi,l)}{T} f^2 e^{-\frac{\Delta(O)T}{k_B T_c}}$$

- **Typical sputtered film defects**

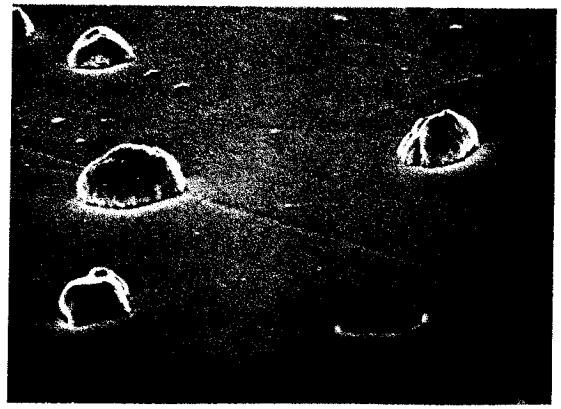

20 μm

- **Possible origins = seeds on the substrate:**
  - from magnetron cathode
  - dust particles on the copper substrate
  - roughness defects

Significant effect on R_{res}

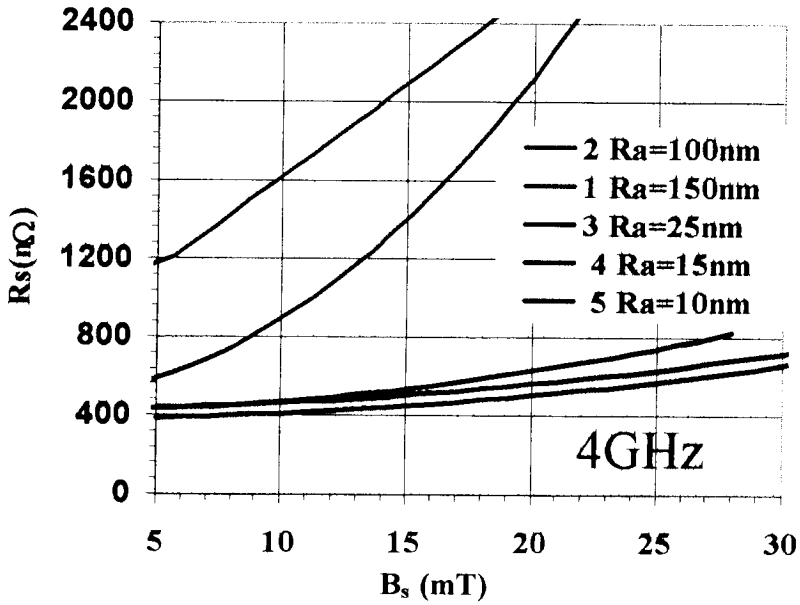

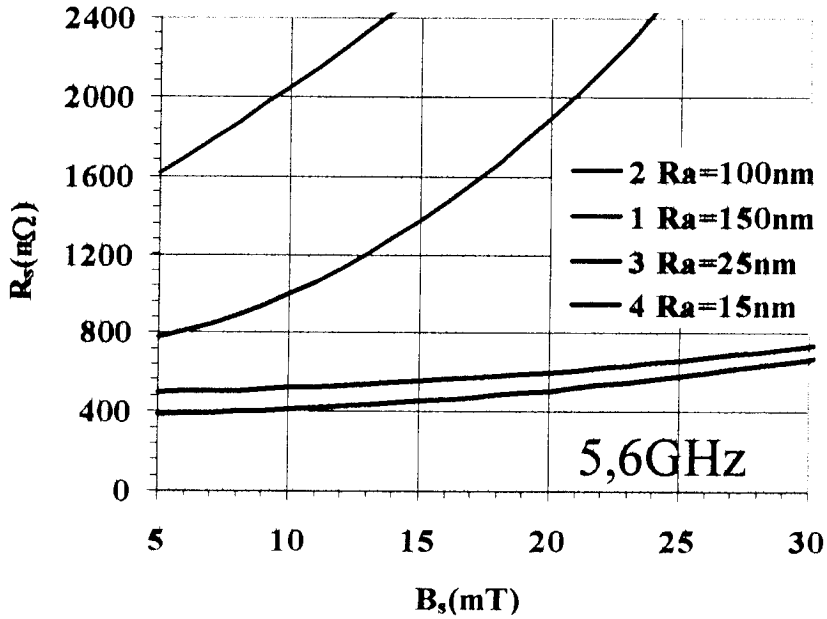

$\Rightarrow$ correlation between defect density and $R_{res}(B_s)$

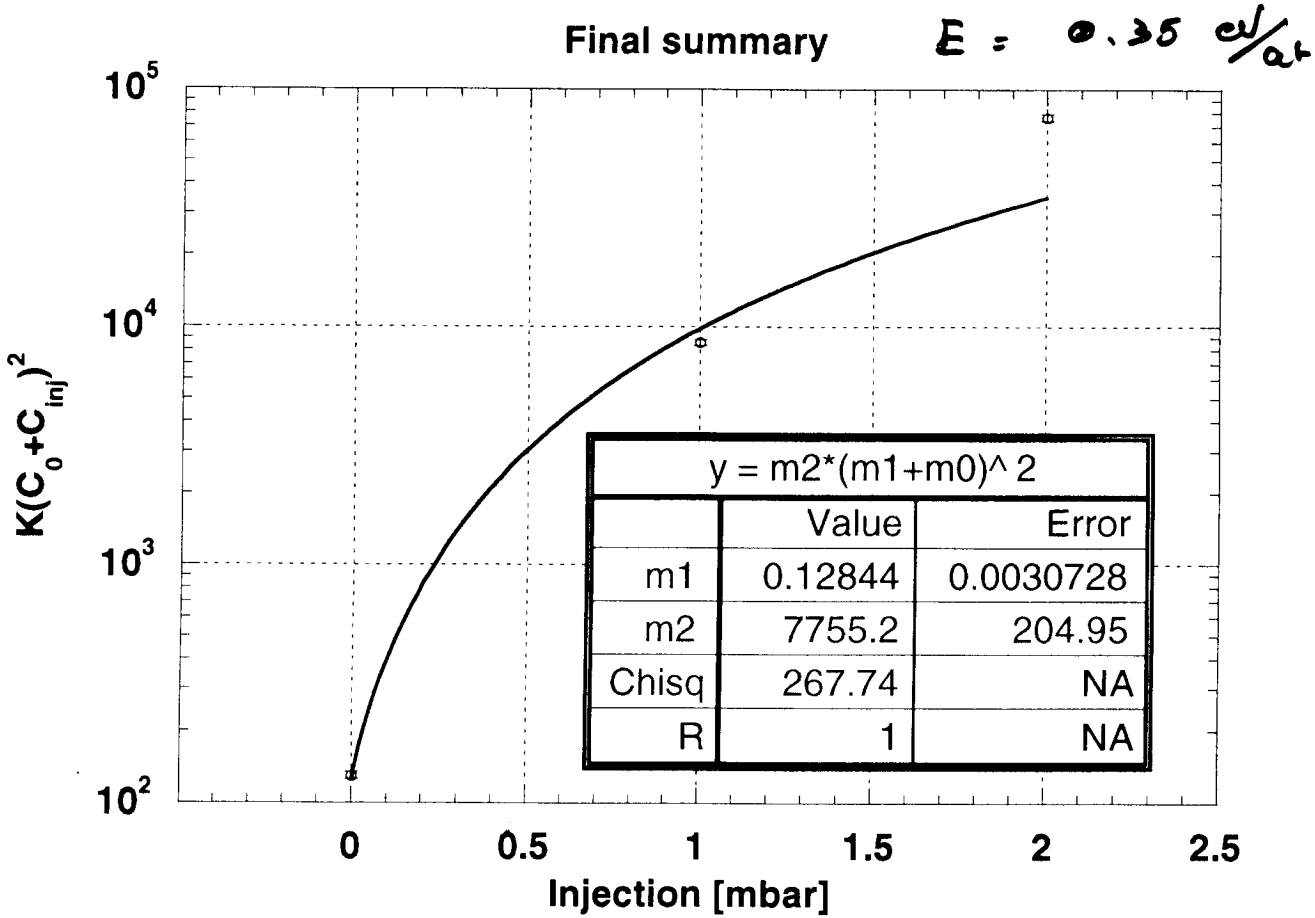

$\Rightarrow C_0 = 0.11\% \; H_2$

Copper underlayer

14

Sputtered cavities

- 1.5 GHz hydroformed at CERN
- 1.3 GHz hydroformed at Saclay

The major limitations of the Nb/Cu cavities performances seems to be linked to the copper surface before deposition rather than to the niobium sputtering itself .

We developed a chemical treatment for the copper cavities:
SN bath
(a mixture of sulphuric and nitric acids)

6 hydroformed 1.3GHz copper cavities

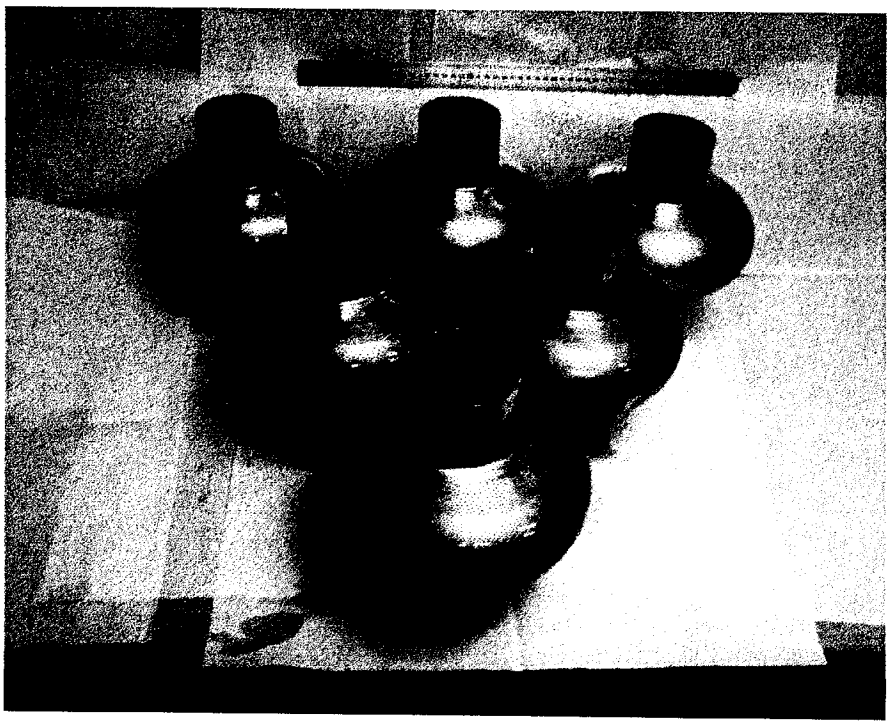

Magnetron sputtering

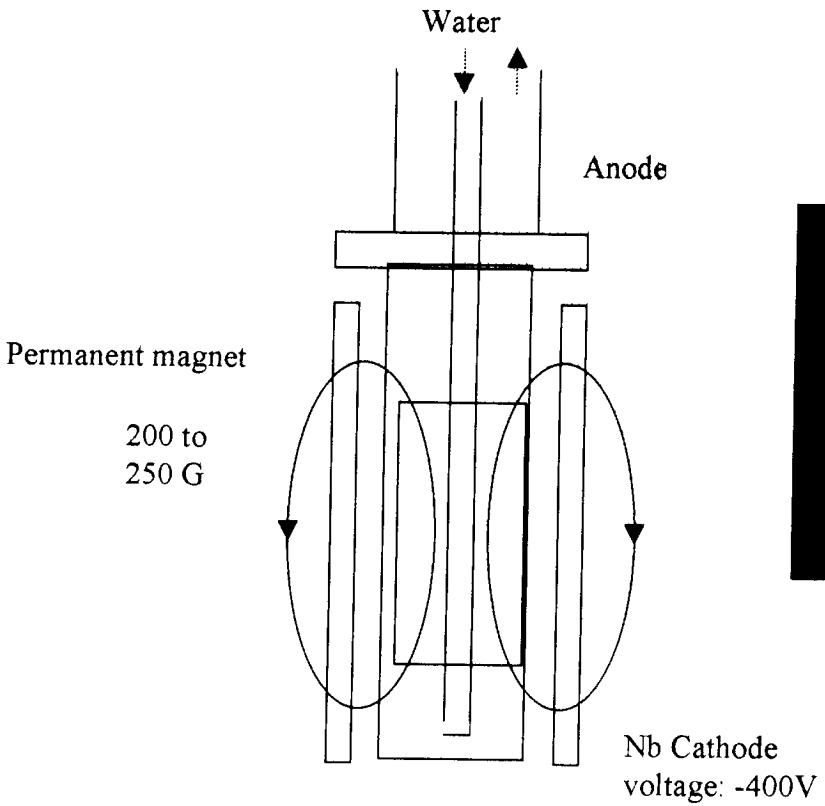

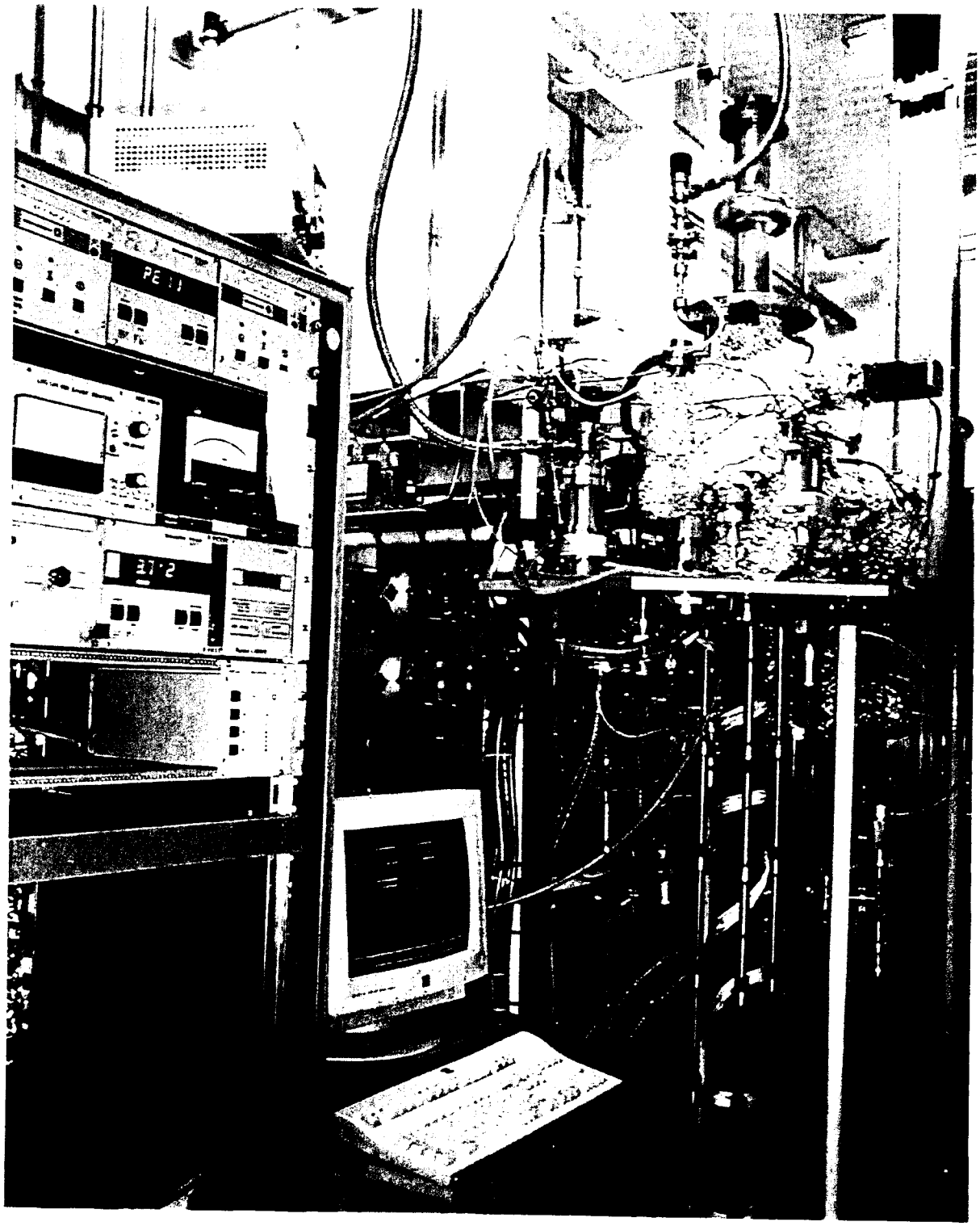
PE 11

Sequence of processing the cavities:

1- chemical polishing
2- HPR at 85 bars
3- drying in class 100 clean air room
4- mounting of flanges and dust free transport to the sputtering set-up
5- slow pumping of the cavities
6- Nb sputtering with argon (400 °C)
7- HPR at 85 or 30 Bars
8- drying in class 100 clean air room (about 3 hours)
9- mounting of flanges and dust free transport to the cryostat insert for RF tests

Hydroformed Nb/Cu cavity at 1.3GHz
S1-14

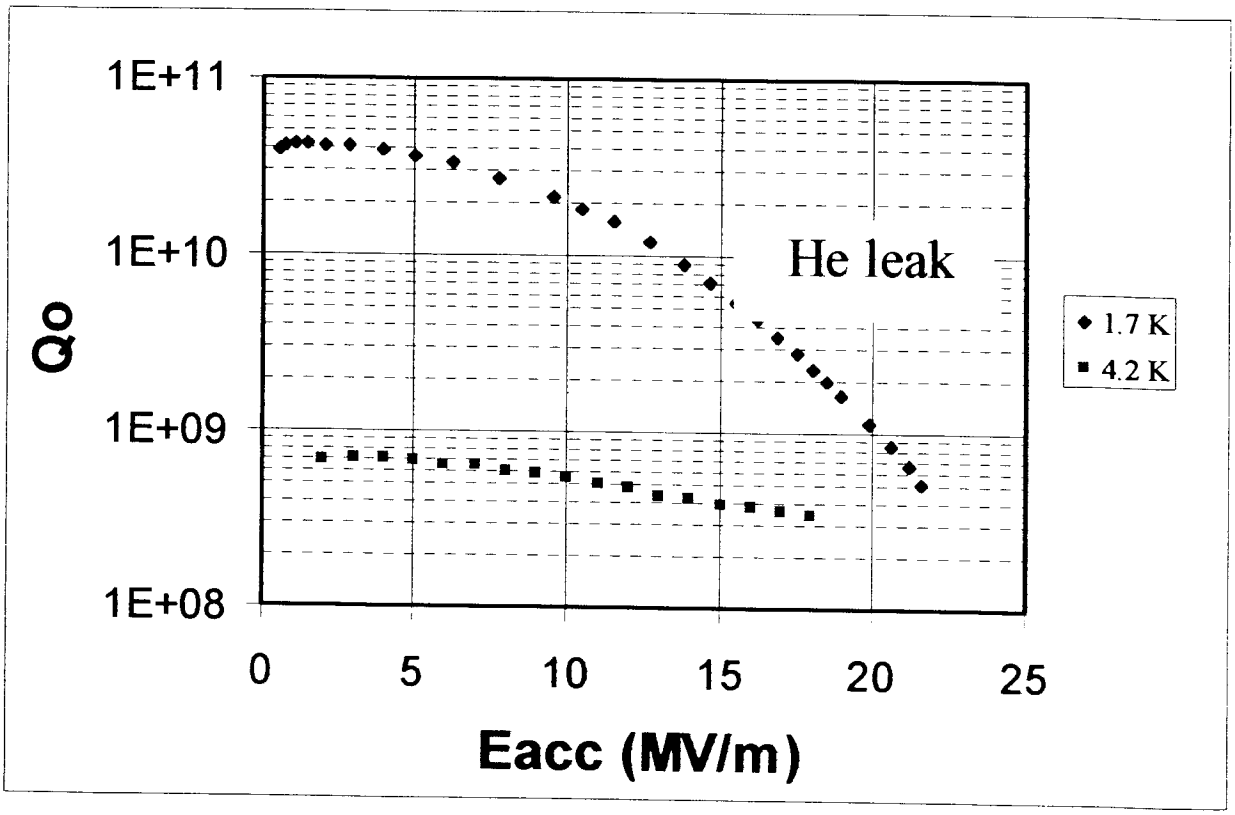

No exponential decrease:

effect of the copper characteristics ?

The five 1.5HGz cavities tested at 1.7 K without baking

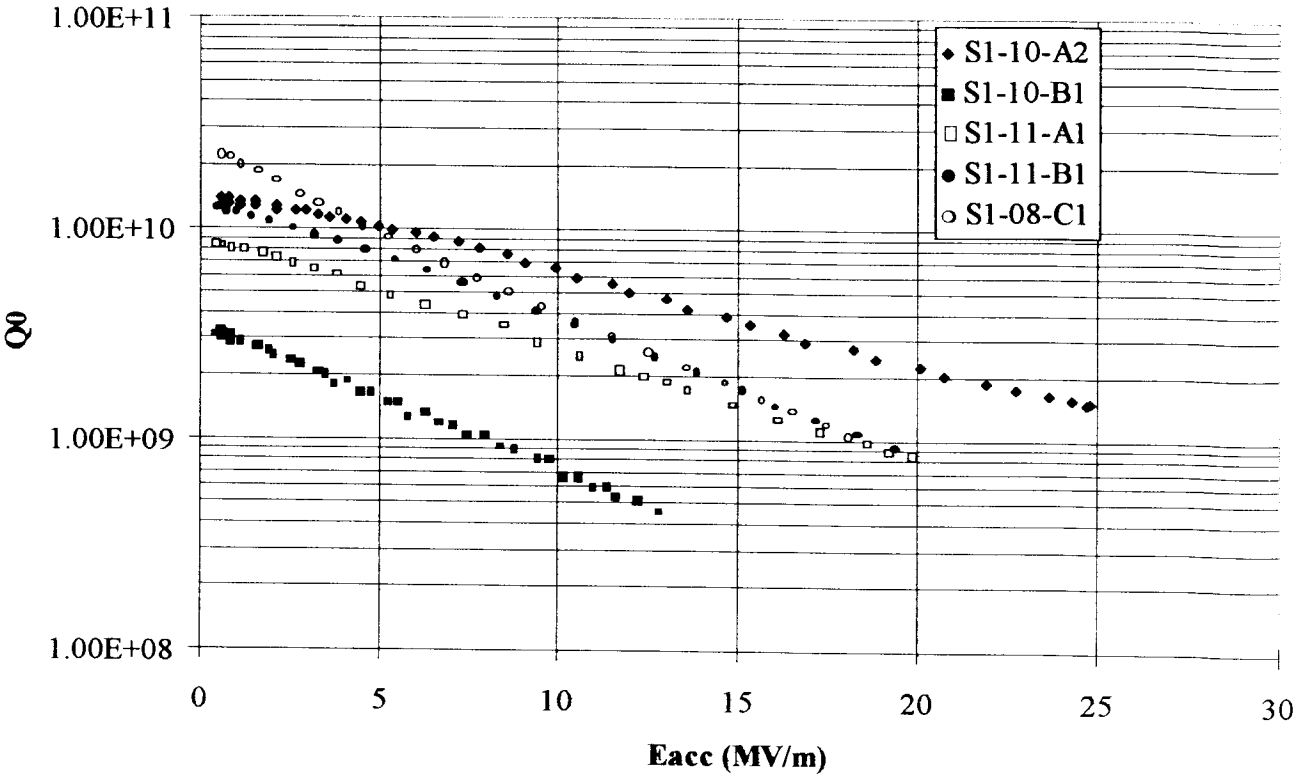

Exponential decrease of Q_0 for all cavities

Best result: E_{cc}=25MV/m with Q_0=1.2 10^9

Effect of baking

(S1-11 cavity baked at 90°C during 20 hours)

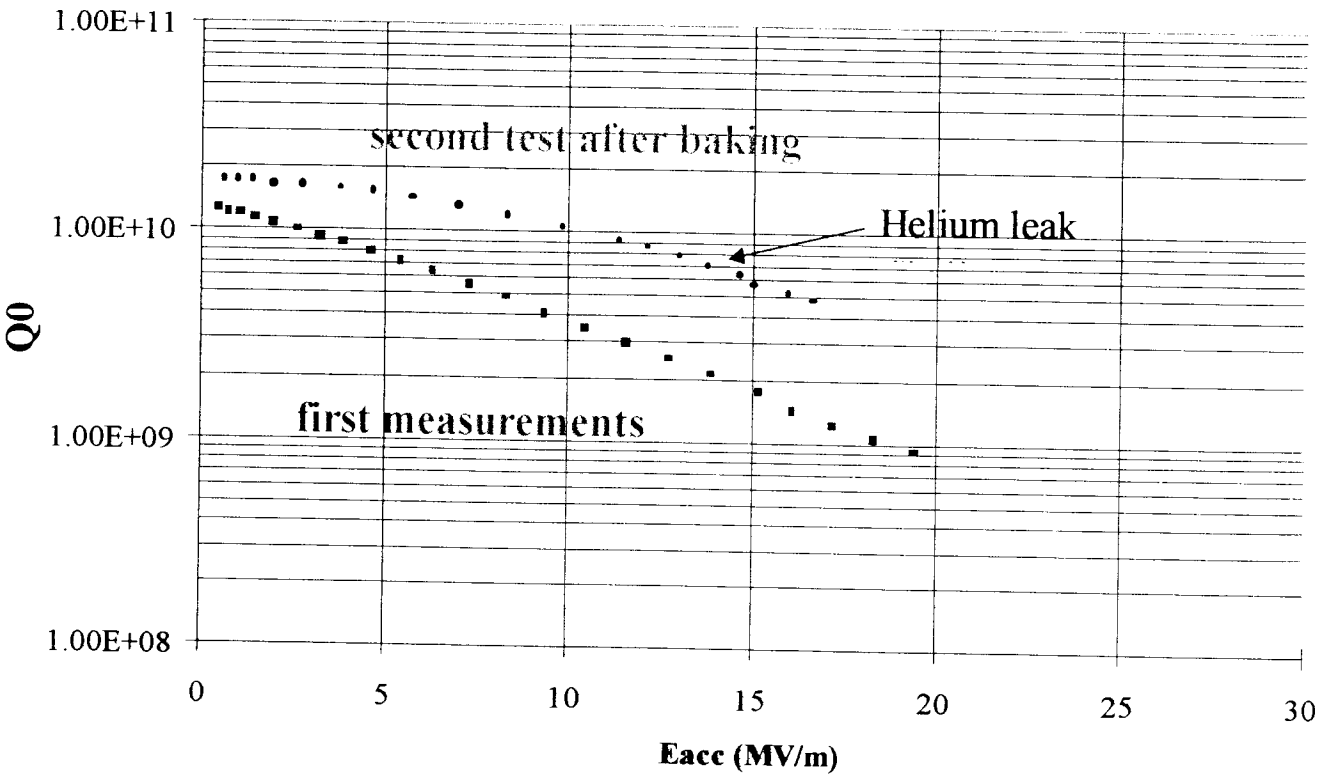

Baking with the same conditions S1-08 cavity had no effect on its Q-slope !

Conclusions:

- 1.5GHz and 1.3GHz Nb/Cu cavities were all limited by power (Q_0 slope)
- Best cavity at 1.5GHz reached:

  E_{acc}=25 MV/m with Q_0=1.2 10^9

- R_{res} and slope correlated to the growth defect density

  => improved cleanliness

  => improved copper polishing

- growth defects are not the only origin of R_{res} and slope:

  Q_0 slope is sometime reduced by a baking at 90°C for 20 hours

Arco

Arco

A new approach for superconductive coating of copper cavity for high accelerating fields

Roberto Russo INFM

Arco

Main participants

- "Roma Tor Vergata"
- **Sect. INFN**
  - Prof S. Tazzari
  - Dr. L. Catani
  - Workshop
- **Sect. INFM**
  - Prof. M. Cirillo (INFM)
  - Dr. R. Russo (INFM)
  - graduate student
- **LNF**
  - Prof. F. Tazzioli

- SINS (**Varsavia**)
  - Dr. J. Langner
  - Dr. S. Kulinski
  - M. Sadowski
  - J. Stanislawski
  - Technical support
- **Tomsk University**
  - Prof. N. Koval consultant
- CERN ? INFM Naples?

Arco

Main goals

- Realisation of a planar cathodic arc source
- Study and optimisation of samples
- RF characterisation of best samples
- Study of a system for cavities deposition (linear arc and/or filtered)

Arco

The Sputtering

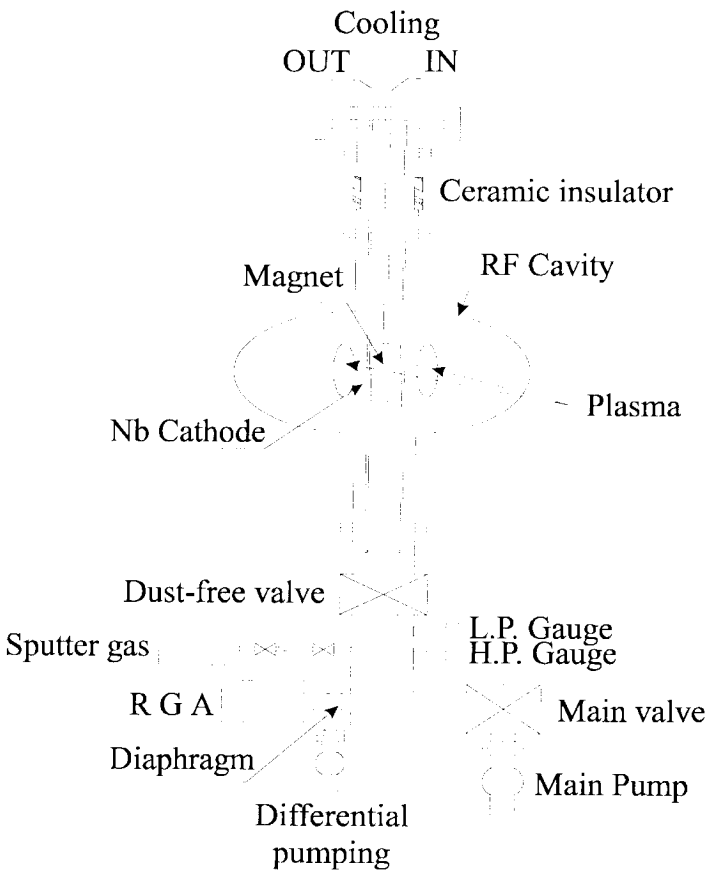

- Voltage 300-600V
- Gas noble , Ar, Kr or Xe at P ~10^{-3} Torr
- Current 1-10Amps
- Rate 1-50 Å/s
- sputtered material is neutral with an energy ranging from 0.1 to 10eV

Arco

Sputtering at "Tor Vergata"

- limit vacuum 10^{-10} Torr with a oil free pumping system (turbo + membrane)
- Gas analyser with differential pumping
- Mixed magnetic configuration
- Voltage 300 - 500V
- From room temperature to 300°C
- Plasma current from 0.2 to 2 Amperes
- Beta from 7 to 30 (RRR)

Arco

Cathodic Arc deposition

- Discharge start in vacuum and is sustained by the evaporated material
- Low Voltage 10-40 V
- High Current 50-200 A
- Discharge current density 10^4-10^6 A/cm^2
- Hot spot speed on the cathode surface1-100m/s
- Plasma density 10^{11}-10^{12} atoms/cm^3
- evaporated material is ionised (>90%)
- Kinetic energy of evaporated ions is 10-100 eV
- From the edge of the cathode active spot microdroplets can be emitted (0.1-100μm size)

Arco

Film properties

- Excellent adhesion
- Very good density
- Very few impurity
- Easy to realise compounds (nitride and carbide)

Arco

Microdroplets

- For refractory materials with good cathode cooling microdroplets are < 1%

- Quantity of microdroplets depends by
  - Discharge conditions , (Mainly current)
  - Cathode purity (Purest the best)
  - Cathode temperature (Cooling system is very important)

- Influence on the film property has to be investigated

Arco

Main steps

Production of samples using a planar arc source to study Nb coating conditions and influence of microdroplets.

Are microdroplets a problem?
(main problems can be Rs and field emission)

YES → Filtered arc system

No → Linear arc source

Arco

Conclusion

- Arc Plasma is a powerful technique to produce coatings (better than magnetron sputtering a-priori, excepted microdroplets)

- In 2-3 years we will know if this technique is suitable for niobium on copper cavities

Muon Collaboration

Superconducting Cavity Requirements and Development

Hasan Padamsee

Cornell University

Background

Short muon lifetime demands high gradient

NC cavities at high gradient
=> very high peak power => $$

With SC cavities filling times can be made long
to lower peak RF power

Based on 400 MHz LHC cavity results
we can optimistically plan for Eacc = 15 MV/m

see example

Muon Collaboration

Fermilab NUFACT design study calls for
200 MHz RF for Linac and RLA1, 500 cells

400 MHz for RLA2, 1500 cells
Higher frequency, less RF, less $$ for
11 - 50 GeV RLA2

Compare to LEP-II, 350 MHz
288 cavities x 4 cells = 1152 cells

Altogether, NuFact Acceleration ≈ 2 x LEP-II !

Development pressure is on the 200 MHz system

If Muon storage ring built at < 15 GeV,
need 200 MHz system
200 MHz is lower than lowest frequency ever
for SC (350 MHz)

400 MHz system very similar to LEP-II
except
we need to increase gradient from 8e-1
10 to 15 MV/m in 4-cell cavities

**Must also explore ways to improve
Nb/Cu quality**

Muon Collaboration

What is the RF power needed for SC cavity?

Example: RLA 1 - 200 MeV

Average beam current =
total charge per RF cycle x repetition rate =
(for 3 x10^{12} muons)

0.48 μC x 4 passes x 15 Hz = 28.8 μA

Beam on time = (no. or recirculations x path length)/c
= 9 μs at rep rate of 15 Hz

=> Beam on duty factor = 0.13%

Peak RF power to match to beam = 2.4 MW/cell

Fill time needed to reach 11.25 MV in cell
= 0.58 ms

Matched Q_L = 5.3x 10^5
BW = 380 Hz

Muon Collaboration

To Reduce Peak Power Cost

Take advantage of long filling time feature of SC cavities

Increase filling time to 2 ms

Passage of bunches extract small fraction of cavity stored energy
0.5% (Linac), 2.2% (RLA1) and 10.8%(RLA2)

Assumption:
Energy extracted by beam does not have to be replenished during the RF pulse

There is also a choice about what QL to use.

If QL is too high
BW becomes small and microphonics
could be a problem

If we keep QL around 5.3×10^5

Ppk = 728 kW/cell

Muon Collaboration

How much microphonics is tolerable?

Calculate how far can we run off resonance and reach 15 MV/m with this power?

Ans: 10 Hz off resonance tolerable
This may not be safe enough.

Muon Collaboration

To be safe, assume we need to tolerate microphonics of 80 Hz , given the large structures

Now we chose Q_L to get lowest power.

See curves:
$Q_L = 6 \times 10^5$, BW = 300 Hz
Power = 850 kW per cell

Longer fill times will allow further RF power and cost reduction for optimum choice of Q_L.

For example, fill time = 3 ms,
$Q_L = 8 \times 10^5$, P = 680 kW/cell

However, RF power cost may go up with longer pulse length.

Also AC power cost goes up

R&D Objective:
What is the best fill time, loaded Q and power level?

Muon Collaboration

Cavity Parameters

RF Frequency	**MHz**	**200**	**400**
R/Q per cell	Ohm	100	100
Active Cell length	m	0.75	0.375
Cell diameter	m	1.5	0.75
Gradient	MV/m	15	15
Voltage per cell	MV	11.25	5.6
Stored Energy per cell	Joules	1000	126
Q0		$6x10^9$	$6x10^9$
Operating Temp	K	2.5 - 4.2?	2.5 - 4.2?
Peak RF Power per cell	kW	820	200
Loaded Q		$6.5x10^5$	$2x10^6$
Bandwidth	Hz	300	200
Fill time	ms	2	2
Duty factor	%	3	3
Dynamic heat load	Watt/cell	6	1.6
Number of cells		551(Linac +RLA1)	1511 (RLA2)

Operating temperature: 2.5 - 4.2 K, needs R&D
Depends on severity of Q-slope

Muon Collaboration

RF System Parameters

	F MHz	Pulsew msec	MW per Linear_m	Cells per klystron	Number cells	Tot. installed Votage /GeV
Linac.	200	2	0.55	10	320	3.6
RLA1	200	2	0.55	10	231	2.6
RLA2	400	2	0.2	60	1,511	8.5
total						14.7
name	Peak MW	Ave Pwr kW /kly	No. of klystrons	Linear_m per kly	Linear_m	Average rf P MW
Linac.	8.25	247.5	32	15	480	7.9
RLA1	8.25	247.5	23	15	347	5.7
RLA2	9	270	25	45	1133	6.8
Total			80		1960	20.4

Roughly 80 klystrons x 10 MW each
= 800 MW, 2 ms pulse length, 3% duty factor

In terms of average power
these klystrons are comparable to other devices

But not in terms of size
Length of klystron
200 MHz, 3 - 4 m, 400 MHz 2 - 3 m

Average RF power = 20 MW
Wall power for RF = 40 MW

Muon Collaboration

Refrigeration Heat Loads

Dynamic Heat load

Linac + RLA 1 = 3300 W

RLA 2 = 2418 W

Total Dynamic heat load = 5700 W

Static Heat Load 5 W/m

Linac + RLA 1 = 4200 W

RLA2 = 5700 W

Total static heat load = 10 kW

Total Heat load = 15 kW

Refrigeratior AC power = 5 MW

Muon Collaboration

Challenges

Fabrication of large scale 200 MHz structure
1.5 m diam x 2 m long (w beam tubes)

Mechanical properties,
resilience against micro-phonics @ 200 Hz BW
esp. in pulsed operation

High Field, high Q performance
Eacc = 15 MV/m, (active gradient) Q = 6 x10^9

One MW pulsed operation
Input power capability one MW @ 2 ms pulse

What is the best fill time, loaded Q and power level?

What is the best operating temperature?
2.5 - 4.2 K?

Muon Collaboration

R&D Program

Aim: 3 year goal : Show 15 MV/m gradient
5 year goal: Cryomodule test

• Develop, design, fabricate and high power test one 200 MHz single-cell cavity.

Approach: Nb/Cu suitable for 200 MHz Why?

1) Significant savings in material cost
If made from Nb sheet, 6 mm thick,
Nb cost for 500 cells will be 70 M$ ($200 per pound)

Copper base cavity will cut material cost
by x 10 - x 100

2) Quench resistance (one kJ stored energy)
copper wall can be made thicker for stiff cavity against microphonics
3) CERN has made substantial headway in Nb/Cu technology
low frequency cavities, 350 MHz, 400 MHz
large number of cavities
Need to improve Q slope.
14 MV/m proof of principle exists at 400 MHz

Muon Collaboration

Improvements

- Cost reduction
- Q-slope reduction

No Welds - cost reduction, better performance

Spin single-cell copper cavity from one sheet
Collaboration with INFN
They have already spun 1300 MHz Nb and Cu cavities from single sheet

Q-slope reduction

Develop collaboration with coating laboratories
to explore high energy niobium deposition.
small samples

Dual ion beam sputtering
Laser ablation, others?

Analyze film properties and
Test RF properties at 6 GHz
Host cavity available

Example for Coating by Sublimation: TiN for RF windows

J. Lorkiewicz, B. Dwersteg

Collaboration: **A. Brinkmann, D. Reschke, X. Singer, K. Twarowski, others**

TiN coated coupler components:

- flat WG (waveguide) windows for the main TTF coupler,

- DESY TTF - III coupler cylindrical 300 K ("warm") windows,

- DESY TTF - III coupler cylindrical 70 K ("cold") windows,

- DESY TTF - II coupler coaxial line components.

Coating method used:

- Ti vapor deposition in NH_3 atmosphere

MEASUREMENT OF MULTIPACTING CURRENTS OF METAL SURFACES IN RF FIELDS

D. Proch, Deutsches Elektronen-Synchrotron DESY, Hamburg, Germany and
D. Einfeld, R. Onken, N. Steinhauser, Fachhochschule Ostfriesland, Emden, Germany

Abstract

Multipacting currents can absorb RF energy and produce breakdown in high power components such as couplers, windows, higher order mode absorbers, etc.. This phenomenon starts if certain resonant conditions for electron trajectories are fulfilled and if the impacted surface has a secondary yield larger than 1. There are known recipes to reduce the secondary yield by coating techniques but the success rate is often unsatisfactory. Therefore we have started systematic measurements of the RF multipacting current. We measure the multipacting current between two electrodes of a specially designed coaxial resonator. Technical surfaces (Cu, plated Cu on stainless steel, Al, stainless steel) have been investigated before and after surface treatments such as chemical cleaning, baking and Ti coating. We present data for the strength of multipacting, start current, processing time and possible reconditioning.

I. INTRODUCTION

Multipacting is a phenomenon of resonant electron multiplication:

- one electron is accelerated by the electric RF field and hits the target surface after one even (odd) number of RF half cycles as resonant condition for one (two) surface multipacting,
- the impacting electron produces more than one secondary electron.

These two conditions have to be fulfilled in order to start an electron avalanche. This electron current might result in severe limitations of the stored energy in microwave components or finally ignite a breakdown. To suppress these limitations, the resonant condition can be avoided by proper choice of geometry. Resonant conditions for a parallel plate geometry in pure electric fields can be easily predicted and thus be avoided by the right gap distance. In the case of electromagnetic fields, however, multipacting is simulated by tracking programs. In the case of complicated three dimensional RF components a simulation of electron trajectories becomes very demanding. Furthermore the RF design might not allow to change the geometry by the needed amount.

Therefore attempts are undertaken to suppress multipacting by proper coating of critical surfaces. A material for coating is chosen which has a secondary yield of smaller than or at least near by one. Different coating materials are known, for example Ti, TiN, CrO_2, etc. [1] . Those materials have been investigated by measuring the secondary yield in DC experiments on sample surfaces. RF components might have complicated geometry to be coated. The improvement also depends on coating conditions of large technical surfaces. Therefore a test resonator was developed to measure the RF multipacting current directly under various coating conditions. For fast turn around this resonator should allow a fast exchange of the multipacting electrodes and should operate at low power. In this paper the design of such a test resonator is given and first measurements on different coatings are presented.

II. DESIGN OF THE TEST RESONATOR

The resonant condition for two side multipacting in an electric field is given by:

$$E_{(n)} = \frac{4m\pi}{e} \cdot \frac{f^2 l}{(2n-1)} \qquad (1)$$

n: order of multipacting (n:1,2,3,...)
f [Hz]: frequency
l [m]: gap distance
m [kg]: mass of electron
e [C]: charge of electron
$E_{(n)}$ [V/m]: resonant electric field gradient

The magnetic RF field in the center gap of a reentrant resonator is small as compared to the electric RF field. Therefore two side multipacting according to equation (1) is expected in such a resonator. The experiment prooved that multipacting actually occures at the predicted field levels. This

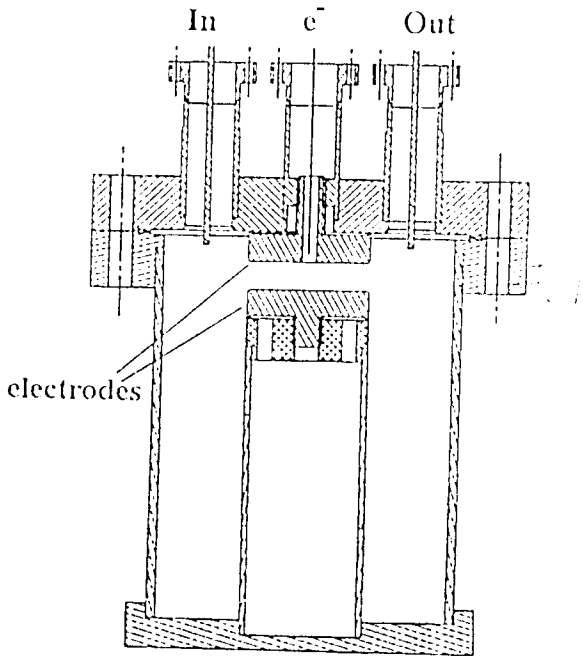

Figure 1: Test resonator

A.Brinkmann 09.11.99

Alu-sample #14, Ti coating test No. 23, Date of coating 04.11.99
Heating current 17 A, deposition time 48 s, Chamber heating off

Multipactingstrom-Verlauf

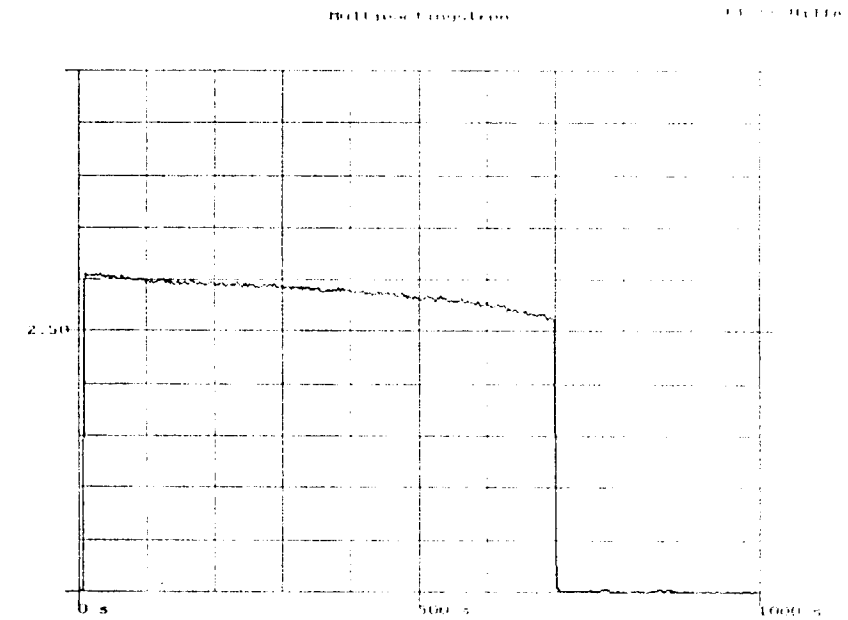

alu_9.dat

Feldstärkenverlauf

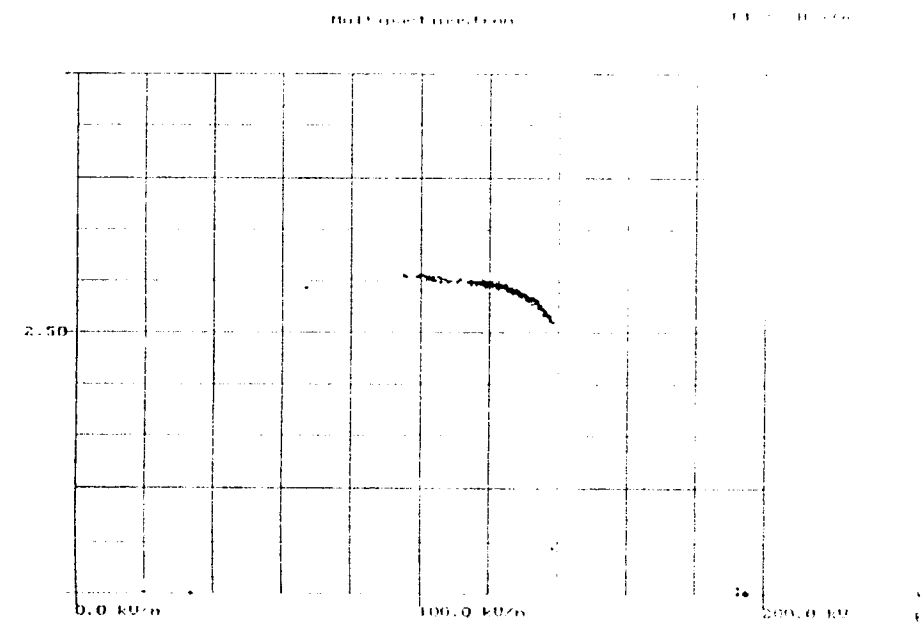

alu_9.dat

Test results from DESY coaxial resonator

Sample	Substrat temperature	Deposition rate (atmosphere)	Layer thickness	Further processing	Layer resistivity (Mohm/sq.) at 3000 K	Layer resistivity (Mohm/sq.) at 70 K
1. Al		before processing				
2. Cu		before processing				
3. Cu	25° C	20 nm/min (res. gas)	ca. 40 nm	no		
4. Cu	25° C	20 nm/min (NH_3)	ca. 40 nm	no		
5. Cu *	150° C	9 nm/min (10^{-3} mbar NH_3)	13 nm	150 mbar NH_3 3 days	960	14600
6. Al	150° C	9 nm/min. (10^{-3} mbar NH_3)	15 nm	300 mbar NH_3 2 days	55	960
7. Al	150° C	9 nm/min. (10^{-3} mbar NH_3	ca. 7 nm	250 mbar NH3 3 days	2900	195000
8. Al *	25° C	9 nm/min. 10^{-3} mbar NH_3	7 nm	700 mbar NH_3 20 hours	11700	195000
9. Al *	25° C	9 nm/min. 10^{-3} mbar NH_3	7 nm	700 mbar NH_3 23 hours	24300	290000
10. Al *	150° C	9 nm/min. 10^{-3} mbar NH_3	ca. 4 nm	200 mbar NH_3 24 hours		
11. Al	150° C	9 nm/min. 10^{-3} mbar NH_3	7 nm	750 mbar NH_3 21 hours	0.6	4.5
12. Al	150° C	9 nm/nim. 10^{-3} mbar NH_3	7 - 8 nm	400 mbar NH_3 1 week		

Multipactoring time

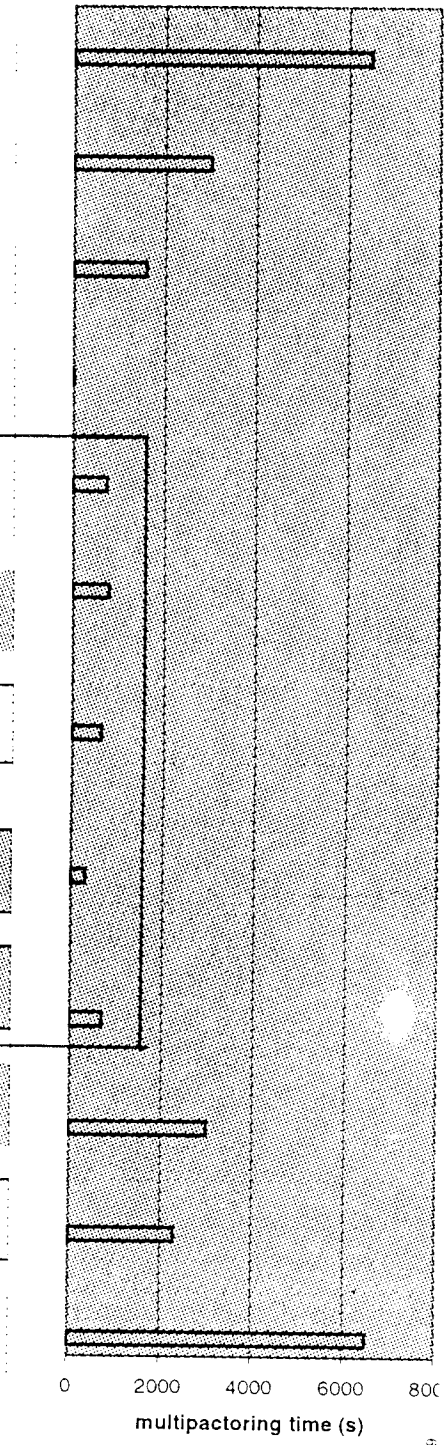

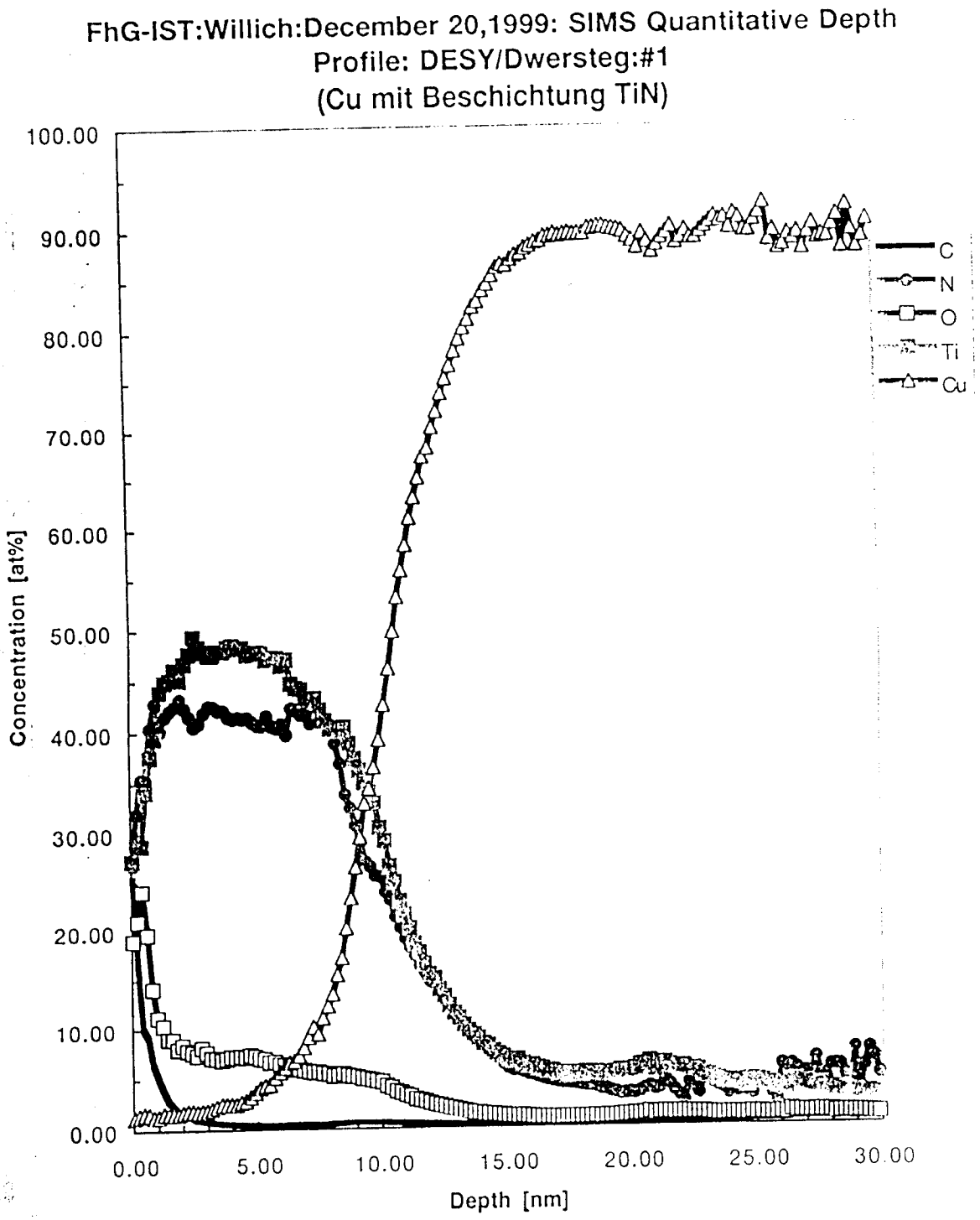
FhG-IST:Willich:December 20,1999: SIMS Quantitative Depth Profile: DESY/Dwersteg:#1
(Cu mit Beschichtung TiN)
Concentration [at%]
100.00
90.00
80.00
70.00
60.00
50.00
40.00
30.00
20.00
10.00
0.00
0.00
5.00
10.00
15.00
20.00
25.00
30.00
Depth [nm]
C
N
O
Ti
Cu

184

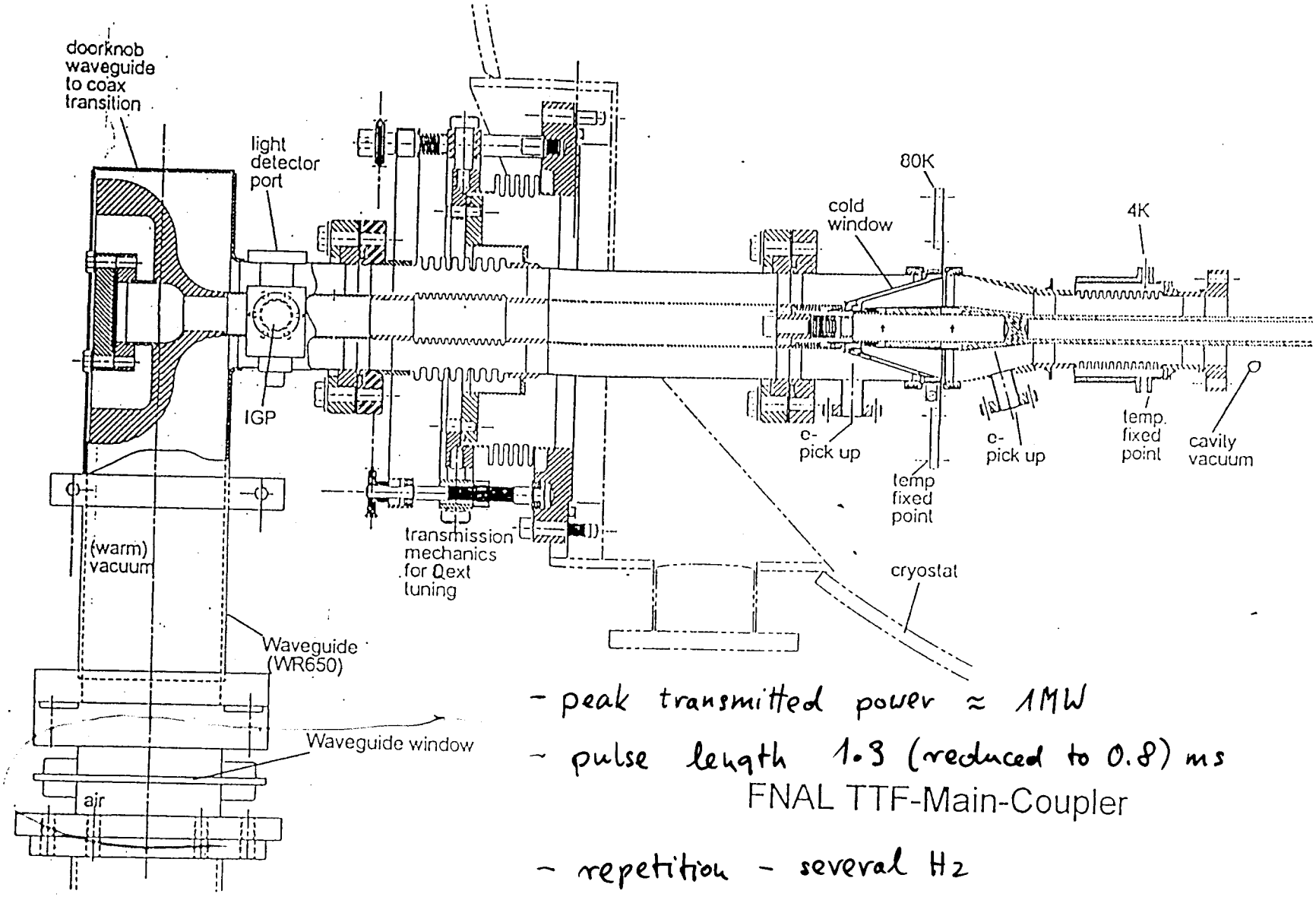

- peak transmitted power ≈ 1MW
- pulse length 1.3 (reduced to 0.8) ms

FNAL TTF-Main-Coupler

- repetition - several Hz

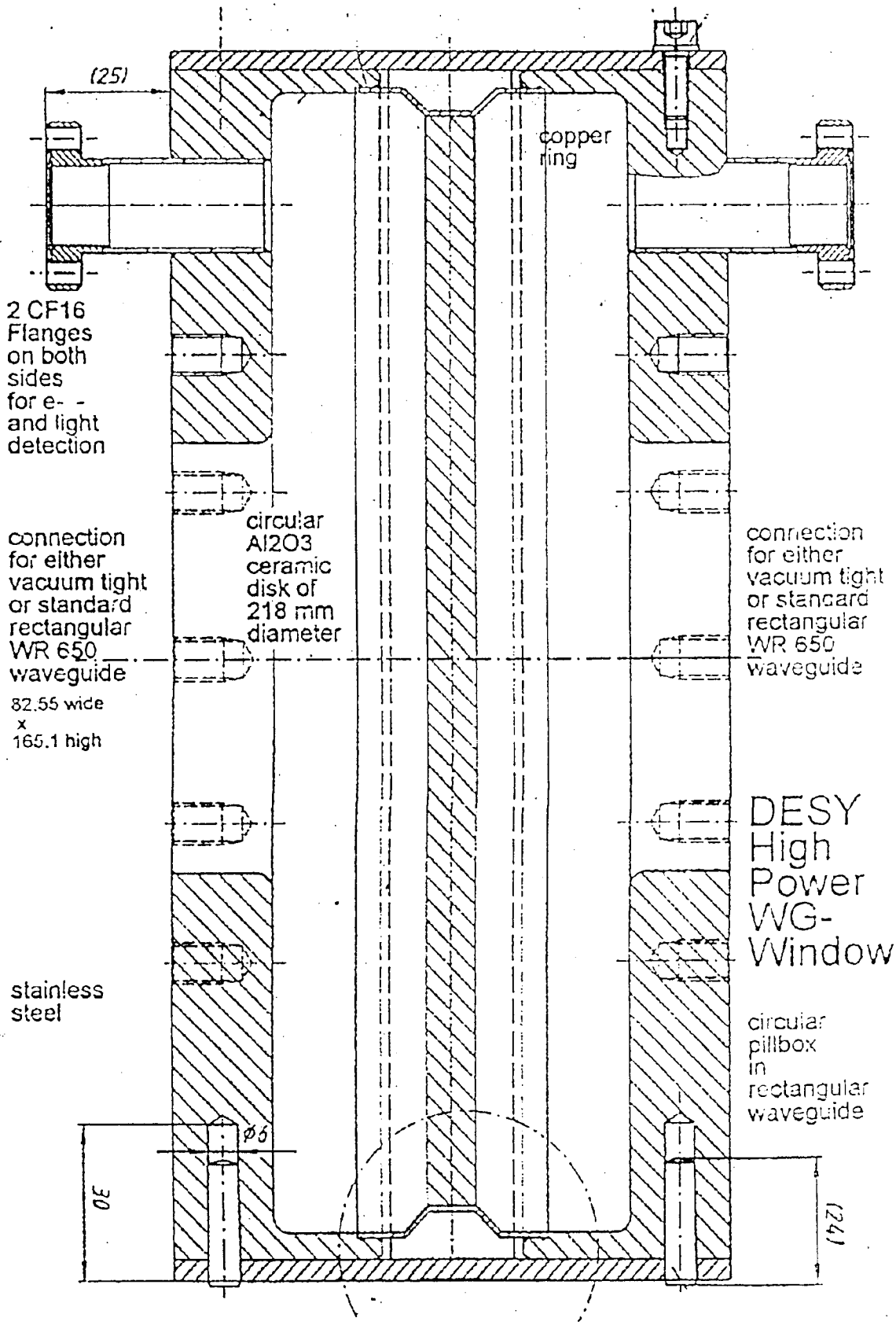
(25)
copper ring
2 CF16 Flanges on both sides for e- - and light detection
circular Al2O3 ceramic disk of 218 mm diameter
connection for either vacuum tight or standard rectangular WR 650 waveguide
82.55 wide x 165.1 high
connection for either vacuum tight or standard rectangular WR 650 waveguide
DESY High Power WG-Window
stainless steel
circular pillbox in rectangular waveguide
ø6
30
(24)

Ti-layer thickness distribution on the ceramic disc

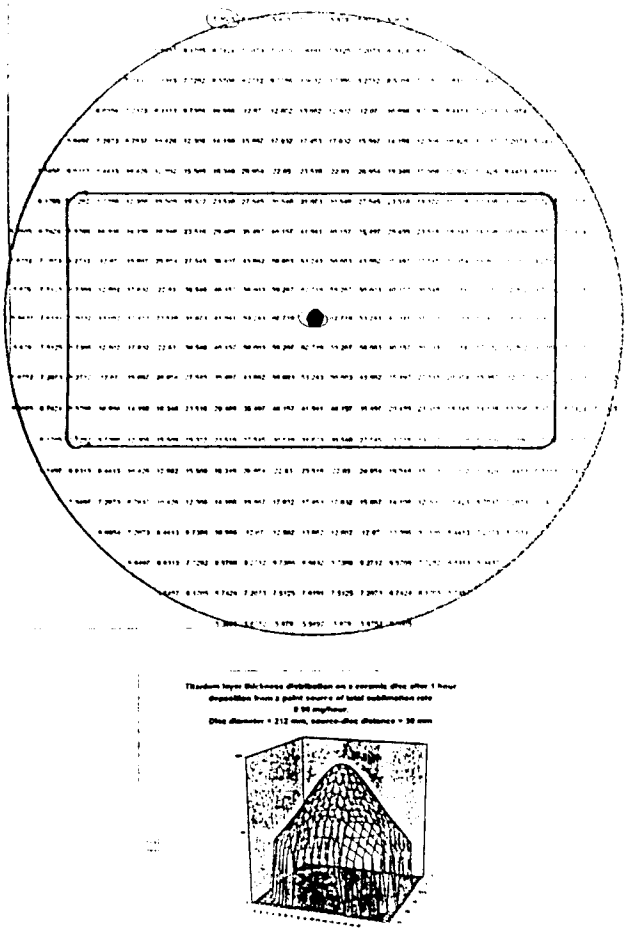

Point source; thickness ratio = 11

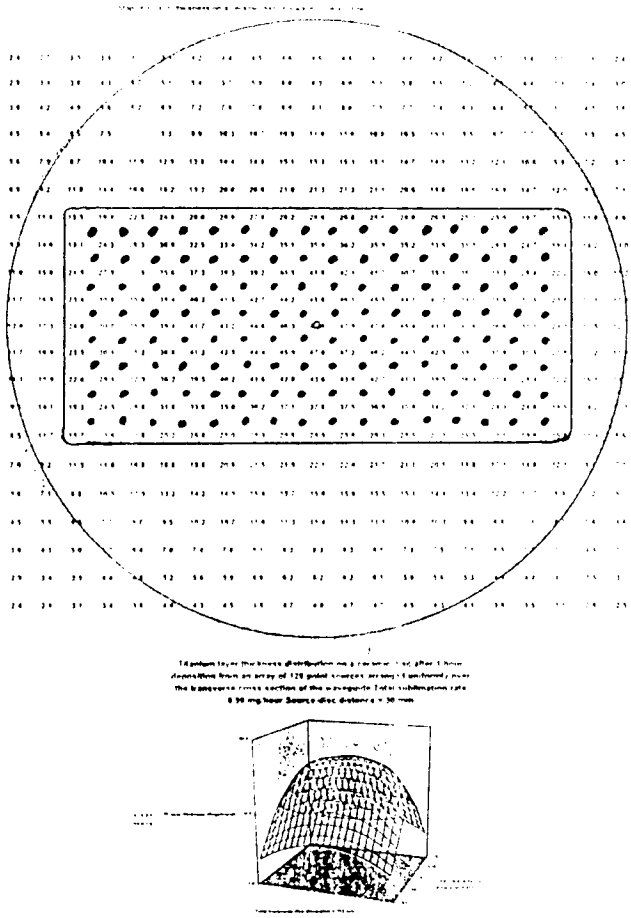

"Surface" source; thickness ratio = 10.4

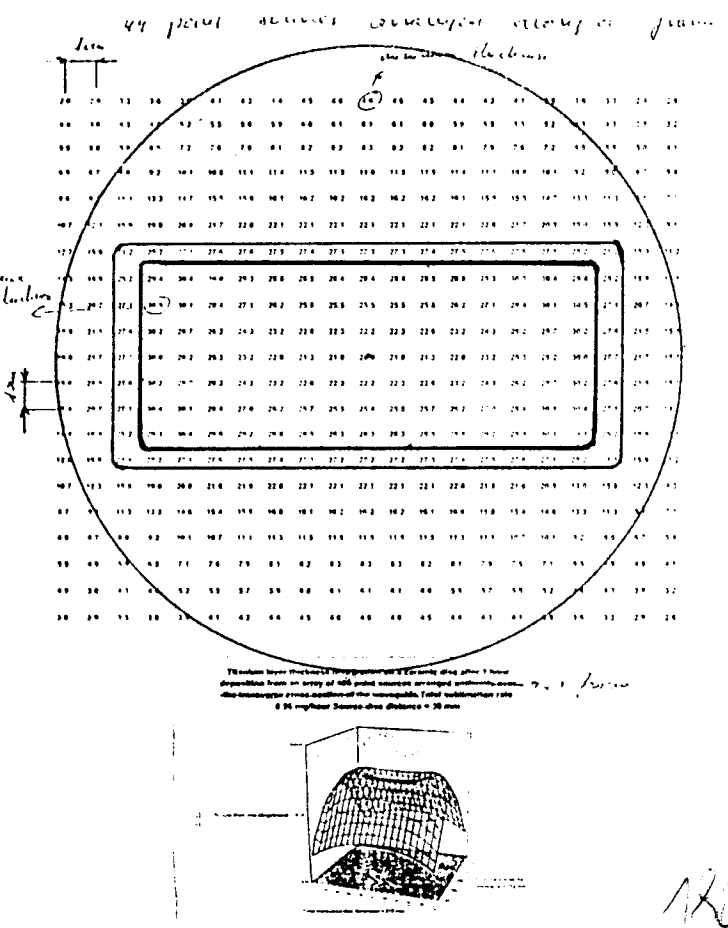

Wire loop in the waveguide;

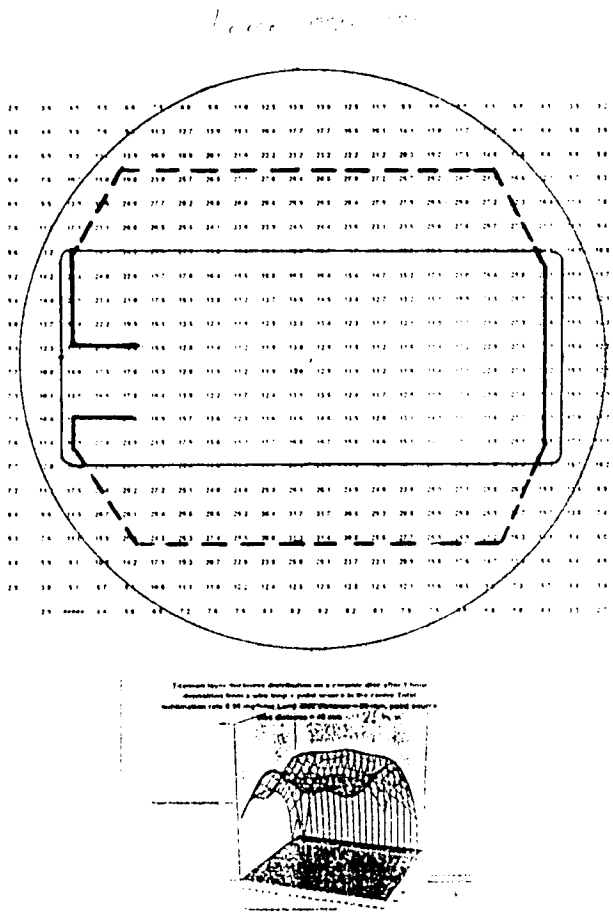

Wire loop inside the pillbox;
Thickness ratio = 4

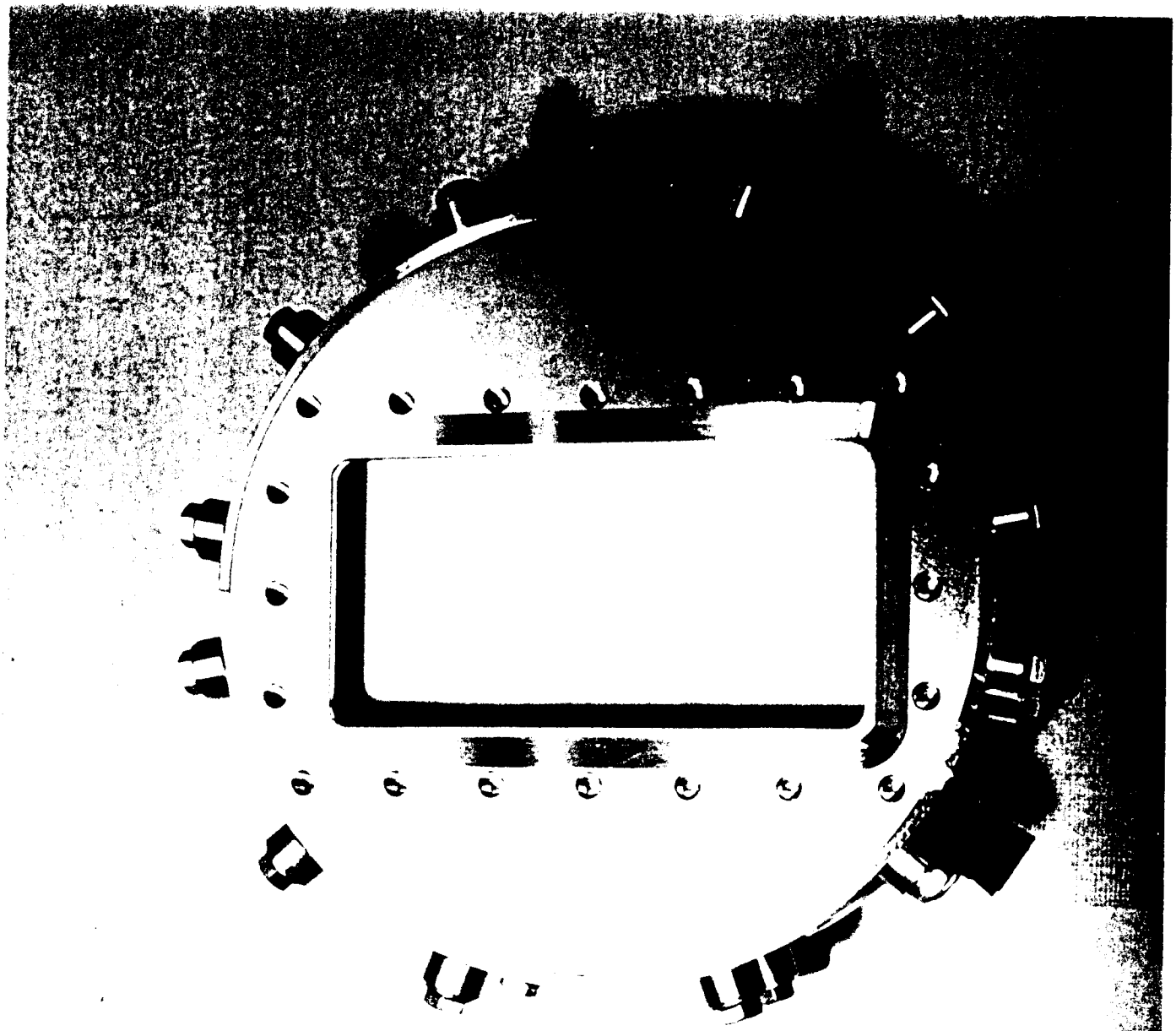

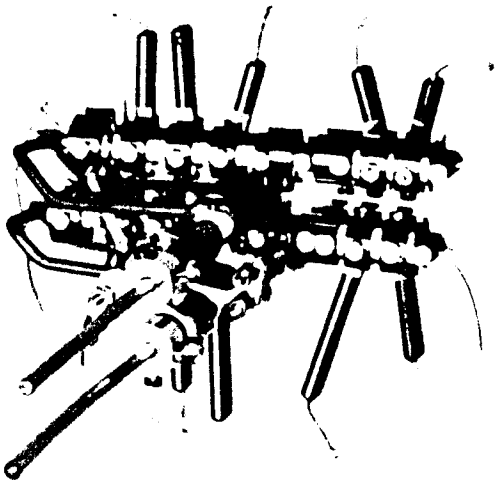

188

Ti wire loop with supporting structure

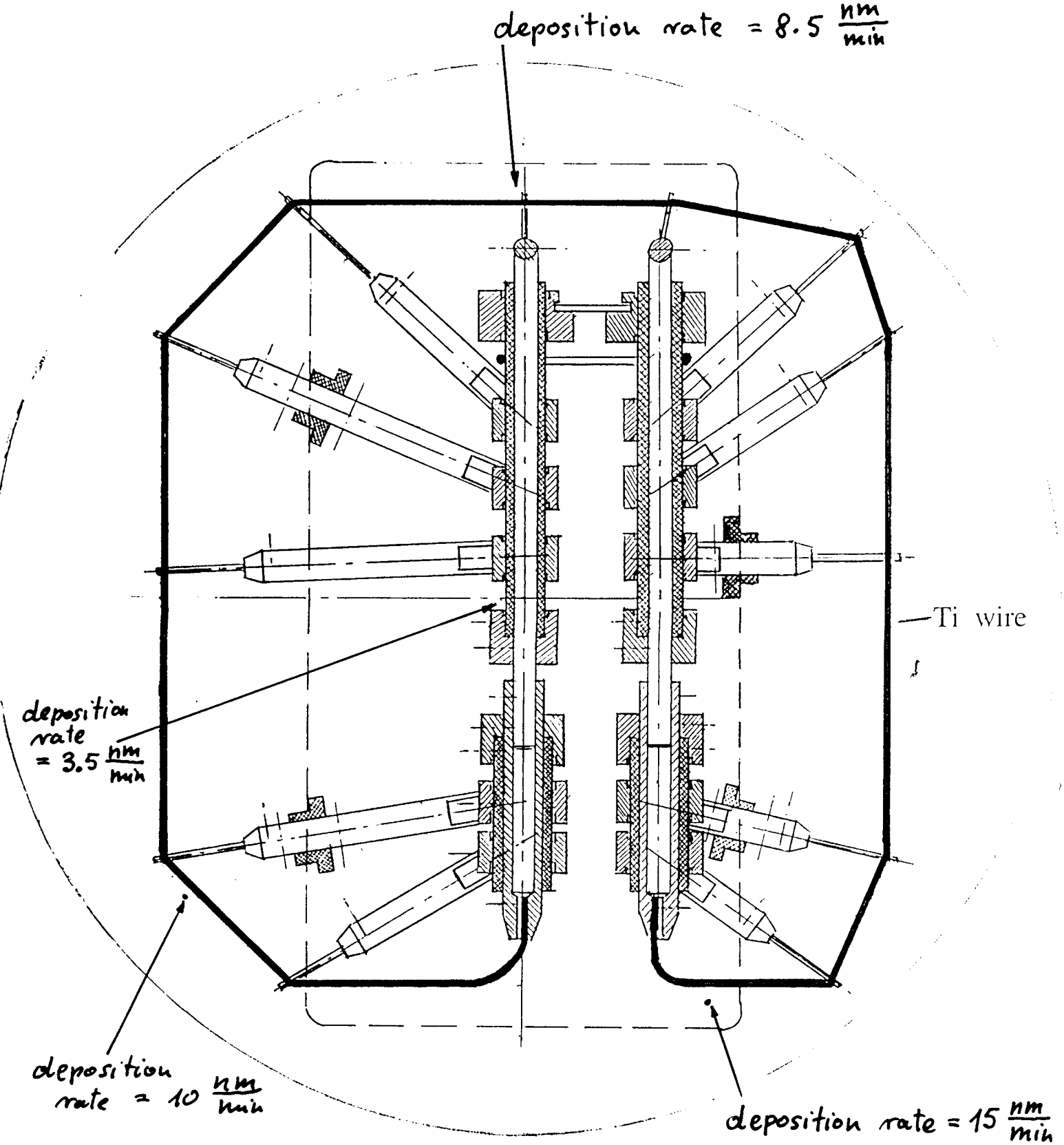

"G"-series waveguide windows coating - processing parameters

of WG window coated	Maximum deposition rate on the disc	Ammonia pressure during coating	Estimated layer thickness range	Postprocessing NH_3 pressure, duration time	Layer resistance after coating / after postprocessing	Colour the disc surface
G-16	12 nm/min	2E-3 mbar	5 - 22 nm	940 mbar (41 hours)		metallic grey, pale in the centre
G-17	12 nm/min	2E-3 mbar	5 - 22 nm	970 mbar (11 hours)	3.3 Kohm/sq. / 7.3 Kohm/sq.	metallic grey, pale in the centre
G-18	12 nm/min	2E-3 mbar	3 - 12 nm	860 mbar (40 hours)	90 Kohm/sq. / 161 Kohm/sq.	metallic grey, grey-yellowish, pale
G-20	12 nm/min	2E-3 mbar	3 - 12 nm	850 mbar (18 hours)	16 Kohm/sq. / 54 Kohm/sq.	metallic grey, grey-yellowish, pale
G-21	12 nm/min	2E-3 mbar	3 - 12 nm	700 mbar (17 hours)	6.7 Kohm/sq. / 28 Kohm/sq.	metallic grey, grey-yellowish, pale
G-22	12 nm/min	2E-3 mbar	3 - 12 nm	650 mbar (38 hours)	12 Kohm/sq. / 223 Kohm/sq.	metallic grey, grey-yellowish, pale
G-23	12 nm/min	2E-3 mbar	3 - 12 nm	ca.900 mbar (60 hours)	25 Kohm/sq. / 949 Kohm/sq.	metallic grey, grey-yellowish, pale
G-24	5 nm/min	2E-3 mbar	3 - 12 nm	780 mbar (88 hours)	32 Kohm/sq. / 1277 Kohm/sq.	grey-yellowish, pale
G-25	5 nm/min	2E-3 mbar	3 - 12 nm	ca.700 mbar (63 hours)	18 Kohm/sq. / 330 Kohm/sq.	grey-yellowish, pale
G-26	5 nm/min	2E-3 mbar	3 - 12 nm	ca.620 mbar (2 weeks)	12 Kohm/sq. / 1500 Kohm/sq.	grey-yellowish, pale

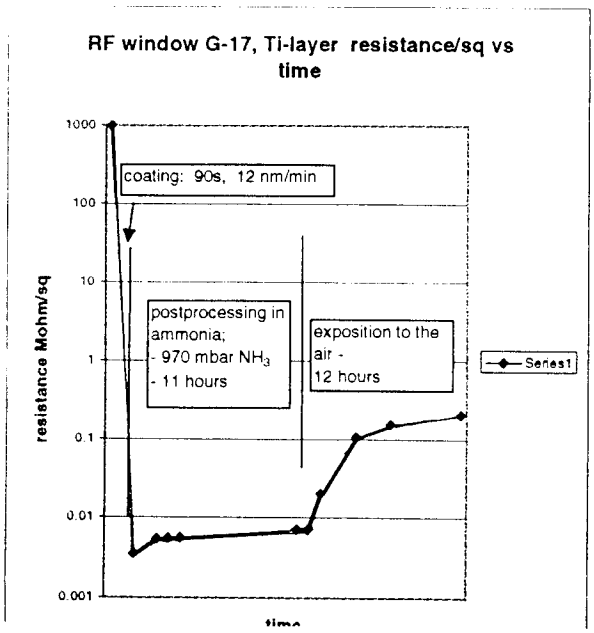

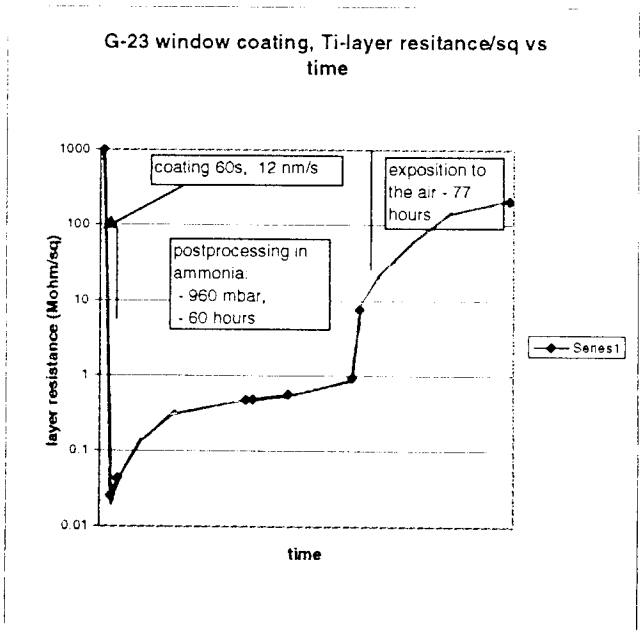

Impact of TiN coating on waveguide windows
RF performance

- number of TiN-coated waveguide windows - 21

- number of RF-tested waveguide windows - 3

- TiN layer thickness - 3 – 15 nm (inhomogeneous)

- RF performance - much improved (*)

  * processing time reduced to 1 day,

  * proper power transmission,

  * no light or electron emission,

  * RF performance insensitive to a previous 1-day exposition to the air.

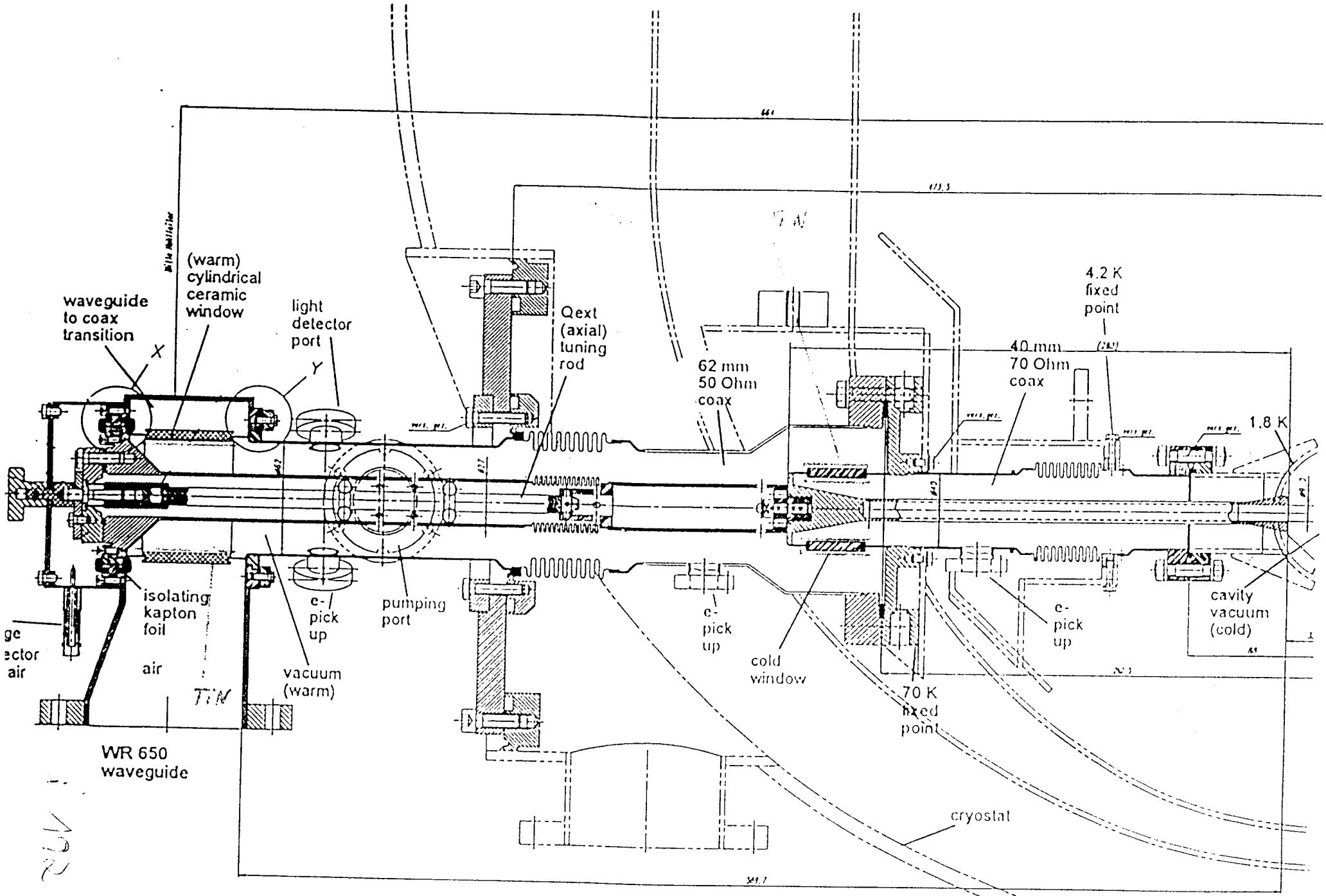

DESY TTF-Main Coupler , Version III

with inner conductor bias

TiN coating of cylindrical windows for DESY-TTF-III coupler

70 K windows - 20 pcs

"warm" windows - 20 pcs

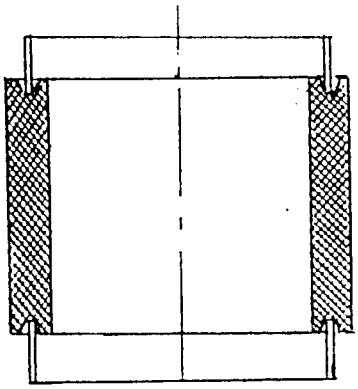

copper collar

Step 2 - coating of cylindrical surfaces

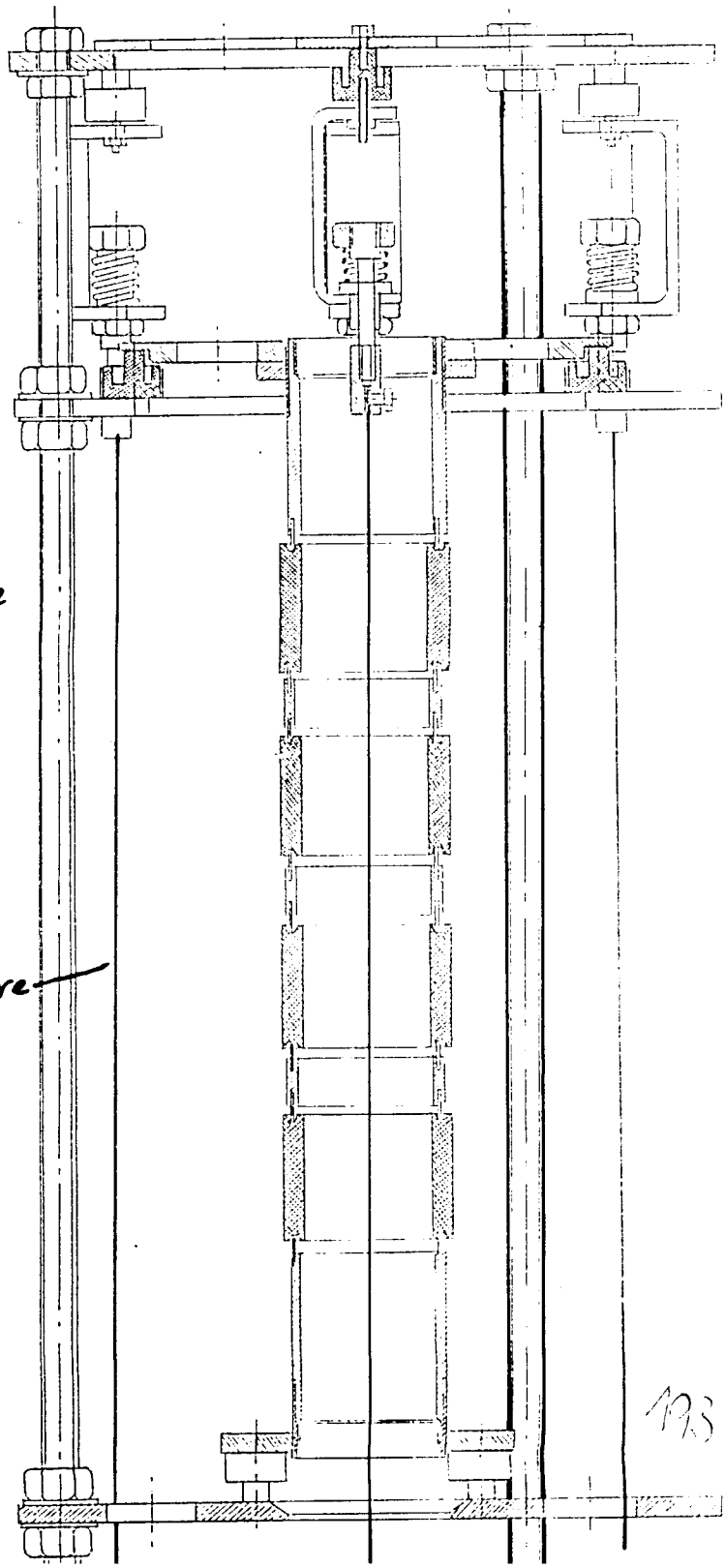

Step 1 - end plates coating

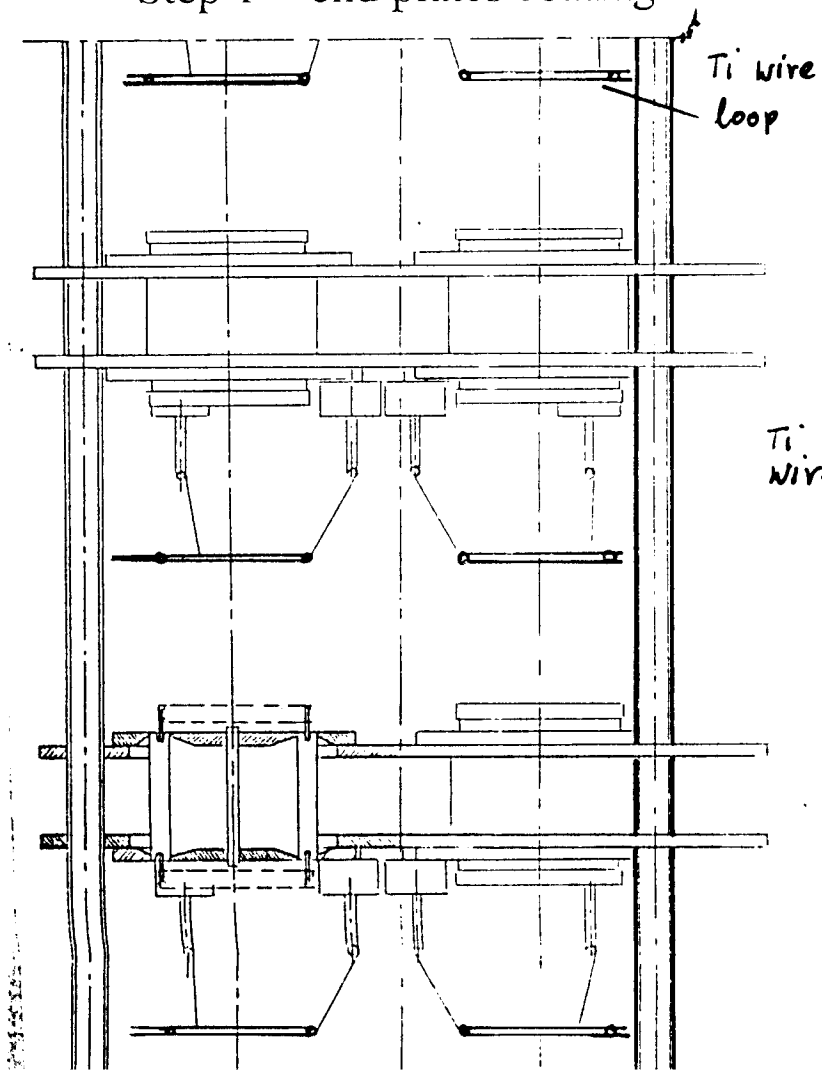

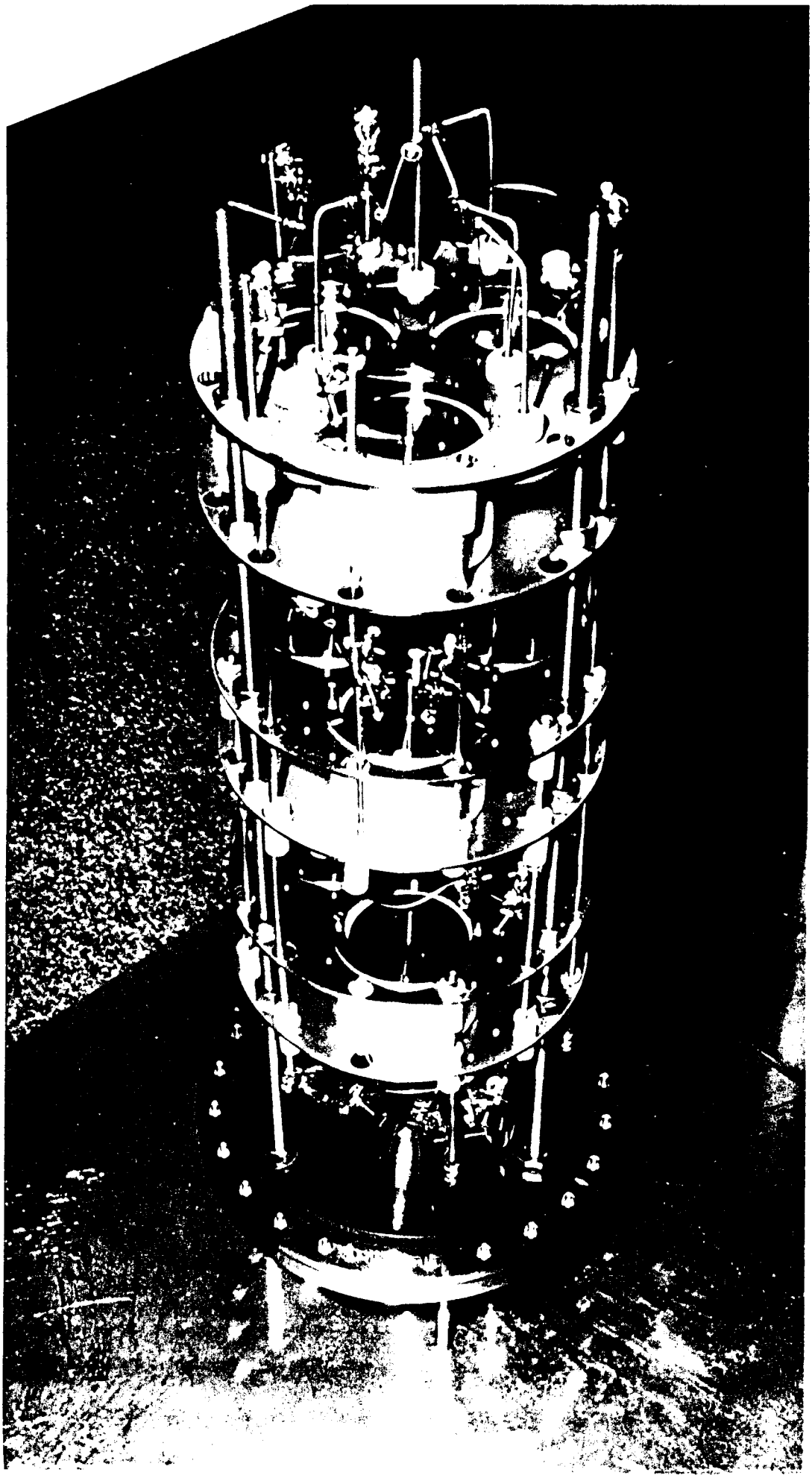

174

300 K windows coating; coating of end

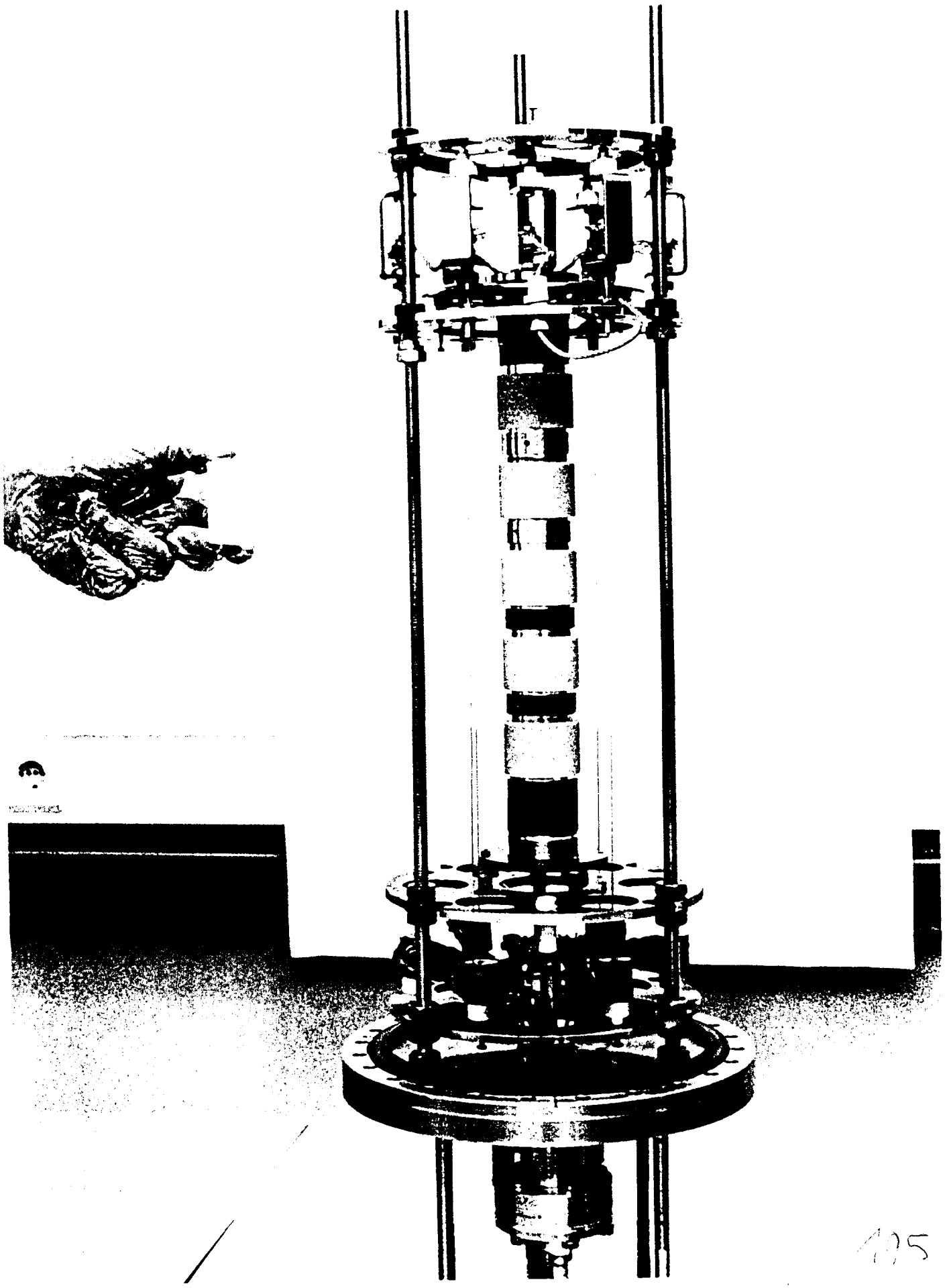

70K windows coating, TiN coating of cylindrical surfaces

Time schedule of cylindrical coupler windows TiN coating

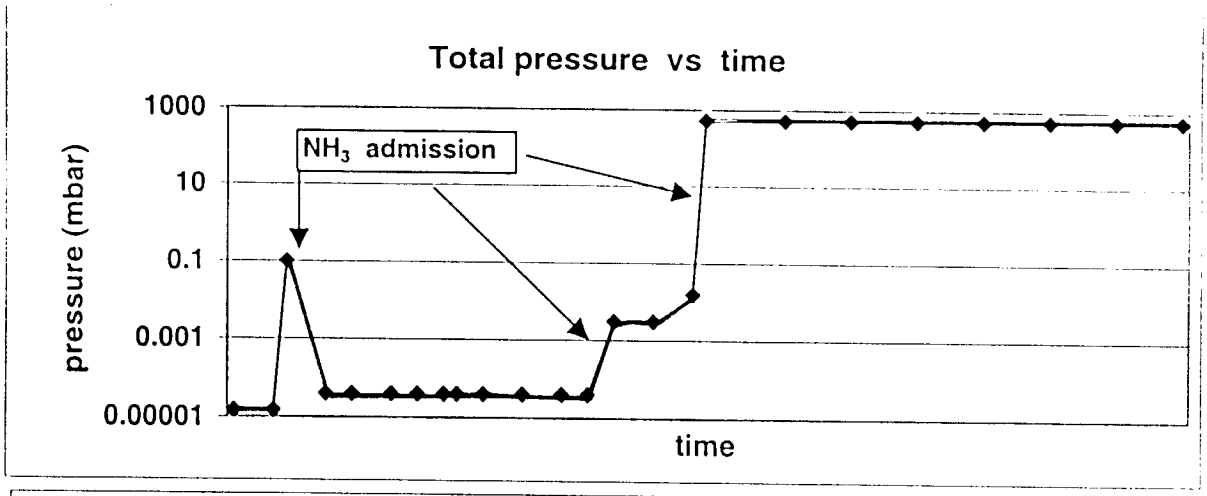

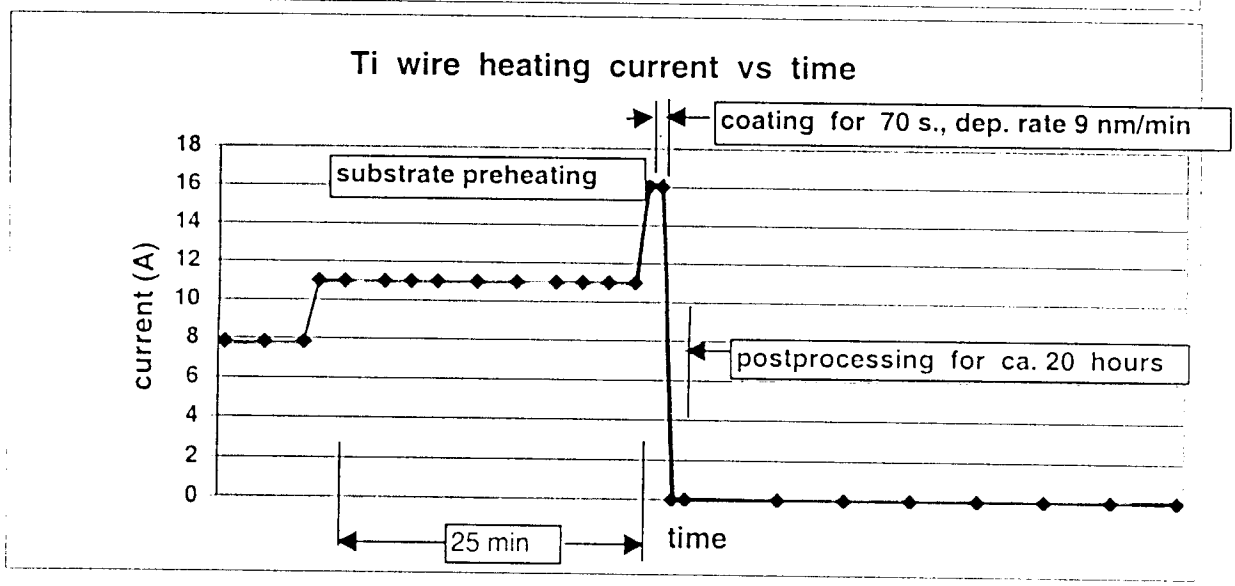

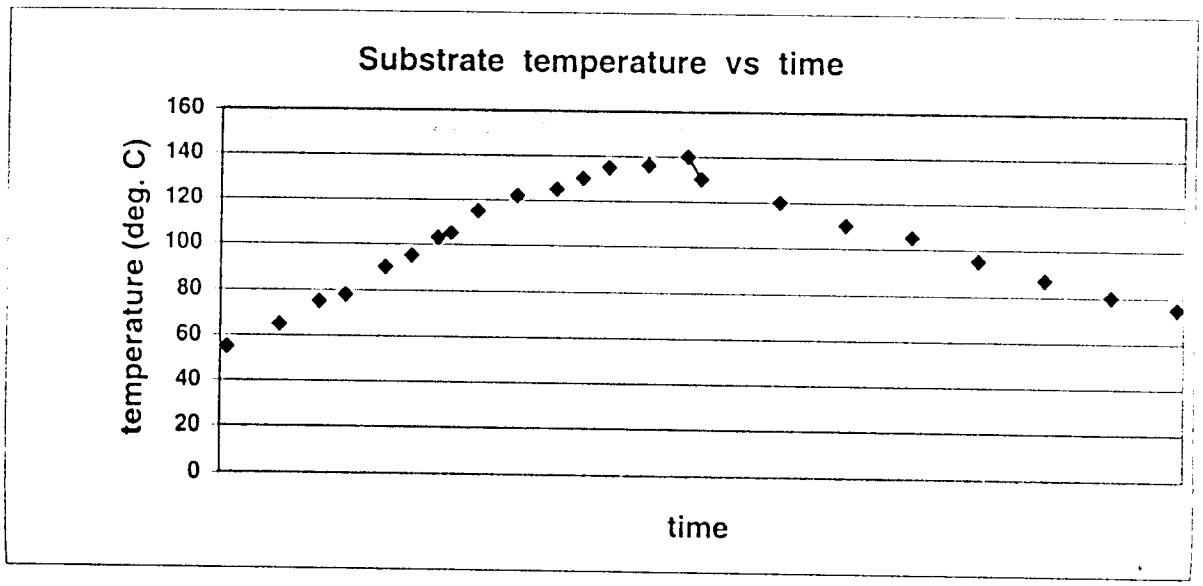

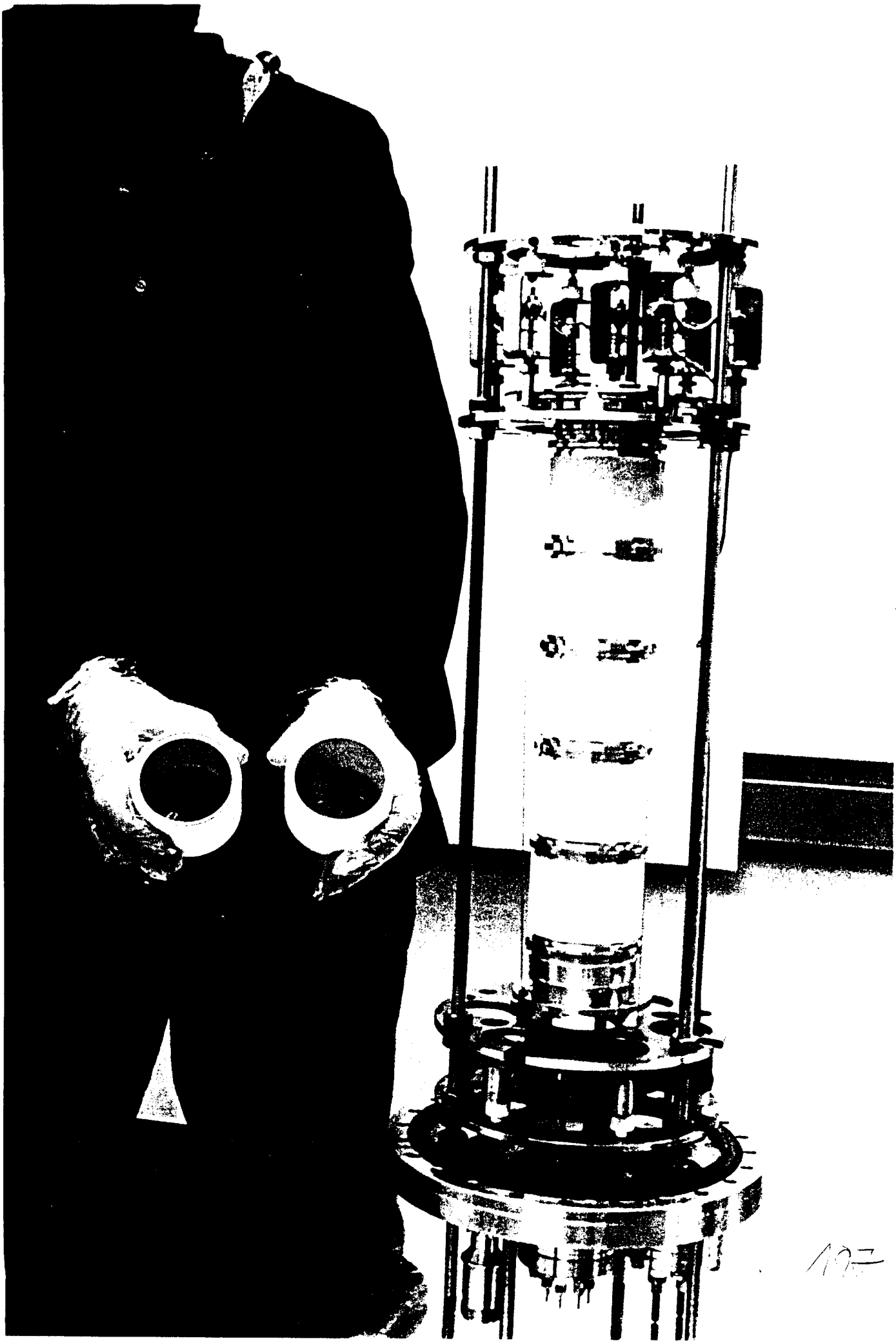

107

DESY TTF-II
coupler

TiN coating

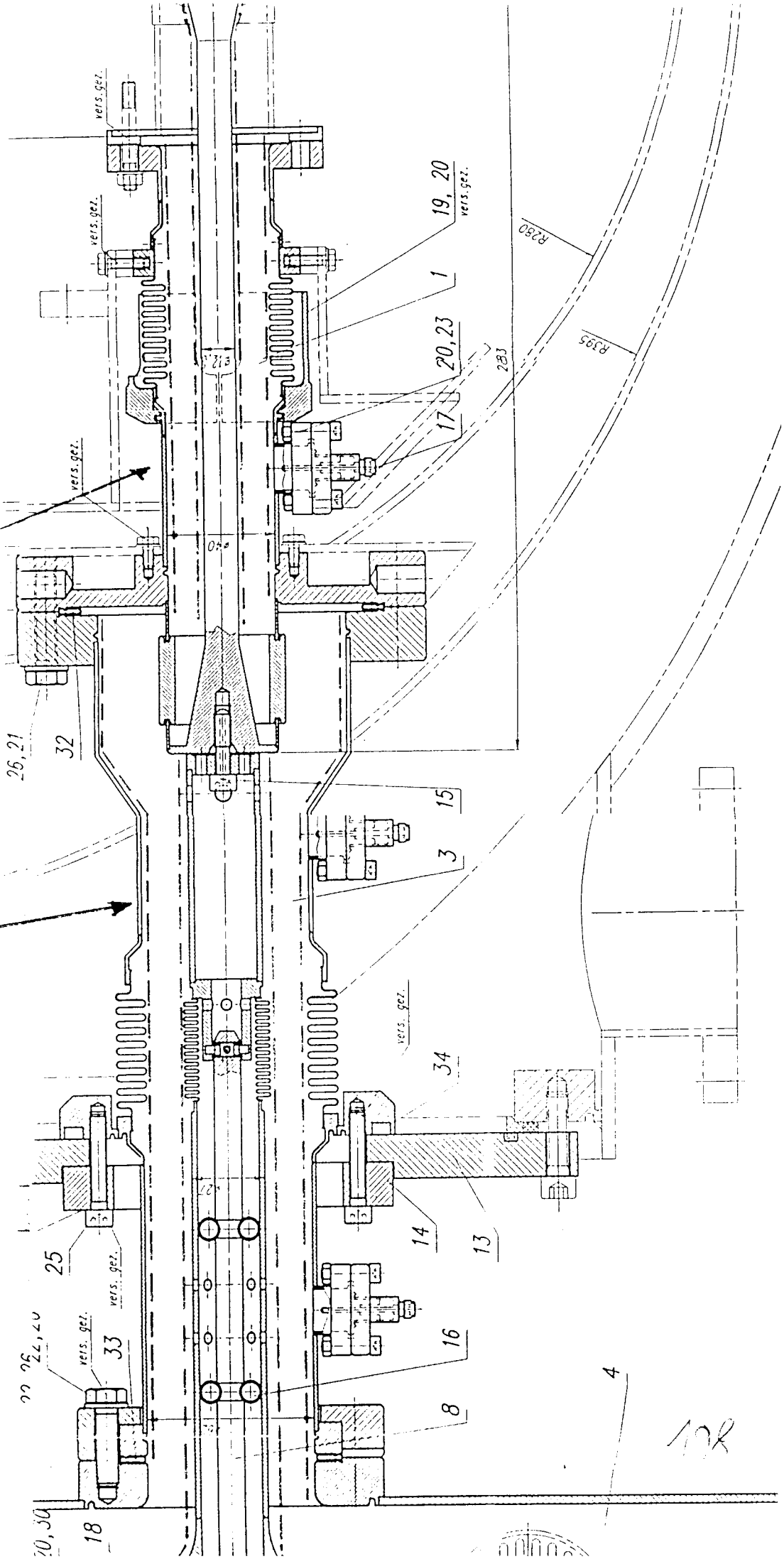

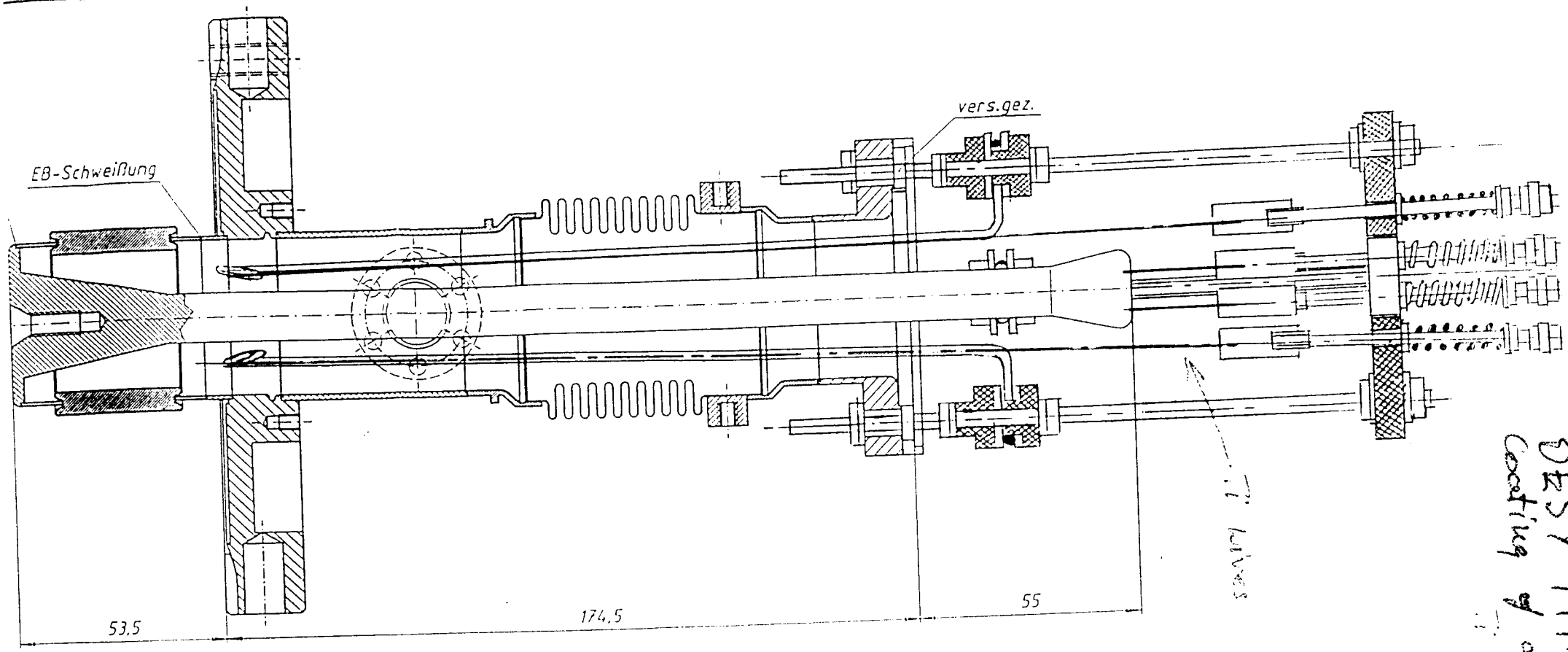

DESY TTF-II coupler, Coating of cold part of coaxial line

chweißen.

und Innenfläche mit Tantalblech abgedeckt.

herung montieren.

Bauteile
20 beachten.
[ ]
[ ]

DIN ISO 8015

DESY-Norm													~
Ra (mikro m)	0.025	0.05	0.1	0.2	0.4	0.8	1.6	3.2	6.3	12.5	25	50	o.B.
ISO Rauhigkeits-Kennzahl	N1	N2	N3	N4	N5	N6	N7	N8	N9	N10	N11	N12	✓

Allg.-toleranzen n. DIN ISO 2768 T1 u. T2 Toleranzkl. m

Oberfl. Angp. n. DIN 3142 oder ISO-1302

Abmaße in micro m

					Datum	Name
				Gez.	8.11.96	Oppe
				Gepr.		
e	174.5; 55; bildl.	07.01.98	Mar	Gen.		
d	Cy-Flansch	10.11.97	Mar	Erzeug.		
c	Antenne	14.10.97	Mar			
b	geändert	25.3.97	Ce			
a	Bohrung hinzu	12.2.97	Ce			

DESY behält sich für diese Zeichnung alle Rechte gem. DIN 34 vor

DESY reserves for this drawing all rights according to DIN 34

Für Rückfragen wenden Sie sich bitte an DESY Abteilung TT

Maßstab: 1:1

20. Juli 1999

Werkstoff:

Kalter Teil

DESY-MHF

3 96 4328/A.000

Blatt von Blättern